THE GEOLOGY AND MINERALOGY OF THE PHOSPHATE DEPOSITS OF CHRISTMAS ISLAND, INDIAN OCEAN

A thesis submitted for the Degree of Master of Science

by

N.A. TRUEMAN, B.E. (Hons)

Geology Department
University of Adelaide

Supervisor
Dr J.B. Jones

Date submitted: 12th July, 1965

Mineralogical research carried out at The Australian Mineral Development Laboratories, Adelaide as part of the exploration and development project of the British Phosphate Commissioners.

CONTENTS

CONTENTS

CONTENTS

STATEMENT

This thesis contains no material which has been submitted for the award of any degree or diploma in any university.

To the best of my knowledge and belief this thesis does not contain any material previously published or written by another person, except where due acknowledgement is made either in the text, or in the bibliography.

1. INTRODUCTION

This investigation of the geology and mineralogy of the phosphate deposits of Christmas Island was undertaken to provide an understanding of the nature and mode of occurrence of the phosphate minerals, their mutual relations and their relations with the other rocks of the island.

The investigation was commenced in June, 1962, at The Australian Mineral Development Laboratories at the request of the British Phosphate Commissioners, with the examination of 27 samples supplied by the British Phosphate Commissioners. These were taken principally from the phosphate workings. Field investigations were undertaken between 20th June and 29th July, 1963, and 28th September and 6th October, 1964. The latter field investigation was concerned primarily with the laying out of location markers for an aerial photographic survey which was to be conducted subsequently. However some additional sampling was carried out during the second visit. Geological and mineralogical investigations of the phosphate deposits and related rocks were undertaken to provide data for the delineation of the reserves, for the development and mining of the deposits, and for beneficiation and utilization tests.

Christmas Island is one of the three principal sources of phosphate for Australia and New Zealand. It is situated in the north-eastern part of the Indian Ocean and is approximately 190 miles south of Java and 900 miles from the north-west coast of Australia. It is an isolated island its nearest oceanic neighbour being in the Cocos-Keeling group over 500 miles to the south-west.

The production of calcium phosphate (apatite) has increased steadily from 396,000 metric tons in 1955/6 to 637,000 metric tons in 1962/3 (British Sulphur Corp, 1964). Phosphate from Christmas Island constitutes approximately one-third of Australia's requirements for the manufacture of phosphatic fertilizers. Approximately 50,000 tons of "phosphate dust" is exported from Christmas Island to Malaya annually.

The island has an area of approximately 55 square miles and the highest point is approximately 1100 feet above sea level. About 3000 people are resident on the island of whom 2800 are of Asian descent, the majority being Malaysians. The remainder are Europeans, principally from Australia, New Zealand and Britian.

The island has an average annual rainfall of approximately 75 inches. The rain is seasonal, the major falls occurring in the summer monsoonal months between January and April.

Extensive tropical vegetation covers most of the island, and in many places reaches a height of over 100 feet.

2. SUMMARY

Christmas Island is of volcanic origin and consists of volcanic and bioconstructed carbonate rocks and their derivatives formed mainly during the Eocene and Miocene epochs. Physiographically, it consists of a series of cliffs and terraces rising to a plateau approximately 700 feet above sea level.

Several prominent hills occur on the plateau, the highest reaching an elevation of the order of 1100 feet. The phosphate deposits occur mainly on the upper plateau and hills and consist essentially of apatite, crandallite and millisite, and barrandite. The apatite occurs on and within the carbonate rocks and the barrandite has been formed by the phosphatization of the volcanics.

The crandallite and millisite have formed by the lateritization of the apatite, the lateritization of carbonate rocks in the presence of phosphate, and as a result of weathering of the barrandite.

It has been found that carbonate and fluorine ions substitute freely in apatite and a possible linear relationship between these ions is postulated. Iron substitutes for aluminium in crandallite and millisite and the chemical data suggest that these minerals may be polymorphs of the same chemical compound corresponding to the formula of crandallite. Barrandite has formed as a result of phosphatization of basic volcanic rocks, presumably of limburgitic composition. The formation of barrandite involves the removal of silicon, magnesium and calcium. It is partially pseudomorphic.

Thermal studies indicate an inverse relationship between the degree of crystallinity and solubility of phosphate in citrate solutions in all the major phosphate mineral groups present on Christmas Island. Thermal studies were carried out on apatite, crandallite, millisite and barrandite.

The geological history of the island is considered to be related to the successive growth of reef limestones and derivative sediments (some of which have been dolomitized) and to contemporaneous volcanism.

The phosphates are ancient guano deposits and their derivatives The phosphatization is post-Miocene and probably Pleistocene in age and the deposition of the phosphate is considered to have taken place when the island formed a small, low-lying atoll, with little vegetation and an arid climate.

3. PHYSIOGRAPHY AND GEOTECTONICS

Christmas Island rises through a series of cliffs and terraces to a central plateau at an average elevation of about 700 feet. A composite photograph of the island from the eastern seaboard is given in Plate 1. The island is irregular in outline and roughly T-shaped. It is approximately 11 miles long in a north-south direction and 9 miles from east to west.

The cliffs vary in height up to 600 feet and are separated by gently-sloping terraces. A fairly continuous terrace of recently raised limestone occurs around most of the island at an average elevation of 50 feet. (Plates 2a and 3b). The upper plateau contains several hills, the highest of which (Murray Hill) is approximately 1100 feet above sea level. The central area of the plateau is slightly depressed and has an average elevation of about 650 feet.

Evidence of wave action is observable on the inland cliffs in many places, and raised beaches, often consisting of accumulations of pebble phosphate, occur on some of the terraces.

There is little available data on the bathymetry of the eastern Indian Ocean. However, it is known that Christmas Island is situated on a small ridge between two oceanic deeps.

The Maclear deep, between Christmas Island and Indonesia, is elongated in an east-west direction and is arcuate in shape, roughly parallel to the Indonesian Archipelago. Depths of over 3800 fathoms have been recorded in this area. To the south of Christmas Island lies the Wharton deep. The outline of this depression has not been reported in detail. However, it appears to be roughly equidimensional in plan, and depths to 2833 fathoms have been recorded.

Christmas Island is an isolated volcanic cone rising some 14,000 feet from the bottom of the ocean. The sea, even close to the island, is of considerable depth and less than half a mile from the coast ships cannot normally record any depth soundings.

Gravity determinations of the Indonesian area have been carried out in the past, notably by Vening Meinesz (Heiskanen and Vening Meinesz (1958)) and Van Bemmelen (1949). According to the compilation by the latter author of the isostatic anomaly map, there is a strong negative gravity (- 135 m gal) anomaly coincident with the Maclear deep and a weak positive anomaly (+ 54 m gal) parallel to the deep and passing through Christmas Island.

The bathymetric and isostatic evidence is taken to indicate that the Maclear deep represents an active geosynclinal zone and the parallel ridge to the south is probably an associated geanticline. The epicentres and depths of earthquakes and the distribution of the volcanics in the Indonesian Archipelago are also interpreted as being connected with this tectonism and it has been suggested that the whole area is influenced by compression or shortening of the earth's crust in a north-west/south-east direction between the Australian and Asian continents.

It is apparent that Christmas Island has been subjected to considerable vertical oscillations and there is much evidence of normal (tensional) faulting. These conditions are consistent with those expected in an active tectonic zone and associated with a geanticline. Coleman (1962) has recorded similar tectonic effects on Choiseul Island in the British Solomons Group which he considers likewise to be situated on a geanticline.

The incidence of volcanism on geanticlines is thought to be related to the general crustal weakness associated with these structures.

Folding and compressional faulting were not observed on Christmas Island.

4. GENERAL GEOLOGY

The island consists essentially of volcanic and carbonate rocks of Eocene and Miocene age. The Eocene rocks consist of andesite, trachybasalt, basalt glass, olivine basalt and limburgite interbedded with foraminiferal limestone and tuffaceous limestone. The upper series, of Miocene age, consists dominantly of foraminiferal and coral limestone, altered limestone and dolomite with interbedded flows of limburgite. The youngest rocks are leached and recrystallized and replaced by phosphate.

From the available palaeontological evidence there appears to be an hiatus in the sequence in Oligocene time (see Section 6 and Appendix A).

5. FIELD INVESTIGATIONS

5.1 Previous Investigations

Previous geological investigations of Christmas Island were conducted in 1898 by C. W. Andrews (1900) of the British Museum and in 1958 by O. N. Warin (1958) of the Bureau of Mineral Resources. The former investigation was sponsored by the British Museum for the purpose of recording not only the geology of the island, but also the fauna and flora. Permanent habitation prior to this was negligible and it was the desire of the British Museum to record the data on the natural science at that stage. Andrews was resident on the island for approximately 10 months and recorded some valuable data on the palaeontology and geology. Unfortunately there has been considerable revision of the palaeontology since Andrews's investigation and this necessitated resampling of many of his sample localities.

O. N. Warin visited Christmas Island for approximately 3 weeks in 1958. The purpose of his visit was to examine the mode of occurrence of the phosphate, but additionally he recorded some important data on the under-lying rocks. In the brief time that Warin was on the island it was not possible for him to sample the phosphate deposits systematically, nor was it possible to collect samples for palaeontological examination.

As well as these investigations, it is reported that a geologist was resident on the island immediately prior to World War II. However, with the impending occupation of the island by the Japanese in 1942, it is reported that this investigator was evacuated to Singapore where, unfortunately, he was killed and his records destroyed.

Systematic drilling for the purpose of evaluating the grade and distribution of the phosphate deposits on the upper area of the island was carried out by the British Phosphate Commissioners in 1957-58. The drill sites were located on a 400-ft grid in areas where drilling was considered possible (i. e. , where rock outcrops were not excessive). The results of this work were plotted on a map on the scale of 1 in. equals 2000 ft and certain areas defined as possible fields. However since that time the potential importance of the iron-aluminium phosphate has been realized and the 1957-58 survey which was concerned only with apatitic phosphate is now only of limited value.

5.2. General

Christmas Island consists of a series of volcanic rocks interbedded with limestones, the latter having formed from coral reefs and shelly beds on and around the volcanic nucleus. Andrews (1900) described the island under four headings and this classification is followed in this report. The areas are:

1. The central nucleus
2. The inland cliffs
3. The plateau and hills
4. The sea cliff

The phosphate deposits, with the exception of minor pebble beds occur on the plateau and hills and therefore the investigation has been primarily concentrated within this area. However, some sampling and examination of the rocks of the nucleus was carried out principally to revise the palaeontology and to obtain geological data on the island core.

5.3 The Central Nucleus – the older carbonate and volcanic rocks

Rocks constituting the nucleus were observed at Flying Fish Cove, at Waterfall, Ethel Beach and Dolly Beach on the eastern coast, and between the Freshwater (Hugh's) Dale and Winifred Beach on the western coast. These rocks are exposed in the shore and first inland cliffs where later reef limestones have not developed. In other coastal areas examined, younger reef limestones form bold cliffs with a terrace of extremely rugged pinnacle limestone behind them. These limestones were sampled on the north and south coast for palaeontological examination to determine the age of the last negative shore movement. Palaeontological examinations (Appendix A) indicate that this reef consists of a fauna of species living at the present day (Sample P36).

The rocks of the nucleus consist of lavas and pyroclasts interbedded with beds of yellow and white limestones. Beds of volcanic debris cemented by calcareous material occur frequently, usually immediately overlying beds of lava. This relationship is suggestive of a period of erosion of the lavas before deposition of the limestone. Good exposures of these rocks occur in Flying Fish Cove and were mapped in detail by Andrews. The author has examined and sampled the sequence at several places but has not remapped it. The sequence is as follows:

	Description	Approximate Thickness ft
4.	Massive white limestone containing foraminifera	150
3.	Light grey tuffaceous limestone	50
2.	Basalt glass and basalt	20
1.	Red-yellow limestone containing numerous microfossils	75

The sequence is complicated by faulting and is frequently overlain by talus and near the base of the cliff, by recently-raised reef limestone. The faulting where observable is normal. Two parallel faults are exposed in the cliff behind the boat club striking NE-SW.

However the northern fault dips to the north and the southern to the south. Possibly resulting from this faulting, fresh volcanic rock is exposed on the first inland cliff behind the Drumsite settlement. This volcanic rock was observed in outcrop in only a few places, principally behind the Asian school, but pebbles of fresh volcanics were observed on the terrace and in the west-bearing gullies between this area and the cliff behind the cove. The relationship of this volcanic rock to the adjacent limestone could not be determined on the eastern limb of the outcrop. From the observed exposures it appears to have a non-tectonic contact with the limestone. The western margin was equally difficult to examine but, according to Warin (1958), it is a faulted junction.

Large (1 cm) radiating crystals of calcite were observed in the fault zones in Flying Fish Cove. These crystals occur in solution cavities and are thought to have resulted from secondary deposition from springs along the faults. The emanation of fresh water from this fault zone could also be responsible for the lack of growth of the reef in the boat channel in front of the Marine Department buildings.

On the east coast, between the golf course and Ethel Beach, extensive outcrops of volcanic rocks were observed. These rocks were found on the sea cliff and the shore terrace and in places form the lower sections of the first inland cliff. Between Ethel Beach and Waterfall well developed columnar jointing was observed in the volcanics and in places they are amygdaloidal. The volcanics at Ethel Beach consist of trachybasalt and about six feet above sea level are overlain by volcanic glass.

At Steep Point, the cliff is interrupted by a vertical fault zone striking approximately 60^0. In this area a saddle was observed, the walls of which on the east and west sides are vertical and appear to be stepped. Faulting is postulated purely on physiographic evidence, because it was not possible to examine the area in detail and marker horizons were not apparent on quick inspection. The floor of the saddle is strewn with pebble phosphate and brown soil and appears to have been worked by the sea before the last shore movement. Similarly a raised beach which also was covered by pebble phosphate was observed behind Lily Beach. The pebbles are smooth and sub-rounded and there appeared to be some degree of sorting, the coarser pebbles occurring closer to the present shore line. The cliffs at Lily Beach consist of recently elevated reef limestone and contain several sink holes.

Between Steep Point and Ross Hill Tank, further outcrops of volcanic rocks were observed. These rocks are basaltic and crop out below limestones at the Ross Hill Tank (RL315) Further to the north the first inland terrace appears to be composed of basalt as much volcanic scree was observed and sago palms, which according to Andrews (1900) are indicative of volcanic rocks, are plentiful. The first terrace terminates against a limestone cliff bearing east-west, about $\frac{1}{2}$ mile north of Ross Hill Tank. According to Warin (1958) this scarp is the result of a major fault which intersects all formations of the island with the exception of the recent reef limestone and is evident again in Sydney's Dale on the

west coast. The present author did not observe any displacement in the formations in Sydney's Dale, nor was any displacement evident in the area north of Ross Hill Tank. However, in the time available, it was not possible to map this area in detail and thus the possibility of faulting is not discarded. It is suggested, however, that the occurrence of large scarps of limestone could result from the irregular development of limestone reefs such as those evident in the first inland cliff on the northern side of the golf course. The scarp north of Ross Hill Tank is weathered and covered by talus in many places. Numerous small caves, which appear to be the result of wave action, occur along the scarp, and secondary carbonate is quite common.

Further outcrops of volcanic rocks occur on the east coast below Ross Hill and at Dolly Beach. On the first inland terrace north of Dolly Beach much volcanic scree was observed, but in this area sporadic outcrops of limestone pinnacles also occur. It is assumed that the scree has been derived from the inland cliff immediately to the west under Ross Hill. Again it was not possible in the time available to explore for the source of this material.

At Dolly Beach volcanic rocks outcrop on the headlands and in the surf zone. These appear to be lavas and tuffs. The lavas contain coarse phenocrysts of feldspar and idiomorphic ferro-magnesian minerals. They consist of andesite (Sample RH6 and RH6T). These volcanics are all considered to be rocks of the nucleus.

On the west coast between the Freshwater (Hugh's) Dale and Winifred Beach, good exposures of rocks of the nucleus were found. Volcanic rocks outcrop in Hugh's Dale and in Sydney's Dale about 250 yards from the coast. These volcanics are underlain by massive limestone and are best exposed at Sydney's Dale. This is a chasm, presumably opened along a joint plane, about 100 feet deep and 30 feet wide. The base, near the coast, consists of massive limestone containing calcareous fragments and weathered in varying degrees to a reddish-brown soil. Corallites up to 4 feet in diameter are exposed in the vertical walls. About 200 yards from the coast, within Sydney's Dale, bedded limestone was observed striking 10^0 and dipping 30^0W. Variations in dip from the horizontal are unusual and, in most cases, this is primary dip or results from current bedding. However in this case the relationship of this limestone to the enclosing rocks could not be determined.

The most extensive outcrops of volcanic rock observed on the island occur south of Sydney's Dale and extend to the south of Winifred Beach. They are limburgitic, at least in part, and crop out on the shore cliff about 50 feet above sea level, and are approximately 100 feet thick. In places boulders up to 30 feet in diameter were observed, which are jointed in a radiating structure. South of Winifred Beach the volcanics are overlain by white limestone (Sample P48) which contains abundant microfossils. This limestone is extremely rugged and appears to cap the centre of the peninsula.

It is possible that the volcanics which outcrop above Winifred Beach are correlative with those behind the Dales. Although outcrops in this area are reasonably continuous, it was not possible to map this area as there is insufficient control and the available base maps are not sufficiently accurate. The volcanic rocks of the lower levels were sampled wherever possible for mineralogical comparisons with the volcanics of the upper levels.

5.4 The Inland Cliffs

The limestone forming the inland cliffs and central plateau is the most common rock type exposed on the island. It overlies the yellow limestones and lower volcanic sequence, and the contact was observed on the north-eastern section of the first inland cliff principally between Flying Fish Cove and Ethel Beach. The contact where exposed appears to be disconformable with the underlying volcanics and shows signs of being exposed underwater prior to deposition of the limestone. In several places, for example in Flying Fish Cove and between Waterfall and Ethel Beach, a bed of calcareous material containing fragments of volcanic rock marks the base of the younger limestones. This bed is normally of the order of 1 to 4 feet thick.

The limestone of the inland cliffs is uniform in appearance and, with the exception of the interbedded volcanics which were observed in only a very few places normally constitutes the entire sequence. These cliffs are up to 500 feet high.

The cliffs are separated by a terrace of variable width. Where the first and second inland cliffs are developed, the terrace separating them is of the order of 300 yards. This terrace is mostly covered by soil and limestone detritus which appears to be corroded by marine weathering. Adjacent to the cliffs a zone of rugged limestone pinnacles is commonly developed and in most cases is now covered by thick pandanus. It is suggested that the pinnacle limestone may be a reef development on the edge of the terrace.

In at least three places the inland cliffs show evidence of incipient phosphatization. The second inland cliff, which runs parallel to the Drumsite to South Point railway near the $10^1/_4$ mile peg (i.e., $10^1/_4$ miles from South Point) consists of massive limestone and contains some banded phosphate. The cliff consists of massive horizontally bedded white limestone, and commonly contains solution cavities in which have been deposited successive bands of secondary carbonate and phosphate. The phosphate mineral appears to be apatite and the centres of the cavities are commonly lined with calcite crystals. Although no fossils were observed at this locality, small foraminifera(?) were collected from the railway cutting on the 10 mile peg. It is thought that the limestone of this locality is of the same age as that at the $10^1/_4$ mile peg.

Other examples of incipient phosphatization in the inland cliff limestone were observed at the cliff to the north of the railway line, at the $7\frac{1}{2}$ mile peg, and also on the eastern side of the railway $1\frac{3}{4}$ miles north of South Point. In both these cases (Samples RL2 and P12 respectively) the phosphate appears to be replacing the limestone.

It is perhaps significant that, in at least two of the above examples, there is no known phosphate field delineated nearby and that it is most unlikely that phosphate-bearing solutions have migrated from the known areas of phosphate deposits to these localities. In the third case, that occuring $1\frac{3}{4}$ miles north of South Point, the sample was taken in the railway cutting. Unfortunately it has not been possible so far to determine if this is immediately adjacent to the phosphate fields of the north-west section of South Point but, if so, it illustrates the ability of the phosphatic solutions to penetrate to considerable depths. This phosphatization occurs some 200 feet below the level of the existing workings.

Volcanic rocks were observed interbedded with the upper limestones in only one locality. On the eastern side of Ross Hill, the inland cliff is well developed and is estimated to be approximately 700 feet high. It consists essentially of massive limestone in which some foraminifera(?) (Sample P54) were observed. Additionally an interbedded volcanic flow was observed about 300 feet from the base of the cliff. This flow is approximately 60 feet thick and is fine-grained without amygdules or vesicles. Its lateral extent was not determined.

5.5 The Central Plateau and Hills

The central plateau is the most extensive physiographic unit of the island and may be generally defined as that area above which no cliffs of considerable lateral extent are developed. However, there are several small and, in some places, steep hills developed on the plateau. This feature may be broadly classified into:

a. Areas consisting of rugged limestone outcrop (karrenfeld or "limestone" pinnacles) with little soil development, and containing sporadic caves and sink-holes.

b. Areas of small limestone outcrop with considerable development of red-brown soil, which may or may not be phosphatic.

c. Areas of brown soil showing no visible outcrops, which are commonly phosphatic and in some cases are considered to be the result of the weathering of volcanic rocks.

d. Areas of volcanic rocks, which show few outcrops, and a thick development of brown soil. These areas are also phosphatized in certain cases.

The main area of pinnacles of carbonate rock occurs in the vicinity of Camp 4 and to the north-east through Grant's Well towards Gannet Hill. The rock is very rugged and usually crops out as large pinnacles up to 8 feet high and several feet in width, and often with a very irregular surface. Near Camp 4, the carbonate rock is recrystallized and consists of dolomite (Sample RL3). In other localities, such as Jedda Cave and between Grant's Well and Ross Hill Tank (Samples P22 and P23), the carbonate rock contains abundant tests of corals. It also outcrops extensively to the west of Camp 4. In some places in this area it contains many shells, as at locality P32, about 1 mile west of the South Point road. This area contains numerous sink-holes and caves, of which Jedda Cave is an example. Underground water has been discovered in Jedda Cave at a depth of 80 feet from the mouth of the cave[a]. Fresh water was found at Grant's Well at a depth of approximately 100 feet and the water flows west along a bed of weathered volcanic rock (Sample GW1). Approximately 200 yards east of Grant's Well a bore was sunk to obtain data on the underground water. Fresh "basalt" was encountered at 72 feet after passing through brown soil (Sample GW6).

The area of rugged limestone crops out in a depression of the central plateau and has a reduced level between 800 and 600 feet. It is bounded by higher ground to the south (Ross Hill and Wharton Hill), to the east (Stronach Hill and Margaret Knoll), to the north (Gannet Hill) and to the west (towards Stewart Hill). Recent discoveries of fresh water at Grant's Well and Jedda Cave give some evidence that there are good supplies of water in the area. Further exploration by drilling and examination of existing caves may reveal further good flows, particularly near the junction between the limestone and underlying volcanic rocks. Small impervious beds may also cause minor accumulations in the form of perched water-tables and therefore the impervious layer should be penetrated to some depth to determine the nature of the flow. It is considered that the accumulations in Grant's Well and Jedda Caves are of this type.

Other areas believed to be composed essentially of carbonate rocks (limestones) in which there are few outcrops occur in several places in the central plateau. A typical area of this type occurs between Field 5 and Grant's Well on top of the inland cliff adjacent to the railway line. The area consists of red to dark brown soil which shows no variation in colour to a depth of about 3 feet. Two auger holes (A8 and A9) were sunk in this area to determine the mineralogical composition of the soil profile. It was found to consist essentially of crandallite with minor goethite. The outcropping limestone is fossiliferous, containing foraminifera, shells and corals (Samples P9 and P10).

(a) Inspection of the underground stream in Jedda Cave in September, 1964, revealed that, as in the case of Grant's Well, the water flows along a bed of weathered volcanic rock. (AMDL Report 386).

A good example of phosphatic soil occurring in association with sporadic limestone outcrops occurs on the northern end of Field 17. Here the soil is light brown to grey and shows only slight colour variation to a depth of 31 inches (Auger Sample A19). The limestone in this area crops out irregularly and is similar to the pinnacles described above.

Areas of brown soil showing no visible outcrop occur in many places of the cental plateau. Typical examples are the phosphate Fields 18, 23 and parts of 25, as well as the area between Murray Hill and Jack's and Ferguson Hills. There are also several examples between Ross Hill and Phosphate Hill. In some places, the soil is obviously phosphatic (for example auger hole A3, in Field 25) and the profile under these circumstances usually varies in the same manner as the phosphate fields presently being worked. These areas were sampled by auger to determine the nature and vertical variation of the mineralogy. The samples gave no indication of the size of the deposits as the depth of penetration was never more than 3 feet and at the most only two holes were sunk in any one field.

To the north-west of Murray Hill at the extremity of Field 25, a large area of phosphate rock is exposed. It occurs on the end of Tom's Ridge at the edge of the inland cliff. The phosphate rock (Samples MH6 and MH7) is crustiform banded and, although normally white to buff, varies in colour from dark brown or black to blue-grey. The phosphatization is thought to have resulted from solution deposition from phosphatic spring water from the Murray Hill area. The rest of Tom's Ridge consists of thick brown soil containing sporadic pebbles of phosphate (Sample MH5).

In some cases, particularly between Murray Hill and Jack's and Ferguson Hills, dark brown soil occurs which shows no colour variation in the upper 3 feet and the area contains no rock outcrops. These soils are thought to be the derivatives of volcanic rocks and were sampled by auger to determine the mineralogical constituents (Samples A1 and A2).

Phosphatized volcanic rocks were observed in outcrop on the southern side of Aldrich Hill in two localities near lines 10 and 1 of the Smithson Bight area drilling grid. These rocks occur as isolated boulders up to 2 feet in diameter. The remainder of the area is covered by light brown soil (Samples A11 and A13). The phosphatized volcanic rocks are interbedded with limestone (Samples P30 and P31). Near line 10, they appeared to be less phosphatized and the area was sampled extensively (Sample Ce2). Veins of green and brown barrandite up to 1 inch wide were observed in some samples. The results of the petrological and mineralogical examinations of this material are included in Section 7.

Several of the hills which occur on the central plateau were also examined. Murray Hill, the highest point on the island (1170 feet), was found to consist mainly of limestone and around its base well developed coral (Sample P26) was found. On the north side of the hill above the coral limestone an area of dark brown soil devoid of rock outcrop was observed. This area contains sub-rounded pebbles of phosphate (Sample MH1) up to six inches in diameter. Towards the summit, brown to brown-green phosphate rock was observed (Sample MH2). Samples of this material from the centre of the island were examined in the laboratory. They were found to consist of barrandite and show remnant igneous textures. Further occurrences of this material were reported from bore-holes sunk in the Murray Hill area on the southern side of the summit.

It is therefore concluded that Murray Hill was originally a volcanic vent.

Phosphatized and fresh volcanic lava was also found on the sides of Stewart Hill and Ross Hill. Stewart Hill contains isolated outcrops of barrandite rock (Sample Ce9) overlain by horizontal bedded limestone containing bands of macerated shells (Sample P50). On the summit of the hill, a scree of limestone detritus (Ce10) was found. Thus it is assumed that Stewart Hill was also a volcanic vent and, once dormant, was under water for a sufficient time for limestone to accumulate on its upper surface. The limestone scree on the summit appears to be water-worn.

Ross Hill is also thought to have been a centre of volcanism. This hill is over 1000 feet high and about 200 feet above the surrounding plateau. Wharton Hill, which adjoins Ross Hill to the east, is a spur that extends to the railway line. The lower slopes of Ross Hill consist of light brown soil with no visible outcrops (Auger Sample A17). Occasional large "boulders" of brown soil may be weathered volcanics. Above this zone extensive limestone crops out. This limestone contains some shells (Sample P33) and, towards the top, foraminifera (Sample RH5/P).

On the southern side of Ross Hill a bed of a limburgitic volcanic flow was observed (Sample RH3). This rock, where exposed, appears to be quite fresh.

The flow extends for at least 300 yards in a southerly direction. It is estimated to be between 20 and 60 feet thick, although difficulty was experienced in determining the extent because of extremely poor outcrop. Soil covering the volcanic rock was sampled by auger, (Sample A18). It is yellowish-brown and did not show any variation to a depth of 27 inches. Below the volcanics, limestone was again found to crop out and weathered limestone fragments are plentiful.

Neither at Phosphate Hill nor at Limestone Hill were any volcanic rocks observed. These areas were examined in particular to determine whether the iron and aluminium of the overburden of the adjacent phosphate fields could have originated from alluvial deposition from the weathering of volcanic rocks on higher ground.

Phosphate Hill consists of massive limestone which outcrops sporadically near the summit. In the vicinity of the radio masts, the limestone is weathered and friable. On the western side of the cricket pitch, light brown phosphatic soil was observed through which sporadic limestone pinnacles are exposed. The soil was sampled by auger to a depth of 17 inches and showed no variation to this depth (Sample A10). The hole was stopped on a limestone floater and some brown pebble phosphate was encountered. This soil-clad plateau extends west to the top of the inland cliff behind the Drumsite settlement. The elevation of the radio masts is 1020 feet.

Beneath Phosphate Hill to the south, the limestone contains some well-preserved corals and shells. These were sampled from a limestone pinnacle at the north end of the airstrip which has an elevation of 889 feet (Sample P6). Further south, on the western road to Grant's Well, the limestone is also fossiliferous (Samples P8 and P9). This road follows a ridge in a south-westerly direction at an elevation of 880 to 925 feet. The limestone contains some large coral colonies.

Limestone Hill could not be examined in much detail because of the dense undergrowth. Approximately 100 yards from the north-west quarry, red phosphatic soil was found (Sample SP6) containing phosphate pebbles. Some pebbles are deep brown in colour (Sample SP7). The limestone which crops out further east is fossiliferous (Samples P16 and P17) but, as in the case of Phosphate Hill, volcanic rocks were not observed.

5.6 The Sea Cliff

In addition to the places so far described in which rocks of the nucleus are exposed, in many places younger limestones constitute the sea cliff. These are particularly well developed on the north coast between Rocky Point and North-East Point and between South Point and Margaret Beach and, presumably, to North-West Point. Similarly on the south coast in Smithson Bight and probably continuing to Egeria Point, this limestone constitutes the cliff and adjacent terrace. (Plate 3B).

The cliff consists of massive limestone, buff to grey in colour and iron stained in part. It contains numerous coral colonies, the largest observed being approximately fifteen feet in diameter (Samples P34, FC6). The limestone is jointed vertically into large blocks up to 50 feet wide, and blocks which have broken and fallen into the sea are evident at numerous places.

The cliff is normally undercut by the sea and blow-holes are quite common. Limestone caves are also common (for example Grime's Cave) and these commonly contain stalactic calcite.

Above the cliff the terrace commonly consists of very rugged limestone which occurs as pinnacles with irregular surfaces. These pinnacles are believed to have formed as a fringing reef which has been elevated during the last negative shore-line movement.

5.7 The Phosphate Fields Currently being Worked

Phosphate is currently being raised at Phosphate Hill and South Point. In the former locality three areas designated Fields 4, 5A and 5EF are being developed. At the latter, three areas designated East Quarry North-West Quarry and West Quarry were being worked during 1963. Field 17, Limestone Hill, was in early stages of development in September 1964.

5.7.1 Phosphate Hill

The most extensive recent workings at Phosphate Hill are those on Field 5A. The overburden in this area is up to 15 feet deep and the best exposure occurs in the western face. It is brown to white-brown in colour and grades into white phosphate at depth. It has an earthy lustre and is compact and hard in the exposed faces.

Within the overburden, a zone of pebble phosphate occurs which is essentially linear in plan and extends from the western face towards the inland cliff on the eastern side of the field. The zone has an average width of approximately 12 feet and is up to 8 feet deep. The contact of this zone with the enclosing overburden is arcuate in cross section and was well exposed near the working face. Sorting was evident in the pebble zone in the eastern section of the field. The pebbles, varying from $^1/_2$ to 4 inches in diameter, are massive and sub-rounded. They are nodular and consist of banded apatite. They are commonly replaced in part by brown crandallite. Small concentric bands of manganese oxide were also observed. It is assumed that the pebble deposit is a prior stream bed and the pebble phosphate has been washed down from the higher ground to the west (Sample PH1).

The overburden grades into a white phosphate (presumably apatite) and this occurs between pinnacles of partly phosphatized to fresh carbonate rock. The depth of the white phosphate is variable but is mostly from 5-10 feet.

The carbonate rock is normally massive and varies from white to buff in colour. The upper level of the pinnacles is irregular in this field which contrasts with those pinnacles occurring at South Point. The pinnacles have an average height of 8 feet and are mostly of the order of 4 to 6 feet thick. Current bedding was observed in the carbonate rock in one place at the northern end of the field (Sample PH2). This sample was found to be dolomite. The pinnacles show numerous indications of replacement by phosphate (Sample P43).

The western face of Field 5A was channel sampled from the overburden into the white phosphate over a distance of approximately 15 feet. The reduced level of Field 5A is approximately 900 feet.

Perhaps the best exposure of the phosphate profile observed is the west face of Field 4. Here the overburden depth is in excess of 6 feet and fluctuates considerably over the face. A typical section is as follows:

Depth ft	Description
0 –3	Dark brown, homogeneous phosphatic overburden containing plant roots.
3 –5	Brown to reddish phosphate containing occasional oolitic patches about $1^1/_2$ in. wide.
5 –$6^1/_4$	Light brown to white mottled zone containing some apatite concretions and apatite fragments.
$6^1/_4$–9	Buff coloured apatite, oolitic and friable in part.

Massive pinnacles of carbonate rock with smooth conchoidal surfaces were observed in this face of the quarry. Vegetation (tree roots) was also observed, even in the lower levels.

A further exposure of the profile was observed in the recent workings on the eastern side of the field. Here the sequence is as follows:

Depth ft	Description
0–4	Dark brown earthy phosphate.
4–6	Mottled zone of white to light brown phosphate.
6–12	White to grey apatite.

Again unaltered pinnacles are exposed in the quarry face. Channel samples were cut in both the above localities for mineralogical examination.

Field 5EF is the most recently developed and at the time of examination only a small area had been worked out. The phosphate here is reported to be high grade and with an overburden depth of only 18 inches. The depth of workings on the eastern side is quite shallow, being little more than 6 feet. However, it is reported that the depth of phosphatization increases to the west. Work is proceeding along a north-south bearing face.

Exploratory drilling was being carried out to the north of the workings at Field 5EF during inspection in 1963. Here the drilling was proceeding on an eighty-foot grid on lines bearing 30^0. North of the existing workings the phosphate grade is reported to be poor and, in one hole observed by the author, approximately 4 feet of overburden (Sample PH6) was penetrated before the drill intersected dark brown pebbles (Sample PH7). It is current practice to cease drilling on reaching any solid rock, this being governed to a large degree by the type of drill being used.

In addition to the fields currently being worked, all of which occur on the east side of Phosphate Hill two large areas have been worked out on the northern side. In these areas the depth of phosphatization was extensive and pinnacles of up to about 100 feet were observed in the workings. The deposits currently being worked all occur over 850 feet above sea level but one of the old areas occurs at approximately 400 feet.

5.7.2 South Point

Phosphate has been raised in this area for some years and the workings are somewhat more extensive than those at Phosphate Hill. Additionally, the depth of phosphatization appears to be greater at South Point and the overburden less extensive.

Of the area being worked at the present time, the deposits at East Quarry appear to be most extensive. The quarry face strikes approximately north-south and is being worked in a westerly direction. This quarry contains a considerable depth of high grade (low iron and alumina) phosphate. The overburden has been stripped to an average depth of approximately 10 feet and below this the phosphate extends up to 60 feet in depth.

The "limestone" pinnacles are massive and buff coloured and, as at Phosphate Hill, appear to be phosphatized in some cases. The phosphate is generally earthy and friable but zones of phosphate rock or crustiform banded apatite occur in patches in many places. This phosphate rock varies in colour from rusty-brown and light blue to white. In other places, small zones of brown phosphate were observed and these occur throughout the profile.

Two channel samples were cut from the working face at the East Quarry. The reduced level of the face is between 770 and 780 feet. The depth of the workings in the North-West Quarry is shallower than in the East Quarry. At the time this quarry was examined, the face was about twelve feet high and an estimated 5 feet of overburden had been stripped prior to mining. The quarry is being advanced to the south along a face bearing 60^0. Again, the overburden appears to grade into the white phosphate and some rock phosphate was observed in joint faces.

It was in the West Quarry that most of the rock phosphate was observed. Here the workings are approximately 20 feet deep and the face is being advanced to the east on a bearing of 160^0. The phosphate rock (Samples SP4 and SP5) is crustiform banded and brecciated in places. In other respects this quarry appears to be similar to the others. The pinnacles were found to be dolomite.

Pebble beds, similar to those described at Field 5A, Phosphate Hill, were observed at the south end of the South Point fields. These pebbles are coarser to the north, reaching a diameter of 8 inches, and are smaller to the south where they extend across the terrace to Lookout Point. This sorting is considered to suggest stream deposition, the source being in the higher ground towards Limestone Hill.

An extensive area of rock phosphate occurs on the terrace south of the phosphate workings. This occurs as large blocks about 12 inches in width and is crustiform banded (Specimen SP1). This deposit is similar to that on Tom's Ridge and is believed to have resulted from secondary deposition from spring water. The banded texture of the material is suggestive of secondary deposition and, if so, it is an example of secondary enrichment.

The depth to which phosphatization has taken place is difficult to estimate, but in several places there is evidence that it extends considerably below the level to which the phosphate is worked. In the "limestone" quarry at South Point there is exposed in the face a considerable amount of white phosphate, presumably apatite, which has been deposited in joint fractures in the carbonate rock. The quarry face is approximately 30 feet high and the carbonate rock is massive and strongly jointed. In addition to the friable and crustiform phosphate, there is a certain amount of phosphate evident in the massive carbonate rock which it appears to be replacing. As the top of of the "limestone" quarry is approximately equivalent to the base of the phosphate workings which adjoin it, this is considered evidence that the phosphatization has occurred to a considerable depth below the level worked. The extent of the phosphate, relative to the carbonate rock, in the quarry is not as high as in the phosphate fields above, and it is doubted that this material could be won by the method of phosphate raising currently being practised (Samples SP2 and SP3). The carbonate rock was found to be dolomite and of detrital origin (Section 7, Plate 10B).

Other areas in which phosphate minerals were observed in massive limestone further indicate the depth and distribution of the mineralization. No attempt was made during this investigation to determine the extent of these "deeper" phosphates, but they are significant in that they indicate the ability of the phosphate to migrate, presumably under the influence of ground water. It is also possible as a result of this migration that secondary enrichment may have taken place under favourable geochemical conditions. These would presumably be associated with evaporation or some process of ionic concentration.

During field investigations in September-October, 1964, the West Quarry had been worked by open cut mining in benches to a depth of about 100 feet below the pinnacles. It was apparent that the phosphate had penetrated the carbonate rocks, replacing them and forming large deposits of high purity. It is considered probable that others of this type will be encountered.

6. PALAEONTOLOGY

Fifty-four samples of the limestones from Christmas Island were collected by the author and submitted to Dr N. H. Ludbrook of the S. A. Government Department of Mines for palaeontological examination. The results of this work are contained in the S. A. Government Department of Mines Report DM693/64 entitled "Tertiary Limestones of Christmas Island (Indian Ocean)" which is included as Appendix A of this report.

Of the collected samples, 12 were found to consist more or less entirely of reef corals, 14 contained molluscan moulds and 7 were recrystallized or leached limestones. The remainder were found to contain foraminifera and were used for dating purposes.

The limestones examined, with the exception of the fringing reef, are of Eocene (Tertiary 'b') and lower Miocene (Tertiary 'e' to 'f'$_{1-2}$ — Aquitanian to lower Burdigalian) age. Both the Upper Eocene and Lower Miocene are reef limestones with abundant corals and calcareous algae and are rich in foraminifera which appear to be localized in their distribution.

It will be shown in Section 7.6 that the fauna, texture and mineralogy of the limestones are indicative of the facies of formation.

The palaeontological examination was also of value for determining the age of the phosphatization. As the phosphate has replaced the underlying limestone, it is possible to obtain an uppper limit of its age. The youngest limestones of the upper plateau which could be dated were found to be of Burdigalian age and thus the phosphate must have been deposited at the close of, or subsequent to, this period.

7. MINERALOGY AND PETROLOGY

7.1 Preamble

Mineralogical and petrological examinations were carried out on a representative selection of samples of the volcanic and carbonate rocks from both the upper and lower series of the Tertiary formations and the post Tertiary reef limestones. Mineralogical and where possible petrological examinations were also carried out on the phosphatic samples. The descriptions are subdivided accordingly.

The mineralogical examination was mainly carried out by x-ray diffraction techniques using both powder photography in 5.73 and 11.46 cm Debye-Scherrer cameras and by diffractometry. Microscopic examination in thin section and immersion oils and differential thermal analysis were carried out to assist in the mineralogical examination of some samples. Owing to the sub-microscopic grain size of many of the carbonate and phosphate samples microscopic examination of these materials was of limited value. Petrological examination of those samples sufficiently coherent for thin section preparation was undertaken, however, and the carbonate rocks sectioned for palaeontological examination were also studied petrographically.

7.2 Terminology

The terminology used in the description and classification of the volcanic rocks is that of Hatch, Wells and Wells (1961) and, for the ultramafic volcanic rocks, that of Williams, Turner and Gilbert (1954). The classification proposed by Schlanger (1964) for reef complex sediments has been used for the carbonate rocks.

Terminology of phosphate minerals and textures is more difficult. Mineralogically, no attempt has been made in this section to differentiate between varieties of apatite. It will be shown in Section 8 that the apatite is a carbonate-fluor-hydroxy variety. The names of other phosphate minerals are those used in Dana's System of Mineralogy (Palache, Berman and Frondel, 1951). Petrologically, two forms of apatite could be distinguished. The first is sub-microscopic in grain size and optically isotropic. It is referred to as collophane. The second occurs in veins or lining cavities and consists of fine crystals oriented normal to the vein. It is anisotropic with a birefringence $n_w - n_e$ of approximately 0.004-0.009 and the crystals are length slow. This variety is termed dahllite. The compositional variations between collophane and dahllite have not been determined owing to the difficulty of extracting sufficient pure material for chemical analysis.

The term barrandite is the group name for members of the variscite-strengite series and the term barrandite rock is used for a rock consisting dominantly of these minerals.

7.3 The Lower Volcanic Rocks

The rocks at the base of the lower volcanic series (elevation = 0-200 ft) which were examined in the laboratory were those from Waterfall (Sample FC6), Ethel Beach (Samples FC7, FC8) and Dolly Beach (Samples RH6, RH6T). These rocks consist of andesites, trachybasalt and volcanic glass.

The andesites crop out in the surf and sea-cliffs at Waterfall and Dolly Beach. At Waterfall the rock is a hypersthene-augite andesite. Hypersthene occurs as phenocrysts which constitute about 5 per cent of the rock and average 0.3 mm in grain size. The matrix consists of microlites of plagioclase, of composition An_{10} to An_{50}, and augite. Opaque grains are a common accessory and appear to be magnetite. Chlorite has formed by alteration of the hypersthene.

At Dolly Beach there are two distinct types of andesite. The lowermost (Samples RH6, Plate 9B) is porphyritic, the phenocrysts consisting of zoned basic plagioclase and clinopyroxene. The plagioclase frequently exhibits reversed zoning, the core being more sodic. On several unzoned crystals the composition was found to be labradorite An_{60}. The composition of the pyroxene phenocrysts could not be determined accurately but refractive index measurements were comparable with those of diopsidic

augite. Phenocrysts of lamprobolite occur in patches throughout the rock. The groundmass is aphanitic and consists dominantly of fine-grained, strained plagioclase. The refractive index of this plagioclase indicates a composition of sodic oligoclase and it constitutes about 70 per cent of the rock. Accessory opaques (15%) occur as large grains in the matrix and anhedral apatite (2%) occurs as grains averaging 0.4 mm in diameter. Sample RH6T which overlies RH6 is of the same composition but is microporphyritic.

Rocks of the trachybasalt type crop out in the sea cliff at Ethel Beach (Sample FC7). This rock is porphyritic and consists of phenocrysts of olivine (10%) and pyroxene (10%) in a groundmass of opaques (30%), plagioclase (10%), pyroxene (30%) and glass (10%). The olivine is euhedral to subhedral and varies from 0.04 to 0.5 mm in diameter. It is commonly altered to a pale green chloritic mineral. Pyroxene phenocrysts which are normally zoned also occur and are commonly fractured and modified by magmatic corrosion. Unzoned crystals were found to be augite. They frequently contain exsolution bodies of titaniferous magnetite. The opaques occur in the groundmass as grains averaging 0.006 mm in diameter and as aggregates of grains. The pyroxene microlites are of similar dimensions and thus difficulty was experienced in determining their composition. The plagioclase occurs as laths varying in length from 0.09 mm to 0.006 mm. Determination of the composition of the plagioclase was not positive but extinction measurements on only a few grains indicated a composition of andesine (An_{35}). The groundmass has been altered to a bright green chloritic mineral. This chlorite was observed in fractures and vesicles where concentric banding was evident. One amygdule was found to contain an inner zone of dark brown chlorite and a nucleus of finely fibrous colourless (?)clay. Calcite also occurs in patches filling vesicles and fractures and is considered to be deuteric. This rock may correspond to the trachybasalt described by Campbell-Smith (1926) from Panchoran Bay (Waterfall). A chemical analysis is given by Campbell-Smith (p 53, Table III, No. 1).

Altered volcanic glass overlies the trachybasalt at Ethel Beach. In hand specimen this rock is massive and brick-red with an irregular surface. Microscopically it was found to contain secondary oolitic bodies and remnant phenocrysts of mafic minerals. The greater part of the rock consists of apparently amorphous or cryptocrystalline brick-red material which is considered to be iron-stained volcanic glass. This glass does not show any flow banding. Irregular cavities occur throughout the rock and in places oolitic red and buff coloured material occurs. Altered rock fragments have acted as nuclei for the deposition of the secondary material in some cases. Remnant phenocrysts of euhedral volcanic minerals occur sporadically throughout the rock. They are up to 0.2 mm in length and have been altered, possibly by weathering. The phenocrysts are not iron-stained.

At an elevation between 200 and 400 feet above sea-level volcanic rocks of the lower series crop out on the inland cliffs and terraces in several areas and samples were examined from Flying-Fish Cove

(Samples FC11, FC11A, FC12B, FC12T), Ross Hill Tank (GW3) on the east coast, and Sydney's Dale (WC2) on the west coast. These rocks consist of andesite, basalt and basalt glass.

Andesite was observed in the cliff at Flying Fish Cove (Sample FC12T) in an outcrop extending between two normal faults at an elevation of approximately 400 feet. Because of the faulting its relationship to the associated rocks is uncertain but it directly overlies Eocene limestone. The rock is light grey in hand specimen and contains numerous white phenocrysts and fine veins of calcite-filled fractures. It is extensively altered. The major constituents are plagioclase (60%), opaques (20%) and calcite (20%). The plagioclase occurs as laths, the average length of which is 0.2 mm, and as interstitial grains as small as 0.002 mm. The composition of the coarser plagioclase is andesine, An_{60}. The opaques are considered to be magnetite and occur as grains associated with the plagioclase and as needles in patches of carbonate. Calcite occurs in three main forms, as a vein mineral, in large patches filling vesicles and replacing feldspar laths. It is considered that the carbonate formation represents an alteration resulting from the action of lime-rich ground waters but it is also possible that some of the carbonate was incorporated during the molten stage of the lava.

The andesite from Sydney's Dale (Sample WC2) is fresh and differs from the andesites of the east coast in having a pronounced subophitic texture. The elevation of this sample locality is estimated to be 200 feet. The rock is dark grey and massive in hand specimen and consists essentially of olivine, labradorite, augite and opaques, in a groundmass of andesine laths. Secondary calcite occurs in some parts of the rock. The olivine occurs as anhedral grains and has been extensively corroded and altered to serpentine. It constitutes about 5 per cent of the rock and fragments up to 0.075 mm are present. The pyroxene, which by colour and 2V was determined to be titan-augite, constitutes 20 per cent of the rock. Subophitic intergrowths of feldspar have replaced about 50 per cent of the pyroxene crystals. Labradorite phenocrysts constitute about 5 per cent of the rock. They average 1.55 mm in length and are commonly zoned. As in the case of the andesite from Dolly Beach, the zoning is reversed. Magmatically corroded opaque grains (10%) are common and are uniformly disseminated throughout the rock. They are considered to magnetite and/or ilmenite. The grain size varies from 0.075 to 0.003 mm, the average being 0.063 mm. Anhedral apatite crystals (2%) are associated with the mafic constituents and average 0.033 mm in diameter. The groundmass consists of interlocking laths of andesine of composition An_{60}. These laths show flow layering and are frequently deformed and fractured. They constitute about 40 per cent of the rock and average 0.184 mm in length.

Basalt was observed at Flying Fish Cove in the inland cliff at about 400 feet above sea level and at Ross Hill Tank at a reduced level of 320 feet. Three specimens from Flying Fish Cove were examined. Sample FC11A, like the andesite of sample FC12T, was taken from an outcrop between the faults x-x, y-y (Andrews (1900)). It is dark grey and

massive. Petrological examination indicates that this rock is an altered, porphyritic olivine basalt, consisting essentially of phenocrysts of olivine and pyroxene in an aphanitic groundmass of feldspar, opaques, pyroxene and glass. The olivine is considerably altered forming a green serpentiniferous mineral. It constitutes about 10 per cent of the rock. Pyroxene phenocrysts are euhedral and rhomb-shaped or tabular. Their composition is that of augite and they average 0.24 mm in diameter. Plagioclase phenocrysts are rare and only one grain was observed which could be used for extinction angle measurements. This was found to be acid labradorite in composition. The groundmass is aphanitic. Opaques (25%) occur as interstitial grains and as fine acicular crystals in the volcanic glass. Fine-grained pyroxene of indeterminate composition constitutes about 30 per cent of the rock and volcanic glass accounts for another 20 per cent. In addition to the serpentiniferous material forming after olivine a bottle green chloritic mineral occurs in spherical bodies approximately 0.20 mm in diameter. These bodies are either vesicle fillings or altered mafic minerals. The chlorite comprises approximately 15 per cent of the rock.

Sample FC11 overlies FC11A and is also a porphyritic basalt but contains no olivine. It consists essentially of phenocrysts of plagioclase (labradorite) and pyroxene (augite) in a much altered groundmass of plagioclase, glass, opaques and chlorite. It has been extensively altered and now contains large masses of secondary calcite. The alteration has affected both phenocrysts and groundmass. The grain size of the carbonate is generally less than 0.006 mm but occasional grains up to 0.01 mm were observed. The larger masses contain areas up to 0.2 mm in optical continuity.

Basalt was also sampled from the base of the inland cliff at Ross Hill Tank. This volcanic flow is interbedded in carbonate rocks and its upper surface gives rise to a series of fresh water springs which were once used as a source of domestic water. The basalt (Sample GW3) has a reduced level of about 320 feet. The rock is dark grey and massive and is porphyritic. Microscopically it was found to consist of an aphanitic groundmass of plagioclase, of composition calcic andesine to sodic labradorite, and pyroxene and containing remnant phenocrysts now consisting of rusty brown nontronite. The plagioclase occurs mainly as fine laths and as interstitial, non-granular material in the groundmass. The composition of the plagioclase was determined by extinction angle measurements on albite twins but owing to the fine grain size (the average length is 0.09 mm) its determination could only be stated between the limits An_{38} to An_{50}. The plagioclase constitutes about 40 per cent of the rock. The pyroxene is granular and tabular and averages 0.025 mm in grain size. It constitutes about 30 per cent of the rock, and is a clinopyroxene of 2V less than 30^0. This is considered to be pigeonite. Opaque grains (15%) are disseminated throughout the rock. These are considered to be magnetite and occur as anhedral grains and acicular crystals. The microphenocrysts are polygonal in form and now consist of a clay mineral which is commonly stained with concentric bands of iron oxides. This was identified by x-ray diffraction

as nontronite and comprises about 10 per cent of the rock. The average diameter of the altered phenocrysts is 0.23 mm. The rock also contains amygdules which are filled with nontronite and calcite. Fractures containing secondary calcite are also common.

Basalt glass was observed in the cliff at Flying Fish Cove (Sample FC12B) overlying the saturated basalt (FC11). In hand specimen the rock is black and vitreous and in thin section was found to consist of light brown glass and coarse crystals of bytownite, augite and opaques (Plate 9A). The glass (85%) is cryptocrystalline or amorphous and occurs in globular masses separated by fine fractures. Small laths of plagioclase are dispersed throughout the glass and these vary in length from 0.02 to 0.3 mm. In addition to the microlites, phenocrysts of bytownite (8%) were observed in patches. These phenocrysts are fractured and interpenetrate and are commonly associated with pyroxene. They average 1.5 mm in length. The pyroxene (5%) is augite and is subidiomorphic. Coarse opaque crystals (2%) were also observed. There is some evidence of magmatic corrosion of the phenocrysts. Flow layering of the glass and microlites is also evident in some sections of the rock.

The volcanic rocks of basaltic compostion from Flying Fish Cove are probably representatives of the last phase of volcanism in the lower (Eocene) series. However as this area shows evidence of extensive faulting the exact stratigraphic relationship of these samples is somewhat obscure.

7.4 The Lower Carbonate Rocks

Carbonate rocks of the lower series crop out in association with the volcanics on the east and west coasts of the island. Several samples were examined petrologically and two were submitted to Dr N. H. Ludbrook of the S. A. Government Department of Mines for palaeontological examination.

The lowest carbonate rocks examined were those from the sea cliff at Flying Fish Cove and are represented by Samples FC8A and P35. These limestones were taken from outcrop $^1/_4$ mile east of Smith Point. They consist of dense yellow foraminiferal coquinoid limestone of the lagoonal facies. They contain 30 to 40 per cent calcareous mud and the remainder consists of whole unsorted foraminifera. The presence of heterostegina saipanensis indicates a shallow water environment (Cole, W. S.[a] (1963) p 751). The limestone lacks planktonic forms indicating an environment insulated from the open sea. The distinctive yellow coloration of these limestones is presumably the result of weathering or volcanic contamination.

Interbedded with this limestone is a tuffaceous limestone composed mainly of well sorted detrital calcite grains and calcitic mud and layers containing volcanic debris (Sample FC7A). Some layers contain foraminiferal tests varying in width from 0.13 mm to 2 cm. These are thin and constitute no more than 5 per cent of the rock. The tuffaceous layers consist of calcite (50%) and rounded masses of opaque minerals and a

(a) This reference appears in the bibliography of Appendix A.

fibrous radiating mineral, possibly chlorite. The opaque minerals are variable in grain size, the maximum being 0.6 mm in diameter and the minimum 0.02 mm. Obvious sorting of the volcanic detritus is suggestive of a pyroclastic origin or graded bedding. The calcite shows a corresponding variation in grain size but recrystallization of the carbonate may have altered the original carbonate crystallites to some degree. The contacts between successive beds are sharp, sutured and commonly stained dark brown. Some of the apparent contacts are considered to be microstylolites.

Sample P51 is from the yellow limestone cropping out in the inland cliff at Flying Fish Cove at an elevation of about 300 feet. It is therefore considered to be equivalent to Andrews' limestone "B" (Andrews 1900, p 272) and since the colour, fauna and texture are similar to that of Sample P35. It is also considered to be of the lagoonal facies.

Towards the upper part of the sequence, at an elevation of approximately 400 feet, a brick red carbonate rock was observed (Sample FC14). It occurs on the eastern (downthrow) side of the fault x-x (Andrews 1900, Fig. 2A) and underlies the Miocene orbitoidal limestone. This rock is considered to correspond to the "Batoe Merah" member described by Andrews (1900, p 277). It is an iron-stained limestone consisting of about 70 per cent calcite with about 30 per cent volcanic debris. The calcite is heavily stained with iron oxides and occurs in aggregates of grains about 0.23 mm in diameter separated by veinlets of less stained carbonate in which the grains are larger. The individual grains of the stained carbonate could not be distinguished but the grain size of the vein carbonate was found to average 0.25 mm. Some patches of clear carbonate associated with altered volcanic fragments consist of aggregates of grains averaging 0.2 mm in diameter. Patches of green nontronite (25%) with associated opaque grains (5%) occur throughout the rock. The nontronite appears to be an alteration of mafic minerals of volcanic origin which were probably included in the sediment prior to consolidation.

7.5 The Upper Volcanic Rocks

Volcanic rocks of the upper series, which are interbedded with Miocene carbonate rocks, crop out at a number of localities on the inland cliffs and on the central plateau and hills. In many of these localities the rocks have been extensively altered by phosphatization obscuring their original identity but where separate occurrences of fresh volcanics were observed these were sampled and examined petrologically. In addition one sample (RH3) was examined by electron probe microanalysis (Section 9) to determine the elemental distribution and to provide data on the mechanism of phosphatization.

The three samples examined petrologically were from localities FC3, EP3 and RH3. These rocks are limburgites. Sample FC3 crops out on the inland terrace between Drumsite and the north coast of the island and, although faulting is evident in this area, it is in association and probably interbedded with the Miocene orbitoidal limestone at an elevation of approximately 600 feet. Sample EP3 occurs on the west coast of the island

on the terrace to the east of Winifred Beach. This rock crops out extensively and boulders up to 15 feet in diameter were observed some of which exhibit marked radial jointing (Plate 4B). The radial jointing is thought to be indicative of submarine volcanism or the ejection of large volcanic bombs which were partially lithified before impact.

Sample RH3 outcrops poorly . Small fragments were observed on the southern side of Ross Hill, at an elevation of about 1000 feet, extending over what is thought to be a strike length of more than 300 yards in a southerly direction.

The limburgites consist mainly of phenocrysts of olivine in a groundmass of tabular crystals of pyroxene and glass. Opaque minerals are also present. Sample RH3 was examined in most detail (Plate 9C). In this rock the olivine phenocrysts are euhedral and constitute approximately 13 per cent. The 2V (75-90^0) indicates a composition of forsterite. The grain size of the phenocrysts varies from 1.25 to 0.01 mm with an average of 0.37 mm. They are commonly fractured and alteration to biotite (5%) has proceeded along cleavage partings in some grains. Clinopyroxene constitutes approximately 50 per cent of the rock, but its composition could not be determined positively by optical methods. Some of the pyroxene is zoned, the zoning being particularly evident on (001) sections, and the extinction is slightly undulose. However electron probe studies revealed an appreciable lime content indicating that this mineral is augite. The crystals vary in length from 0.002 to 0.32 mm with an average of 0.076 mm. Glass constitutes 20 per cent of the rock and occurs interstitially between the pyroxene microlites and surrounding the olivine phenocrysts. The refractive index of the glass is between 1.5400 and 1.5500 which, according to the determinative curves of Kittleman (1963), corresponds to a silica content of 60 per cent. The remainder is essentially alumina.[a] Granular opaque minerals determined by electron probe microanalysis to be chromite and ilmenite account for a further 5 per cent of the rock. These opaque minerals are angular and mainly, but not exclusively, associated with the groundmass. The average grain size is 0.036 mm. In addition, acicular ilmenite crystals occur in arborescent aggregates in some of the volcanic glass. A white clay mineral occurring in amygdules proved to be nontronite.

Sample FC3 differs from RH3 in that it contains more opaques and less pyroxene. Some iddingsite was observed in this rock surrounding the olivine crystals. Magmatic resorption of the olivine phenocrysts is also evident.

Sample EP3, like FC3, contains iddingsite. In this sample the pyroxene has a small 2V and is probably pigeonitic. Amygdules were observed in this specimen approximately 0.12 mm in diameter. They are lined firstly by a zone of cloudy volcanic glass containing a number of acicular crystals which could not be positively identified and secondly by a zone of fibrous zeolite. The zeolite which is optically similar to heulandite constitutes approximately 5 per cent of the rock.

(a) See Section 9.

7.6 The Upper Carbonate Rocks

The carbonate rocks of the upper series were sampled from a number of localities distributed on the central plateau and hills and the inland cliffs and terraces. The majority of these samples were examined in the laboratory. Those containing or thought to contain fossils were submitted to Dr. N. H. Ludbrook of the South Australian Government Department of Mines for palaeontological description. For examination of the microfossils and for petrological description many of these samples were thin sectioned. X-ray diffraction was used for the identification of the carbonate minerals in many of the samples and some of those found to contain dolomite were prepared for microscopic examination and stained with alizarin red S dye to determine the distribution of the carbonate minerals.

The majority of the carbonate rocks of the upper series were found to consist entirely of calcite. However dolomite was detected in samples taken from the top of the inland cliffs in many places and from the carbonate rock in the central depressed area of the plateau. The rocks underlying and forming the pinnacles in the phosphate fields at South Point and Field 5A, Phosphate Hill, were also found to be dolomite and loose, unconsolidated dolomite was observed in the inland cliff near Ross Hill Tank. Aragonite was detected in the carbonate rock on the Egeria Point peninsular. (The Post Tertiary recently raised reef at Flying Fish Cove was also found to contain a considerable amount of aragonite).

Incrustate, particulate and metasomatic carbonate rocks (Schlanger, 1964) were identified from the upper series.

Incrustate carbonate rocks crop out on the inland cliffs and on the edges of the inland terraces. The samples of this type which were examined petrologically are P12 and P40, near the railway line 3-4 miles north of South Point, P21 one mile north-west of Middle Point, P53 $^{1}/_{2}$ mile north of Ross Hill Tank, P54 $^{3}/_{4}$ mile north of Ross Hill and P101 on the Settlement – Drumsite roadway. The elevation of these localities is between 300 and 600 feet. These rocks consist dominantly of calcite but in some samples dolomite was detected in minor quantities. The incrustate limestones which were examined petrologically are of the algal-foraminiferal and coral-algal-foraminiferal sub-groups. They characteristically exhibit a crust-like texture and have formed largely from the in situ growth of the fauna. Tests of other varieties of foraminifera are often present in minor amounts in cavities between the crustose forms. Calcareous mud is also subordinate or absent. The fauna of these limestones is that normally found in the reef-wall facies and includes such foraminifera as species of Carpentaria together with lithothamnion algae and miliolids. Sample P40 consists essentially of incrustate forms but unlike the other samples is brecciated and contains more lime mud. This sample is therefore considered to be of a fore-reef transitional facies. The others are classified on the basis of fauna, texture and mineralogy in the reef-wall facies.

The remaining samples of fossiliferous limestones from the upper series are of the particulate class and of the lagoonal facies. It is

reported[1] that planktonic foraminifera are not present in any of these limestones and thus it is concluded that they were formed in lagoons with restricted access to the open sea. Limestones of the coquinite, paracoquinite, microparacoquinite, coquinoid and breccia types were identified.

Sample P13, the orbitoidal limestone of Jones and Chapman (1900), is of the coquinite type and contains abundant foraminifera including large lepidocyclina. This rock contains less than 25 per cent mud matrix. The presence of other foraminifera such as Borelis pygmaeus indicates a lagoonal facies of depths less than 40 fathoms (Cole, 1963).

Samples P45 and P52 are algal-foraminiferal paracoquinites. They consist of poorly sorted fossils in a mud matrix which constitutes between 30 and 40 per cent of the rocks. Microparacoquinites are more common and are represented by Samples P4, P6, P26, P30 and P33. They contain many species of foraminifera together with miliolids and a mud matrix constituting from 25 to 50 per cent of the rock.

Samples P9, P31, P37 and P53 are classified as coquinoids and consist of a mud matrix (50-70%) and whole unsorted foraminifera, molluscan moulds and algae. The foraminifera are benthonic forms.

Two limestone breccias were found, Samples P28 and P48. These consist of fragments of algae and foraminifera in a mud matrix comprising about 50 per cent of the rock. Sample P48 contains fragments of incrustate foraminifera, together with shallow water benthonic forms and is therefore considered to have formed close to the reef-wall.

Carbonate rocks of the metasomatic class[2] (Schlanger, 1964) are common in the upper series and are of the dolomitic and phosphatic types.

Recrystallized dolomitic limestone outcrops as massive pinnacles in the central depressed area of the upper plateau at an elevation between 650 and 700 feet. Sample RL3 is of this type. Calcite is the dominant constituent comprising about 80 per cent of the rock. It occurs in two forms; as zones of fine crystals forming a mosaic in which individual crystals are not differentiated, and as large crystals, of a second generation, which cement the zones of finer carbonate. The larger crystals are up to 0.64 mm in diameter. One fragment of a fossil was observed in a zone of fine calcite but the rock is otherwise devoid of fossils. Dolomite also occurs in two forms; as patches of equidimensional, interlocking grains averaging 0.11 mm in diameter, and as overgrowths on the vein calcite. The dolomite of the first type is commonly cloudy and some grains contain a cloudy nucleus approximately 0.04 mm in diameter. In yet other grains of

---

1. Personal communication, N.H. Ludbrook.

2. The term metasomatism as used by Schlanger (1964) and in this thesis is of the general sense of replacement. The metasomatism is supergene and the use of the term is not to imply elevated temperatures.

dolomite a nucleus of calcite was observed but in most cases the dolomite did not appear to be deposited around a nucleus of different composition. The paragenesis of this rock appears to be:

1. the deposition of fine calcite mud with some fossil remains,
2. partial dolomitization leading to the formation of patches of cloudy dolomite of fine grain size and
3. a second generation of calcite in fractures and cavities forming coarse crystals and the contemporaneous crystallization of dolomite overgrowths on the calcite rhombs.

Schlanger (1964) describes similar dolomitic sediments from the Alifan limestone of Guam and suggests that the textural evolution indicates "post-depositional uplift and solution, post-solution submergence and dolomitization and finally post-dolomitization emergence and cementation" (p D16). The dolomitized sediment from Christmas Island is not strictly comparable in texture and paragenesis with that described by Schlanger. However it is suggested that emergence and submergence in a restricted shallow water environment is the most likely condition for the formation of this rock. The conditions thought to be responsible for the dolomitization are further discussed in Section 11.

Some of the dolomite from the old limestone quarry at South Point also appears to be a metasomatic replacement of fossiliferous limestone. One sample examined petrologically (Sample SP2B) was found to exhibit an incrustate texture and contain some algal fragments. However dolomite was the only carbonate mineral detected in this rock. It is also extensively replaced by irregular veins of apatite which are massive and crustiform banded.

A similar crystalline dolomite rock was sampled from a railway cutting approximately $1\frac{3}{4}$ miles north of South Point, at an elevation of about 650 feet (Sample SP8A). This rock consists entirely of rhombic sections of dolomite averaging 0.195 mm in diameter. The rhombic crystals commonly show growth zoning. Replacement of the crystalline dolomite by white homogenous veins is common. The rock contains minor apatite and this occurs in the veinstone. Another sample from this locality which is a uniform fine-grained carbonate rock (Sample SP8B) was found to consist of calcite with accessory apatite. In thin section this rock is homogeneous and most of the calcite and apatite is less than 0.001 mm in grain size. Some calcite (approximately 20%) is coarser and has an average grain size of 0.006 mm. The texture of this rock is suggestive of chemical precipitation and fossil fragments are absent. It is possible that the apatite is likewise a chemical precipitate, as the rock is not veined and there is no evidence of metasomatism. Apatite is thought to constitute less than 5 per cent of the rock. Unfortunately it was not possible to determine the relationship of the phosphatic limestone and the crystalline dolomite.

Fine-grained, homogeneous dolomite was obtained from outcrop on the top of the inland cliff approximately 1 mile north of Jones Point (Sample EP1). The grain size of this dolomite is less than 0.001 mm but there is some suggestion of bedding. A vein of brown calcite occurs in one section of this rock which shows comb-structure on the margins indicating it to be of the cavity-filling variety. The cause of the brown coloration is not known but is thought to be due to the presence of iron. This rock is also considered to have originated from chemical precipitation.

Detrital dolomitic sediments, cross-bedded in places, were observed in the carbonate rocks forming the pinnacles of the phosphate fields at South Point and in Field 5A at Phosphate Hill. Graded bedding was evident in detrital dolomite in the old limestone quarry at South Point (Sample SP2A). Layers of coarse dolomite grains occur at irregular intervals and are spaced between 6.8 mm to 0.55 mm apart. These layers are separated by progressively finer dolomite, the grain size varying from 0.025 mm to less than 0.001 mm. The contact between the coarse and fine layers is characteristically sharp (Plate 10B).

The cross-bedded detrital dolomite from Field 5A, Phosphate Hill, contains some quartz (Sample PH2). Dolomite was also found to constitute the massive carbonate rock outcrop on the edge of the inland cliff adjacent to the golf course (Sample PH11). The elevation of this outcrop is approximately 600 feet. The dolomite is veined with calcite. A similar occurrence approximately $\frac{1}{2}$ mile north of Ross Hill at an elevation of 800 feet (Sample RH5) was also found to contain dolomite but calcite forms the bulk of this rock. Similar material was observed on the Tom's Ridge track (Sample P19). In this case molluscan moulds are plentiful.

Unconsolidated, detrital dolomite was also observed in the inland cliff near Ross Hill Tank at an elevation between 500 and 600 feet. This dolomite is partially lateritized forming goethite. The exposed thickness is about 50 feet and it is overlain by younger limestone (Plate 5B).

Phosphate metasomatism of the upper carbonate rocks was observed in samples from the old limestone quarry at South Point. One such sample (SP3) was found to be a partially recrystallized detrital dolomite (Plate 10C). Approximately 50 per cent of the dolomite is fine-grained or sub-microscopic and is bedded. The remainder is recrystallized forming grains averaging approximately 0.045 mm in diameter. Some algal fragments are preserved in the rock. Replacement of the unaltered dolomite by apatite was evident but this replacement was found to be restricted to the finer carbonate. It is considered that the recrystallization of the dolomite reduced the permeability, preventing the access of phosphatic solutions and the coarser grain size decreased the amenability to phosphatic replacement. The lack of apatite in the recrystallized part of this specimen indicates that this mineral has not been deposited contemporaneously with the dolomite and is a late stage mineral. Some crustiform

banded apatite occurs in cavities but most of this mineral was found replacing the carbonate.

7.7 The Post-Tertiary Carbonate Rocks

The post-Tertiary carbonate rocks comprise the shore cliff and terrace surrounding most of the island at an elevation of about 60 feet and the fringing reef. These limestones consist of calcite and aragonite. Sample P36, taken from the shore terrace at Rocky Point, consists of approximately equal quantities of poorly crystallized calcite and aragonite. This sample contains incrustate foraminifera (Homotrema) and planktonic foraminifera. Planktonic fauna is absent from the Tertiary carbonate rocks.

7.8 The Phosphate Samples

The phosphate samples examined mineralogically were selected from the channel and grab samples of the present workings and the auger and rock samples obtained in undeveloped areas. They are generally of two textural types, the first being friable and earthy or granular (incoherent phosphate) and the second being massive (coherent phosphate).

Mineralogical examination was carried out principally by x-ray diffraction techniques. Differential thermal analysis (DTA), thermo gravimetric analysis (TGA), complete and partial chemical analysis and electron probe microanalysis (EPMA) were carried out on certain selected samples for confirmation of the mineralogical identification and to provide additional data for the utilization and studies of ore genesis. Results of these additional techniques are included in Sections 8, 9 and 10 but reference is also made to these studies in this section. Owing to the sub-microscopic grain size of most of the phosphate, the use of optical microscopy was of limited value with these materials. Refractive index determinations using oil immersion techniques were also of little value, owing to the high refractive index of the iron-aluminium phosphates and iron hydroxides.

Petrological examination of thin sections of the phosphate was restricted to the massive varieties, but even here the sub-microscopic nature of much of the phosphate made petrological examination difficult. Where possible material was extracted from the samples being described petrographically and identified by x-ray diffraction.

7.8.1 General Statement

All the samples of soil obtained from the upper plateau were found to contain phosphate minerals. The main species identified were apatite (carbonate-fluor-hydroxy-apatite – approx. $Ca_5(PO_4, CO_3)_3(F, OH)$), crandallite (theoretically $CaAl_3(PO_4)_2(OH)_5H_2O$), millisite (theoretically $(Na, K)CaAl_6(PO_4)_4(OH)_9 . 3H_2O$) and barrandite ($(Fe, Al)PO_4 . 2H_2O$).

Apatite is the principal mineral of the phosphate fields currently being worked and it is overlain by an overburden of varying thickness consisting of crandallite and/or millisite. The transitional zone consists of a mixture of the crandallite-millisite and apatite.

The samples of soil obtained from the unworked areas and where not associated with apatite (as reported by the British Phosphate Commissioners' drilling results 1957-58) were also found to contain crandallite and/or millisite together with goethite ($Fe(OH)_3$) and/or boehmite ($Al_2O_3.H_2O$). Accessory clays (kaolin and a 14A mineral) were also detected in some of these samples and quartz was detected in one sample. The material obtained by hand-auger was frequently contaminated with carbonate minerals which were present in the soil profile as fragments of the bedrock and as floaters.

Barrandite was identified in the massive phosphate rocks which crop out as boulders in several localities on the upper plateau. The barrandite is commonly the dominant constituent of such samples but may be associated with crandallite, montgomeryite ($Ca_4Al_5(PO_4)_6(OH)_5.11H_2O$) and chromite. The soil profile formed on the barrandite was found to contain crandallite as the dominant constituent together with minor goethite and accessory kaolin, quartz and a 14A mineral.

Wavellite ($Al_3(PO_4)_2(OH)_3.5H_2O$) was observed in one sample from the West Quarry workings submitted subsequent to the author's field investigations. This is a minor constituent in a sample consisting dominantly of crandallite. The mode of occurrence of this material is not clear but is thought to be of late stage development occurring in a vertical joint in the apatite or carbonate bedrock.

7.8.2 The Phosphate Workings

Mineralogical examination of the channel samples taken from the phosphate workings at Fields 4, 5A and 5EF, Phosphate Hill, and East Quarry, North-West Quarry, and West Quarry at South Point were carried out. Twenty-five grab samples submitted by the British Phosphate Commissioners prior to the field investigations by the author were also examined mineralogically. These were taken from the East, Main, West, No. 8, Old No. 9, New No. 9, and North-West quarries at South Point, and from Fields 4 and 5A at Phosphate Hill. Samples of pebble phosphate from Field 5A, Phosphate Hill, and from South Point and samples of massive phosphate from the West Quarry at South Point were also examined.

Field 4, Phosphate Hill

Two channel samples of the phosphate profile in Field 4 were cut and examined mineralogically. The first, taken from the western border of the field, was designed to include the transition from overburden into apatite. The profile in this face was irregular and interrupted by massive white pinnacles of carbonate rock. The junction between the overburden and the apatite tends to parallel the surface of the limestone, rising

over pinnacles and becoming deeper in sections where limestone was not visible. The junction between the overburden and apatite was marked by a thin zone of mottled brown and white phosphate. At the point of sampling the overburden was approximately 8 feet thick. The mineralogy is as follows.

Depth ft	Description
0- 2	Crandallite dominant,[(a)] millisite and boehmite accessory
2- 8	Crandallite dominant, boehmite sub-dominant, millisite accessory
8- 9	Apatite dominant, crandallite accessory
9-12	Apatite

Samples from 2 to 4 feet and 11 to 12 feet were submitted for chemical analysis. The results, together with modal computations, are included in Tables 1 and 2.

A profile exposed on the eastern side of the quarry on the working face (Plate 6B) was also examined. Here the overburden had been stripped to an average depth of 5 feet. The profile was 12 feet deep at the point of sampling. The first 6 feet were found to consist of apatite with accessory crandallite and below this depth the profile consists entirely of apatite.

Field 5A, Phosphate Hill

One channel sample was cut from the western face of this quarry. The sample was taken from approximately 10 feet below the top of the exposed face and extended down vertically for 16 feet, passing from overburden into white phosphate. This profile was found to contain crandallite and millisite in the upper section and apatite at the base. The intermediate section consists of mixtures of these minerals in varying proportions but the crandallite and millisite were found to maintain a fairly constant ratio.

Two grab samples of white phosphate taken from 40 to 45 feet below the working bench of the quarry were examined (Samples 16 and 17). The first is white and friable and the x-ray diffraction pattern indicated

---

(a) The abundance is estimated visually from the intensity of characteristic x-ray diffraction lines, referable to standards. The terminology is as follows:

Dominant:	greater than 50%
Co-dominant:	one of several equal major components
Sub-dominant:	50-20%
Accessory:	less than 20%

apatite as the only constituent. No secondary apatite was observed and neither dahllite nor carbonate minerals were detected. The second sample is massive and contains numerous small cavities. It is coated with light brown earthy crandallite. It is similar to the first in that it consists dominantly of homogeneous buff coloured collophane but fine bands of dahllite are common around cavities. These bands are approximately 0.01 mm thick. The crandallite constitutes about 5 per cent of the samples and is also sub-microscopic. Other grab samples taken from this quarry (Numbers 18 to 23) are similar.

Pebble phosphate, which occurs in a linear zone running in an east-west direction through this field, was also sampled and examined in the laboratory (Samples 15 and 22). Sample 15 consists of irregular, sub-rounded pebbles averaging 1 cm in diameter. They were found to consist essentially of apatite and a few pebbles contain an outer shell of black manganiferous apatite. Secondary crandallite and apatite oolites, 0.65 mm to 1 mm in diameter, occur in cavities in the pebbles. The majority of the pebbles consist of collophane with minor bands of dahllite. No carbonate minerals were detected.

Feild 5EF, Phosphate Hill

At the time of inspection the workings at Field 5EF were not very advanced. Overburden stripping was in progress and approximately $^1/_2$ acre had been worked out. The average depth of the apatite was about 6 feet. Mineralogical examination of a channel sample cut from the western face indicated that apatite, crandallite and millisite were co-dominant constituents in the upper part of the profile which passed into apatite with depth.

East Quarry, South Point

The East Quarry was being advanced to the west along a north-south face, the height of whichaveraged 40 feet. The face appeared to contain little iron/aluminium phosphate. However approximately 10 feet of overburden had been stripped from this quarry prior to mining. Small zones, possibly joint cavities, containing rusty brown phosphate (crandallite) were observed, and these were found to occur sporadically to some considerable depth. Two channel samples were taken from the working face of this quarry approximately 100 yards apart. At the southern end the face was about 40 feet high and the top 2 feet were not sampled. At the northern end the face was about 20 feet high. The southern channel sample consisted dominantly of crandallite and millisite in the upper part which graded into apatite with depth. The northern sample consisted dominantly of apatite but millisite was detected between 6 and 12 feet from the surface.

Massive white to buff coloured phosphate from this quarry was examined mineralogically and petrologically and found to consist of collophane and secondary dahllite. The dahllite which constitutes about 5 per cent of

the sample occurs in crustiform bands lining cavities. Oolites of apatite, approximately 0.3 mm in diameter, were observed in cavities.

West Quarry, South Point

When first examined in June, 1963, the West Quarry was in the early stages of development. The phosphate was being won by the conventional "Phosphate Raising" method leaving the massive carbonate rock pinnacles in situ. During the second inspection in October, 1964, the quarry was being worked in benches to a depth of about 100 feet, the carbonate pinnacles having been removed revealing extensive apatite deposits beneath.

Large blocks of massive and crustiform banded apatite, varying in colour from white to light blue and brick red, were also observed. Sample SP5 is of this type. It consists of irregularly banded white and red apatite with a resinous variety (nauruite) occurring in cavities. X-ray diffraction examination of this material did not reveal any differences in mineralogy. A chemical and modal analysis of this sample is included in Table 15.

During the first inspection two channel samples were taken from the working face, the first to a depth of 20 feet and the second to 10 feet. Approximately 5 feet of overburden had been stripped from this area prior to mining. The channel samples were found to consist entirely of apatite.

A sample of banded apatite from the lower levels of West Quarry was submitted subsequent to the second visit. This rock is massive and varies in colour from dark brown to white. Most of the rock in hand specimen appears to be fine-grained or granular and well sorted. Irregular porous zones which appear to be detrital were observed in places and microfaulting is evident. Approximately 95 per cent of the rock consists of submicroscopic apatite. The bedding features are accentuated by the inclusion of carbonaceous material which in its distribution shows evidence of graded bedding. The width of the beds varies from more than 1 cm to less than 1 mm. The porous irregular zones appear to be organic and it has been suggested[(a)] that these may be remnants of green algae. The "granular" layers consist of cylindrical organic bodies which could not be positively identified in the thin section[(b)]. The spherical sections of these bodies

---

(a) Personal communication Mr W. Harris, S.A. Government Department of Mines.

(b) The author is indebted to Dr N.H. Ludbrook and Mr W. Harris of the S.A. Government Department of Mines for brief examination of this specimen.

vary from 0.16 to 0.30 mm in diameter and contain dendritic markings. Rectangular sections average 0.4 mm in length and frequently contain two horizontal markings parallel to the long dimension. These organic bodies are thought to be seeds[a]. They now consist of apatite which optically appears amorphous and commonly contain numerous opaque flecks of carbonaceous matter. The apatite of the markings is weakly birefringent. The matrix is dahllite, deposited in fine bands around the organic particles.

This rock was not observed in outcrop. It is obviously sedimentary and much of the apatite is probably the result of precipitation from an aqueous solution or from the coagulation of colloids. The presence of (?)green algae and other possible plant material is suggestive of a lagoonal rather than a marine facies. It may be the result of deposition of phosphate in a restricted lagoon, the phosphate having been derived from adjacent guano bearing land.

North-West Quarry, South Point

At the time of the first inspection in July 1963, the North-West Quarry was being developed in a southerly direction along a face striking 245°. The height of the face was variable but averaged 10 feet. Overburden appeared to be more abundant in this than at East Quarry and a thickness of 9 feet was estimated in one exposure. The apatite is generally friable and oolitic. Patches of crustiform banded apatite (nauruite) occur throughout the profile. Mineralogical examination of a channel sample of the working face indicated that the upper 4 feet consist dominantly of apatite with accessory crandallite and millisite. Below this depth the profile consists entirely of apatite.

A profile of the overburden about 5 feet thick was exposed in a cutting along the access road to this quarry. A channel sample taken approximately 150 yards from the working face is of light brown earthy phosphate without visible variation. Mineralogical examination revealed that this material consists of millisite and apatite, the former being dominant in the upper 4 feet.

Chemical and modal analyses of a sample from North-West Quarry (depth, 12 ft) are included in Table 9.

7.8.3 The Worked Out Phosphate Quarries

Samples of phosphate from the older sections of East Quarry and No. 8 and 9 Quarries at South Point which were submitted prior to field inspection in July 1963 were also examined. These samples consisted of oolitic, earthy, massive crustiform banded and brecciated apatite. Samples of pebble phosphate from the southern end of the South Point fields and blue

---

(a) Personal communication Mr W. Harris.

phosphate rock were also submitted. The oolitic, massive and crustiform banded varieties are similar to those described above. Phosphate breccia was submitted from the old section of the East Quarry. The samples were taken at a depth of 40 feet from the top of the working face. The breccia fragments consist of both massive and colloform banded apatite. The colour varies from dark brown to white and alternate dark and light banding of some fragments is common. The fragments vary in size, the maximum length being 1.7 mm and the average approximately 0.33 mm. Collophane is the main constituent and makes up approximately 70 per cent of the sample. Dahllite makes up 15 per cent and birefringent apatite a further 13 per cent. The remaining 2 per cent consists of calcite and/or dolomite which occurs as individual crystals about 0.03 mm in diameter and as aggregates of fine crystals. The carbonate occurs within breccia fragments.

A sample of blue phosphate rock (Sample 7, Plate 11A) which was taken from the workings of Number 8 Quarry at a depth of 40 feet was also found to be a breccia. It varies considerably in colour. Most of the cement is white but some is khaki and red-brown. The colour variations are gradational. This sample was found by x-ray diffraction to consist dominantly of apatite. Small fragments of carbonate were extracted and identified as dolomite. In thin section the white phosphate was found to be opaque and is generally homogeneous. Fine bands of dahllite occur in some places surrounding cavities in the white phosphate. The dolomite fragments are cemented by apatite, principally dahllite. They consist of granular dolomite crystals frequently showing growth zoning. The apatite appears to be cementing the dolomite without obvious signs of replacement. Qualitative analysis of fragments of brick red apatite showed a greater quantity of iron and strontium than in the white phosphate.

The pebble phosphate from South Point is similar to that described above from Field 5A, Phosphate Hill.

7.8.4 The Unworked Areas

Phosphate samples were obtained from the unworked areas by hand auger and grab sampling. In many areas massive specimens of phosphate rock occur as scree and floaters and these were examined both mineralogically and petrographically. Some samples were also submitted for chemical analysis and the results are included in Section 8.

The massive samples were found to consist of three mineralogical types: (a) apatite, (b) barrandite and (c) crandallite. Pebbles and sub-rounded fragments of apatite occur in many areas and massive deposits of concretionary apatite occur on the end of Tom's Ridge (Sample MH7) and on the inland terrace below the phosphate workings at South Point (Sample SP1). Barrandite crops out as spheroidal boulders and was observed in samples from five localities on the upper plateau (Samples Ce1, Ce2, Ce9, MH9 and A13). Other "massive" samples were found to consist dominantly of crandallite, together with apatite, barrandite and goethite (Samples MH8, MH10, Ce3 and Ce6).

(a) Apatite

Most of the samples consisting of apatite occur as loose scree and are dispersed over the surface of many of the unworked phosphate fields. These samples are normally sub-rounded and are white, buff or brown in colour and crustiform banded or oolitic. They are thought to be nodules weathered from the underlying phosphate deposits or are floaters. They are commonly coated with, and are sometimes weathered to, crandallite.

The extensive deposit of massive phosphate rock cropping out on the end of Tom's Ridge also consists entirely of apatite. This material is crustiform banded, light to dark brown in transmitted light but white to buff in hand specimen. The apatite is fine, approximately 70 per cent being sub-microscopic; 25 per cent shows weak birefringence but without visible grain boundaries, and 5 per cent is fibrous and banded (dahllite). The fine crystals frequently occur in globular aggregates suggestive of precipitation from solution of aggregation from colloidal suspension. The crustiform banded texture, the mode of occurrence and grain size of this apatite are suggestive of deposition from ground water and it probably represents a spring deposit. A chemical and modal analysis of this material is included in Table 17, Section 8.

Similar massive apatite occurs on the terrace below the workings at South Point. This sample is impure however, containing a minor amount of dolomite. It also could be a spring deposit.

(b) Barrandite

Barrandite crops out at several localities on the plateau. It commonly occurs as spheroidal boulders which are dark brown or grey on the weathered surface. In some cases the rocks consist entirely of barrandite but not uncommonly crandallite is also present. Montgomeryite was detected in one sample of barrandite rock. Texturally, these rocks are either massive, brecciated, oolitic or crustiform banded. In the more massive samples, polygonal outlines of remnant igneous phenocrysts are discernible. Sample Cela (Plate 12, A to C) is one such sample. In hand specimen this consists of dark brown altered volcanic rock in which small prism shaped bodies are visible. The rock is extensively replaced by light green phosphate, the replacement having taken place initially along fractures. Microscopically, the rock was found to consist of fine-grained barrandite and accessory opaque grains. It is veined by secondary, pale coloured barrandite and light brown crandallite. Polygonal sections of remnant volcanic phenocrysts are common. In rare instances these phenocrysts contain a fine, fibrous chloritic mineral (Plate 12B). Small andhedral opaque grains were observed principally within the barrandite which has replaced the groundmass. The phosphatized phenocrysts are

relatively free of opaques although occasional large opaque grains were observed. The distribution of the fine opaque grains and the texture of the barrandite serves to outline the phenocrysts which were shown by electron probe microanalysis (Section 9) to be of essentially the same composition as the matrix. The electron probe microanalysis showed the opaque grains to consist mainly of chromite. However every grain examined was found to be surrounded by an outer rim of titanium phosphate. A secondary vein of light green barrandite occurs in this specimen replacing the phosphatized volcanic rock. This barrandite is crustiform banded and is similar in habit and anisotropism to dahllite. Parts of the central sections of this vein contain light brown crandallite, deposited after the formation of the barrandite vein. Numerous cavities which contain fine acicular crystals occur in the crandallite. These later crystals are optically similar to apatite but could not be positively identified because of the fine grain size.

A specimen of brecciated and oolitic barrandite rock was also examined from locality Ce1 (Sample 26). The breccia fragments are irregular in shape and are composed of sub-microscopic to fine-grained barrandite. The outlines of pre-existing volcanic minerals, now represented by lath and prism-shaped phosphate aggregates, are common within the breccia fragments. These fragments vary from 4.5 to 0.25 mm in length and constitute about 25 per cent of the rock. The breccia fragments are cemented by a light brown phosphatic matrix which also consists dominantly of barrandite. This barrandite is more homogeneous in texture and is optically isotropic. Oolitic barrandite is also common within the matrix. The oolites vary in diameter from 0.05 to 0.9 mm, the average being 0.32 mm.

A sample of brecciated barrandite rock cemented with crandallite was examined from locality Ce2. X-ray diffraction showed the breccia fragments to be barrandite and montgomeryite. Oolites with nuclei of barrandite and dark brown overgrowths of crandallite are set in a matrix of earthy brown crandallite. Cavities between the oolites commonly contain small prismatic crystals of apatite, in somecases in radiating aggregates. The paragenetic sequence appears to be (1) barrandite, (2) crandallite and (3) apatite. Hematite and goethite may also occur in the matrix of this rock, in association with crandallite, but neither of these minerals was positively identified.

(c) Crandallite

The "massive" samples consisting dominantly of crandallite resemble the barrandite rocks in outcrop. They typically consist of a fine-grained, earthy material and were found by x-ray diffraction to be dominantly crandallite with sub-dominant goethite. It is likely that they have formed by the weathering of barrandite but solid outcrop is rare in these areas which generally consist of light to dark brown soil.

The soil and phosphate profiles in many of the unworked areas were sampled to a limited depth by hand-auger. The samples so collected

were packed in core-boxes and subsequently examined in the laboratory by x-ray diffraction and in some cases by chemical and differential thermal analysis.

The auger samples taken from areas delineated as phosphate fields by the B. P. C. drilling programme of 1957-58 were numbers A3, A4, A10, A14, A19, A20 and A22. These samples were found to contain some apatite and in several profiles this mineral became more abundant in depth. Millisite and/or crandallite were also present in all the profiles. Samples A4 and A14 contain very little crandallite and in these cases the main iron-aluminium mineral is millisite. These samples were both taken from depressed areas of the central plateau which have poor drainage and become swampy after rain. Sample A10, the only one with no millisite, consists of crandallite and apatite and pebbles of apatite were encountered during the drilling. The remaining samples contain both crandallite and millisite in varying proportions but no systematic distribution of millisite and crandallite is apparent.

Auger samples of the soil in areas in which carbonate rocks are plentiful are represented by numbers A2, A6, A7, A8, A12 and A21. All these soils were found to contain some crandallite, and millisite was detected in Samples A7, A8 and A12. In some cases the samples contain boehmite and/or goethite. Kaolin was detected in two samples (A12 and A21) and accessory quartz in one (A21).

The soil profiles in areas of outcropping barrandite rock (numbers A11 and A13) were also examined. The soil is light to yellow brown and to the depth sampled showed no colour variation. These soils consist of crandallite with goethite and kaolin, and in Sample A11 a 14A mineral was also detected but low concentration prevented identification.

Soil developed on fresh volcanic rock was obtained on the south side of Ross Hill (Sample A18) and on the inland terrace at Drumsite (Sample A23). In both cases the volcanic rock is limburgite. Sample A23, the only auger sample not taken on the central plateau, is the only one without iron-aluminium phosphate minerals. The profile in this case is dark brown and consists of disordered kaolin, sub-dominant quartz and accessory goethite. Sample A18 consists of yellow brown soil and is composed dominantly of millisite and sub-dominant crandallite and accessory goethite.

The remaining auger samples (numbers A1, A5, A9, A15, A16 and A17) were taken in areas devoid of rock outcrop and thus in most cases it was not possible to deduce the nature of the parent material from which they were formed. They vary in colour from dark reddish brown to yellow brown and usually show no variation in colour throughout the depth sampled. All samples of this group were found to contain crandallite and, with the exception of Sample A9, all contain some millisite. In addition goethite is commonly present and kaolin was observed in Sample A5. Sample A17 is almost identical to A18 which was taken in an area of outcropping fresh volcanic rock. The similarity of mineralogy suggests a similar parent rock for these samples and, as they both occur at approximately the same elevation but on opposite sides of Ross Hill, it is suggested that the volcanic

flow is continuous. "Boulders" of crandallite and goethite also occur at locality A17.

The mineralogical composition of the surface and near surface soils is indicative of the lateritic origin of these materials. Phosphate minerals were found in all samples of the soil on the central plateau.

8. CHEMISTRY

8.1 Preamble

Chemical analysis was carried out[(a)] on representatives of the major types of phosphate occurrence, some carbonate rocks and one volcanic rock. The inorganic constituents of a sample of bird excrement were also determined to provide data on the origin of the phosphate.

Additional samples of apatite were also partially analysed to determine the fluorine distribution throughout the phosphate profile. Phosphorus (as P_2O_5) and fluorine were determined on these samples.

The trace elements were determined by emission spectroscopy[(b)]. The results obtained are semi-quantitative, visual determination of line intensities being used to estimate the abundance of these elements. These results were obtained for use in exploration and for the delineation of phosphatic soils derived from volcanic and carbonate rocks by the determination of certain elements. The trace element constitution was also determined to provide data on the formation of the phosphate minerals.

8.2 The Apatite Samples

Eleven samples of apatite were analysed completely and the ionic proportions computed. The results of these analyses and the computations are recorded in Tables 2, 6, and 9 to 17 inclusive[(c)]. One sample containing both apatite and iron/aluminium phosphate was also analysed and the modal analysis computed, the results being included in Table 4.

The theoretical formula of apatite is $Ca_5(PO_4)_3(F, Cl, OH)$, the fluorine, chlorine and hydroxyl groups substituting for each other to form the almost pure end members fluorapatite, chlorapatite and hydroxy-apatite respectively. Six samples of Christmas Island apatite were analysed for chlorine and in every case this element was found to constitute less than 0.01 per cent of the sample. A considerable variation in the content and ratio of the fluorine and hydroxyl ions was recorded. The

---

(a) The chemical analyses were carried out principally by D. K. Rowley, Analytical Section, AMDEL. Other officers of the Analytical Section made some specific determinations.

(b) The spectrographic analyses were by A. B. Timms and G. R. Holden, Analytical Section, AMDEL.

(c) Tables are included at the end of this section, pp 53-86

fluorine content of these samples is, however, generally lower than that reported from other insular phosphate deposits (Hutchinson, 1950). In addition to the substitutions involving the monovalent radical, many substitutions have been reported in apatites, and there appears to be a similar variation in the material from Christmas Island.

All the apatite contained minor quantities of titanium, iron, aluminium, magnesium, manganese, zinc, sodium, potassium, and lithium. The presenceof these elements in the apatite crystal lattice has been recorded previously (Deer, Howie and Zussman, 1962). These ions, substitute for calcium and, in the case of the trivalent and monovalent ions, the balance of charge is maintained by the collective substitution for calcium and phosphorus, as in $Ca_2^{+2}P^{+5} \rightleftharpoons 3(Al, Fe)^{+3}$. It will be demonstrated that substitutions of calcium by alkalis are also probable, with the concomitant replacement of oxygen by fluorine and/or hydroxyl to balance the charge.

The source of the metal ions is considered to be related to the initial guano and to the carbonate rocks with which it has reacted. In the case of the sesquioxides, the ratio of aluminium to iron was found to be remarkably constant, being approximately 2.5: 1. Moreover, this constancy has been demonstrated over a large number of routine analyses of cargo samples which have been made in recent years[a]. The ratio is also preserved in the iron/aluminium phosphates which occur as overburden on the apatite deposits.

Determination of the sesquioxide content of three carbonate rocks is reported in Table 28. In these cases the iron is in excess of the aluminium. However, in the analysis of the recent bird excrement (Table 28), the relation of alumina to iron oxide is more comparable with that of the apatite deposits, the ratio being 1.83: 1. It is therefore concluded that the sesquioxides of the apatite samples are essentially of biogenic origin. However, some solid solution of hematite and apatite is also possible (Hogarth, 1957), and is considered to be responsible for the brick red banded apatite which occurs in minor amounts in some deposits (Sample SP5).

The occurrence of manganiferous apatite and the presence of finely dispersed manganese oxides in apatite has been reported previously. Such occurrences were also observed in the Christmas Island samples, principally in the nodular pebble phosphate. Minor quantities of zinc are also characterisitic of the Christmas Island apatite. According to Goldberg (Graf 1960), marine vertebrates concentrate zinc from sea-water by a factor of approximately 30,000 compared with a factor of 1000 in the case of marine invertebrates. The average zinc content of sea-water is reported by Mason (1958, p 187) as being between 0.009 and 0.021 ppm. Rankama and Sahama (1949, p 714) report that zinc accumulates in phosphorite of organic origin. The presence of between 0.1 and 0.01 per cent of this element in the apatites is a further indication of the avian origin of these deposits.

(a) Personal communication, D. K. Rowley.

The presence of carbonate radicals in the apatite samples was studied in some detail. These radicals constitute a deleterious impurity in apatite in the manufacture of superphosphate, because the consumption of sulphuric acid becomes excessive. The tolerable content of carbonate, expressed as CO_2, is of the order of 5 per cent[a]. In some cases the physical inclusion of calcite or dolomite in the apatite was detected. This contamination results from the admixture of the underlying limestone (or dolomite) pinnacle in the phosphate during mining, or by the partial replacement of the bedrock by the phosphate (Sample A7, Plate 11A).

Much of the carbonate, however, is not present as separate minerals but is included in the crystal structure of the apatite. Some research has been carried out into the nature of the carbonate replacement in apatites, but as yet complete understanding of the substitution laws has not been reached. It has been shown (Deer, Howie and Zussman, 1962, p 327) that the lattice parameters and optical properties of the carbonate apatite are distinctly different from those of hydroxyapatite and fluorapatite. However, the carbonate can be selectively leached from some varieties of carbonate apatite by some acids (Deer, Howie and Zussman, 1962, p 327).

The substitution of carbon for calcium and for phosphorus has been suggested previously. McConnell, (1952) has denied the possibility of the carbonate radical substituting for the (F,Cl, OH) group. Deer, Howie and Zussman (1962) have suggested that there may be some direct function between the (F, Cl, OH) content and the carbonate, and Borneman-Starynkevich and Belov (Deer, Howie and Zussman, 1962, p 329) have suggested the formula for carbonate apatite as being $xCa_{10}P_6O_{24}F_2 + yCa_{10}P_5CO_{23}F_3$.

In the accompanying modal analyses the ionic proportions have been calculated on a basis of 10 Ca, etc., ions per two formula units and also on a basis of 26 (O, F, Cl, OH) ions per two formula units. From these tables the total (F, Cl, OH) ions were graphed against the C ions and the results are shown in figures 6 and 7. On the sample graphs, the analyses of carbonate apatites reported by Deer, Howie and Zussman (1961, p 328), Palache, Berman and Frondel (1951, p 883) and by McConnell (1960) have been plotted. Analyses carried out for the British Phosphate Commissioners on samples submitted to AMDEL from the Sechura Desert and an undisclosed locality in Peru have also been included in these calculations and graphs.

The results indicate that at least two and possibly three functions relating the carbonate and monovalent radicals may be operative. The first involves the substitution:

$$(PO_4)^{-3} \rightleftharpoons (CO_3.F)^{-3} \qquad (1)$$

This is essentially the reaction postulated by Borneman-Starynkevich and Belov.

(a) Personal communication T. A. Adams, The British Phosphate Commissioners.

The correlation of the analyses in the region of this proposed function as shown in Figures 6 and 7 is not close.

McConnell (1952 and 1960) has disputed the possibility of this form of substitution and states (1960, p 212)

> "the data on francolite do not fit the assumption that $(CO_3OH)^{-3}$ substitutes for $(PO_4)^{-3}$ because there is not a straightforward relation between the water and carbon dioxide contents. The best interpretation still posulates CO_3 groups entering the structure in such a manner that some Ca ions are omitted i. e., some CO_3 groups lie parallel to (00. 1) whereas approximately three times as many CO_3 groups are essentially perpendicular to (00. 1) and are distributed symmetrically about an axis which has essentially (pseudo) threefold symmetry. "

McConnell (1952) proposes the structural formula of francolite as being:

$$(Ca_{10-a}(H_2O)_a)X_2(P_{6-3a-b}C_{4a}H_{4b})(O_{24-a-b}X_{a+b})$$

In the case of dahllite, McConnell (1938) proposes that O substitutes for $(F, OH, Cl)_2$ and suggests that the name should be extended to include carbonate oxy-apatite as well as carbonate hydroxyapatite.

In the results of these analyses two other functions relating carbonate and (F, OH, Cl) are indicated. They are essentially parallel but contain differing amounts of monovalent radical in the non-carbonate end member. The slope of the line indicates substitutions of the type:

$$3(PO_4)^{-3} \rightleftharpoons 2(CO_3 . F_{2.5})^{-4.5} \qquad (2)$$

Those analyses, corresponding to the function 3, Figures 6 and 7, contain three fluorine, etc., atoms in the non-carbonate end member instead of the normal number of two, per two formula units. The analyses of both relationships 2 and 3 were therefore examined to determine the possibility of other substitutions. Both sets of analyses were found to contain approximately the same quantities of trivalent ions but those of relationship 3 were found to contain an average of approximately three times more monovalent ions than those of relationship 2. There was found to be a corresponding decrease in divalent ions (Ca, etc). Figure 8 is a graph of the monovalent to divalent ions in these samples.

It is indicated that in addition to the substitution of monovalent and carbonate ions for phosphate ions, the monovalent ions substitute for oxygen with the replacement of monovalent positive ions for divalent positive ions to balance the charge.

It can be seen, therefore, that the carbonate ions may be present in a variety of ways in the apatite samples, both within the phosphate mineral lattice and as contamination by calcite or dolomite. Furthermore the fluorine may be present in the apatite structure in either the monovalent radical, in conjunction with carbonate ions, in place of phosphate radical, or in place of oxygen in conjunction with the replacement of calcium by monovalent positive ions (sodium, potassium and lithium).

Unfortunately it has not been possible, within the scope of this investigation, to study the structural effects of these substitutions on the apatite crystal lattice.

In addition to the apatite samples analysed completely, a number were analysed for fluorine and phosphorus to determine the distribution of the fluorine throughout the deposits as excessive fluorine is deleterious in phosphate used as stock food.

The analyses of Table 30 suggest a random distribution of the fluorine content with depth. In the upper parts of the profile where crandallite and/or millisite dominate, the fluorine content is low and there is some suggestion that in the intermediate zones consisting of a mixture of apatite and iron/aluminium phosphate, the fluorine content of the apatite is highest. Samples of concretionary apatite ("rock phosphate") which occur on the lower terrace at South Point (Sample SP1, Table 28) and on Tom's Ridge (Sample MH7, Table 17) have fluorine contents of 2.50 and 3.44 per cent, respectively. The mode of occurrence and the petrography of these deposits suggest that they have been formed by spring deposition.

The evidence therefore suggests that the fluorine is of atmospheric origin and is introduced into the phosphate by infiltrating meteoric waters. It is known that apatite will take up fluorine from solution to form the most stable structural variety, fluorapatite (Trautz et al, 1964). The higher fluorine content of the apatite in the upper portions of the profile is consistent with it having been introduced by downward percolating waters, as is the much higher fluorine content of the apatites deposited by precipitation or colloidal coagulation by surface springs. Further work on complete profiles would probably resolve the problem of the possible concentration of fluorine in the transitional sections between iron/aluminium and calcium phosphates ("B-grade"). Table 31 is a summary of the fluorine determinations available. The amount of this element in recent bird excrement is considerably less than that in the apatites. Likewise the fluorine content of the volcanic rocks (Table 31) and the carbonate rocks is considerably lower.

The trace element determinations of some Christmas Island apatites and carbonate rocks are recorded in Table 32. A sample of apatite from the Bone Valley Formation, Florida, is also included for comparison. This sample was made available by Mr. R.K. Johns of the S.A. Government Department of Mines,

There is some similarity in the trace element content of the Florida and Christmas Island samples, although these deposits have been formed by different processes. The principal differences are the slightly greater concentration of the rare earths and vanadium in the Bone Valley apatite over that from Christmas Island. The former deposits originated as a sedimentary formation of shallow water marine facies.

8.3 The Crandallite Samples

Iron-aluminium phosphates, consisting dominantly of crandallite occur in many areas of the upper plateau and it is estimated that this is the most abundant phosphate mineral of the island. It occurs in the weathered horizons of carbonate and volcanic rocks and the apatite deposits. Samples consisting entirely of crandallite were not observed, however. In some areas it occurs with goethite and rarely boehmite; in others associated with millisite or barrandite.

The overburden on the apatite deposits also contains crandallite, commonly as a major constituent. It is associated with apatite and millisite but free oxides and hydroxides of iron and aluminium are generally absent.

Chemical and modal analyses of samples containing crandallite in major proportions are recorded in Tables 1, 3, 7, 8, 18, 21 and 29.

Crandallite is a member of the plumbogummite group of hydrous aluminium phosphates containing calcium, strontium, barium, lead and (?)caesium in varying amounts, crandallite being the calcium end member, goyazite the strontium end member, gorceixite the barium end member and plumbogummite the lead end member. In the accompanying analyses, strontium has not been determined separately from calcium except in Samples Ce2 and Ce2a. However determination by emission spectroscopy (Table 33) indicates that in these samples the strontium content is less than 0.1 per cent.

In most analyses the phosphate content is slightly less than the theoretical requirement. This deficiency is believed to be compensated by an excess of hydroxyl groups, $4(OH)^{-1}$, presumably substituting for $(PO_4)^{-4}$. Arsenate does not substitute for phosphate in any of the recorded analyses and sulphate ions are likewise not recorded.

The accepted formula for crandallite (Palache, Berman and Frondel (1951, p 831)) is $CaAl_3(PO_4)_2(OH)_5.H_2O$. This formula accords with analyses of this mineral from Utah (Larsen, 1940) and Florida (Owens et al., 1960) and the analyses of the Christmas Island crandallite samples could be calculated in terms of it. However, in several cases it was found that the alumina content was considerably less than the theoretical requirement. This is considered to be compensated by the presence of iron. Those samples consisting of a mixture of crandallite and goethite (e.g., Samples A2 (30 in.) Table 7; MH8, Table 18) were found to contain sufficient alumina to assign to the crandallite mineral. However in other cases (e.g., Sample 3, Table 29), the alumina is less than the stoicheiometric requirements for the calcium and phosphate. The combined sesquioxides are stoicheiometric in such cases. The analyses indicate that where sufficient aluminium ions are available, these are taken into the crandallite lattice in preference to iron but, when deficient, iron may substitute.

Wambeke (1958) reports a plumbogummite mineral from the Belgian Congo, called lusungite, in which iron, phosphorus, strontium and lead are the main constituents. The formulation is stated as being $(Sr, Pb)Fe_3(PO_4)_2(OH)_5H_2O$. This mineral was found in a phosphate-rich zone of a uraniferous pegmatite.

The trace element constitution of the crandallite samples (Table 33) show a definite resemblance between the samples from Christmas Island and that from Florida. By comparison of Tables 32 and 33, it can be seen that there is a marked increase in the hydrolzate elements in the crandallite-millisite samples compared with those consisting of apatite. This is a further indication of the essentially lateritic origin of the iron-aluminium phosphates (Frederickson, 1952, Rankama and Sahama, 1949, p 202). The relative abundance of certain trace elements in the crandallite and millisite samples and the influence of the parent rock are discussed in Section 8.4

The average fluorine content of samples consisting of crandallite and millisite is recorded in Table 31. It can be seen that the fluorine content of these minerals (0.2%) is independent of the source rock from which they have formed and is considerably less than that of the apatite minerals (1.95%). The fluorine is possibly present in the iron-aluminium phosphate in substitution for hydroxyl groups but this was not established.

8.4 The Millisite Samples

Three samples which were found by x-ray diffraction and differential thermal analysis to consist dominantly of millisite were chemically analysed. These samples (Numbers A7 (0-2ft), A16 (0-2ft) and A17 (0-4 ft)) also contain some crandallite. The analyses are included in Tables 19 and 20. In addition, three samples containing both crandallite and millisite in major proportions were analysed and these results are included in Tables 1, 3 and 29. No sample consisting entirely of millisite was examined.

The formula of millisite is reported by Larsen and Shannon (1930, p 329) as being $Na_2O.2CaO.6Al_2O_3.4P_2O_5.17H_2O$. This composition was derived from the average of two analyses after correcting for minor impurities consisting of dennisonite and wardite. Capdecomme and Pulou (1954, p 288) report the occurrence of similar material from the Thies district, Senegal, which these authors termed pallite. The Senegal mineral differed in composition from that reported by Larsen and Shannon from Utah in that it was almost free from alkali and a considerable proportion (of the order of 10%) of the alumina was replaced by iron. Capdecomme and Pulou suggested a theoretical composition of pallite as being $3CaO.6(Al,Fe)_2O_3.4P_2O_5.17H_2O$. Subsequently, millisite was reported by Owens, Altschuler and Berman (1960) from Fairfield, Utah. This material which was associated with crandallite was analysed and modal analyses were computed in terms of the formula for millisite given by Larsen and Shannon.

Owens et. al. (1960) found that a pallite sample from Senegal (which also contained minor augelite) contained 1.5 per cent sodium. They state that

> "..... it appears (in the absence of more complete analyses of pure pallite) that the pallite may be a normal millisite in which much of the iron is in associated goethite." (p 560)

The chemical analyses of the Christmas Island samples containing both crandallite and millisite were computed by modal analysis in the same way as those of Owens et al (1960), the alkali being used as an index of the millisite content. These analyses are recorded in Tables 1, 3 and 29. It was found that the alkali, calcium, phosphorus and water contents were nearly stoicheiometric. However, the alumina content was insufficient for these minerals. By use of the combined iron oxide and alumina, the analyses were found to be in good agreement. It is thus concluded that iron can substitute for aluminium in the millisite lattice as suggested by Capdecomme and Pulou (1954). Efforts were made to remove the iron oxides or hydroxides by heavy media separation and by leaching with sodium dithionite solution. (Sodium dithionite leaching is the normal method for removing iron or aluminium oxides or hydroxides from soils in a neutral solution). The results of these tests were negative and no difference in the x-ray diffraction pattern was observed after treatment. The constancy of the ratio iron/aluminium in the crandallite-millisite samples forming the overburden on the apatite deposits further suggests that they are associated in the same minerals. The ratio of the sesquioxides in the overburden is the same as that of the apatite, namely $Al_2O_3 : Fe_2O_3 = 2.5 : 1$. It is therefore concluded that, in the Christmas Island phosphate, iron substitutes for aluminium in the minerals crandallite and millisite.

The chemical analyses of samples consisting dominantly of millisite are included in Table 19. By determination of the area of the crandallite peaks on the differential thermal traces[(a)] and by difference, these samples were estimated to contain 80 $\pm$ 5 per cent millisite. The crandallite standard used for these determinations was Sample MH8, the crandallite content of which was determined from the chemical and modal analyses.

The ionic ratios of the Christmas Island millisite samples are included in Table 20. It can be seen that in Sample A16 and A17 the alkalis are in lower proportions than those required for the formula of millisite of Larsen and Shannon (1930). Moreover the RO ions, which are essentially calcium oxides, are approximately twice the required value for this formula. The sesquioxides are approximately comparable. The water content is slightly excessive, but these determinations, which were carried out by the Penfield method, may include some organic matter[(b)].

The mole ratios of these samples are more comparable with those of crandallite, the theoretical ratios of which are also included in Table 20. It is apparent that the results do not conform to the formula of Larsen and Shannon (1930), and these results suggest that:

(a) DTA by B.H.J. Waters, AMDEL.
(b) Personal communication, D.K. Rowley.

a. alkalis are not essential constituents of millisite,

b. iron may substitute for aluminium in the millisite crystal lattice, and

c. there is some indication that crandallite and millisite are polymorphic.

Further work on purer samples of millisite would be necessary to establish these hypotheses.

The trace element determinations of these samples are included in Table 33. The constituency is comparable with those containing major amounts of crandallite. The assemblage is characterized by hydrolzate elements, indicative of a lateritic origin.

Those samples taken from soils derived from volcanic rocks were found to contain significantly higher concentrations of titanium than those occurring on carbonate rocks or apatite deposits. The titanium content possibly indicates the rock type from which these minerals were derived.

8.5 The Barrandite Samples

Chemical analysis of five samples consisting dominantly of barrandite and two consisting of barrandite and crandallite are included in Table 21. With the exception of one sample (Ce2), which contains both crandallite and montgomeryite, modal analyses were also computed and these are included in Tables 22 to 27.

The barrandite has formed as a result of phosphatic metasomatism of volcanic rocks. Barrandite, the name proposed by McConnell (1940) for the variscite-strengite series, has the general formula $(Al, Fe)PO_4 . 2H_2O$. There is an isodimorphous series variscite $(AlPO_4 . 2H_2O)$ - barrandite - strengite $(FePO_4 . 2H_2O)$, and metavariscite-clinobarrandite-phosphosiderite, the former series being orthorhomic and the latter monoclinic. (McConnell, 1940).

The Christmas Island samples which were examined do not contain members of the clinobarrandite series. They contain varying amounts of aluminium and iron, the atom ratios varying from Al: Fe = 3.23: 1 to Al: Fe = 1.15: 1. Minor amounts of calcium and other divalent ions were detected and up to 0.2 per cent alkali was found in some samples. In Samples Ce2, Ce2a and Ce2b, the presence of crandallite was observed by x-ray diffraction. It was assumed, however, that in all cases the divalent ions were present in minerals of the gorceixite (crandallite) series. In the accompanying modal analyses, these elements were used as an index of the amount of gorceixite minerals present in the samples, and the equivalent amounts of the sesquioxides, phosphate and water were subtracted before computation as barrandite. The assumption that these divalent and monovalent ions were not within the barrandite lattice may not be justified but their low concentration in doubtful cases is considered to make this assumption of little consequence.

In one sample (Ce1) barium was detected, and therefore the crandallite-type mineral is considered to be gorceixite. Barium and strontium determinations were not carried out on all samples as the spectrographic results (Table 33) indicate that these elements are insignificant in most cases.

Sample Ce2 was found to contain montgomeryite ($Ca_4Al_5(PO_4)_6(OH)_5 . 11H_2O$) as well as crandallite and barrandite. This mineral was also reported from the variscite nodules of Utah (Larsen, 1940). The presence of the two calcium aluminium phosphates makes modal analysis of this sample unfeasible.

The fluorine content of the barrandite samples is included in Table 21 and is summarized in Table 31. The $F: P_2O_5$ ratios of these samples are less than those of the other mineral groups. The lack of monovalent radicals in the barrandite crystal structure may be partly responsible for the lack of fluorine.

Semi-quantitative trace element determinations were carried out on the samples consisting dominantly of barrandite, namely Ce1, Ce1a, Ce2b, MH2 and MH2a. The results are included in Table 34. Further reference to these results will be made in Section 8.6.

8.6 Non-Phosphatic Samples

Chemical analysis was carried out on two samples of carbonate rocks, Samples PH2 and SP2, and on one sample of the upper volcanics, Sample RH3.

The carbonate rocks were previously determined to be dolomite (Section 7). They were taken from the pinnacles in Field 5A at Phosphate Hill and from the "limestone"quarry at South Point. They both show bedding structures (Plate 10B) and are obviously detrital. Both samples contain sesquioxides, the first with an $Al_2O_3: Fe_2O_3$ ratio of 0.25: 1 and the second 0.5: 1. This is in marked contrast to that of the phosphate samples (2.5: 1). Fluorine and phosphorus were detected in both samples in minor amounts. The $F: P_2O_5$ ratio of these rocks (Table 30) is 0.33:1, the highest ratio recorded for the Christmas Island samples. In the absence of apatite, fluorine has been found to be present in carbonate rocks as fluorite (CaF_2). However, in the presence of apatite, the fluorine is absorbed by this mineral preferentially (Graf, 1960, vol 3, p 21). The trace element content of these rocks is recorded in Table 32.

An analysis of a sample of the upper volcanic rock from the south side of Ross Hill (Sample RH3) is recorded in Table 21. This rock is a limburgite and a petrological description is included in Section 7. The low silica content (40.7%) is indicative of the basic nature of this rock.(a) The elemental distribution was examined by electron probe microanalysis (Section 9).

(a) A limburgite has been reported by Hayton (1947) with a silica content as low as 32.1 per cent.

The trace element constituency of the limburgite is recorded in Table 34. It is apparent that there has been considerable migration of the more acid soluble constituents from these rocks during conversion to barrandite.

The principal reactions involved in the phosphatization of the volcanic rocks are the removal of alkali and alkaline earths and silica. Iron, aluminium and titanium are apparently mobilized (Section 10) but not removed from the rock.

According to Britton (1956) the precipitation of iron and aluminium phosphates takes place in an acid environment (pH $\leq$4), whereas calcium and magnesium are not deposited until the pH reaches approximately 10. Figure 9 is a graph of the experimental data on the precipitation of phosphates reported by Britton (p 146). In these experiments the hydrogen ion concentration was recorded when a N/10 solution of trisodium phosphate was added to 100 cc of salt solution the hydrogen ion concentration being followed electrochemically. The concentration curve for zirconium is considered to be comparable with that for titanium which was not recorded. Iron is likewise expected to be roughly comparable with aluminium.

It can be seen from Figure 9 that there is a considerable "pH gap" between the deposition of R_2O_3 and RO phosphates. This is considered to be relevant to the formation of barrandite in the first stage of phosphatization, which involves the removal of calcium and magnesium, and the later formation of crandallite and apatite. It is considered that the pH is low during the initial stage but the solution becomes more alkaline during the final stages of phosphatization. Britton (p 152) notes that the only phosphates precipitated from solutions more acid than pH5 are those of zirconium, thorium, aluminium and beryllium.

8.7 Tables 1-34 – Chemical and Modal Analyses

Explanation

In the chemical analyses the major constituents were largely determined by wet methods and the trace elements were determined semi-quantitatively by emission spectroscopy.

The samples containing iron-aluminium phosphates are computed in accordance with the mineralogy by assigning the appropriate mole content based on the theoretical mole ratio.

In samples containing millisite the alkalies were used as an index and the equivalent amounts of other moles subtracted.

The term "subtract" used in Tables 1 and 3 is an abbreviation of subtraction and the figures represent the moles subtracted according to the theoretical mole ratios for each mineral.

In the analyses of samples of apatite ionic proportions were used rather than moles. This enabled adjustment on the basis of 10 divalent positive ions (Ca etc.) and 26 anions per two formula units.

TABLE 1: CHEMICAL AND MODAL ANALYSIS
Sample Ch4, 2-4 ft

	Chemical Analysis %	Adjusted for Insoluble H_2O^-, rem[a]	Mole Ratios	Sum	Millisite			Crandallite		
					Theoretical Mole Ratio	Subtract	Difference	Theoretical Mole Ratio	Subtract	Difference
P_2O_5	23.3	25.6	0.1804	-	4	0.0152	0.1652	2	0.1652	Nil
CO_2	0.49	0.53	0.0121	-	-	-	-	-	-	-
Al_2O_3	27.9	30.6	0.3057	0.3797	6	0.0228	0.3569	3	0.2478	0.1091[b]
Fe_2O_3	10.8	11.82	0.0740							
CaO	8.9	9.8	0.1748	0.1773	2	0.0076	0.1697	2	0.1652	0.0025[c]
MgO	0.09	0.10	0.0025							
MnO	0.89	0.10	-	-	-	-	-	-	-	-
ZnO	0.07	0.08	-	-	-	-	-	-	-	-
TiO_2	0.42	0.46	-	-	-	-	-	-	-	-
Na_2O	0.16	0.18	0.0029	0.0038	1	0.0038	Nil	-	-	-
K_2O	0.08	0.09	0.0009							
F	0.19	0.21	0.0110	-	-	-	-	-	-	-
Cl	< 0.01[d]	< 0.01	-	-	-	-	-	-	-	-
H_2O^+	18.0	19.75	1.0970	-	15	0.0570	1.0400	7	0.5782	0.4618[e]
H_2O^-	0.95	-	-	-	-	-	-	-	-	-
Insoluble	4.76	-	-	-	-	-	-	-	-	-
Total	97.00	-	-	-	-	-	-	-	-	-
$-O \equiv F$[f]	0.08	-	-	-	-	-	-	-	-	-
TOTAL	96.92									

(a) Remainder is most probably organic matter. (b) Represents approximately 14.21% excess R_2O_3. (c) Represents 0.21% excess CaO. (d) < Less than.

(e) Represents approximately 8.3% excess combined water (H_2O^+). (f) ≡ Equivalent.

TABLE 2: CHEMICAL AND MODAL ANALYSIS
Sample Ch4, 11-12 ft

	Chemical Analysis %	Adjusted for Insoluble H_2O^-, rem[a]	Mole Ratios	Apatite Ions		Apatite Adjusted to 10 Cations	Apatite Sum	Apatite Equivalent F, O, OH
P_2O_5	37.5	37.8	0.2663	P	0.5326	5.436	6.140	13.59
CO_2	2.66	2.68	0.0690	C	0.0690	0.7041		1.408
Al_2O_3	0.94	0.95	0.0094	Al	0.0188	0.1920	9.998	0.288
Fe_2O_3	0.37	0.37	0.0023	Fe	0.0046	0.0470		0.070
CaO	52.5	53.0	0.9452	Ca	0.9452	9.6450		9.645
MgO	0.03	0.03	0.0007	Mg	0.0007	0.0071		0.007
MnO	0.03	0.03	0.0004	Mn	0.0004	0.0041		0.004
ZnO	0.01	0.01	0.0001	Zn	0.0001	0.0010		0.001
TiO_2	0.02	0.02	0.0002	Ti	0.0002	0.0020		0.004
Na_2O	0.28	0.28	0.0045	Na	0.0090	0.0920		0.046
K_2O	0.04	0.04	0.0004	K	0.0008	0.0082		0.004
F	3.71	3.74	0.1968	F	0.1968	2.008	4.885	2.008
Cl	<0.01	<0.01	-	-	-	-		-
H_2O^+	2.6	2.6	0.1410	OH	0.2820	2.877		2.877
H_2O^-	0.70	-	-	-	-	-	-	-
Insoluble	0.08	-	-	-	-	-	-	-
Total	101.51	100	-	-	-	-	-	29.952
$-O \equiv F$[b]	1.56	-	-	-	-	-	-	2.442
TOTAL	99.95	-	-		-	-	-	27.510

(a) Remainder is most probably organic matter. (b) ≡ Equivalent. (c) < Less than.

TABLE 3: CHEMICAL AND MODAL ANALYSIS
Sample Ch 5A, 2-4 ft

	Chemical Analysis %	Adjusted for Insoluble H_2O^-, rem[a]	Mole Ratios	Sum	Millisite			Crandallite		
					Theoretical Mole Ratio	Subtract	Difference	Theoretical Mole Ratio	Subtract	Difference
P_2O_5	29.7	30.8	0.2167	0.2167	4	0.0180	0.1987	2	0.2156	0.0169
CO_2	0.17	0.18	0.0040	-	-	-	-	-	-	-
Al_2O_3	27.4	28.4	0.2783	0.2503	6	0.0270	0.3233	3	0.3233	Nil
Fe_2O_3	11.1	11.5	0.0720							
CaO	12.1	12.5	0.2235	0.2253	2	0.0090	0.2163	2	0.2156	0.0007
MgO	0.07	0.07	0.0018							
MnO	0.36	0.37	0.0052	-	-	-	-	-	-	-
ZnO	0.11	0.11	0.0014	-	-	-	-	-	-	-
TiO_2	0.32	0.33	0.0041	-	-	-	-	-	-	-
Na_2O	0.26	0.27	0.0043	0.0045	1	0.0045	Nil	-	-	-
K_2O	0.02	0.02	0.0002							
F	0.28	0.29	0.0153	-	-	-	-	-	-	-
Cl	< 0.01[c]	-	-	-	-	-	-	-	-	-
H_2O^+	14.8	15.3	0.8506	0.8506	15	0.0675	0.7831	7	0.7546	0.0285
H_2O^-	0.91	-	-	-	-	-	-	-	-	-
Insoluble	1.46	-	-	-	-	-	-	-	-	-
Total	99.06	-	-	-	-	-	-	-	-	-
$-O \equiv F$[b]	0.12	-	-	-	-	-	-	-	-	-
TOTAL	98.94	-	-	-	-	-	-	-	-	-

(a) Remainder is most probably organic matter. (b) ≡ Equivalent. (c) < Less than.

TABLE 4: CHEMICAL AND MODAL ANALYSIS
Sample Ch. EQ[1], 0-2 ft

	Chemical Analysis %	Adjusted for Insoluble, H_2O^-, rem[a]	Mole Ratios	Millisite			Crandallite			Apatite				
				Theoretical Mole Ratio	Subtract.	Difference	Theoretical Mole Ratio	Subtract.	Difference	Ions		Adjusted to 10 Cations	Sum	Equiv. F, O, OH
P_2O_5	33.1	34.2	0.2409	4	0.0176	0.2233	2	0.1322	0.0911	P	0.1822	5.23	5.604	13.07
CO_2	0.70	0.72	0.0164	-	-	-	-	-	-	C	0.0164	0.374		0.748
Al_2O_3	17.4	18.0	0.1765	6	0.0264	0.1983	3	0.1983	Nil	-	-	-	-	-
Fe_2O_3	7.4	7.6	0.0482											
CaO	26.1	27.0	0.4815	2	0.0088	0.4727	2	0.1322	0.3405	Ca	0.3405	9.78		9.78
MgO	0.10	0.10	0.0025	-	-	-	-	-	-	Mg	0.0025	0.071		0.071
MnO	0.10	0.10	0.0014	-	-	-	-	-	-	Mn	0.0014	0.041	9.988	0.041
ZnO	0.16	0.17	0.0021	-	-	-	-	-	-	Zn	0.0021	0.060		0.060
TiO_2	0.10	0.10	0.0093	-	-	-	-	-	-	Ti	0.0093	0.036		0.070
Na_2O	0.25	0.26	0.0042	1	0.0044	Nil	-	-	-	-	-	-	-	-
K_2O	0.02	0.02	0.0002											
F	1.51	1.56	0.0821	-	-	-	-	-	-	F	0.0821	2.360	2.360	2.360
Cl	< 0.01[c]	< 0.01	-	-	-	-	-	-	-	-	-	-	-	-
H_2O^+	10.5	10.8	0.5992	15	0.1800	0.4192	7	0.4627	-0.0435	-	-	-	-	-
H_2O^-	0.94	-	-	-	-	-	-	-	-	-	-	-	-	-
Insoluble	1.50	-	-	-	-	-	-	-	-	-	-	-	-	-
Total	99.88	-	-	-	-	-	-	-	-	-	-	-	-	26.200
-O≡F [b]	0.64	-	-	-	-	-	-	-	-	-	-	-	-	1.18
TOTAL	99.24	-	-	-	-	-	-	-	-	-	-	-	-	25.020

(a) Remainder is most probably organic matter. (b) ≡ Equivalent. (c) < Less than.

TABLE 5: CHEMICAL AND MODAL ANALYSIS
Sample Ch. EQ[1], 8-10 ft

	Chemical Analysis %	Adjusted for Insoluble H_2O^-, rem[a]	Mole Ratios	Millisite			Crandallite			Apatite				
				Theoretical Mole Ratio	Subtract.	Difference	Theoretical Mole Ratio	Subtract.	Difference	Ions		Adjusted to 10 Cations	Sum	Equiv. F, O, OH
P_2O_5	37.9	38.5	0.2713	4	0.0168	0.2545	2	0.0294	0.2251	P	0.4502	5.762	6.117	14.405
CO_2	1.20	1.22	0.0277	-	-	-	-	-	-	C	0.0277	0.355		0.710
Al_2O_3	5.5	5.6	0.0549	6	0.0252	0.0441	3	0.0441	Nil	-	-	-	-	-
Fe_2O_3	2.3	2.3	0.0144											
CaO	44.7	45.4	0.8097	2	0.0084	0.8013	2	0.0294	0.7719	Ca	0.7719	9.777		9.777
MgO	0.13	0.13	0.0032	-	-	-	-	-	-	Mg	0.0032	0.041		0.041
MnO	0.12	0.12	0.0017	-	-	-	-	-	-	Mn	0.0017	0.022	9.941	0.022
ZnO	0.20	0.20	0.0039	-	-	-	-	-	-	Zn	0.0039	0.050		0.050
TiO_2	0.03	0.03	0.0004	-	-	-	-	-	-	Ti	0.0004	0.005		0.010
Na_2O	0.25	0.25	0.0040	1	0.0042	Nil	-	-	-	-	-	-	-	-
K_2O	0.02	0.02	0.0002											
F	2.56	2.60	0.1369	-	-	-	-	-	-	F	0.1369	1.752	5.236	5.236
Cl	< 0.01[c]	< 0.01	-	-	-	-	-	-	-	-	-	-		
H_2O^+	4.7	4.8	0.3020	15	0.0630	0.2390	7	0.1029	0.1361	OH	0.2722	3.484		
H_2O^-	1.00	-	-	-	-	-	-	-	-	-	-	-	-	-
Insoluble	0.44	-	-	-	-	-	-	-	-	-	-	-	-	-
Total	101.05	-	-	-	-	-	-	-	-	-	-	-	-	30.251
$-O \equiv F$[b]	1.08	-	-	-	-	-	-	-	-	-	-	-	-	2.618
TOTAL	99.97	-	-	-	-	-	-	-	-	-	-	-	-	27.633

(a) Remainder is most probably organic matter. (b) ≡ Equivalent. (c) < Less than.

TABLE 6: CHEMICAL AND MODAL ANALYSIS
Sample Ch. EQ[1], 32-34 ft

	Chemical Analysis %	Adjusted for Insoluble H_2O^-, rem[(a)]	Mole Ratio	Apatite			
				Ions	Adjusted to 10 Cations	Sum	Equivalent F, O, OH
P_2O_5	40.3	40.9	0.2948	P 0.5896	5.992	6.2503	14.980
CO_2	1.11	1.12	0.0254	C 0.0254	0.2583		0.5166
Al_2O_3	0.66	0.66	0.0065	Al 0.0130	0.1322		0.1983
Fe_2O_3	0.21	0.21	0.0013	Fe^{3+} 0.0026	0.0264		0.0396
CaO	53.4	53.7	0.9576	Ca 0.9576	9.730		9.730
MgO	0.07	0.07	0.0017	Mg 0.0017	0.0173		0.0173
MnO	0.01	0.01	0.0001	Mn^{2+} 0.0001	0.0055	9.9927	0.0055
ZnO	0.05	0.05	0.0006	Zn 0.0006	0.0060		0.0060
TiO_2	0.02	0.02	0.0002	Ti 0.0002	0.0020		0.0020
Na_2O	0.21	0.21	0.0034	Na 0.0068	0.0692		0.0346
K_2O	0.02	0.02	0.0002	K 0.0004	0.0041		0.0020
F	2.28	2.30	0.1211	F 0.1211	1.231		
Cl	<0.01[(c)]	< 0.01	-	- -	-	3.489	3.489
H_2O^+	2.0	2.0	0.1110	OH 0.2220	2.258		
H_2O^-	0.70	-	-	- -	-	-	-
Insoluble	0.02	-	-	- -	-	-	-
Total	101.06	-	-	- -	-	-	27.0209
$-O \equiv F$[(b)]	0.96	-	-	- -	-	-	0.615
TOTAL	100.10	-	-	- -	-	-	26.3059

(a) Remainder is most probably organic matter. (b) ≡ Equivalent. (c) < Less than.

TABLE 7: CHEMICAL AND MODAL ANALYSIS
Sample A2, 30 inch

	Chemical Analysis %	Adjusted for Insoluble, H_2O^-, rem[a]	Mole Ratios	Crandallite		
				Theoretical Mole Ratio	Subtraction	Difference
P_2O_5	19.0	22.2	0.1563	2	0.1563	Nil
CO_2	0.46	0.54	0.0122	-	-	-
Al_2O_3	26.8	31.3	0.3068	3	0.2343	0.1770
Fe_2O_3	14.3	16.7	0.1045			
CaO	8.2	9.6	0.1707	2	0.1563	0.0144
MgO	0.16	0.19	0.0046	-	-	-
MnO	0.28	0.33	0.0046	-	-	-
ZnO	0.06	0.07	0.0009	-	-	-
TiO_2	0.96	1.12	0.0140	-	-	-
Na_2O	0.18	2.04	0.0034	-	-	-
K_2O	0.12	0.14	0.0015	-	-	-
F	0.14	0.16	0.0086	-	-	-
Cl	0.01	0.01	-	-	-	-
H_2O^+	15.3	17.9	0.9913	7	0.5467	0.4446
H_2O^-	4.63	-	-	-	-	-
Insoluble	7.68	-	-	-	-	-
Total	98.0	-	-	-	-	-
$-O \equiv F$ [b]	0.06	-	-	-	-	-
TOTAL	97.94	-	-	-	-	-

(a) Remainder is most probably organic matter. (b) ≡ Equivalent. (c) ~ Less than.

TABLE 8: CHEMICAL AND MODAL ANALYSIS
Sample A8, 36 inch

	Chemical Analysis %	Adjusted for Insoluble, H_2O^-, rem[a]	Mole Ratios	Crandallite		
				Theoretical Mole Ratios	Subtraction	Difference
P_2O_5	17.7	20.7	0.1458	2	0.1458	Nil
CO_2	0.51	0.60	0.0135	-	-	-
Al_2O_3	29.9	35.0	0.3428	3	0.2187	0.2141
Fe_2O_3	12.3	14.4	0.0900			
CaO	8.0	9.3	0.1668	2	0.1458	0.0210
MgO	0.12	0.14	0.0035	-	-	-
MnO	0.20	0.23	0.0033	-	-	-
ZnO	0.04	0.05	0.0006	-	-	-
TiO_2	0.50	0.58	0.0073	-	-	-
Na_2O	0.05	0.06	0.0009	-	-	-
K_2O	0.15	0.17	0.0019	-	-	-
F	0.07	0.08	0.0043	-	-	-
Cl	< 0.01[c]	< 0.01	-	-	-	-
H_2O^+	16.0	18.7	1.038	7	0.5003	0.5377
H_2O^-	2.93	-	-	-	-	-
Insoluble	9.10	-	-	-	-	-
Total	97.57	-	-	-	-	-
$-O \equiv F$ [b]	0.03	-	-	-	-	-
TOTAL	97.54	-	-	-	-	-

(a) Remainder is most probably organic matter. (b) ≡ Equivalent. (c) < Less than.

TABLE 9: CHEMICAL AND MODAL ANALYSIS
Sample NW, 12 ft

	Chemical Analysis %	Adjusted for Moisture Insoluble	Apatite							
			Mole Ratios	Ions		Adjusted to 10 Cations	Sum	Equivalent F, O, OH	Adjusted to 26 F, O, OH	Equivalent Ions
P_2O_5	38.3	38.7	0.2727	P	0.5454	5.556	6.188	13.89	13.31	5.324
CO_2	2.70	2.73	0.0620	C	0.0620	0.632		1.264	1.211	0.605
Al_2O_3	0.64	0.67	0.0066	Al	0.0132	0.134	10.000	0.201	0.193	0.116
Fe_2O_3	0.28	0.28	0.0017	Fe	0.0034	0.035		0.052	0.050	0.030
CaO	52.8	53.3	0.9504	Ca	0.9504	9.682		9.682	9.276	9.276
MgO	0.17	0.17	0.0042	Mg	0.0042	0.043		0.043	0.041	0.041
MnO	0.00	0.00	-		-	-		-	-	-
ZnO	0.01	0.01	0.0001	Zn	0.0001	0.001		0.001	0.001	0.001
TiO_2	0.01	0.01	0.0001	Ti	0.0001	0.001		0.002	0.002	0.001
Na_2O	0.30	0.30	0.0048	Na	0.0096	0.098		0.049	0.047	0.094
K_2O	0.03	0.03	0.0003	K	0.0006	0.006		0.003	0.003	0.006
Li_2O	nd(a)	-	-		-	-		-	-	-
F	2.53	2.56	0.1347	F	0.1347	1.372	3.905	1.372	1.314	1.314
Cl	nd	-	-		-	-		-	-	-
H_2O^+	2.22	2.24	0.1243	OH	0.2486	2.533		2.533	2.427	2.427
H_2O^-	0.88	-	-		-	-	-	-	-	-
Insoluble	0.18	-	-		-	-	-	-	-	-
Total	101.11	-	-		-	-	-	29.092	27.875	-
$-O \equiv F$	1.07	-	-		-	-	-	1.952	1.870	-
TOTAL	100.04	-	-		-	-	-	27.140	26.005	-

(a) nd = not determined

TABLE 10: CHEMICAL AND MODAL ANALYSIS
Sample W/1, 0-4 ft

	Chemical Analysis %	Adjusted for Moisture, Insoluble	Mole Ratios	Apatite						
				Ions		Adjusted to 10 Cations	Sum	Equivalent F, O, OH	Adjusted to 26 F, O, OH	Equivalent Ions
P_2O_5	39.1	39.4	0.2769	P	0.5538	5.624	6.030	14.06	13.43	5.372
CO_2	1.67	1.76	0.0400	C	0.0400	0.406		0.812	0.776	0.388
Al_2O_3	2.19	2.21	0.0217	Al	0.0434	0.446	10.002	0.669	0.639	0.383
Fe_2O_3	0.78	0.79	0.0049	Fe	0.0098	0.099		0.148	0.141	0.085
CaO	51.0	51.4	0.9166	Ca	0.9166	9.302		9.302	8.887	8.887
MgO	0.17	0.17	0.0042	Mg	0.0042	0.043		0.043	0.041	0.041
MnO	0.02	0.02	0.0003	Mn	0.0003	0.003		0.003	0.003	0.003
ZnO	0.14	0.14	0.0017	Zn	0.0017	0.017		0.017	0.016	0.016
TiO_2	0.01	0.01	0.0001	Ti	0.0001	0.001		0.002	0.002	0.001
Na_2O	0.27	0.27	0.0043	Na	0.0086	0.087		0.043	0.041	0.082
K_2O	0.02	0.02	0.0002	K	0.0004	0.004		0.002	0.002	0.004
Li_2O	nd[a]	-	-		-	-		-	-	-
F	1.66	1.67	0.0879	F	0.0879	0.892	4.227	0.892	0.852	0.852
Cl	<0.01[b]	-	-		-	-		-	-	-
H_2O^+	2.80	2.96	0.1643	OH	0.3286	3.335		3.335	3.186	3.186
H_2O^-	0.60	-	-		-	-	-	-	-	-
Insoluble	0.16	-	-		-	-	-	-	-	-
Total	100.65	-	-		-	-	-	29.328	28.016	-
$-O \equiv F$	0.70	-	-		-	-	-	2.113	2.019	-
TOTAL	99.95	-	-		-	-	-	27.215	25.997	-

(a) nd = not determined.
(b) < = less than.

TABLE 11: CHEMICAL AND MODAL ANALYSIS
Sample W/2, 0-2 ft

	Chemical Analysis %	Adjusted for Moisture Insoluble	Mole Ratios	Apatite						
				Ions		Adjusted to 10 Cations	Sum	Equivalent F, O, OH	Adjusted to 26 F, O, OH	Equivalent Ions
P_2O_5	39.3	38.5	0.2714	P	0.5428	5.646	6.203	14.105	13.601	5.44
CO_2	2.40	2.35	0.0535	C	0.0535	0.557		1.114	1.074	0.537
Al_2O_3	0.21	0.21	0.0020	Al	0.0040	0.042	10.001	0.063	0.061	0.037
Fe_2O_3	0.07	0.07	0.0004	Fe	0.0008	0.008		0.012	0.012	0.007
CaO	53.7	52.6	0.9389	Ca	0.9389	9.768		9.768	9.419	9.419
MgO	0.18	0.18	0.0044	Mg	0.0044	0.046		0.046	0.044	0.044
MnO	<0.03(a)	-	-		-	-		-	-	-
ZnO	0.01	0.01	0.0001	Zn	0.0001	0.001		0.001	0.001	0.001
TiO_2	0.01	0.01	0.0001	Ti	0.0001	0.001		0.002	0.002	0.001
Na_2O	0.40	0.39	0.0063	Na	0.0126	0.131		0.065	0.063	0.126
K_2O	0.02	0.02	0.0002	K	0.0004	0.004		0.002	0.002	0.004
Li_2O	nd(b)	-	-		-	-		-	-	-
F	1.61	1.56	0.0831	F	0.0831	0.865	3.570	0.865	0.834	0.834
Cl	<0.01	-	-		-	-		-	-	-
H_2O^+	2.39	2.34	0.1300	OH	0.2600	2.705		2.705	2.608	2.608
H_2O^-	0.55	-	-		-	-	-	-	-	-
Insoluble	0.12	-	-		-	-	-	-	-	-
Total	101.03	-	-		-	-	-	28.748	27.721	-
-O≡ F	0.68	-	-		-	-	-	1.785	1.721	-
TOTAL	100.35	-	-		-	-	-	26.963	26.000	-

(a) < = less than.
(b) nd = not determined.

TABLE 12: CHEMICAL AND MODAL ANALYSIS
Sample W/2, 4-6 ft

	Chemical Analysis %	Mole Ratios	Apatite						
			Ions		Adjusted to 10 Cations	Sum	Equivalent F, O, OH	Adjusted to 26 F, O, OH	Equivalent Ions
P_2O_5	39.8	0.2804	P	0.5608	5.732	6.263	14.330	14.082	5.632
CO_2	2.29	0.0520	C	0.0520	0.531		1.062	1.044	0.522
Al_2O_3	0.23	0.0022	Al	0.0044	0.045		0.067	0.066	0.040
Fe_2O_3	0.07	0.0004	Fe	0.0008	0.008		0.012	0.012	0.007
CaO	54.0	0.9629	Ca	0.9629	9.842		9.842	9.672	9.672
MgO	0.09	0.0022	Mg	0.0022	0.022		0.022	0.022	0.022
MnO	<0.01(b)	-		-	-	10.000	-	-	-
ZnO	<0.01	-		-	-		-	-	-
TiO_2	0.01	0.0001	Ti	0.0001	0.001		0.002	0.002	0.001
Na_2O	0.24	0.0039	Na	0.0078	0.080		0.040	0.039	0.078
K_2O	0.01	0.0001	K	0.0002	0.002		0.001	0.001	0.002
Li_2O	nd(a)	-		-	-		-	-	-
F	0.77	0.0405	F	0.0405	0.414	2.160	0.414	0.407	0.407
Cl	<0.01	-		-	-		-	-	-
H_2O^+	1.54	0.0854	OH	0.1708	1.746		1.746	1.716	1.716
H_2O^-	0.58	-		-	-	-	-	-	-
Insoluble	0.10	-		-	-	-	-	-	-
Total	99.80	-		-	-	-	-	27.538	-
$-O \equiv F$	0.32	-		-	-	-	-	1.080	-
TOTAL	99.48	-		-	-	-	-	26.458	-

(a) nd = not determined.
(b) < = less than.

TABLE 13: CHEMICAL AND MODAL ANALYSIS
Sample W/2, 8-10 ft

	Chemical Analysis %	Adjusted for Moisture, Insoluble	Mole Ratios	Apatite						
				Ions		Adjusted to 10 Cations	Sum	Equivalent F, O, OH	Adjusted to 26 F, O, OH	Equivalent Ions
P_2O_5	37.4	37.57	0.2646	P	0.5292	5.373	6.638	14.062	13.174	5.269
CO_2	5.45	5.47	0.1244	C	0.1244	1.265		2.530	2.370	1.185
Al_2O_3	0.07	0.07	0.0007	Al	0.0014	0.014		0.021	0.020	0.012
Fe_2O_3	0.03	0.03	0.0002	Fe	0.0004	0.004		0.006	0.006	0.004
CaO	53.7	53.9	0.9618	Ca	0.9618	9.784		9.784	9.166	9.116
MgO	0.23	0.23	0.0057	Mg	0.0057	0.058		0.058	0.054	0.054
MnO	0.01	0.01	0.0001	Mn	0.0001	0.001	10.000	0.001	0.001	0.001
ZnO	<0.01 (a)	-	-		-	-		-	-	-
TiO_2	0.01	0.01	0.0001	Ti	0.0001	0.001		0.002	0.002	0.001
Na_2O	0.42	0.42	0.0068	Na	0.0136	0.138		0.069	0.065	0.130
K_2O	<0.01	-	-		-	-		-	-	-
Li_2O	nd (b)	-	-		-	-		-	-	-
F	0.36	0.36	0.0190	F	0.0190	0.193		0.193	0.181	0.181
Cl	<0.01	-	-		-	-	2.439	-	-	-
H_2O^+	1.98	1.99	0.1104	OH	0.2208	2.246		2.246	2.104	2.104
H_2O^-	0.52	-	-		-	-	-	-	-	-
Insoluble	0.10	-	-		-	-	-	-	-	-
Total	100.35	-	-		-	-	-	28.972	27.143	-
-O≡ F	0.15	-	-		-	-	-	1.219	1.142	-
TOTAL	100.2	-	-		-	-	-	27.753	26.001	-

(a) < = less than
(b) nd = not determined

TABLE 14: CHEMICAL AND MODAL ANALYSIS
Sample 5A

	Chemical Analysis %	Mole Ratios	Apatite Ions		Adjusted to 10 Cations	Sum	Equivalent F, O, OH	Adjusted to 26 F, O, OH	Equivalent Ions
P_2O_5	39.6	0.2826	P	0.5652	5.733	6.1763	14.330	13.901	5.560
CO_2	1.90	0.0437	C	0.0437	0.4433		0.8866	0.8601	0.4300
Al_2O_3	0.40	0.0040	Al	0.0080	0.0812		0.1218	0.1181	0.0709
Fe_2O_3	0.16	0.0010	Fe	0.0020	0.0203		0.0303	0.0294	0.0176
CaO	53.6	0.9681	Ca	0.9681	9.819		9.819	9.526	9.526
MgO	nd[a]	-		-	-		-	-	-
MnO	nd	-		-	-	9.9996	-	-	-
ZnO	nd	-		-	-		-	-	-
TiO_2	nd	-		-	-		-	-	-
Na_2O	0.23	0.0038	Na	0.0076	0.0771		0.0385	0.0373	0.0746
K_2O	0.01	0.0001	K	0.0002	0.0020		0.0010	0.0097	0.0194
Li_2O	nd	-		-	-		-	-	-
F	0.76	0.0405	F	0.0405	0.4109	3.1479	0.4109	0.3986	0.3986
Cl	nd	-		-	-		-	-	-
H_2O^+	2.40	0.2698	OH	0.2698	2.737		2.737	2.655	2.655
H_2O^-	nd	-		-	-	-	-	-	-
Insoluble	0.3	-		-	-	-	-	-	-
Total	99.36	-		-	-	-	28.375	27.535	-
$-O \equiv F$	0.32	-		-	-	-	1.574	1.527	-
TOTAL	99.04	-		-	-	-	26.801	26.008	-

(a) nd = not determined.

TABLE 15: CHEMICAL AND MODAL ANALYSIS
Sample SP5

	Chemical Analysis %	Mole Ratios	Apatite						
			Ions		Adjusted to 10 Cations	Sum	Equivalent F, O, OH	Adjusted to 26 F, O, OH	Equivalent Ions
P_2O_5	38.5	0.2713	P	0.5426	5.535	6.277	13.84	13.20	5.280
CO_2	3.2	0.0727	C	0.0727	0.742		1.484	1.415	0.707
Al_2O_3	0.42	0.0041	Al	0.0082	0.084	10.000	0.126	0.120	0.072
Fe_2O_3	0.25	0.0016	Fe	0.0032	0.033		0.049	0.047	0.028
CaO	52.6	0.9380	Ca	0.9380	9.579		9.579	9.135	9.135
MgO	0.48	0.0119	Mg	0.0119	0.121		0.121	0.115	0.115
MnO	0.07	0.0010	Mn	0.0010	0.010		0.010	0.009	0.009
ZnO	0.12	0.0015	Zn	0.0015	0.015		0.015	0.014	0.014
TiO_2	0.01	0.0001	Ti	0.0001	0.001		0.002	0.002	0.001
Na_2O	0.32	0.0052	Na	0.0104	0.106		0.053	0.050	0.100
K_2O	0.02	0.0002	K	0.0004	0.004		0.002	0.002	0.004
Li_2O	0.05	0.0023	Li	0.0046	0.047		0.023	0.022	0.044
F	1.78	0.0937	F	0.0937	0.957	3.923	0.957	0.913	0.913
Cl	nd[a]	-		-	-		-	-	-
H_2O^+	2.65	0.1470	OH	0.2940	2.966		2.966	2.828	2.828
H_2O^-	0.69	-		-	-	-	-	-	-
SiO_2	nd	-		-	-	-	-	-	-
Total	101.16	-		-	-	-	29.227	27.872	-
$-O \equiv F$	0.83	-		-	-	-	1.961	1.870	-
TOTAL	100.3	-		-	-	-	27.266	26.002	-
Insoluble	nd	-		-	-	-	-	-	-

(a) nd = not determined.

TABLE 16: CHEMICAL AND MODAL ANALYSIS
Sample PH1

	Chemical Analysis %	Adjusted for SiO_2 Insoluble	Mole Ratios	Apatite						
				Ions		Adjusted to 10 Cations	Sum	Equivalent F, O, OH	Adjusted to 26 F, O, OH	Equivalent Ions
P_2O_5	37.4	37.4	0.2635	P	0.5270	5.254	5.899	13.137	12.866	5.146
CO_2	2.85	2.85	0.0647	C	0.0647	0.645		1.290	1.263	0.631
Al_2O_3	2.60	2.60	0.0255	Al	0.0510	0.508	10.005	0.762	0.746	0.448
Fe_2O_3	1.50	1.50	0.0094	Fe	0.0188	0.187		0.280	0.274	0.164
CaO	50.5	50.5	0.9005	Ca	0.9055	8.978		8.978	8.793	8.793
MgO	0.48	0.48	0.0119	Mg	0.0119	0.119		0.119	0.116	0.116
MnO	0.12	0.12	0.0017	Mn	0.0017	0.017		0.017	0.017	0.017
ZnO	0.07	0.07	0.0008	Zn	0.0008	0.008		0.008	0.008	0.008
TiO_2	0.05	0.05	0.0006	Ti	0.0006	0.006		0.012	0.012	0.006
Na_2O	0.37	0.37	0.0060	Na	0.0120	0.120		0.060	0.059	0.118
K_2O	0.04	0.04	0.0004	K	0.0008	0.008		0.004	0.004	0.008
Li_2O	0.06	0.06	0.0027	Li	0.0054	0.054		0.027	0.026	0.052
F	2.00	2.00	0.1052	F	0.1052	1.049	3.703	1.049	1.027	1.027
Cl	nd(a)	-	-		-	-		-	-	-
H_2O^+	2.40	2.40	0.1331	OH	0.2662	2.654		2.654	2.599	2.599
H_2O^-	0.46	-	-		-	-	-	-	-	-
SiO_2	0.04	-	-		-	-	-	-	-	-
Total	101.14	-	-		-	-	-	28.397	27.810	-
- O≡ F	0.84	-	-		-	-	-	1.851	1.813	-
TOTAL	100.3	-	-		-	-	-	26.546	25.997	-
Insoluble	0.24	0.24	-		-	-	-	-	-	-

(a) nd = not determined.

TABLE 17: CHEMICAL AND MODAL ANALYSIS
Sample MH7

	Chemical Analysis %	Adjusted for Moisture, to 100%	Mole Ratios	Apatite						
				Ions		Adjusted to 10 Cations	Sum	Equivalent F, O, OH	Adjusted to 26 F, O, OH	Equivalent Ions
P_2O_5	35.3	35.9	0.2710	P	0.5420	5.487	6.476	13.718	12.561	5.024
CO_2	4.2	4.3	0.0977	C	0.0977	0.989		1.978	1.811	0.905
Al_2O_3	0.28	0.28	0.0027	Al	0.0054	0.055		0.082	0.075	0.045
Fe_2O_3	0.19	0.19	0.0012	Fe	0.0024	0.024		0.036	0.033	0.020
CaO	51.4	52.2	0.9309	Ca	0.9309	9.426		9.426	8.631	8.631
MgO	0.65	0.66	0.0164	Mg	0.0164	0.166		0.166	0.152	0.152
MnO	0.01	0.01	0.0001	Mn	0.0001	0.001	10.000	0.001	0.001	0.001
ZnO	0.04	0.04	0.0005	Zn	0.0005	0.005		0.005	0.005	0.005
TiO_2	0.02	0.02	0.0002	Ti	0.0002	0.002		0.004	0.004	0.002
Na_2O	0.87	0.88	0.0142	Na	0.0284	0.287		0.143	0.131	0.262
K_2O	0.03	0.03	0.0003	K	0.0006	0.006		0.003	0.003	0.006
Li_2O	0.03	0.03	0.0014	Li	0.0028	0.028		0.014	0.013	0.026
F	3.44	3.50	0.1842	F	0.1842	1.865	5.639	1.865	1.708	1.708
Cl	nd[a]	-	-		-	-		-	-	-
H_2O^+	3.30	3.36	0.1864	OH	0.3728	3.774		3.774	3.456	3.456
H_2O^-	0.59	-	-		-	-	-	-	-	-
SiO_2	nd	-	-		-	-	-	-	-	-
Total	100.40	101.40	-		-	-	-	31.215	28.584	-
- O≡ F	1.45	1.47	-		-	-	-	2.819	2.581	-
TOTAL	98.9	99.93	-		-	-	-	28.396	26.003	-
Insoluble	nd	-	-		-	-	-	-	-	-

(a) nd = not determined.

TABLE 18: CHEMICAL AND MODAL ANALYSIS
Sample MH8

	Chemical Analysis %	Adjusted for Insoluble, to 100 %	Mole Ratios	Crandallite			Goethite			
				Theoretical Mole Ratios	Subtraction	Difference	Theoretical Mole Ratios	Subtraction	Difference	Equivalent %
P_2O_5	20.7	21.9	0.1549	2	0.1549	nil	-	-	-	-
CO_2	0.45	0.48	0.0109	-	-	-	-	-	-	-
Al_2O_3	23.7	25.1	0.2468	3	0.2322	0.1742	1	0.1742	nil	-
Fe_2O_3	24.0	25.5	0.1596	-	-			-	-	-
CaO	7.8	8.3	0.1478	2	0.1549	- 0.0071	-	-	-	- 0.4
MgO	nd(a)	-	-	-	-	-	-	-	-	-
MnO	nd	-	-	-	-	-	-	-	-	-
ZnO	nd	-	-	-	-	-	-	-	-	-
TiO_2	nd	-	-	-	-	-	-	-	-	-
Na_2O	0.09	0.10	0.0015	-	-	-	-	-	-	-
K_2O	0.03	0.03	0.0003	-	-	-	-	-	-	-
Li_2O	nd	-	-	-	-	-	-	-	-	-
F	0.09	0.10	0.0050	-	-	-	-	-	-	-
Cl	<0.01(b)	-	-	-	-	-	-	-	-	-
H_2O^+	17.33	18.4	1.021	7	0.5418	0.479	3	0.522	-0.043	-0.75
H_2O^-	nd	-	-	-	-	-	-	-	-	-
Insoluble	3.70	-	-	-	-	-	-	-	-	-
Total	97.89	99.8	-	-	-	-	-	-	-	-
- O≡ F	0.04	-	-	-	-	-	-	-	-	-
TOTAL	97.85	-	-	-	-	-	-	-	-	-

(a) nd = not determined.
(b) < = less than.

TABLE 19: CHEMICAL ANALYSES OF SAMPLES CONSISTING MAINLY OF MILLISITE

	Sample A16, 0-2 ft		Sample A17, 0-4 ft		Sample A7, 0-2 ft		Mean, Chemical Analysis	
	Chemical Analysis %	Moles	Chemical Analysis %	Moles	Chemical Analysis %	Moles	Millisite Samples %	Crandallite Samples %
P_2O_5	27.0	0.2036	27.7	0.2062	25.4	0.1858	26.7	22.33
CO_2	0.41	0.0100	0.43	0.0106	0.5	0.0118	0.45	0.75
Al_2O_3	26.6	0.2794	24.5	0.2538	26.0	0.2647	25.7	27.3
Fe_2O_3	11.1	0.0745	13.2	0.0873	13.9	0.0904	12.7	14.55
TiO_2	0.46	0.0064	1.55	0.0205	nd[a]	-	1.00	1.17
CaO	11.1	0.2121	11.5	0.2167	9.0	0.1666	10.5	6.83
MgO	0.09	0.0025	0.23	0.0060	nd	-	0.16	0.16
MnO	0.58	0.0087	0.15	0.0022	nd	-	0.36	0.15
ZnO	0.06	0.0008	0.05	0.0006	nd	-	0.06	0.04
Na_2O	0.52	0.0094	0.74	0.0126	0.49	0.0082	0.58	0.09
K_2O	0.03	0.0003	0.02	0.0002	0.05	0.0005	0.03	0.07
Li_2O	0.02	0.0008	0.02	0.0009	nd	-	0.02	0.02
F	0.27	0.0158	0.52	0.0289	0.12	0.0007	0.30	0.11
Cl	nd	-	nd	-	nd	-	-	-
H_2O^+	15.34	0.9105	14.2	0.8326	18.9	1.040	16.15	16.21
H_2O^-	1.56	-	1.42	-	nd	-	1.49	3.44
Insoluble	2.24	-	2.58	-	3.45	-	2.76	5.26
Total	97.38	-	99.83	-	99.81	-	-	-
- O≡ F	0.11	-	0.22	-	0.05	-	-	-
TOTAL	97.27	-	99.61	-	99.76	-	-	-
Org matter	nd	-	2.9	-	nd	-	-	-
SiO_2	nd	-	0.64	-	nd	-	-	-

(a) nd = not determined.

TABLE 20: MODAL ANALYSES OF SAMPLES CONSISTING MAINLY OF MILLISITE

	Moles	Mole Ratios	Millisite Theoretical Mole Ratios	Crandallite Theoretical Mole Ratios
		Sample A16, 0-2 ft		
P_2O_5	0.2036	1	1	1
RO_2	0.0064	0.031	-	-
R_2O_3	0.3539	1.716	1.5	1.5
RO	0.2346	1.152	0.5	1
R_2O	0.0105	0.052	0.25	-
H_2O	0.9105	4.472	3.75	3.5
		Sample A17, 0-4 ft		
P_2O_5	0.2062	1	1	1
RO_2	0.0205	0.099	-	-
R_2O_3	0.3411	1.654	1.5	1.5
RO	0.2255	1.094	0.5	1
R_2O	0.0137	0.066	0.25	-
H_2O	0.8326	4.038	3.75	3.5
		Sample A7, 0-2 ft		
P_2O_5	0.1858	1	1	1
RO_2	nd(a)	-	-	-
R_2O_3	0.3551	1.911	1.5	1.5
RO	0.1666	0.897	0.5	1
R_2O	0.0087	0.047	0.25	-
H_2O	1.040	5.599	3.75	3.5

(a) nd = not determined.

TABLE 21: CHEMICAL ANALYSIS OF SAMPLES CONSISTING MAINLY OF BARRANDITE AND UPPER VOLCANICS (LIMBURGITE)

	Sample Number							
	Ce1	Ce1a	Ce2	Ce2a	Ce2b	MH2	MH2a	RH3
Mineralogy: major	Barrandite	Barrandite	Crandallite	Crandallite	Barrandite	Barrandite	Barrandite	Limburgite
minor	Gorceixite	-	Barrandite, Montgomeryite	Barrandite	Crandallite	-	-	-
P_2O_5	40.1	37.67	28.64	29.23	37.7	38.56	37.22	1.13
CO_2	0.11	0.31	0.28	0.34	0.15	0.11	0.08	0.21
TiO_2	0.52	1.85	4.08	2.05	2.71	3.29	2.95	1.61
Cr_2O_3	nd[a]	0.39	nd	nd	nd	nd	nd	0.25
Al_2O_3	23.4	20.0	14.2	25.7	19.6	15.3	17.7	11.1
Fe_2O_3	10.7	14.84	23.26	12.63	15.59	20.42	19.23	4.00
FeO	nd	nd	nd	nd	nd	nd	nd	6.80
NiO	nd	nd	nd	nd	nd	nd	nd	0.09
CaO	0.30	3.0	8.20	8.95	2.60	0.2	0.60	11.7
BaO	1.32	nd	0.13	0.15	nd	nd	nd	nd
SiO	nd	nd	0.16	0.17	nd	nd	nd	nd
MgO	0.03	0.25	0.62	0.15	0.08	0.07	0.07	15.5
MnO	0.01	0.03	0.07	0.04	0.03	0.03	0.02	0.17
ZnO	0.02	0.02	0.03	0.02	0.01	0.02	0.03	nd
Na_2O	0.04	0.11	0.08	0.06	0.09	0.08	0.18	1.00
K_2O	0.03	0.02	0.66	0.03	0.01	0.04	0.04	1.08
Li_2O	0.02	0.02	0.05	0.02	0.02	0.03	0.03	nd
F	0.12	0.10	0.05	0.08	0.05	0.01	0.01	0.04
SiO_2	0.14	0.22	0.28	0.14	<0.01[b]	<0.01	<0.01	40.7
Remainder	0.10	0.69	0.68	0.34	0.30	0.25	0.39	-
Total H_2O	22.9	20.10	19.75	18.9	20.85	21.25	21.75	H_2O^+ 2.55 H_2O^- 2.25
Total	99.90	99.62	99.22	99.00	99.79	99.66	100.30	100.18
$-O\equiv F$	0.05	0.04	0.02	0.03	0.02	0.00	0.00	0.02
TOTAL	99.90	99.6	99.20	99.0	99.8	99.66	100.30	100.16

(a) nd = not determined.
(b) $<$ = less than.

TABLE 22: CHEMICAL AND MODAL ANALYSIS
Sample Cel

	Analysis %	Mole Ratios	Ions		Sum	Gorceixite			Barrandite			Difference Moles	Difference Weight %
						Theoretical Atom Ratios	Subtraction	Difference	Theoretical Atom Ratios	Subtraction	Difference		
P_2O_5	40.12	0.2826	P	0.5652	0.5652	2	0.0370	0.5282	1	0.5460	- 0.0178	- 0.0089[a]	- 1.26[a]
CO_2	0.11	0.0025	C	0.0025	-	-	-	-	-	-	-	-	-
SiO_2	0.14	0.0233	Si	0.0233	-	-	-	-	-	-	-	-	-
TiO_2	0.52	0.0065	Ti	0.0065	-	-	-	-	-	-	-	-	-
Cr_2O_3	nd[c]	-		-	-	-	-	-	-	-	-	-	-
Al_2O_3	23.4	0.2304	Al	0.4608	0.6015	3	0.0555	0.5460	1	0.5460	nil	-	-
Fe_2O_3	10.72	0.0671	Fe	0.1342									
CaO	0.30	0.0053	Ca	0.0053	0.0185	1	0.0185	nil	-	-	-	-	-
BaO	1.32	0.0086	Ba	0.0086									
SrO	nd	-		-									
MgO	0.03	0.0007	Mg	0.0007									
MnO	0.01	0.0001	Mn	0.0001									
ZnO	0.02	0.0002	Zn	0.0002									
NaO	0.04	0.0006	Na	0.0012									
K_2O	0.03	0.0003	K	0.0006									
Li_2O	0.03	0.0009	Li	0.0018									
F	0.12	0.0063	F	0.0063	2.548	7	-	1.209[b]	2	1.092	0.117	0.117[b]	2.16[b]
Total H_2O	22.9	1.271	OH	2.542									
Total	99.90	-		-	-	-	-	-	-	-	-	-	-
$-O \equiv F$	0.05	-		-	-	-	-	-	-	-	-	-	-
TOTAL	99.90	-		-	-	-	-	-	-	-	-	-	-

(a) P_2O_5
(b) H_2O
(c) nd = not determined.

TABLE 23: CHEMICAL AND MODAL ANALYSIS
Sample Cela

	Analysis %	Mole Ratios	Ions		Sum	Crandallite			Barrandite			Difference Moles	Difference Weight %
						Theoretical Atom Ratios	Subtraction	Difference	Theoretical Atom Ratios	Subtraction	Difference		
P_2O_5	37.67	0.2655	P	0.5310	0.5310	2	0.1322	0.3988	1	0.4067	-0.0079	-0.0039[a]	-0.55[a]
CO_2	0.31	0.0070	C	0.0070	-	-	-	-	-	-	-	-	-
SiO_2	0.22	0.0366	Si	0.0366	-	-	-	-	-	-	-	-	-
TiO_2	1.85	0.0232	Ti	0.0232	-	-	-	-	-	-	-	-	-
Cr_2O_3	0.39	-	-	-	-	-	-	-	-	-	-	-	-
Al_2O_3	20.69	0.2096	Al	0.4192	0.6050	3	0.1983	0.4067	1	0.4067	nil	-	-
Fe_2O_3	14.84	0.0929	Fe	0.1858									
CaO	3.0	0.0535	Ca	0.0535	0.0661	1	0.0661	nil	-	-	-	-	-
BaO	nd[c]	-		-									
SrO	nd	-		-									
MgO	0.25	0.0062	Mg	0.0062									
MnO	0.03	0.0004	Mn	0.0004									
ZnO	0.02	0.0002	Zn	0.0002									
Na_2O	0.11	0.0018	Na	0.0036									
K_2O	0.02	0.0002	K	0.0004									
Li_2O	0.02	0.0009	Li	0.0018									
F	0.10	0.0053	F	0.0053	2.2353	7	0.4627	0.8863[b]	2	0.8134	0.0729	0.0729[b]	1.31[b]
Total H_2O	20.10	1.115	OH	2.230									
Total	99.62	-	-	-	-	-	-	-	-	-	-	-	-
$-O \equiv F$	0.04	-	-	-	-	-	-	-	-	-	-	-	-
TOTAL	99.6	-	-	-	-	-	-	-	-	-	-	-	-

(a) P_2O_5
(b) H_2O
(c) nd = not determined.

TABLE 24: CHEMICAL AND MODAL ANALYSIS
Sample Ce2a

	Analysis %	Mole Ratios	Ions		Sum	Crandallite			Barrandite		
						Theoretical Atom Ratios	Subtraction	Difference	Theoretical Atom Ratios	Subtraction	Difference
P_2O_5	29.23	0.2059	P	0.4118	0.4118	2	0.3426	0.0692	1	0.0692	nil
CO_2	0.34	0.0077	C	0.0077	-	-	-	-	-	-	-
SiO_2	0.14	0.0233	Si	0.0233	-	-	-	-	-	-	-
TiO_2	2.05	0.0257	Ti	0.0257	0.6947	3	0.5139	0.1808	1	0.0692	0.1116
Cr_2O_3	nd[a]	-		-							
Al_2O_3	25.7	0.2554	Al	0.5108							
Fe_2O_3	12.63	0.0791	Fe	0.1582							
CaO	8.95	0.1596	Ca	0.1596	0.1713	1	0.1713	nil	-	-	-
BaO	0.15	0.0010	Ba	0.0010							
SrO	0.17	0.0016	Sr	0.0016							
MgO	0.15	0.0037	Mg	0.0037							
MnO	0.04	0.0006	Mn	0.0006							
ZnO	0.02	0.0002	Zn	0.0002							
Na_2O	0.06	0.0009	Na	0.0018							
K_2O	0.03	0.0003	K	0.0006							
Li_2O	0.02	0.0011	Li	0.0022							
F	0.08	0.0042	F	0.0042	2.102	7	1.1991	0.903	4	0.2768	0.626
Total H_2O	18.9	1.049	OH	2.098							
Total	99.00	-		-	-	-	-	-	-	-	-
$-O \equiv F$	0.03	-		-	-	-	-	-	-	-	-
TOTAL	99.0	-		-	-	-	-	-	-	-	-

(a) nd = not determined.

TABLE 25: CHEMICAL AND MODAL ANALYSIS
Sample Ce2b

	Analysis %	Mole Ratios	Ions		Sum	Crandallite			Barrandite			Difference Moles	Difference Weight %
						Theoretical Atom Ratios	Subtraction	Difference	Theoretical Atom Ratios	Subtraction	Difference		
P_2O_5	37.7	0.2656	P	0.5312	0.5312	2	0.1146	0.4166	1	0.5474	- 0.1308	- 0.0654[a]	- 9.28[a]
CO_2	0.15	0.0034	C	0.0034	-	-	-	-	-	-	-	-	-
SiO_2	<0.01[c]	-		-	-	-	-	-	-	-	-	-	-
TiO_2	2.71	0.0339	Ti	0.0339	0.6193	3	0.1719	0.5474	1	0.5474	nil	-	-
Cr_2O_3	nd[d]	-		-									
Al_2O_3	19.9	0.1951	Al	0.3902									
Fe_2O_3	15.59	0.0976	Fe	0.1952									
CaO	2.60	0.0464	Ca	0.0464	0.0573	1	0.0573	nil	-	-	-	-	-
BaO	nd	-		-									
SrO	nd	-		-									
MgO	0.08	0.0020	Mg	0.0020									
MnO	0.03	0.0004	Mn	0.0004									
ZnO	0.01	0.0001	Zn	0.0001									
Na_2O	0.09	0.0014	Na	0.0028									
K_2O	0.01	0.0001	K	0.0002									
Li_2O	0.02	0.0009	Li	0.0018									
F	0.05	0.0026	F	0.0026	2.317	7	0.4011	0.953[b]	2	1.0948	- 0.142	- 0.142[b]	- 2.52[b]
Total H_2O	20.85	1.157	OH	2.314									
Total	99.79	-		-	-	-	-	-	-	-	-	-	-
$-O \equiv F$	0.02	-		-	-	-	-	-	-	-	-	-	-
TOTAL	99.77	-		-	-	-	-	-	-	-	-	-	-

(a) P_2O_5
(b) H_2O
(c) < = less than.
(d) nd = not determined.

TABLE 26: CHEMICAL AND MODAL ANALYSIS
Sample MH2

	Analysis %	Mole Ratios	Ions		Sum	Crandallite			Barrandite			Difference Moles	Difference Weight %
						Theoretical Atom Ratios	Subtraction	Difference	Theoretical Atom Ratios	Subtraction	Difference		
P_2O_5	38.56	0.2717	P	0.5434	0.5434	2	0.0238	0.5196	1	0.5659	- 0.0463	- 0.0231[a]	- 3.28[a]
CO_2	0.11	0.0025	C	0.0025	-	-	-	-	-	-	-	-	-
SiO_2	<0.01[c]	-		-	-	-	-	-	-	-	-	-	-
TiO_2	3.29	0.0412	Ti	0.0412	0.6016	3	0.0357	0.5659	1	0.5659	nil	-	-
Cr_2O_3	nd[d]	-		-									
Al_2O_3	15.55	0.3048	Al	0.3048									
Fe_2O_3	20.42	0.1278	Fe	0.2556									
CaO	0.20	0.0036	Ca	0.0036	0.0119	1	0.0119	nil	-	-	-	-	-
BaO	nd	-		-									
SrO	nd	-		-									
MgO	0.07	0.0017	Mg	0.0017									
MnO	0.03	0.0004	Mn	0.0004									
ZnO	0.02	0.0002	Zn	0.0002									
Na_2O	0.08	0.0012	Na	0.0024									
K_2O	0.04	0.0004	K	0.0008									
Li_2O	0.03	0.0014	Li	0.0028									
F	0.01	0.0005	F	0.0005	2.358	7	0.0833	1.137[b]	2	1.132	0.005	0.005[b]	0.01[b]
Total H_2O	21.25	1.179	OH	2.358									
Total	99.66	-		-	-	-	-	-	-	-	-	-	-
- O≡ F	nil	-		-	-	-	-	-	-	-	-	-	-
TOTAL	99.66	-		-	-	-	-	-	-	-	-	-	-

(a) P_2O_5
(b) H_2O
(c) < = less than.
(d) nd = not determined.

TABLE 27: CHEMICAL AND MODAL ANALYSIS
Sample MH2a

	Analysis %	Mole Ratio	Ions		Sum	Crandallite			Barrandite			Difference Moles	Difference Weight %
						Theoretical Atom Ratios	Subtraction	Difference	Theoretical Atom Ratio	Subtraction	Difference		
P_2O_5	37.22	0.2622	P	0.5244	0.5244	2	0.0420	0.4824	1	0.5709	- 0.0885	- 0.0442[a]	- 6.27[a]
CO_2	0.08	0.0002	C	0.0002	-	-	-	-	-	-	-	-	-
SiO_2	< 0.01[c]	-		-	-	-	-	-	-	-	-	-	-
TiO_2	2.95	0.0369	Ti	0.0369	0.6339	3	0.0630	0.5709	1	0.5709	nil	-	-
Cr_2O_3	nd[d]	-		-									
Al_2O_3	18.09	0.1781	Al	0.3562									
Fe_2O_3	19.23	0.2408	Fe	0.2408									
CaO	0.60	0.0107	Ca	0.0107	0.0210	1	0.0210	nil	-	-	-	-	-
BaO	nd	-		-									
SrO	nd	-		-									
MgO	0.07	0.0002	Mg	0.0002									
MnO	0.02	0.0003	Mn	0.0003									
ZnO	0.03	0.0004	Zn	0.0004									
Na_2O	0.18	0.0029	Na	0.0058									
K_2O	0.04	0.0004	K	0.0008									
Li_2O	0.03	0.0014	Li	0.0028									
F	0.01	0.0005	F	0.0005	2.419	7	0.1470	1.133[b]	2	1.1418	- 0.009	- 0.009[b]	- 0.162[b]
Total H_2O	21.75	1.207	OH	2.414									
Total	100.30	-		-	-	-	-	-	-	-	-	-	-
- O≡ F	nil	-		-	-	-	-	-	-	-	-	-	-
TOTAL	100.30	-		-	-	-	-	-	-	-	-	-	-

(a) P_2O_5
(b) H_2O
(c) < = less than.
(d) nd = not determined.

TABLE 28: CHEMICAL ANALYSES CARBONATE ROCKS, PHOSPHATIZED CARBONATE ROCKS AND BIRD EXCREMENT

	Sample Number			Bird Excrement
	PH2	SP2	SP1	
P_2O_5	0.27	0.75	27.6	12.6
CO_2	45.8	45.8	13.3	nd[a]
SiO_2	0.28	nd	nd	0.05[c]
TiO_2	<0.01[b]	<0.01	<0.01	nd
Al_2O_3	0.08	0.07	0.11	0.11
Fe_2O_3	0.31	0.14	0.11	0.06
CaO	32.8	33.0	48.1	12.6
MgO	19.3	19.2	4.3	0.57
MnO	0.01	0.01	0.01	0.005
ZnO	0.01	0.06	0.03	0.025
Na_2O	0.28	0.17	0.82	0.62
K_2O	0.02	0.01	0.04	1.51
Li_2O	0.12	0.12	0.08	0.01
F	0.08	0.24	2.50	0.04
H_2O^+	1.00	0.90	1.90	-
H_2O^-	0.02	0.02	0.38	71.4[d]
Total	100.54	100.49	99.28	99.6
$-O \equiv F$	0.03	0.10	1.05	-
TOTAL	100.5	100.4	98.2	99.6

(a) nd = not determined.
(b) < = less than.
(c) Acid insoluble.
(d) Loss on ignition.

TABLE 29: PARTIAL CHEMICAL AND MODAL ANALYSIS
Sample 3

	Analysis %	Adjusted for Insoluble	Mole Ratios	Sum	Millisite			Crandallite			Equivalent %
					Theoretical Mole Ratios	Subtraction	Difference	Theoretical Mole Ratios	Subtraction	Difference	
P_2O_5	28.2	28.9	0.2035	0.2035	4	0.0256	0.1779	2	0.1994	- 0.0215	- 3.0
Al_2O_3	26.7	27.3	0.2680	0.3375	6	0.0384	0.2991	3	0.2991	nil	-
Fe_2O_3	10.8	11.1	0.0695								
CaO	11.8	12.1	0.2107	0.2107	2	0.0128	0.1979	2	0.1994	- 0.0015	- 0.1
Na_2O	0.32	0.33	0.0053	0.0064	1	0.0064	nil	-	-	-	-
K_2O	0.09	0.09	0.0011								
H_2O^+	14.2	14.5	0.8056	0.8056	15	0.0960	0.7096	7	0.6979	0.0117	+ 0.2
H_2O^-	1.63	-	-	-	-	-	-	-	-	-	-
Insoluble	2.7	-	-	-	-	-	-	-	-	-	-
TOTAL	96.44	-	-	-	-	-	-	-	-	-	-

TABLE 30: FLUORINE – PHOSPHORUS CONTENTS
Christmas Island Apatite and Carbonate Rocks

Sample No.	ft	Fluorine F %	Phosphorus P_2O_5 %	Ratio F: P_2O_5
		Apatites		
EQ'	16-18	2.26	39.9	0.0566
EQ'	20-22	2.12	40.1	0.0528
EQ'	24-26	2.14	40.6	0.0527
EQ'	28-30	2.26	41.1	0.0537
EQ'	36-38	2.13	40.5	0.0526
W2	2-4	0.93	40.3	0.0204
W2	6-8	0.59	38.5	0.0153
		Limestone		
P30		0.04	0.37	0.108
RL2		0.15	0.19	0.7895

TABLE 31: AVERAGE FLUORINE – PHOSPHORUS CONTENT
Christmas Island Phosphate and Related Rocks

Material	Number of Analyses	Source	F	P_2O_5	$F:P_2O_5$	R_2O_3
Crandallite/millisite not associated with apatite	6	AMDEL	0.20	22.8	0.0088	34.22
Crandallite/millisite "overburden" on apatite deposits	2	AMDEL	0.23	26.5	0.0087	38.8
Crandallite/millisite and apatite ("B grade")	3	AMDEL	2.15	36.7	0.0586	12.9
	6	BPC	2.28	36.37	0.0627	11.71
Phosphate consisting dominantly of apatite ("A grade")	18	AMDEL	1.95	38.42	0.0508	1.11[a]
	9	BPC	0.73	37.92	0.0192	1.84
Carbonate rocks (Limestone and dolomite)	4	AMDEL	0.13	0.39	0.3333	0.30[b]
Upper volcanic rocks (Limburgite)	1	AMDEL	0.04	1.13	0.0354	21.72
Phosphatized volcanic rocks (Barrandite)	4	AMDEL	0.05	38.3	0.0016	35.5

(a) Average of 11 analyses.
(b) Average of 2 analyses.

Note The Christmas Island analyses are not strictly comparable with those of AMDEL as different analytical methods were used. In the former case a gravimetric technique was used, whereas the AMDEL fluorine determinations were carried out by the Willard-Winter distillation method.

TABLE 32: SEMI-QUANTITATIVE SPECTROGRAPHIC ANALYSIS OF APATITE AND DOLOMITE SAMPLES FROM CHRISTMAS ISLAND AND OF FLORIDA APATITE[a]

Sample	Over 10 %	10-1 %	1-0.1 %	1000-100 ppm	100-10 ppm	10-1 ppm
NW/12 ft North-west Quarry South Point Apatite	Ca, P	-	Al, Fe, Na	Cu, Zn, K, Li, Mg	Mn, Ti, Pb Sr	Cr, Ni, Sn, Cd, Bi, Ag, Ba
W/2 0-2 ft West Quarry, Sth Point Apatite	Ca, P	-	Al, Na	Fe, K, Li,	Zn, Ti, Cu, Pb, Mn, Sr	Ni, Cd, Bi, Ag, Ba, Cr
W/2 4-6 ft West Quarry, Sth Point Apatite	Ca, P	-	Al, Na	Fe, Li, Mg, Cu	K, Zn, Ti, Pb, Mn, Sr	Ni, Sn, Bi. Ag, Ba, Cr
W/2 8-10 ft West Quarry, Sth Point Apatite	Ca, P	-	Na, Mg	Al, Fe, Li	K, Zn, Ti, Cu, Pb, Mn, Sr	Ni, Sn, Bi, Ba Cr
W/1 0-4 ft West Quarry Sth Point Apatite	Ca, P	Al	Na, Mg, Zn, Fe	K, Li, Mn, Cu	Ti, Pb, Cd, Ba, Sr, Zr,	Ni, Sn, Bi, Ag, B, Cr
PH1 Pebble Phosphate Phosphate Hill (Field 5A) Apatite	Ca, P	Al, Fe	Mn, Mg, Na	Ba, Sr, Si, Ti, Zn, K, Li, Cu	Pb, Co, Ni, Sn, Cd, Cr	B, V, Bi, Ag, Be, Mo, Ga
SP5 West Quarry, Sth Point Massive Phosphate Apatite	Ca, P	-	Al, Fe, Zn, Mg, Na	Ti, Mn, K, Li, Sr,	Cu, Pb, Ni, Cd	Ba, Sn, Bi, Mo, B, Cr
SP1 South Point Concretionary Phosphate Dolomite and Apatite	Ca, P	Mg	Na, Sr	Al, Fe, Zn, K, Li, Cu	Pb, Ni, Mn, Ti	Sn, Bi, Mo B, Ba, Cr
MH7 Toms Ridge Concretionary Phosphate Apatite	Ca, P	-	Fe, Al, Na, Mg, Sr	Ti, Zn, K, Li	Cu, Pb, Co, Ni, Mn, Ba	Cr, V, Sn, Cd, Bi, B
PH2 Phosphate Hill Field 5A Dolomite	Ca, Mg	-	Si, P, Fe, Na	Al, K, Sr, Li	Pb, Cr, Cu, Zn, Ni, Sn, Mn, Ti	Bi, Mo, B, Ba, V
SP2 South Point Dolomite	Ca, Mg	-	P, Fe, Na	Al, K, Li, Sr	Cu, Pb, Ni, Mn, Ti	Cr, Sn, Bi, Be, Mo, B, Ba
Bone Valley Bone Valley Formation Florida, USA Apatite	Ca, P	[Fe, Al, Na, K][b]		Mn, Ti, Ba, Sr, La, Zn	Ni, Cd, Cr, V, Y, Sc, Rb, Li, Cu, Pb	Sn, Bi, Be, Mo, Ga, B

(a) Analysis by A.B. Timms, AMDEL.
(b) 10 to 0.1 %.

TABLE 33: SEMI-QUANTITATIVE SPECTROGRAPHIC ANALYSIS OF CRANDALLITE AND MILLISITE SAMPLES FROM CHRISTMAS ISLAND AND FLORIDA[a]

Sample	Over 10 %	10-1 %	1-0.1 %	1000-100 ppm	100-10 ppm	10-1 ppm
Ch4 2-4 ft Phosphate Hill, Field 4 overburden Cr + M(c-d) B(ac)	Al, P	Si, Ca, Fe	Na, Ti, Mn	Mg, Ba, Cr, Sr, Zn, K	Ni, Sc, Cu Cd, V, B, Li, Rb, Pb	Be, Co, Sn Bi, Ga, In
Ch5A 2-4 ft Phosphate Hill, Field 5A overburden Cr + M(c-d)	Al, P	Si, Ca, Fe	Na, Ti, Mn	Mg, Ba, Sr, Zn, K	Ni, Sc, Cu, Cd, V, B, Li, Pb, Co,Cr	Be, Sn, Bi Ga, In, Mo
A2 2 ft 6 in. Between Murray and Ferguson Hills Lateritic soil Cr(d), G(s-d)	Al	Si, Ca, Fe, P	Na, Ti	Mg, Ba, Sr, Zn, K, Mn, Cr, Li	Ni, Sc, Cu, Cd, V, B, Rb, Pb, Co	Be, Sn, Bi, Ga, In, Mo
A7 0-2 ft East of Grants Well Lateritic soil M(d), Cr(s-d)	Al, P	Si, Ca, Fe	Na, Ti, Mn, Sr, Zn	Mg, Ba, Cr, Sc, La, B Co	Ni, Cu, Cd, V, Pb, Sn, Y, Li	Be, Bi, Ga Rb
A8 2 ft 6 in. North of Grants Well Lateritic soil Cr, M (c-d)	Al	Si, Ca, Fe P	-	Mg, Ba, Sr, Zn, K, Na, Mn, Cr, Ti	Ni, Sc, Cu, V, B, Pb, Li	Be, Sn, Bi Ga, In, Co, Cd
A16 0-2 ft North of Ross Hill Tank Lateritic soil M (d), Cr (s-d)	Al, P	Si, Ca, Fe	Na, Ti, Mn	Mg, Ba, Sr, Zn, K, La	Cr, Sc, Ni, Cu, B, Pb Li, Co, Cd	Be, Sn, Bi, Ga, V
A17 0-4 ft Ross Hill Lateritic soil M (d), Cr (s-d)	Al, P	Si, Ca, Fe	Na, Ti, Mn, Sr	Mg, Ba, Zn, K, Cr, La	Ni, Sc, Cu, Cd, V, B Pb, Co	Be, Sn, Bi Ga, Li
MH8 Murray Hill (?) Weathered barrandite Cr (d), G (s-d)	Al, Fe	Si, Ca, P	Ti	Cr, Ni, Cu, B, Co, Na, Mn, Mg, Ba, Sr, Zn, K	Sc, Cd, V Pb, Sn,	Be, Bi, Ga Li
Ce2 Aldrich Hill Massive and pisolitic Cr (d), B(s-d) and Montg.	Fe, P	Al, Ca, Ti	Si, K, Mg	Li, Rb, La, Na, Mn, Ba, Sr, Zn, Cr	Ni, Sc, Cu, V, B, Pb, Co, Sn	Be, Bi, Ga, Mo
Leached Zone, Bone Valley formation Florida Cr and M (d), Qtz (s-d)	Al	Si, Ca, P, Fe	Na, Ti	B, V, Zr, Mg, Ba, Pb, Cr, Sr, Cu	Ga, Ni, Y Mn, Sc	Be, Yb

(a) Analysis Christmas Island Samples, A.B. Timms, AMDEL. Florida Sample, H.W. Worthing USGS (Owens et al, 1960).

Key to abbreviations in first column

Cr = Crandallite.
M = Millisite.
B = Boehmite.
G = Goethite.
Montg= Montgomeryite
Qtz = Quartz

(d) = dominant.
(c-d) = co-dominant.
(s-d) = sub-dominant.
(ac) = accessory.

TABLE 34: SEMI-QUANTITATIVE SPECTROGRAPHIC ANALYSIS OF BARRANDITE ROCKS AND UPPER VOLCANICS (LIMBURGITE)[a]

Sample	Over 10 %	10-1 %	1-0.1 %	1000-100 ppm	100-10 ppm	10-1 ppm
Cel West of Camp 5 Green Massive Barrandite	Al, P	Fe	Ca, Ti, Ba	Mg, La, Zn, Na, K, Sr, Cr, V	Mn, Cu, Pb B, Li	Ni, Sn, Be Bi, Mo, Ga, Ge
Cela As for Cel Dk brown phosphatized volcanic rock Barrandite	Al, P, Fe	Ca	Si, Ti, Mg	Zn, Na, Cr, V, K	Co, Cd, Sc, Ba, Sr, Mn, Cu, Pb, Li Ni, Sn	B, Be, Bi, Mo, Ga
Ce2b Southern side Aldrich Hill Barrandite (d) Crandallite (s-d)	Al, P, Fe	Ca, Ti	Mn	Mg, Na, Cr, Ba	Zn, K, Sr, V, Cu, Pb, Sn, Co, Cd, Sc, Li	B, Be, Bi, Mo Ga
MH2 Murray Hill Oolitic Barrandite	P, Fe	Al, Ti	Ca, Mn	Mg, Zn, Na, K, Li, Cr	Ba, V, Cu Pb, Sn	Sr, Ni, Cd, Bi, Ga, B
MH2a Murray Hill Oolitic Barrandite	P, Fe	Al, Ti,	Ca, Na	Mg, Zn, K, Li, Cr, La	Sn, Cd, Ba, Mn, Sr, V, Cu, Pb, Co, Ni	B, Be, Bi, Ga
RH3 Ross Hill Limburgite	Si, Mg, Al	Fe, Ti, Ca,	P, Mn, Na K, Cr	Li, Cu, Co, Ni, Zn, La, Ba, V, Zr, Sc, Rb	Pb, Sn, Mo	B, Bi, Ga, Ge

(a) Analysis by A.B. Timms and G.R. Holden, AMDEL.

Key to abbreviations in first column

(d) = dominant.

(s-d) = sub-dominant.

9. ELECTRON PROBE MICROANALYSIS

Electron probe microanalysis was undertaken to determine the mode of occurrence of the titanium in the barrandite samples and to provide chemical data of the phosphatization of the volcanic rocks.

The electron probe microanalyser (EPMA) is an instrument capable of analysing elements within the periodic range magnesium to uranium in small areas (down to 3 microns in diameter) and to display by potentiometric chart recording and cathode ray oscillocopes the distribution of these elements throughout the surface of a solid sample.

The EPMA examination of the Christmas Island phosphate samples was semi-quantitative.

It was found during chemical analysis that a considerable proportion of the barrandite samples was insoluble after acid digestion. This digestion involved the addition of concentrated hydrochloric acid, followed by concentrated nitric acid and, finally, concentrated perchloric acid, the mixture being heated on a hot plate to the production of perchloric fumes.

The acid insoluble fraction was chemically analysed separately and the results are included in Table 35. Complete chemical analyses of these samples are included in Tables 21 to 27, Section 9.

It can be seen that the insoluble fraction consists dominantly of titanium and phosphorus, together with some iron. Aluminium was not determined but it is likely[(a)] that the remainder would consist mainly of this element.

The acid digestion was repeated on Sample MH2 and the insoluble fraction collected. It was found to consist mainly of an earthy yellow material and some black granular matter. This fraction was examined by x-ray diffraction and the pattern was found to be not comparable with any titanium oxide, titanium pyrophosphate or barrandite standard. A mixture of apatite and titanium oxalate with a Ti: P_2O_5 ratio the same as in the above insoluble fractions was then digested in the same acids. The insoluble fraction so obtained was poorly crystallized but contained x-ray diffraction lines comparable to some of those of the initial insoluble fraction.

It was concluded, therefore, that the insoluble titanium phosphate was not a residue from the acid digestion but was essentially a precipitate. The acid insoluble fractions of other phosphate samples, principally those consisting of crandallite and/or millisite, are possibly also of this constitution.

As a result of these findings, it was considered important to determine the distribution of the titanium in the barrandite samples. Two samples were examined, Sample MH2 and Sample Cela.

Sample MH2 is an oolitic barrandite rock. Its chemical composition is recorded in Tables 21 and 26.

(a) Personal communication, D.C. Bowditch, AMDEL.

TABLE 35: ACID INSOLUBLE FRACTION
Barrandite Samples[a]

Sample No.	Acid Insoluble %	SiO_2 %	TiO_2 %	P_2O_5 %	ZnO %	MgO %	MnO %	Fe_2O_3 %	CaO %
Ce1a	3.98	0.22	1.36	1.37	nd[b]	nd	nd	0.34	nd
Ce1	0.48	0.14	0.10	0.12	<0.01[c]	<0.01	<0.01	0.02	<0.01
Ce2	8.04	0.28	3.51	2.24	0.01	0.03	0.03	1.26	<0.01
Ce2a	3.74	0.14	1.58	1.33	<0.01	0.01	0.01	0.33	<0.01
Ce2b	5.06	<0.01	2.46	2.10	<0.01	<0.01	0.01	0.19	<0.01
MH2	7.66	<0.01	3.21	3.96	0.01	<0.01	0.01	0.22	<0.01
MH2a	6.40	<0.01	2.63	3.12	0.01	0.01	0.01	0.23	<0.01

(a) Chemical analysis by D.K. Rowley, AMDEL.
(b) nd = not determined.
(c) < = less than.

A line scan by the electron probe microanalyser across one of the oolites was carried out, recording the distribution of iron, aluminium, titanium and phosphorus. The results are included in Figure 10 and Plates 14E and F.

The scans indicate that the titanium is deposited in certain specific bands of the oolith. Although the effect of absorption of the characteristic x-rays was not allowed for, it is also indicated that the titaniferous layers are not devoid of phosphorus and it is likely that the titanium is present in the barrandite lattice, possibly in place of R^{3+} ions. The results indicate that the titanium of the original volcanic rock is mobilized during phosphatization and re-deposited.

Sample RH3 (the upper volcanic limburgite) and Cela were then examined to determine the elemental distribution in these rocks. Sample RH3 is a limburgite from the upper series taken on the south side of Ross Hill. Petrological description is included in Section 9 and chemical analysis in Table 21. Plate 9C is a photomicrograph of this sample.

A line scan across a section of the sample consisting of pyroxene and glass of the matrix, ilmenitic and chromitic opaque grains, and an olivine phenocryst is shown in Figure 11. Analysis was carried out for silicon, titanium, chromium, iron, aluminium, calcium and magnesium and photographs of the characterisitic radiation for calcium, titanium, chromium, iron and silicon and the absorbed electron image, which were displayed on the cathode ray tubes, are included in Plate 13, A to F.

The results indicate that the opaques are essentially of two types; chromite and ilmenite. Some titanium is present in the chromite, however, and the pyroxene is also titaniferous. The distribution of calcium suggests that the pyroxene is augite rather than the lime-poor pigeonite. The glass consists essentially of aluminium and silicon.

Sample Cela is a barrandite rock showing remnant igneous phenocrysts. The petrological description is included in Section 9 and is illustrated in Plate 12, A to C. Chemical and modal analyses are included in Tables 21 to 23. Scans for iron, aluminium, chromium, titanium, phosphorus and silicon were directed across the remnant volcanic phenocrysts and across the opaque grains.

The results so obtained revealed that there is no essential difference in the iron and aluminium contents of the replaced volcanic phenocrysts and the replaced matrix. It is apparent that during the process of phosphatization, these elements are mobilized and redistributed throughout the rock.

It was also found that, in every grain examined, the opaques consist of an inner core of chromite and an outer zone of a titanium compound. The line scan of this sample is reproduced in Figure 12. The phosphorus has not penetrated the chromite grains of the original volcanic rock during phosphatization. However, the ilmenite grains have

been dissolved and the titanium from these grains, together with that from the pyroxene, has been redeposited around the chromite residuals. Photographs of the absorbed electron image and the characteristic radiation for titanium, chromium and phosphorus are included in Plate 14, A to D.

These results suggest:

a. The titanium is not present as rutile and/or ilmenite inclusions in the barrandite (phosphatized volcanic) rocks.

b. All the major elements present in the original volcanic are mobilized during phosphatization, with the exception of those constituting the chromite grains.

c. The acid insoluble fraction of the barrandite rocks cannot be regarded as siliceous matter but consists dominantly of precipitated titanium-phosphorus compound(s). Brief examination of the acid insoluble constituents of the crandallite and millisite samples showed that these contained major amounts of titanium and phosphorus.

10. THERMAL STUDIES

10.1 Preamble

The modifications of the various mineral components on heating are of considerable importance in the manufacture of citrate soluble phosphatic fertilizers. Preliminary experiments were conducted to determine the behaviour of the main Christmas Island phosphate minerals under thermal treatment and to determine the relationship between crystallinity and the citrate solubility of the phosphate.

Thermal studies of samples consisting dominantly of apatite, crandallite and millisite were given in AMDEL Report 349 (1964).[a] In that investigation the samples were heated in a muffle furnace to a series of temperatures between 250 and 1350°C and the phosphate solubility determined in neutral ammonium citrate, 2 per cent citric acid, and alkaline ammonium citrate (Petermann's) solutions.

The differential thermal analysis (DTA) of these samples was carried out prior to the calcination tests. In this investigation samples of barrandite were also examined. The results of the previous tests are summarized in Sections 10.2 to 10.4.

10.2 Apatite

The differential thermal analysis (DTA) and thermal balance examination of apatite shows no reaction to temperatures under 850°C. Above this temperature there is a slight weight loss to 1000°C and above this temperature again a sharper weight loss was observed. The DTA and thermal balance traces of apatite are included in Figures 13 and 18. There was found to be no crystallographic modification of the apatite up to 1000°C and it is believed that the weight loss recorded above this temperature is due to the volatilization of hydroxyl and phosphate ions.

For the purpose of calcination studies, the apatite is considered to be inert. The proportion of phosphate in this mineral soluble in citric acid after heating to various temperatures up to 1347°C was found to be no greater than 29.1 per cent. This solubility decreased with increase in temperature. Solubility in neutral and alkaline citrate solutions was less than that of the 2 per cent citric acid in samples heated to between 250° and 1350°C.

10.3 Crandallite

The DTA trace of a sample consisting mainly of crandallite together with minor goethite (Sample MH8) is recorded in Figure 14. The principal thermal reactions are:

i. an endothermic peak at 114°C corresponding to the loss of non-essential water and organic matter;

(a) Gooden, J.E.A., Ryan, W. and Trueman, N.A. (1964).

ii. an endothermic peak at 290°C corresponding to the loss of combined water from the goethite;

iii. an endothermic peak at 445°C corresponding to the loss of combined water from the crandallite;

iv. an exothermic peak at 808°C and two minor exotherms at 730 and 860°C.

The thermogravimetric trace of a sample consisting of both crandallite and millisite is included in Figure 19. It can be seen from this trace that the main weight loss occurs between 200° and 600°C, corresponding to the loss of combined water.

Citrate solubility determinations indicate that over 80 per cent of the phosphate is citrate soluble in samples after heating to between 500 and 700°C. Below 500°C the citrate solubility decreases considerably.

Examination of the heated products by x-ray diffraction indicates that above 500°C the crandallite is non-crystalline and exhibits a broad, amorphous halo at approximately 4 Angstrom units. Above the exothermic peak at 808°C, the crandallite has recrystallized, forming aluminium orthophosphate, whitlockite ($Ca_3(PO_4)_2$), and iron oxide. The loss of structural water from the goethite caused hematite (Fe_2O_3) to form immediately.

The main citrate solubility occurs in the temperature range in which the crandallite is amorphous.

The examination therefore confirms the findings of Hill, Armiger and Gooch (1950) on crandallite (pseudowavellite) from Florida. However these authors reported that "one of the compounds formed by recrystallization is apatite, which was present in material heated to 800°C and had become a prominent phase at 1000°C", (p 701).

10.4 Millisite

The DTA trace of a sample (A7, 0-2 ft) consisting dominantly of millisite is included in Figure 15.

This sample contains a minor amount of crandallite. The principal thermal reaction exhibited on the DTA trace are:

i. an endotherm at 112°C, corresponding to a loss of moisture and organic matter;

ii. an exotherm at 260°C (unassigned);

iii. a strong endotherm at 365°C, corresponding to the loss of structural water from the millisite;

iv. a weaker endotherm at 460°C corresponding to the loss of structural water in the crandallite;

v. an exotherm at 750°C;

vi. a small exotherm at 840°C.

The weight loss curve reported in Figure 19 also indicates that most of the structural water is given off below 600°C.

X-ray diffraction photographs above 460°C indicate that between this temperature and 750°C the millisite crystal structure is disintegrated and the phosphate is non-crystalline. Above 800°C aluminium orthophosphate and whitlockite were found to have crystallized, together with hematite.

The citrate solubility determinations of the calcined samples indicate that the phosphate is citrate soluble after the crystal structure of the millisite has collapsed and before crystallization of the aluminium orthophosphate and whitlockite.

Millisite is therefore similar to crandallite in its thermal behaviour except that the initial temperature of the transition to the amorphous state is lower (365° as against 445°C) and the temperature of crystallization of aluminium orthophosphate and whitlockite is lower (750° as against 800°C for crandallite).

A difference in temperature of the endotherms of crandallite between Samples MH8 and A7 (0-2 ft) were recorded. Variations in the temperature of thermal reactions of some minerals are commonly recorded by DTA. The reasons for these variations are not completely understood but they are thought to be related to the concentration of the components and the nature of other constituents present in the samples. (Personal communication R. E. Wilmshurst, Amdel).

10.5 Barrandite

Brief examinations of two samples of barrandite were carried out to determine the citrate solubility on calcination. The samples selected for the thermal experiments were those consisting essentially of barrandite, namely Samples Ce1 and Ce2b.

The DTA trace of the Sample Ce1 is reproduced in Figure 17. A strong endothermic peak occurs at 165 to 180°C, but beyond this temperature no thermal reaction was detected to 1000°C. The thermal characteristics of this material are therefore different from those of crandallite and millisite both of which show crystallization exotherms in the temperature region 730 to 850°C.

The two samples, Ce1 and Ce2b were heated in a muffle furnace at 200°C, for 16 hours and at 300°C for 12 hours and the citrate solubility determined. The results are tabulated below.

Sample Ce1:	Total P_2O_5	=	39.9%
	Total H_2O	=	22.9%
Sample calcined at 200°C for 16 hours:			
	Weight loss	=	18.4%
	∴ water loss	=	80.0%
	Citrate soluble P_2O_5	=	26.2%
	Amount of P_2O_5 citrate soluble	=	53.2%
Sample calcined at 300°C for 12 hours:			
	Weight loss	=	20.0%
	∴ water loss	=	87.2%
	Citrate soluble P_2O_5	=	29.7%
	Amount of P_2O_5 citrate soluble	=	59.3%
Sample Ce2b:	Total P_2O_5	=	37.7%
	Total H_2O	=	20.85%
Sample calcined at 200°C for 16 hours:			
	Weight loss	=	16.7%
	∴ water loss	=	80.0%
	Citrate soluble P_2O_5	=	14.4%
	Amount of P_2O_5 citrate soluble	=	32.0%
Sample calcined at 300°C for 12 hours:			
	Weight loss	=	20.0%
	∴ water loss	=	96.0%
	Citrate soluble P_2O_5	=	21.4%
	Amount of P_2O_5 citrate soluble	=	45.2%

The samples heated at 200°C were retained in stoppered phials for about six months, after which time re-heating to 200°C for 16 hours caused a weight loss of 18.32 per cent for Sample Ce1 and 16.03 per cent for Sample Ce2b. This indicates that, after heating at low temperatures, the barrandite re-absorbes water. Sample Ce2b, after heating for 200°C for 6 hours showed a weight loss of 15.59 per cent. On standing an atmosphere of 50 per cent humidity for 12 hours it re-absorbed 2.8 per cent of its weight.

The interpretation of the citrate solubility values stated above is therefore uncertain. It is possible that between the time of calcination and the determination of the citrate solubility some of the barrandite re-absorbed moisture becoming citrate insoluble.

Thermogravimetric analysis of Sample Ce1 was also carried out. A weighed ground sample was placed firstly in a silica-gel desiccator for 48 hours and subsequently transferred to an evacuated desiccator over sulphuric acid to remove moisture. The weight loss recorded was 1.15 per cent. The sample was then heated slowly to 150°C on the thermal balance for 1 hour 45 minutes. The temperature was then increased at a rate of 5°C per minute. The resultant trace is included in Figure 20. It can be seen that the main weight loss (corresponding to the volatilization of structural water) occurs below 300°C. At 1000°C a further slight weight loss was recorded, corresponding, it is thought, to the initial volatilization of phosphorus.

The x-ray diffraction patterns of the samples heated at 200°, 300° and 1200°C were then examined. Portions of typical diffractometer traces are reproduced in Figures 4 and 5. It was found that at temperatures below 300°C and after removal of the water of crystallization, the barrandite remains crystalline but the crystal structure is considerably modified. The x-ray diffraction pattern has some similarities with that of tridymite but the strong basal reflection of tridymite at approximately 4.1A units is absent. Derivative crystal structures (Buerger, 1947) of the tridymite type, formed by the calcination of variscite are reported by Eitel (1952, p 72) and Hummel (1949). The diffraction patterns obtained from the Christmas Island samples suggest that up to 300°C the barrandite structure is essentially intact, but marked changes of intensities of the diffraction lines result from the loss of the water molecules. After the samples heated at 200°C had been standing for about 6 months they re-absorbed water forming the normal barrandite structure. Approximately 18 per cent of weight loss was recovered.

Between 300° and 1200°C the barrandite recrystallized forming the aluminium orthophosphate structure (ASTM Card 11-500). However some diffraction lines referable to the lower temperature phase were detected in the sample heated to 1200°C. The x-ray diffraction pattern at 1200°C shows similarities to that of α-cristobalite.

The presence of a crystal structure above the water-loss temperature of barrandite and the re-absorption of water are probably responsible for the low citrate solubility of the phosphate. The possibility of calcination in the presence of other ions may be of value in breaking down the crystal structure and thereby increasing the citrate solubility of the phosphate.

10.6 Conclusions

The above results indicate that there is an inverse relationship between the crystallinity of the phosphate minerals and the citrate solubility of the phosphorus. The use of x-ray diffraction for the determination of the degree of solubility therefore appears to be feasible.

11. DISCUSSION

11.1 Stratigraphy

The results of the field, mineralogical and petrological investigations indicate that the oldest rocks are of volcanic and organic origin and consist of lavas and bioconstructed limestones. Contamination of these limestones with volcanic debris is common.

Most of the younger carbonate rocks, which are of Miocene age occur over 400 feet above sea level. They are generally whiter than those of the lower areas which are of Eocene age. The white colour is probably due to less volcanic contamination or weathering.

The junction between the Eocene and Miocene rocks was observed only at Flying Fish Cove. Palaeontological evidence (Section 6 and Appendix A) suggests that in this area there was no development of limestone during the Oligocene and this may be true of the whole island. The lack of growth of limestone during this period would indicate that the surface of the island was above sea level. The absence of Oligocene sediments has been reported from other areas of Tertiary sedimentation in the Indo-Pacific area. (Van Bemmelen, 1949).

Petrological description of the volcanic rocks indicates that the lower volcanics of Eocene age are more acidic than the Miocene upper volcanics and there is a general decrease in acidity from the oldest to the youngest rocks. The succession may be summarized as follows:

Series	Elevation	Age	Description
Upper volcanics	600-1000 ft	Miocene	Limburgite
Lower volcanics	300- 600 ft	Eocene	Basalt, limburgite
Lower volcanics	0- 300 ft	Eocene	Andesite, trachybasalt

Volcanic rock samples, collected by C. W. Andrews (1900) and housed in the British Museum, were examined petrologically and chemically by Campbell-Smith (1926).

Campbell-Smith recorded alkali-trachyte, trachybasalt, olivine-basalt with normative nepheline, and limburgitic basalt within the lower volcanic series, and basalt, limburgite and palagonite tuff in the upper volcanic series. He compared the volcanics of Christmas Island with those of eastern Australia and concluded that they were more comparable to the Tertiary volcanics of Australia than those reported from the Indonesian Archipelago. Chemical analyses of seven of the rocks were carried out by Campbell-Smith and, by plotting the variation diagram for Na_2O, K_2O, CaO, MgO, FeO and Al_2O_3 against SiO_2, he concluded that these showed regular variations, with no break between the Eocene and Miocene and therefore indicated a single petrological series.

The only volcanic rock chemically analysed in this investigation is one from the upper volcanic series (Sample RH3) and is probably the youngest volcanic rock so far examined, all of Campbell-Smith's analyses having been carried out on samples from Flying Fish Cove and Panchoran Bay. Sample RH3 crops out on the southern side of Ross Hill at an elevation of about 1000 ft and was found to be a limburgite (Section 7). The results were plotted against those of Campbell-Smith on the variation diagram and it was found that ratios of this sample do not conform to those recorded previously. It is suggested, therefore, that, although there is possibly some relationship with the Eocene volcanics, more probably a change in magmatic composition occurred during later Miocene time. Comparison between Campbell-Smith's data and those determined in this investigation may be open to question, however, as the methods of chemical analysis are probably somewhat different. Furthermore, the basicity of the limburgite may limit the linearity of the variation diagram.

The volcanic rocks are generally of the alkalic (Atlantic) type. According to Van Bemmelen (1949, p 231) the composition of the volcanics from Christmas Island corresponds to those of other volcanic islands of the central parts of the Atlantic, Indian and Pacific Oceans. It differs however, from the composition of the plutonic and volcanic rocks of the orogenic belts of the Indonesian Archipelago, the bulk of which belong to the calc-alkaline (Pacific) suite. Some Atlantic-type volcanics have been reported from the Permian of Timor.

Mineralogical, petrological and palaeontological examinations of the carbonate rocks indicate that the majority are bioconstructed limestones. The observed Eocene limestones contain abundant foraminifera and the organic limestones of Miocene Age consist of corals, foraminifera, gastropods, molluscs and algae. Some of the younger limestones, particularly those of the summits of the hills of the upper plateau, are leached and recrystallized. Limestone scree was also observed in a number of areas on the upper plateau. It occurs as subrounded fragments suggestive of reworking by marine erosion. The limestone occurring on the edge of the terraces is frequently composed of incrustate foraminifera, coral and algae and it is considered to be of the reef-wall facies. Further inland outcrops generally become less frequent and the particulate limestones are more abundant in these areas. Molluscan limestone is well developed in places in the centre of the island, surrounding the generally depressed area between Camp 5 and Grant's Well.

The carbonate rock is partly or completely dolomitized in several areas and detrital dolomite was also observed. The central area near Camp 4 consists of strongly outcropping, recrystallized dolomite. Detrital dolomite was observed at South Point and in Field 5A, Phosphate Hill, in which areas it constitutes the pinnacles beneath the phosphate deposits. Unconsolidated, granular dolomite was observed on the inland cliff between the upper plateau and Ross Hill Tank at an elevation of 550 ft. This unconsolidated dolomite is partly lateritized and is overlain by limestone. (Plate 7B).

The mineralogy, nature of outcrop and, to some extent, the assemblage of the carbonate rocks is thought to reflect the environment of formation or deposition. Considerable research has been carried out in the past on the nature of reef complexes and on the structure of coral atolls. (Ladd, Tracy, Wells, Emery(1950); Clarke and Wheeler (1922); J. Dunbar and Rodgers, (1957)). It is known from studies of present-day reefs, such as those of Bikini Island, that a reef complex consists of several zones. On the seaward side there exists, firstly, an outer zone of talus formed by the mechanical destruction (by wave action) of the reef. This is followed by the growing reef proper which, in turn, is followed by a zone of lime-sand and debris, together with some patches of coral. The reef proper occupies less than 10 per cent of the volume and yet is responsible for most of the material of the whole reef complex.

The reef development of Christmas Island, both ancient and modern, could be observed to some extent, although the volcanism, phosphatization and weathering obscure some of the detail. The fringing reef is estimated to be no more than 100 yards wide in most places and consists of massive and extremely irregular carbonate rock. Mineralogical examination of one recent (unidentified) coral from Flying Fish Cove showed it to be composed of aragonite.

Surrounding much of the island, at an elevation of 40 to 60 feet, is a recently raised fringing reef which contains species living at present (Sample P36). This reef consists of both calcite and aragonite and is also extremely irregular (Plate 3B). In many places the reef abuts the first inland cliff but, on the south coast behind the recently elevated reef, there exists a large terrace consisting dominantly of lime-sand and calcareous soil with occasional limestone outcrops. This latter zone is believed to be representative of a pre-existing reef-flat, the constituents of which were derived from the massive reef on the seaward side. The presence of considerable detritus and the placid waters on the shoreward side of the reef would inhibit the development of much of the fauna and there is an obvious facies change between the reef and the adjacent terrace.

These facies variations are apparent on the inland terraces up to and on the upper plateau. The terraces sometimes contain accumulations of pebble phosphate which has probably been derived from the phosphatic areas above and has been reworked by the sea. They also form raised beaches, such as that above Lily Beach.

The upper plateau likewise shows evidence of reef formation on the edge of the inland cliffs. Furthermore, the occurrence of leached limestone detritus on the hills, and in particular on the top of Murray Hill, indicates that the whole of the island was once under the sea. Some of the carbonate rock is detrital and exhibits graded and false bedding structures (Plate 10B). This carbonate rock is frequently dolomitic.

The central area of the upper plateau is slightly lower than that surrounding it and contains much recrystallized dolomite. Andrews (1900, p 288) considered that this area represented a lagoon and evidence from this investigation tends to support this contention.

The crystallized dolomite of the central area gives way to limestone crowded with molluscan moulds to the west towards Stewart Hill and Jack's Hill. To the east the facies change was more obscure, the higher areas being covered by phosphate and phosphatic soil.

The dolomite rocks were possibly formed by two different processes. Firstly, the nature of the tests of the rock-forming organisms probably influenced the formation of the dolomite. Studies of other coral islands such as Funafuti have shown that, throughout a stratigraphic section, changes from limestone to dolomite occur sometimes with sharp junctions. This has been interpreted as being the result of the higher solubility of the aragonitic organic limestones which react with sea-water and change to dolomite as a result of mass action and other physico-chemical functions (Clarke and Wheeler, 1922, p 60; Dunbar and Rodgers, 1957, p 243).

Secondly, the conversion of aragonitic sediments to dolomite in restricted lagoonal environments has been demonstrated (Alderman, 1964) from the lakes of the Coorong, South Australia. This dolomitization is accompanied by a marked increase in pH of the lagoons when isolated from the sea. A pH of 10.2 has been reported from one lagoon in the Coorong in which the sediments were found to consist of ordered dolomite and magnesite. This isolated lagoonal environment is considered to be comparable with that existing in the central area of the upper plateau of Christmas Island where the carbonate rocks are recrystallized and contain dolomite. The negative shore-line movement, it is thought, would have formed on enclosed body of water in this area, and similar alkaline conditions possibly were associated with such eustatic changes. The general distribution of the main phosphate deposits around the central area suggests that these deposits were possibly formed whilst the upper plateau was an atoll and the central area was below sea-level, forming an atoll lagoon.

Further field and laboratory examination of rocks of the upper plateau is considered important in establishing the environment of formation of the carbonate rocks; the relationship between the dolomitic and calcitic sediments also needs clarification.

The tectonic movements on the island are essentially epeirogenic. It is apparent that there has been considerable vertical movement resulting in the formation of wave-cut cliffs and fringing reefs which have been elevated to 1000 feet above sea-level. Normal faulting is evident in Flying Fish Cove and at Steep Point.

11.2 Phosphate Deposits

The phosphate deposits occur mainly on the upper plateau at more than 700 feet above sea level.

It is concluded that the deposition took place when this was the only part of the island above sea level. One phosphate deposit, that of the old workings at the 400-feet level at Phosphate Hill, is a possible exception. This quarry occurs near the base of the Miocene formations and may

be indicative of a period of phosphatization in the Oligocene during which period an hiatus in the rock sequence exists. Such an hiatus is interpreted as indicating that the island was above sea level in Oligocene time. However, the disconformity between the Miocene and Eocene has not been examined in many areas, and such an investigation would be necessary to provide data to test this hypothesis. Hutchinson (1950) does not refer to avian guano deposits of pre-Pleistocene age. It is possible that this phosphate has been derived from the fields in the adjacent higher areas of Phosphate Hill.

Mineralogical examination was carried out on a number of samples taken more or less at random over the central plateau and on several channel and grab samples from the phosphate workings. It was found that the principal phosphate minerals are apatite, barrandite, crandallite and millisite. The distribution of the apatite was delineated in the drilling programme conducted by the British Phosphate Commissioners in 1957-58. It overlies and replaces limestone and dolomite and occurs in irregular bodies ("Phosphate Fields") throughout the central plateau. Crandallite and/or millisite were detected in the brown overburden on the apatite deposits and in the soil profiles overlying carbonate and volcanic rocks. Barrandite was observed in a number of localities on the central plateau and has been shown to have formed by the phosphatization of volcanic rocks. The general distribution of the apatite and the observed barrandite deposits is shown on Map 1.

In addition to the principal phosphate minerals stated above, montgomeryite and gorceixite were detected in some of the barrandite rocks. These minerals were minor constituents.

11.2.1 Apatite Deposits

The phosphate currently being worked and treated for the manufacture of superphosphate is of this type. The deposits occur on, and as a replacement of, limestone and dolomite, these rocks having been denuded to form a karrenfeld or irregular pinnacle-like surface prior to or during phosphate emplacement. The apatite deposits are irregular in size and shape, vary considerably in depth and are distributed over much of the upper plateau. There is some suggestion that these deposits are associated with the higher areas of the plateau, the central depressed area between the railway and Grant's Well being noticeably devoid of apatite.

Below the overburden, the greater part of the apatite in most deposits was found to be free of contaminants. However, in some of the deeper workings and in the shallow apatite deposits, there was some evidence of inclusion of fragments of dolomite. The carbonate fragments in places were cemented by the apatite (Plate 11A) and fragments of pinnacle rock, which obviously had been introduced during mining, were also observed in the apatite in some of the workings.

In the overburden the apatite is associated with crandallite and millisite, these latter minerals varying in their concentration and relative abundance. A sample of crandallite with minor wavellite was also examined from one of the phosphate deposits.

The apatite occurring on the limestone, as distinct from that which has reacted with it is commonly earthy or oolitic and granular. However, some of this phosphate is concretionary and massive and, under these conditions, is often hard and of a waxy lustre. Large areas of the latter type occur in the South Point deposits. Brecciated and recemented blocks of apatite are also common. The colour of this apatite is usually white or buff, but may be pale blue and brick red. Black nodules which also consist of apatite, are common both in the phosphate workings and pebble beds. These colour variations result from the presence of certain elements, principally iron and manganese.

It is not possible under some circumstances to differentiate between the phosphate formed by metasomatic alteration of the carbonate rock and that derived directly from guano However, in many places, the replacement of carbonate rock by apatite is obvious. Much of the pinnacle exposed in the workings at Phosphate Hill and South Point is partially phosphatized and it was evident at South Point that this alteration had proceeded to at least 100 feet below the depth of the workings (Plate 8A). The apatite of this type is fine-grained usually white in colour and massive.

Apatite also occurs in massive rock outcrop, and occurrences of this type were observed on the end of Tom's Ridge and at South Point. This material is grey to white in colour and is crustiform banded It is considered to be the result of spring deposition from phosphatic ground waters.

Beds of pebble phosphate, consisting mainly of apatite, also occur at several localities on the island. One such deposit occurs in Field 5A at Phosphate Hill. The deposit in this case is lenticular in plan and, as exposed in the workings, appears to have an arcuate cross-section. This material is thought to be of detrital origin, the phosphate nodules having been derived from higher areas and washed into an earlier stream bed which passes through the field. A similar deposit occurs at South Point but here the shape of the deposit is not apparent.

Further deposits of pebble phosphate occur on the lower terraces of the island and are thought to be raised beaches. A deposit of this type occurs behind Lily Beach and in the fault zone at Steep Point. The pebbles consist entirely of fine-grained apatite occurring as roughly elliptical-shaped pebbles averaging 2 inches in the longer axis. The pebbles are generally sub-rounded (water-worn) and weathered superficially to a grey colour.

The apatite is generally fine-grained and for the most part is submicroscopic (less than 1 micron in grain size). Some of this mineral, however, is dahllite and exhibits weak birefringence (Plate 11). This variety occurs mainly in concretionary masses. The grain size of the apatite is typical of that of biogenic origin. Electron microscopic studies of phosphate of this type have indicated a grain size of a few hundred Angstrom units. (Vol'fkovich et. al, 1952).

Chemical analyses of 11 samples of pure apatite indicate that this material is francolite or carbonate-fluor-hydroxy apatite ($Ca_5(PO_4)_3(F, OH, {}^1/_2CO_3)$). It contains less than 0.01 per cent chlorine. The relative contents of carbonate, fluorine and combined water are variable. Studies on the elemental substitutions within apatites have been conducted by several researchers in the past and the crystal structure of fluorapatite was determined by McConnell (1938) and has been refined by others. Substitutions of strontium, magnesium, manganese, iron and aluminium for calcium; silicon for phosphorus; hydroxyl ions and chlorine for fluorine are common. Most of these simple substitutions are evident in the apatite from Christmas Island. The presence of carbonate in apatite is somewhat contentious, there being some division of opinion as to whether it is present in the apatite structure or admixed with or adsorbed on the apatite crystals. DTA and x-ray studies tend to support the view that it is contained in the structure, but chemical tests suggest that it is present as an impurity in the form of calcite or aragonite. The Christmas Island apatite analysed in this investigation contains between 0.84 and 5.45 per cent carbon dioxide, the mean being 2.34 per cent. Only one sample assayed more than 3 per cent and this specimen, taken from the lowest part of the workings in the West Quarry, South Point, probably contains some free calcite or dolomite. In the other cases it is probably present in the apatite structure.

The distribution of fluorine in the apatite minerals at Christmas Island was examined and the data indicate a relationship between the fluorine and carbonate content. Considerable research into the forms of apatite has been carried out in the past, and not only is there considerable substitution between fluorine, chlorine and hydroxyl ions, but fluorine may substitute for oxygen in the other radicals, the balance of charge being maintained by substitution of other ions. Some apatites have been recorded in which the fluorine content exceeds that of theoretical fluorapatite (3.8%).

The chemical and modal analyses (Section 8) indicate three linear relationships of the carbonate and monovalent radicals, as well as substitutions of the monovalent radicals for oxygen with the attendant replacement of monovalent metal ions for the calcium.

There is some suggestion that the fluorine content of the apatite decreases with depth from the surface (Section 8.2). It is known that the fluorine content of apatite constituting fossil bones increases with the age, and there is some data indicating a similar increase in the phosphate of insular deposits (Graf, 1960, Vol. 3, p 21).

The fluorine content of the volcanic rocks, the carbonate rocks and fresh avian excrement is considerably less than that of the apatite deposits and it is therefore considered that the bulk of the fluorine of the phosphate has not been derived from these sources. It is suggested that this element is of atmospheric origin (possibly resulting from volcanic exhalatives in parts of the Indonesian Archipelago) and is introduced by meteoric waters. A summary of the fluorine content of volcanic rocks is

recorded by Correns (1955) and of marine organisms by Vinogradov (1953). The replacement of hydroxyl groups of the apatite by fluorine from circulating ground waters is feasible. This may account for the higher fluorine value in the upper part of the phosphate profile, as the ground water movement would be generally from top to bottom of the profile. The presence of phosphate minerals other than apatite will cause some variation in the pattern, however.

The fluorine content of the Christmas Island phosphorite is considerably less than that of the islands of the western Pacific Ocean.

11.2.2 The Variscite-Strengite (Barrandite) Deposits

Minerals of the variscite-strengite group were found at several localities on Christmas Island. The observed deposits all occur on the upper plateau and on the sides or near the top of the hills. Deposits were sampled at Murray Hill, Aldrich Hill, Stewart Hill and the un-named elevated area approximately 1 mile due west of Camp 4.

These deposits do not crop out extensively and are usually represented by spheroidal boulders up to about 4 feet in diameter. They resemble weathered volcanic rocks in habit. The thickness of the deposits was not estimated as the outcrops in all cases are heavily weathered and are covered by talus. Costeaning and/or drilling would be necessary to determine the thickness and lateral extent of these deposits.

Mineralogical and petrological examinations of selected samples from the above localities were carried out (Section 7). Chemical analyses of a number of samples were also carried out (Section 8) and the electron probe microanalyser was used to determine the distribution of certain elements (Section 9). It was found that all samples contain considerable amounts of both aluminium and iron, the former usually being the more abundant. The term barrandite (McConnell, 1950) has been proposed for this mineral series. Titanium is the principal contaminant and is considered to be present in the barrandite structure (Section 9, Plates 13 and 14).

The rocks consisting of these minerals vary considerably in texture and colour. They are granular, brecciated, pisolitic and crustiform banded and are light green, grey, light brown, yellow-brown and chocolate brown. These variations reflect differences in mode of formation and chemical composition. One sample of light green cellular texture was found to have an aluminium to iron ratio of 1.79:1, whereas brown material from the same deposit had an aluminium to iron ratio of 0.63:1.

It is apparent from petrological and field observations that this material was formed by the phosphatic alteration (metasomatism) of volcanic rocks. The alteration has proceeded along fractures. Partially altered material from the locality west of Camp 4 was observed in which the shapes of the ferromagnesian and feldspar phenocrysts were preserved (Section 7, Plate 12). The brecciated texture of some of the samples has resulted from partial phosphatization.

The chemical process involved in this metasomatism is essentially one of removal of silica and introduction of phosphorus. The volcanic rocks when fresh contain over 35 per cent silica, whereas the phosphatized rocks contain less than 5 per cent. The phosphorus, as pentoxide, can be as high as 40 per cent.

On weathering, these rocks produce a dark brown soil consisting mainly of crandallite, and this mineral has been found constituting large "boulders" which have probably weathered in situ. The conversion to crandallite would involve both hydration and calcification presumably resulting from the action of lime-bearing ground waters and a change in pH from acid to alkaline (Section 8). Calcium is either accessory or absent in the barrandite rock. Some goethite may also form from excess iron in the weathering process.

11.2.3 Crandallite and Millisite Deposits

Crandallite and millisite are the most common phosphate minerals at Christmas Island. They occur over a large area of the upper plateau and constitute the bulk of the soil formed on both limestone and volcanic terrain. Considerable amounts of these minerals also occur in the overburden of the calcium phosphate (apatite) deposits.

Both crandallite and millisite are earthy minerals, submicroscopic in grain size, and vary in colour from light to chocolate brown. In composite samples these minerals are difficult to differentiate optically, and their presence has been determined in all cases by x-ray diffraction examination.

As mentioned in Section 8, crandallite was observed as an alteration product of barrandite, and the soil profiles on the phosphatized volcanic rocks contain crandallite as a dominant constituent. Millisite was observed, however, in the soil developed on the fresh volcanic rock at Ross Hill, and millisite and crandallite were detected in the soil derived from the phosphatized volcanics to the east of Aldrich Hill.

Crandallite and millisite were found to be the dominant constituents of the soil formed from the weathering of the limestones where they are associated with goethite, boehmite and (?)gibbsite. The soil profile is essentially lateritic, as clays and free silica constitute only a minor portion of this material. Laterite and bauxite are frequently formed from the weathering of limestone and 20 per cent of the world's bauxite reserves are of this type. Table 36 shows a comparison of the chemical composition of the lateritic soils from Jamaica and those of Christmas Island. The Jamaican data are thos recorded by Hose (1963).

There are several marked similarities between the geology of Jamaica and that of Christmas Island. Both islands consist mainly of volcanic and pyroclastic rocks and organic limestone; are of middle to lower Tertiary age; occur in approximately the same equatorial zone and have similar climates. Jamaica is much larger than Christmas Island however (4,411 square miles as against approximately 50 square miles)

and is somewhat higher (1500 to 2500 feet above sea level in the upland regions of Jamaica, whereas Christmas Island rises to 700-1100 feet). Jamaica in 1961 was the world's largest producer of bauxite with a production exceeding 5,000,000 tons per annum.

TABLE 36: SOME CHEMICAL ANALYSES OF JAMAICAN AND CHRISTMAS ISLAND SOILS

	Sample Number[c]					
	J-1	J-2	J-3	CI-A/17	CI-A/8	CI-A/2
H_2O	28.1	30.8	15.6	15.6	18.93	19.93
SiO_2	0.4	0.6	23.2	0.64	9.10[a]	7.68[a]
Fe_2O_3	16.3	6.5	16.4	13.24	12.3	14.3
Al_2O_3	49.2	58.9	42.9	24.5	29.9	26.8
TiO_2	2.4	3.2	1.9	1.56	nd[b]	0.96
CaO	0.7	-	-	11.5	8.0	8.2
MgO	0.1	-	-	0.22	0.12	0.16
MnO	0.2	-	-	0.15	0.20	0.28
CO_2	-	-	-	0.43	0.51	0.46
P_2O_5	2.3	-	-	27.0	17.7	19.0
Al_2O_3/Fe_2O_3	3.02	9.08	2.62	1.85	2.43	1.88
R_2O_3/SiO_2	164	109	2.57	63	4.64[a]	5.37[a]

(a) SiO_2 figure here quoted is total acid insoluble and may contain TiO_2 and R_2O_3 (Al_2O_3 + Fe_2O_3), in major proportions, with corresponding decreases in R_2O_3 figures quoted.

(b) nd - Not determined.

(c) J-1 Yellow bauxite, Manchester Parish, Jamaica.
Mineralogy: Major – gibbsite;
Lesser – goethite, anatase;
Minor – hematite, quartz, boehmite, Ca-Al phosphate.

J-2 White bauxite pocket 44 feet deep in yellow bauxite, St Elizabeth Parish, Jamaica.
Mineralogy: Major – gibbsite (75%);
Lesser – boehmite (11%), goethite, anatase;
Minor – kaolinite and/or halloysite.

J-3 Low lying terra rossa on Upper Eocene limestones, Trelawny Parish, Jamaica.
Mineralogy: Major – kaolinite and/or halloysite;
Lesser – hematite, boehmite, gibbsite;
Minor – Ca-Al phosphate, goethite.

CI-A/17 Phosphatic soil near summit, Ross Hill, Christmas Island.
Mineralogy: Major – millisite;
Minor – crandallite, apatite.

CI-A/8 Phosphatic soil between Grant's Well and Phosphate Hill, Christmas Island.
Mineralogy: Major – crandallite;
Minor – goethite, boehmite.

CI-A/2 Phosphatic soil east side of Murray Hill, Christmas Island.
Mineralogy: Major – crandallite;
Minor – goethite and/or gibbsite.

Table 36 illustrates the lateritic nature of the crandallite and millisite bearing soil profiles at Christmas Island. The principal difference between those of Christmas Island and those of Jamaica is the presence of considerable phosphate in the former, but the alumina to iron oxide and the combined sesquioxides (R_2O_3) to silica ratios are comparable. There is some controversy as to the origin of some of the Jamaican bauxites and laterites, some arguing that these minerals are derived from the weathering of limestone and others considering that they originate from the weathering of volcanic detritus. The trace element constituents of the limestones, volcanic rocks and soils will possibly assist in the solutions of these problems.

The conditions favouring the formation of crandallite and the formation of millisite are not known. Both these minerals dominate the soil profiles developed from limestones and volcanic rocks. It was found, however, that the samples collected between Grant's Well and South Point consist mainly of millisite, those north of Grant's Well contain only minor millisite and those west of the railway contain both millisite and crandallite. This regional distribution may be an over simplification as the areas were sampled rather sporadically and no soil profile was sampled to more than 3 feet in depth.

Published data on the occurrence and distribution of millisite and crandallite are meagre. Millisite was originally reported as a constituent of variscite nodules from Fairfield, Utah, (Larsen and Shannon, 1930) and was reported in the aluminium phosphate zone of the Bone Valley Formation, Florida, (Owens et al, 1960). Ferruginous millisite (pallite) was reported from Senegal, French West Africa (Capdecomme et al, 1954). The Fairfield millisite differs in habit and mineralogical association from other reported occurrences and is considered to be an alteration product

after variscite. Most data available on the occurrence of millisite is that relating to the Bone Valley Formation, Florida. According to Owens et al (1960), the millisite is an important intermediate phase in the paragenesis of lateritically altered phosphorites. The aluminium phosphate zone of the Bone Valley Formation is the result of progressive replacement of calcium phosphate and clay by aluminium phosphate and quartz. Of the phosphate minerals, apatite characterizes the unaltered basal part; calcium-aluminium phosphates, crandallite and millisite the middle part; and wavellite, the pure aluminium phosphate, is the stable and commonly the sole phosphate mineral in the upper, most altered, part. The Senegal ferruginous millisite is reported to have formed by the reaction of tricalcium phosphate with montmorillonites. Owens et al (p 560) question the presence of iron in the millisite lattice in the Senegal millisite which Capdecomme et al (1954) consider to be in substitution for about 10 per cent of the alumina. The latter authors also report calcium in substitution for alkalis in millisite.

Chemical analyses of the millisite samples from Christmas Island (Section 8) suggest that the atomic ratios of calcium, phosphorus and aluminium (and iron) are more comparable with those of crandallite than with the reported formulae of millisite, and there is some indication that these minerals are polymorphs of the chemical compound $Ca(Al, Fe)(PO_4)_2(OH)_5.H_2O$. It was found that iron substitutes for aluminium in millisite, and the deficiency of alkalis in some of the millisite samples supports the conclusions of Capdecomme et al (1954). The samples consisting dominantly of millisite were found to contain approximately 2.5 times the amount of alkali present in the samples consisting dominantly of crandallite (Table 19). The absence of pure samples of millisite from any reported occurrence makes precise formulation of this mineral difficult.

Much of the crandallite and millisite at Christmas Island does not occur in direct association with calcium phosphate (apatite) deposits and it is considered that the term phosphorite used by the authors mentioned above refers to these deposits. Millisite and crandallite do occur in the overburden on the apatite deposits at Christmas Island, but considerable deposits of these minerals have apparently formed directly from the weathering of the limestone and volcanic rocks in the presence of phosphorus. This phosphate may be present in ground waters. In some cases, however, the alteration of the apatite to crandallite and to millisite may be complete. Wavellite was only detected in one of the samples examined, but the formation of aluminium phosphate is not completely comparable with that of the Bone Valley Formation. It might also be mentioned that the Bone Valley phosphorite is essentially a continental phosphate deposit, as distinct from the insular phosphates of the islands. The former deposits commonly contain considerable clay contamination and are formed by a different mechanism.

Hutchinson (1950) has recorded analyses of iron and aluminium phosphates from insular phosphate deposits. One such analysis, that of material from Navassa (p 324), has been calculated by the writer in terms of crandallite and apatite and found to be consistent with this mineralogy. It is probable that minerals of these types are common and widespread in occurrence in insular phosphate deposits as well as in continental deposits.

These calculations are included in Table 37. The analysis is that of the "red phosphate" and was given by D'Invilliers in 1891.

TABLE 37: CHEMICAL AND MODAL ANALYSIS OF RED PHOSPHATE FROM NAVASSA ISLAND

	Analysis[a]	Moles	Sum	Crandallite			Apatite		
				Theoretical Mole Ratio	Subtraction	Difference	Theoretical Mole Ratio	Subtraction	Difference
	%								
P_2O_5	29.78	0.21	-	2	0.162	0.048	3	0.048	-
CO_2[b]	3.53	0.08	-	-	-	-	-	-	-
Al_2O_3	18.42	0.181	0.243	3	0.243	-	-	-	-
Fe_2O_3	9.80	0.062							
CaO	23.09	0.41	-	2	0.162	0.25	10	0.16	0.09[d]
H_2O[c]	14.22	0.79	-	7	0.57	0.22	-	-	-
Insoluble	-	-	-	-	-	-	-	-	-
SO_3	1.16	0.014	-	-	-	-	-	-	-
Total	100.0								

(a) Analysis by D'Invilliers (1891).
(b) CO_2 by difference.
(c) H_2O is loss on ignition.
(d) The excess moles of CaO (0.09) is equivalent to the CO_2 and SO_3 and may represent calcite and anhydrite (or gypsum).

It is evident from the mole ratios that the sesquoixides are present in phosphate minerals, as there is an excess of P_2O_5 over the stoicheiometric requirements of CaO for apatite.

Crandallite and millisite are the dominant mineral constituents in the overburden of the phosphorite (apatite) deposits at Christmas Island. Both these minerals are present in the overburden in the workings at Phosphate Hill, but at South Point millisite appears to dominate. Both minerals were detected in the overburden on the phosphorite on the west side of Murray Hill (Sample A3), but in the deposits near Camp 5 (Sample A4) millisite is the only iron-aluminium mineral present. The overburden at this last locality differs in appearance from the others, the colour being light grey.

The iron-aluminium phosphate decreases with depth and apatite dominates the mineralogy of the phosphorite. The junction between the iron-aluminium phosphate zone and the apatite is gradational and laterally very irregular (Plate 5A). A mottled brown-white zone, consisting of apatite, crandallite and millisite, occurs between the two deposits in some of the workings at Phosphate Hill. This zone is not well developed in the East Quarry at South Point or in Field 5A at Phosphate Hill, and in these areas apatite is present in the overburden.

The analyses of the crandallite samples also indicate that the iron present is an essential constituent of this material in some cases and is in substitution for aluminium. However, some of the samples, namely those taken from areas devoid of apatite, do contain minor amounts of free iron and/or aluminium hydroxides. The results indicate that, in the presence of phosphate, crandallite and millisite form at the expense of the iron or aluminium hydroxides, these minerals occurring only in areas relatively deficient in phosphorus.

Sweatman (1961, p 115 et seq) found that under severe or prolonged weathering conditions, phosphatic rocks produced soil containing minerals of the gorceixite group, the species formed being dependent to a large degree on the composition of the parent rock. Thus rocks containing accessory or minor quantities of apatite and monazite were found to produce gorceixite and florencite in the residual soils. These minerals accounted for most of the phosphate from the parent rock. The weathering of the calcareous rocks of Christmas Island in the presence of phosphate ions has likewise formed a mineral of the gorceixite group, the abundance of lime leading to the formation of crandallite.

In the soils formed with insufficient phosphate ions for the inclusion of all the sesquioxides in crandallite or millisite, the iron and aluminium hydroxides, goethite and boehmite, have formed. Thus, in soil profiles formed from the weathering of carbonate and volcanic rocks, in the absence of apatite, the crandallite and millisite are associated with these minerals.

Gorceixite (the barium member of the group) was observed in the phosphatized volcanic rocks and goyazite (the strontium member) may also be present. The formation of these minerals is considered to be related to the presence of barium and strontium of volcanic origin. Sweatman (p 121), concluded that the formation of minerals of the gorceixite group was

largely responsible for the fixation of phosphorus in soils. He found also that many elements (such as copper, chromium and lead) were taken up by these minerals, reducing their availability to vegetation.

Some fluorine was found to be present in the crandallite and millisite. The fluorine and phosphorus pentoxide content of 6 samples from Christmas Island, which are known not to contain apatite but are dominantly crandallite and/or millisite, are recorded in Section 9, Table 31. This table shows that the fluorine content of the apatite is about 18 times greater than that of the iron-aluminium phosphate and the fluorine to phosphate ratio 5.2 times greater. Seven analyses of crandallite and the average of 2 analyses of millisite are reported by Palache, Berman and Frondel (1951), pp 836, 942), none of which recorded fluorine determinations. Owens et al (1960) likewise do not report any fluorine determinations on the Florida material. However, Pikrovskii and Grigor'ev (1963) report the loss of fluorine from crandallite upon heating to 600^{0}C. This crandallite from the Middle Urals, occurs in the upper horizons of greisenized aluminium silicate-carbonate rocks and muscovite-fluorite greisens in contact with low grade metamorphic sandy-clayey sediments and albite-amphibole biotite schists. Hill, Armiger and Gooch (1950, p 699) report 0.73 per cent fluorine in crandallite (pseudowavellite)-bearing beds of the Bartow-Pembroke region of Florida. Here the fluorine to phosphorous pentoxide ratio is 0.0084 and is therefore comparable with the material from Christmas Island. The fluorine present in crandallite and millisite is considered to replace hydroxyl ions in the same manner as it does in fluorapatite.

The trace element constituents of some crandallite and millisite samples are summarized in Table 33 and are compared with a similar summary of Florida material recorded by Owens et al (1960). Spectrographic analyses of the Christmas Island apatite are included in Table 32. The data show a marked similarity between the crandallite-millisite from Christmas Island and from Florida. This is particularly significant as the primary phosphorites from which they were formed differ in origin. The hydrolzate elements (that is those of lower solubility in ground waters) are of higher concentration in the crandallite-millisite samples than in the apatites. The results suggest that the crandallite and millisite are lateritic derivatives.

Variations in the content of some elements, notably titanium and chromium, were recorded and it is possible that these variations reflect the parent rock from which the crandallite/millisite-bearing soils were formed. Those formed from volcanic rocks contain a higher concentration of titanium and chromium than those formed from carbonate rocks or apatite. The results obtained in this investigation are semi-quantitative and the parent rock composition of many of the samples is not known. However the use of certain trace elements for the determination of bedrock under crandallitic and millisitic residual soils is likely to be of some value in future exploration and further studies of the variations of these elements is considered desirable.

11.3 The Origin of the Christmas Island Phosphate Minerals

The exploration and development of the phosphate deposits at Christmas Island will depend to a large degree on an understanding of their origin.

Commercial phosphate deposits of the world are of igneous or sedimentary origin and those of the latter group are classified as primary bedded phosphorites, secondary phosphorites, or guano deposits.

The igneous phosphates are apatitic and occur as segregations in large basic igneous intrusions. The main deposits of this type occur in the USSR, Norway, Sweden, Canada, Uganda and Brazil. The principal deposit in the USSR averages 30 per cent phosphorus pentoxide as mined, and the gangue minerals are aluminium and ferromagnesian silicates.

The primary sedimentary phosphates or phosphorites are normally thin stratigraphic units interbedded in marine sediments. The main phosphate mineral of these deposits is also apatite, sometimes of nodular habit, having formed on continental shelves. The phosphatic limestone of the Phosphoria Formation of the USA are of this type. The mode of formation of this phosphate is still unknown, but it is believed to be contemporaneous with the deposition of the sediments. Certain brachiopods which secrete a phosphatic shell may also be responsible for the phosphatic members in certain marine sediments.

The secondary phosphorites are those formed by the weathering of phosphatic sediments, the phosphate being concentrated in the weathered derivatives. Some of the Florida deposits are of this type.

A more complete review of the primary and secondary phosphate deposits is given by Warin (1961).

Guano deposits are not strictly sedimentary but are of biogenic origin. Most, if not all, insular phosphate deposits are of this type. Guano is formed by the accumulation of the excreta and egesta of vertebrate organisms and may be classified as modern, when formed by contemporary organisms, or ancient, when the accumulation of excrement has ceased as a result of the desertion of the deposit by the guano producing organisms. Such deposits are generally no older than Pleistocene.

It is known from oceanographic studies that Christmas Island is an isolated, conical mountain rising approximately 15,000 feet from the ocean floor. The geological investigations of the rocks now outcropping indicate that the island is an extinct volcano and the limestones which are interbedded with the volcanic rocks were developed by reef building organisms such as corals, molluscs, foraminifera and algae. The geological environment in which the phosphate occurs at Christmas Island is not comparable with that of the continental deposits of the USA and elsewhere. The environment is, however, comparable to that of other island phosphate deposits (insular phosphates), some of which are being formed at the present time. It must be concluded that formation of the phosphate is not the result of conditions similar to those existing on continental slopes or the floors of oceans.

Field observations also indicate that in all probability there is no relationship between the formation of the phosphate and the volcanic rock. Some extrusives, principally those of basic composition, do contain accessory apatite, but the phosphate content of the rocks is usually less than 2 per cent. Furthermore, if the phosphate were of igneous origin, it would be expected that the phosphate deposits would be associated primarily with these rocks. Field observations do not support this contention, the phosphate being associated with the volcanics and with the limestones.

Likewise there is little evidence to suggest that the phosphate has been deposited by the reef building organisms. Clarke and Wheeler (1922) have studied the inorganic constituents of the marine organisms found in sedimentary rocks and have detected only a trace of phosphorus in most foraminifera, corals, molluscs and algae. These are the principal organisms of the limestones of Christmas Island. Also it is considered that, if the phosphate had originated in the limestones, the deposits would be preferentially associated with these rocks, but field observation indicates that a considerable amount of the volcanic material outcropping in the upper areas of the island has been extensively phosphatized as well as the limestones.

An external origin, such as that of guano deposits, then appears to be the only feasible explanation of the geological condition. The similarity of the occurrence of the Christmas Island phosphate and that of known guano deposits further supports this contention.

The conditions favouring the accumulation of guano deposits are discussed in some detail by Hutchinson (1950). Generally, guano deposits are formed only when the organisms producing the guano are large and feed over a large trophophoric field and return to a limited site for rest and reproduction. Additionally, certain physical conditions must apply, namely that the substratum must be of such a form as to retain the deposit and that the rainfall must be low so as to limit denudation. The area of a guano deposit must also be reasonably free from predatory animals.

The biological conditions are fulfilled mainly by birds, although small guano deposits have been formed by mammals such as seals and cave-dwelling bats and by ants. Birds have several advantages; they have the necessary intelligence to develop a colony, they feed over a large trophophoric area and,unlike mammals, they excrete a semi-solid urine in which the main nitrogenous constituent is uric acid. The compositional difference between mammal and avian excreta are thought to be related to the egg stage, the more easily diffusible waste (urea) being substituted by the more convenient uric acid, and this function is retained throughout the life of the bird. This situation is similar to that of reptiles.

Not all colonial sea birds produce guano deposits. Certain varieties, such as several species of Pelecaniformes (pelicans, boobies, cormorants), Sphenisciformes (penguins), albatrosses and terns, appear to deposit the excrement on the colony for nest-making. Other species such as gulls generally avoid the deposition of excrement near the colony.

The physical conditions most suitable for the support of large bird colonies are related to the distribution of ocean currents. Those zones in which the distribution of the currents is such as to cause the upwelling of colder water, which contains more nutrient elements, more frequently contain guano-bearing land masses. Furthermore the major guano deposits are associated with areas of low rainfall. In the southern hemisphere these conditions are most typically fulfilled along the west coasts of the continents (Africa and South America) and in equatorial zones. The seas adjacent to west coasts of the continents of the southern hemisphere are influenced by the influx of cold currents which move in a counter-clockwise system, originating in the higher latitudes. These currents, under the influence of the land masses, bring nutrient elements into the surface waters. The friction set up between this current, together with its counterpart in the northern hemisphere which flows clockwise, and the equatorial counter current produce vertical divergences which likewise bring nutrient elements into surface waters near the latitudes 5^0 north and 5^0 south (Barnes, 1957).

The physical conditions stated above are applicable to the west coast of the Australian continent as well as those coasts of Africa and South America, and it is the author's opinion that some thought might be given to the exploration for guano deposits along this coastline. Some minor deposits are known from the Abrolhos Islands near Geraldton (British Sulphur Corp., 1964), and Cretaceous phosphatic sediments occur at Dandaragan, 108 miles north of Perth. These deposits are not of economic proportions.

Christmas Island, as well as Ocean Island and Nauru in the Pacific, is located in the low latitudes and therefore is probably influenced by the frictionally produced vertical divergences in the ocean currents. The rainfall, vegetation and physiography of the island are not considered conducive to bird colonization. However, the distribution of the phosphate deposits suggests that they were probably formed at a time when the island was emerging and existed as an atoll consisting of what is now the upper plateau. Under such conditions the climate was probably more arid and the vegetation less prolific. These conditions may have existed as early as late Miocene time and there is no evidence available of the age of the phosphatization.

It is concluded therefore, that the three essential rock types of Christmas Island are:

a. volcanic rocks,

b. organic limestones and derivative calcareous sediments,

c. guano.

From the available data the formation of the phosphate minerals is summarized below and presented diagrammatically in Figure 21. The three primary rock types, guano, limestone and volcanic rocks are enclosed in rectangular blocks. The processes summarized in the diagram are as follows.

Removal of Nitrogenous (organic) Matter from the Guano by Aerobic Decay, Leading to the Formation of Apatite. Little data on this process exists in spite of the number of deposits of modern guano in other parts of the world which are available for study. According to Hutchinson (1950, p 71) an approximate analysis of Pelecanus occidentalis thagus is:

	%	
H_2O	9.40	
Organic matter	81.75	
Total N	21.66	
P_2O_5	4.30	(≡ 1.88% P)
Alkali	3.70	
Sand	0.85	

Nitrogen constitutes 26.5 per cent of the organic matter which, in all probability, according to Hutchinson, is mainly uric acid. The nitrogen to phosphorus ratio is 11.5 to 1 and, on a moisture free basis, nitrogen constitutes 24.13 per cent of the sample and phosphorus 2.09. It is apparent that a considerable quantity of the original guano would be lost during aerobic decay, leaving dominantly (calcium) phosphate compounds.

Weathering of Limestone in the Absence of Phosphate. Samples of the soil developed from the weathering of limestone in the absence of phosphorus have not been observed from Christmas Island. However, it has been shown that this is the normal condition for the formation of laterite and/or bauxite. The minerals constituting laterite and bauxite are dominantly iron and aluminium oxides and hydroxides, together with minor quartz and clay.

Reaction of Guano with Lateritic Soil. This leads to the formation of crandallite and millisite, and mixtures of these minerals, together with normal laterite minerals or apatite, are common in limestone areas at Christmas Island. The presence or absence of apatite or iron/aluminium oxides or hydroxides is controlled by the amount of phosphorus available.

Metasomatism of Limestone by Phosphate-bearing Solutions Derived from the Guano. Examples of this reaction are commonplace in the limestones underlying the major phosphorite deposits, and the depth at which this takes place may be in excess of a hundred feet from the leached guano. The apatite thus formed is massive and white.

The Lateritization of Apatite. This is apparent in the phosphate workings where crandallite and millisite have formed as a result of leaching and removal of the more soluble constituents.

Lateritization of the phosphatized limestone also leads to the formation of crandallite and millisite, together with the oxides and hydroxides of iron and aluminium. It has not been possible to differentiate between the crandallite and millisite formed by the lateritization of phosphatized limestones and those formed by the phosphatization of laterite.

Weathering of Volcanic Rocks in the Absence of Phosphate. This process is also difficult to observe on the upper plateau owing to the ubiquity of the phosphate. The soil formed in this way, however, was observed on the volcanic rocks on the inland terrace behind the Asian school at Drumsite The profile here developed consists of iron oxides and hydroxides and disordered kaolin minerals.

The metasomatic reaction of phosphate with the laterite formed from the weathering of volcanic rocks is similar to that formed from limestones.

The Phosphatic Metasomatism of the Volcanic Rocks. The minerals of the variscite-strengite series (barrandite) are formed by this process. The replacement of the original igneous minerals by the iron-aluminium phosphates is, in part, pseudomorphic. Silica is removed during this reaction.

The Weathering of the Phosphatized Volcanic Rocks. Crandallite and/or millisite are again formed by this process.

It can be seen therefore that the crandallite and millisite may form in three different ways; from the limestones, from the volcanic rocks and from the guano.

12. CONCLUSIONS

In this investigation of the geology and mineralogy of the phosphate and related rocks of Christmas Island, an attempt has been made to delineate, in general terms, the nature and mode of occurrence of the principal rock types and mineral deposits. The investigation has been in the nature of a reconnaissance, as it has not been possible to map the extent and distribution of the rock types, nor to compute the size of the phosphate deposits. The conclusions from the investigation are summarized as follows:

12.1 Nature of the Island

The island consists essentially of volcanic rocks and bio-constructed limestones and their derivatives. It is an isolated volcanic cone, probably initiated in the Mesozoic era and extending into Tertiary time.

12.2 Period of Formation of the Island

From palaeontological evidence it has been found that the majority of the rocks above sea level were formed during the Eocene and lower and middle Miocene epochs, there having been an hiatus in the Oligocene epoch. Recently elevated reef limestone has been identified in the shore terrace.

12.3 The Volcanic Rocks

The volcanic rocks are contemporaneous with the carbonate rocks and exposures in the Eocene and Miocene formations were examined. There is a general decrease in acidity of these rocks from the oldest to the youngest. Their compositions range from andesites and trachybasalts to limburgites. Volcanic rocks were observed on the highest areas of the island.

12.4 The Carbonate Rocks

The geological history and the mode of occurrence of the carbonate rocks are discussed. It is concluded that the carbonate rocks were formed in and adjacent to organic reefs and that atoll conditions existed in the centre of the upper plateau. The processes of dolomitization, thought to have been operative during carbonate deposition, diagenesis are considered to be related to the mineralogical composition of the tests and to the geochemical environment of enclosed saline lagoons.

12.5 Situation of the Phosphate Deposits

The phosphate deposits occur on the upper plateau, generally at an elevation higher than 700 feet above sea level. One deposit now exploited occurs on a terrace between Drumsite and the Settlement at an elevation of about 400 feet.

12.6 The Age of the Phosphate Deposits

The age of the phosphate deposits could not be determined accurately. They overlie the youngest identifiable rocks which are of the Burdigalian stage of the Miocene epoch. Much of the upper carbonate rock is recrystallized, dolomitized and phosphatized, any fossils thus being destroyed.

12.7 Mineralogy of the Phosphate Deposits

The phosphate deposits are of three main types: apatite, crandallite and millisite and barrandite.

Apatite was observed mainly in association with carbonate rocks which it overlies and replaces. Some alluvial pebble beds of apatite occur on terraces between the upper plateau and the sea.

Crandallite and millisite occur extensively on the upper plateau. These minerals form the overburden of the phosphorite (apatite) deposits, from which they have formed by lateritization, as major constituents of the weathered derivatives of the carbonate rocks (phosphatic lateritization) and as a result of the weathering of phosphatized volcanic rocks (barrandite).

Barrandite was observed in several areas on the plateau and has formed as a result of phosphatic metasomatism of volcanic rocks which were presumably of limburgitic composition.

12.8 Chemistry of the Phosphate Minerals

Chemical, x-ray diffraction and differential thermal analyses of the phosphate minerals were carried out. The substitutions involving fluorine and carbonate radicals in apatite were examined and several conditions for these substitutions were postulated. Some tentative data on the distribution of fluorine in the phosphorite deposits were obtained.

The composition of the crandallite and millisite minerals was examined. It was concluded that iron substitutes for alumina in both these minerals and that alkalis are not essential constituents of millisite. The data available suggest that crandallite and millisite may be polymorphs of the one chemical compound corresponding essentially to the formula stated for crandallite but including some iron in place of alumina.

Chemical analysis and semi-quantitative electron probe micro-analysis indicate that considerable (up to 17%) titanium may be present in some of the barrandite samples. This element appears to be incorporated in the barrandite structure.

The elemental distribution in the barrandite samples was examined by electron probe microanalysis. It was found that the metasomatism of the original volcanic (lumburgitic) rocks to form barrandite involves the initial removal of silicon, magnesium and calcium and the redistribution of iron and aluminium, together with the introduction of phosphorus and the hydration of the rock. The process is partly pseudomorphic, preserving the outlines of the original volcanic (olivine) phenocrysts. Subsequently crandallite is deposited in veins in the barrandite rock and cements barrandite fragments. Minor apatite may be deposited in the final stages.

The metasomatism occurs in two distinct chemical environments; the first being acid and the second alkaline.

Semi-quantitative determinations of the trace elements of the major phosphates were carried out. It was found that there is a significantly higher concentration of the hydrozates in the crandallite and millisite samples than in those of the apatites. There is a marked similarity of the trace element content of these minerals with those of the Florida deposits. Variations in certain elements in the crandallite/millisite, notably titanium and chromium, are considered to reflect differences of parent rock.

12.9 The Relationships of the Phosphate Minerals

The greater part of the apatite in the phosphorite deposits (phosphate fields) is free of contaminants but in shallow deposits and in deeper sections of other deposits carbonate minerals may be present. In the upper sections of the deposits the apatite is associated with crandallite and millisite. Oxides and hydroxides of iron and aluminium are rare and subordinate in the overburden on apatite deposits.

Crandallite and millisite occur in association together with apatite when forming overburden on phosphorite deposits, with goethite, boehmite and (?)gibbsite in the soil profiles on carbonate and volcanic rocks and with barrandite in the soils overlying phosphatized volcanic rocks.

Barrandite is associated with accessory chlorite and chromite, and with montgomeryite, crandallite and gorceixite.

In the phosphatic overburden on apatite deposits, the combined sesquioxide content can generally be used as an index of the content of crandallite and millisite. In other samples containing these minerals, the phosphorus content is a more reliable index of their abundance, owing to the presence of goethite and boehmite. Samples consisting of apatite and free oxides or hydroxides of iron or aluminium were not observed.

12.10 Thermal Studies of the Phosphates

Thermal studies of the apatite, crandallite, millisite and barrandite were carried out to obtain an understanding of the reaction of these minerals to calcination. Apatite was found to be essentially inert to 1000°C. Crandallite and millisite become essentially amorphous after loss of water

of crystallization at 400 to 500°C and recrystallize as anhydrous orthophosphate compounds above 750°C. Barrandite losses water of crystallization readily below 150°C and adopts a derivative crystal structure. At higher temperatures (between 300°C and 1200°C) it recrystallizes forming the anhydrous orthophosphate compound.

An inverse relationship between crystallinity and the citrate solubility of the phosphate is indicated.

12.11 Origin of the Phosphate

The majority of the phosphate deposits are considered to be of avian guano origin. The biogeochemical and physical factors affecting the formation of the phosphate are reviewed and the processes of the derivation of the various phosphate minerals outlined.

13 ACKNOWLEDGEMENTS

The author wishes to express his gratitude to the considerable number of people who have contributed by the organization of the field investigations, for assistance on the island and for technical discussion and encouragement during the laboratory work.

He is particularly indebted to Messrs T. A. Adams, Assistant General Manager, R. L. Nevile, Superintendent Engineer, and Dr. B. Doak of the British Phosphate Commissioners for their assistance, encouragement and patience during the course of the investigation. He further wishes to record his appreciation to the Island Manager for Christmas Island, Mr. N. Cooke, and his staff for their assistance on the island. He is also indebted to Messrs R. Bishop, D. Forrestor, M. Manners and D. Powell in this respect.

Considerable technical assistance was received from members of AMDEL, notably Messrs A. L. Keats, J. D. Hayton, D. K. Rowley, B. H. J. Waters and A. B. Timms as well as colleagues in the Mineralogy and Petrology Section.

Others with whom discussions were held on various aspects of the investigation include Professors A. R. Alderman and M. F. Glaessner and Drs J. B. Jones and B. Neville of the University of Adelaide and Dr. K. Norrish and Mr. T. R. Sweatman of the CSIRO, Division of Soils.

Finally he wishes to express his gratitude to Dr. N. H. Ludbrook of the S. A. Department of Mines for carrying out the palaeontological investigation and for discussions on the island geology.

14. BIBLIOGRAPHY

1. ALDERMAN, A.R., (1964) "The Origin of Dolomite". Pres. Address, Royal Soc. of South Australia (unpub) (1964).

2. ANDREWS, C.W., (1900), "A Monograph of Christmas Island (Indian Ocean)". Brit. Mus. Nat. Hist. (1900).

3. AUBERT, G., (1960), "The Phosphoric Acid of the Soils of Tropical Regions" Intern. Superphosphate Manufacturers' Assc. Agric. Comm. Paris Extr. Bull Docum. No. 27, (May, 1960).

4. BARNES, H., (1957), "Nutrient Elements" in "Treatise on Marine Ecology and Palaeoecology. Vol 1, Ecology". Geol. Soc. Amer. Mem. 67. J.W. Hedgpeth (Ed) (1957).

5. British Sulphur Corporation Ltd, The, (1964), "A World Survey of Phosphate Deposits". Woodalls Ltd, 2nd ed. (1964).

6. BRITTON, H.T.S., (1956), "Hydrogen Ions – Their Determination and Importance in Pure and Industrial Chemistry". Vol 2, Chapman and Hall Ltd, Lond. (1956).

7. BUERGER, M.J., (1947), "Derivative Crystal Structures" Journ. Chem. Phys., Vol 15, pp 1-16, (1947).

8. CAMPBELL-SMITH, W., (1926), "The Volcanic Rocks of Christmas Island". Quart. Journ. Geol. Soc. Lond. 82, pp 44-66, (1926).

9. CAPDECOMME, L., and PULOU, R.M., (1954), "Sur la radio-activite des phosphates de la region de Thies (Senegal)". Acad. Sci. Paris, Comptes Rendus, 239, pp 288-290, (1954).

10. CLARKE, F.W., and WHEELER, W.C., (1922), "The Inorganic Constituents of Marine Invertebrates". U.S.G.S. Prof. Paper, 124 (1922).

11. COFFER, L.W., and TRUEMAN, N.A., (1964), "Field Investigations – Christmas Island, September-October 1964". AMDEL Report 386, unpub, (1964).

12. COLE, C.V., and JACKSON, M.L., (1951). "Solubility Equilibrium Constant of Dihydroxy Aluminium Dihydrogen Phosphate relating to a Mechanism of Phosphate Fixation in Soils". Soil Sci. Soc. Am. Proc., 15, pp 84-9 (1951).

13. COLEMAN, P.J., (1962), "An Outline of the Geology of Choiseul, British Solomon Islands". Journ. Geol. Soc. Aust., Vol 8, Pt. 2, p 135 et seq, (1962).

14. CORRENS, C.W., (1956), "Geochemistry of the Halogens" in "Physics and Chemistry of the Earth". Ahrens, Rankama and Runcorn (Ed), Pergamon Press, Lond. Vol 1, p 181 et seq. (1956).

15. COWGILL, U.M., HUTCHINSON, G.E., and JOENSEW, O., (1963), "An Apparently Triclinic Dimorph of Crandallite from a Tropical Swamp Sediment in El Peten, Guatemala". Am. Min., Vol 48, No. 9 and 10, p 1144, (Sept-Oct, 1963).

16. DEER, W.A., HOWIE, R.A., and ZUSSMAN, J., (1962). "Rock Forming Minerals" Vol 5 – Non-Silicates. Longmans (1962).

17. DUNBAR, C.O., and RODGERS, J., (1957), "Principles of Stratigraphy". John Wiley and Sons, New York (1957).

18. EITEL, W., (1952), "The Physical Chemistry of the Silicates". Uni. of Chicago Press. (1952).

19. EVANS, R.C. (1952). "An Introduction to Crystal Chemistry". Camb. Uni. Press, 1st Ed., (1952).

20. FISHER, D.J. (1958), "Pegmatite Phosphates and their Problems". Am. Min., Vol 43, No. 3 and 4 pp 181 et seq. (March-April, 1958).

21. FREDERICKSON, A.F., (1952), "The Genetic Significance of Mineralogy" in "Problems of Clay and Laterite Genesis, a Symposium". Am. Inst. Mining and Met. Eng. (1952).

22. GOODEN, J.E.A., RYAN, W., and TRUEMAN, N.A., (1964). "Laboratory Calcination of Phosphate Samples, 250-1350 Degrees Centigrade". AMDEL Report 349, unpub., (June, 1964).

23. GRAF, D.L., (1960), "Geochemistry of Carbonate Sediments and Sedimentary Carbonate Rocks".
Part 1 – Carbonate Mineralogy, Carbonate Sediments
Part 11 – Sedimentary Carbonate Rocks
Part 111 – Minor Element Distribution
Part 1VA – Isotopic Composition – Chemical Analyses
Part 1VB – Bibliography
Illinois State Geol. Surv., Circ. 297, 298, 301, 308, 309, (1960).

24. GRUBB, P.L.C., (1963), "Lateritization of Basalt near Hamilton, Western Victoria". CSIRO Minerag. Rep. No. 869, (June, 1963).

25. GALBRANDSEN, R.A., (1960), "Petrology of the Meade Peak Phosphatic Shale Member of the Phosphoria Formation at Coal Canyon, Wyoming". U.S.G.S. Bull 1111 C, (1960).

26. HABASHI, F., (1962), "Correlation between Uranium Content of Marine Phosphates and Other Rock Constituents". Econ. Geol., Vol 57, No. 7, p 1081, (Nov. 1962).

27. HATCH, F.H., WELLS, A.K., and WELLS, M.K., (1961). "The Petrology of the Igneous Rocks". Thos. Murby and Co. Lond., 12th Ed, (1961).

28. HAYTON, J.D., (1947), "An Unusual Rock Type from the Iron King Mine, Norseman". W.A. Dept. of Mines Govt. Chem. Lab, Unpub. Analyses, (1947).

29. HEIFKANEN, W.A., and VENING MEINESZ, F.A., (1958), "The Earth and its Gravity Field". McGraw Hill, New York, (1958).

30. HILL, W.L., ARMIGER, W.H., and GOOCH, S.D., (1950). "Some Properties of Pseudowavellite from Florida". Trans AIME, Vol 187, Mining Eng., pp 699-702, (June, 1950).

31. HOGARTH, D.D., (1957). "The Apatite-bearing Veins of Nisikkatch Lake, Saskatchewan". Canadian Min., Vol 6 p 140, (1957).

32. HOSE, H.R., (1963), "Jamaican Type Bauxites developed on Limestone". Econ. Geol., Vol 58, No. 1, pp 62 et seq. (Jan-Feb, 1963).

33. HUMMEL, F.A., (1949), "Properties of Some Substances Isostructural with Silica". Journ. Am. Ceram. Soc., Vol 32, No. 10, pp 320-326, (1949).

34. HUTCHINSON, G.E., (1950), "Survey of Exisiting Knowledge of Biogeochemistry -3- The Biogeochemistry of Vertebrate Excretion". Bull. Am. Mus. of Nat. History, Vol 96, (1950).

35. KITTLEMAN, J.R. (Jr.) (1963), "Glass-bead Silica Determination for a Suite of Volcanic Rocks from Owyhee Plateau, Oregon". Geol. Soc. Amer. Bull. V 74, pp 1405-1410, (Nov. 1963).

36. KOCH, S., and SORUDI, I., (1963), "The Hydrous Basic Aluminium Phosphates of Zeleznik (Vashegy), Slovakia (USSR)". Acta Min-Pet. Hung., Vol XVI, No. 1, pp 3-10, (1963).

37. LADD, H.S., TRACY, J.I. Jnr, WELLS, J.W. and EMERY, K.O., (1950), "Organic Growth and Sedimentation on an Atoll". Journ. Geol., V 58, pp 410-425, (1950).

38. LARSEN, E.S. (3rd), (1940), "Overite and Montgomeryite: Two New Minerals from Fairfield, Utah". Am. Min. Vol 25, p 315, (1940).

39. LARSEN, E.S. (3rd) and SHANNON, E.V., (1930), "The Minerals of the Phosphate Nodules from near Fairfield, Utah". Am. Min., Vol 15, pp 307-337, (1930).

40. MASON, B., (1958), "Principles of Geochemistry", John Wiley and Sons, 2nd Ed., (1958).

41. McCONNELL, D., (1938), "The Problem of the Carbonate Apatites. A Carbonate Oxy-apatite (Dahllite)". Am. Journ. Sci., Vol 236, pp 296-303, (1938).

42. McCONNELL, D., (1940), "Clinobarrandite and the Isodimorphous Series Variscite – Metavariscite". Am. Min., Vol 25, p 719 et seq, (1940).

43. McCONNELL, D., (1950), "Petrography of the Rock Phosphates". Journ. Geol., Vol 58, pp 16-23, (1950).

44. McCONNELL, D., (1952), "The Problem of the Carbonate Apatites IV. Structural Substitutions Involving CO_3 and OH". Bull. Soc. Franc. Min. Crist., Vol 75, pp 428-445, (1952).

45. McCONNELL, D., (1960), "Crystal Chemistry of Dahllite". Am. Min., Vol 45, No. 1 and 2, p 209, (Jan-Feb, 1960).

46. NUTTALL, W.L.F., (1926), "A Revision of the Orbitoides of Christmas Island (Indian Ocean)". Quart. Journ. Geol. Soc. Lond., Vol 82, pp 22-43, (1926).

47. OWENS, J.P., ALTSCHULER, Z.S., and BERMAN, R.. (1960), "Millisite in Phosphorite from Homeland, Florida". Am. Min., Vol 45, No. 5 and 6, pp 547-561, (1960).

48. PALACHE, C., BERMAN, H., and FRONDEL, C., (1951), "Dana's System of Mineralogy – Seventh Edition". John Wiley and Sons, New York, Vol 11, (1951).

49. PIRSON, S.J., (1959), "Recovery of Phosphate by In Situ Mining". Soc. of Mining Eng. of AIME, Preprint No. 59H4, (1959).

50. POKROVSKII, P.V., and GRIGOREV, N.A., (1963), "Crandallite from Hydrothermal – Pneumatolytic Zones in the Middle Urals". Inst. Geol. Ural Branch Acad. Sci. USSR., Sverdlovsk Zap. Vses Mineralogy. Obshchestva 92, (5), pp 601-607, 1963, (Chem. Abs. 60, No. 4, Feb. 1964, p 3878).

51. PORTER, J. L., (1958), "Recovery of Phosphate and Alumina from Minerals of the Wavellite and Crandallite Group". Chem. Abs., (1958), p 20955a.

52. RANKAMA, K., and SAHAMA, Th. G., (1949), "Geochemistry". Uni. of Chicago Press, (1949).

53. SCHLANGER, S. O., (1964), "Petrology of the Limestones of Guan" U. S. G. S. Prof. Paper 403D, (1964).

54. SCHULTZ, J. R., and CLEAVES, R. B., (1958), "Geology in Engineering". John Wiley and Sons, New York (1958).

55. SPRY, A., (1962), "The Origin of Columnar Jointing, Particularly in Basalt Flows". Journ. Geol. Soc. Aust. Vol 8, pt. 2, p 191 et seq., (1962).

56. SWAINE, D. J., (1962), "The Trace-Element Content of Fertilizers". Comm. Agric. Bur., Farnham, Royal, Bucks, England (1962).

57. SWEATMAN, T. R., (1961), "The Mineralogy and Chemistry of Phosphate Minerals in Some Soils". Uni. of Adelaide, M. Sc. thesis, (unpub), (1961).

58. TRAUTZ, O. R., ZAPANTA-LEGEROS, R. and KLEIN, E., (1964), "X-ray Diffraction in Dental Research". Norelco Reporter, Vol XI, No. 1, pp 29-33, (Jan-March, 1964).

59. TUREKIAN, K. K., (1963), "Chromium and Nickel in Basaltic Rocks and Eclogites". Geochem et Cosmochim. Acta, Vol 27, pp 835-846, (1963).

60. VAN BEMMELEN, R. W., (1949), "The Geology of Indonesia". Govt. Printing Office, The Hague – 3 Vols (1949).

61. VINOGRADOV, A. P., (1953), "The Elementary Composition of Marine Organisms". Sears Found. for Marine Research Mem. 2, (1953).

62. VINOGRADOV, A. P., (1963), "Biogeochemical Provinces and their Role in Organic Evolution". Geochemistry, No. 3, pp 214-228, (1963).

63. VOL'FKOVICH, S. I., et al (1952), "The Electron Microscope Study of Natural Phosphates". Chem. Abs., 49, p 20629, (1952).

64. WAMBEKE, L. Van (1958), "Une nouvelle espece minerale: la lusungite en provenance de la pegmatite de Kobokobo (Kivu – Congo Belge)". Bull de la Soc. belge de Geol de Paleontol et d'Hydrol LXV11, pp 162-169, (1958).

65. WARIN, O.N., (1958), "Notes on the Geology and the Phosphate Deposits of Christmas Island, Indian Ocean". Bur. Min. Resources. Rec. 1958/98 (1958).

66. WARIN, O.N., (1961), "Continental Phosphate Deposits and the Search for Phosphates in Australia". Bur. Min. Resources, Rec. 1961/120, (1961).

67. WILLIAMS, H., TURNER, F.J., and GILBERT, C.M., (1954) "Petrography. An Introduction to the Study of Rocks in Thin Section". W.H. Freeman and Co., San. Francisco.

68. WHITE, D.E., HEM, J.D., and WARING, G.A., (1963) "Data on Geochemistry, 6th Edition, Chapter F. – Chemical Composition of Sub-surface Waters". U.S.G.S. Prof. Paper 440-F, (1963).

69. WHITE, D.E., and WARING, G.A., (1963), "Data on Geochemistry, 6th Edition, Chapter K – Volcanic Emanations". U.S.G.S. Prof. Paper 440-K (1963).

70. WHITE, W.C. and WARIN, O.N., (1964), "A Survey of Phosphate Deposits in the South-West Pacific and Australian Waters". Bur. Min. Resources. Bull 69, (1964)

71. YODER, H.S., Jnr. and TILLEY, C.E., (1962), "Origin of Basalt Magmas: An Experimental Study of Natural and Synthetic Rock Systems". Journ. Pet., Vol 3, pt 3, pp 342-532, (1962).

PLATES

KEY TO PLATES

Plate 1. The East Coast of Christmas Island.

Plate 2.
A – Loading Phosphate Dust, Flying Fish Cove.
B – Flying Fish Cove from the East.

Plate 3.
A – Lower Volcanics, Dolly Beach. ΔΔ RH6.
B – Recent Reef Limestone, South Coast.

Plate 4.
A – Lower Volcanics and Recent Coral, Flying Fish Cove. ΔΔ FC7A.
B – Radially jointed Upper Volcanics, West Coast. ΔΔ EP3.

Plate 5.
A – Phosphate Profile, West Quarry.
B – Lateritized, Unconsolidated Dolomite, Ross Hill Tank.

Plate 6.
A – Worked-out Area, East Quarry, South Point.
B – Phosphate Profile, Field 4, Phosphate Hill.

Plate 7.
A – Phosphate Recovery beneath Pinnacles, West Quarry.
B – Phosphatized "Limestone" Pinnacle, West Quarry.

Plate 8.
A – Phosphate in fractures and replacing Dolomite, Old Limestone Quarry, South Point. ΔΔ SP2, SP3.
B – Phosphate Rock (massive apatite), Tom's Ridge. ΔΔ MH7.

Plate 9.
A – Basalt Glass (x100, ppl) ΔΔ FC12B.
B – Andesite (x25, XN) ΔΔ RH6.
C – Limburgite (x100, ppl) ΔΔ RH3.

Plate 10.
A – Eocene Foraminiferal Limestone (x25, ppl) ΔΔ FC8A.
B – Graded bedding in Dolomite (x25, ppl) ΔΔ SP2A.
C – Phosphatized Dolomite (x25, ppl) ΔΔ SP3.

Plate 11.
A – Collophane and Dolomite cemented by later Dahllite (x25, XN) ΔΔ 7A.
B – Collophane, Dahllite and later Crandallite (x25, ppl) ΔΔ 18A.

Plate 12. Phosphatized Volcanic Rock (Barrandite containing secondary vein of Barrandite, Crandallite and (?)Apatite. ΔΔ Cela.

A – x25, ppl
B – x40, XN
C – x40, ppl

Plate 13. Electron Probe Microanalysis ΔΔ RH3.

A – Absorbed Electron Image
B – Calcium
C – Titanium
D – Chromium
E – Iron
F – Silicon

Plate 14. Electron Probe Microanalysis ⩚ Cela, MH2.

A – Cela, Titanium
B – Cela, Phosphorus
C – Cela, Absorbed Electron Image
D – Cela, Chromium
E – MH2, Absorbed Electron Image
F – MH2, Titanium

Legend

⩚	–	Sample Locality
volc	–	volcanic rock
ls	–	limestone
phos	–	phosphate
dol	–	dolomite
pl	–	plagioclase
gl	–	glass
px	–	pyroxene
ov	–	olivine
dah	–	dahllite
Cr	–	crandallite
Bar	–	barrandite
Ap	–	apatite
Chl	–	chlorite

PLATE 1

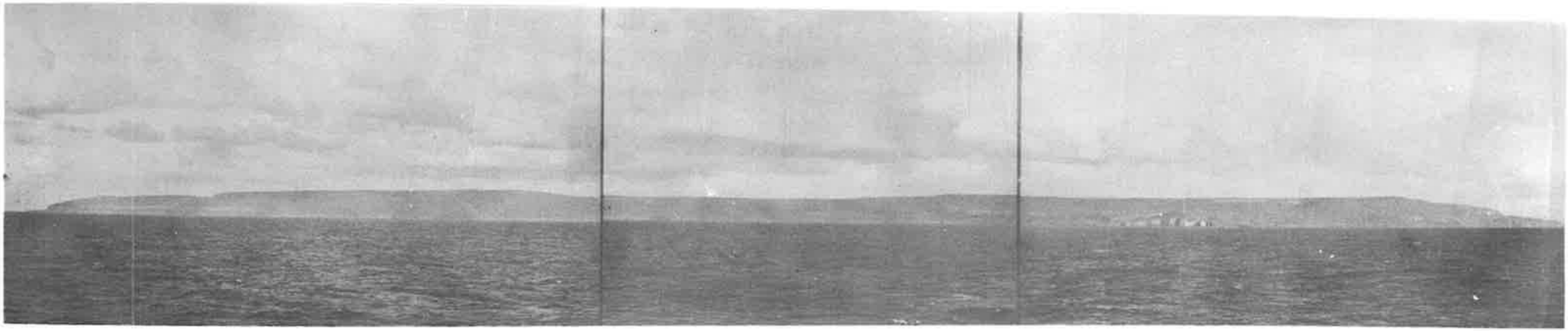

The East Coast of Christmas Island

PLATE 2

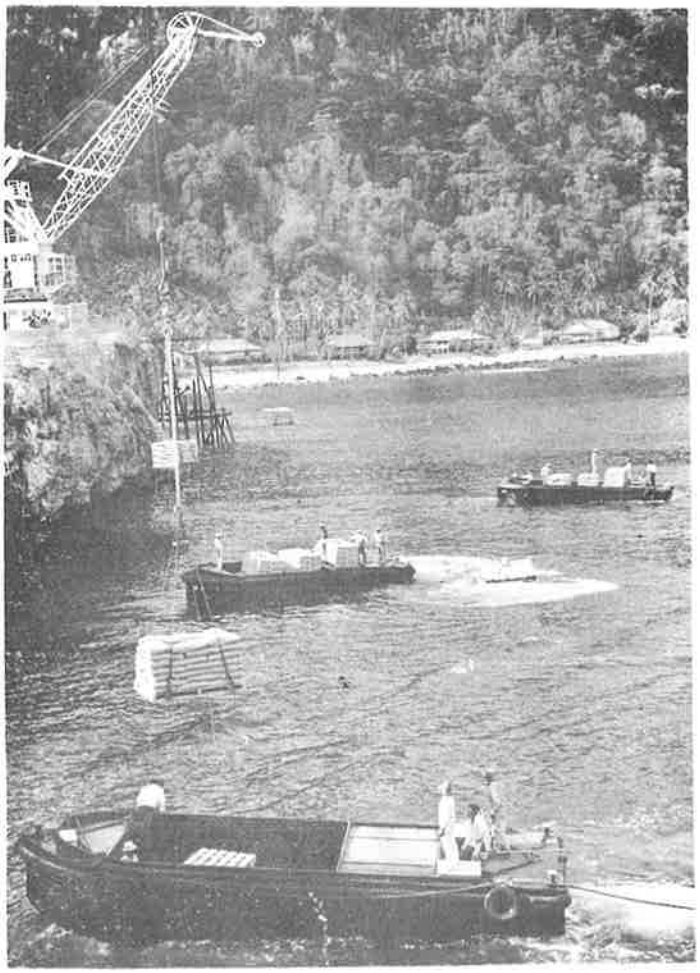

A - Loading Phosphate Dust, Flying Fish Cove

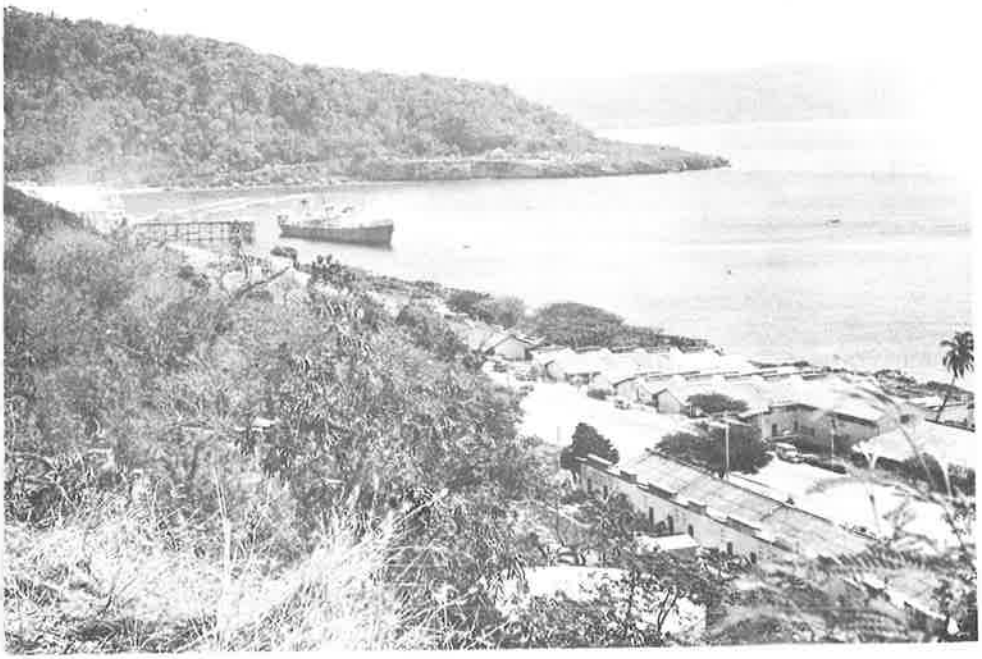

B - Flying Fish Cove from the East

PLATE 3

A. Lower Volcanics, Dolly Beach. ΔΔ RH6

B. Recent Reef Limestone, South Coast

PLATE 4

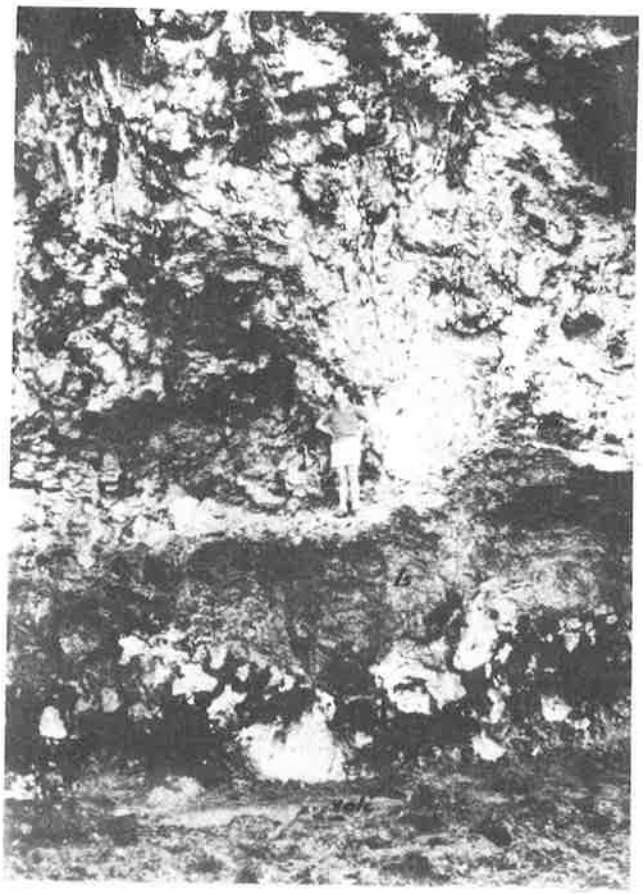

A. Lower Volcanics and Recent Coral, Flying Fish Cove. ΔΔ FC7A.

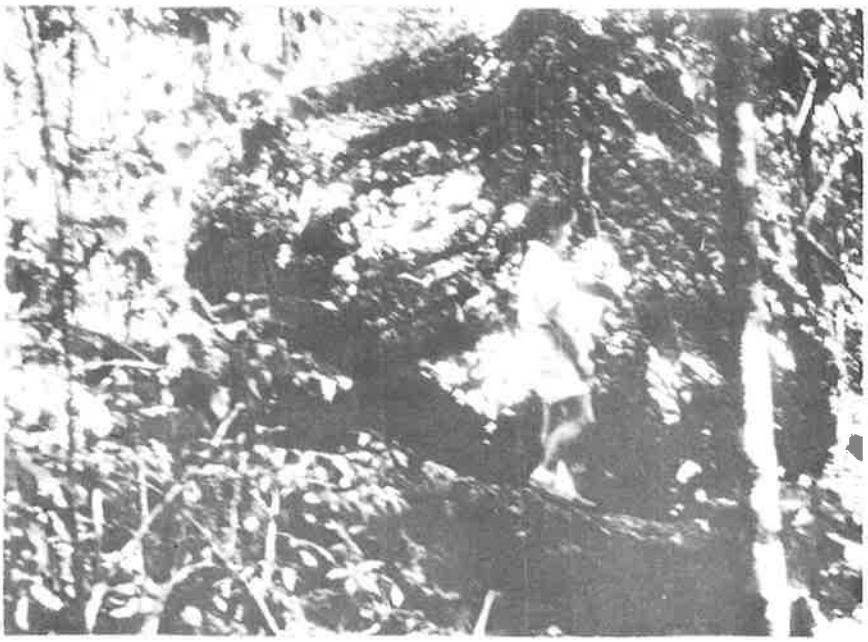

B. Radially jointed Upper Volcanics, West Coast. ΔΔ EP3.

PLATE 5

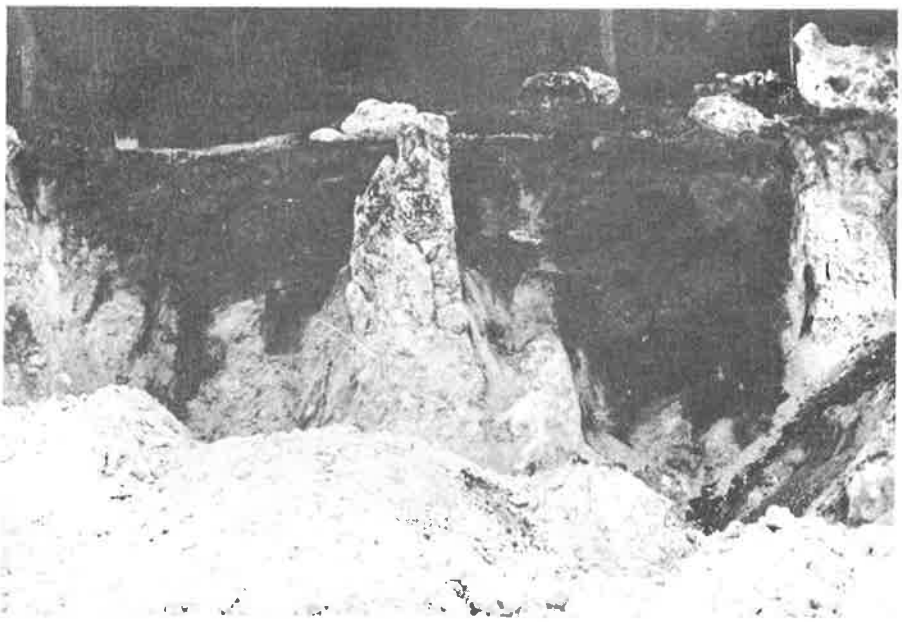

A - Phosphate Profile, West Quarry

B - Lateritized, Unconsolidated Dolomite, Ross Hill Tank

PLATE 6

A. Worked-out Area, East Quarry South Point.

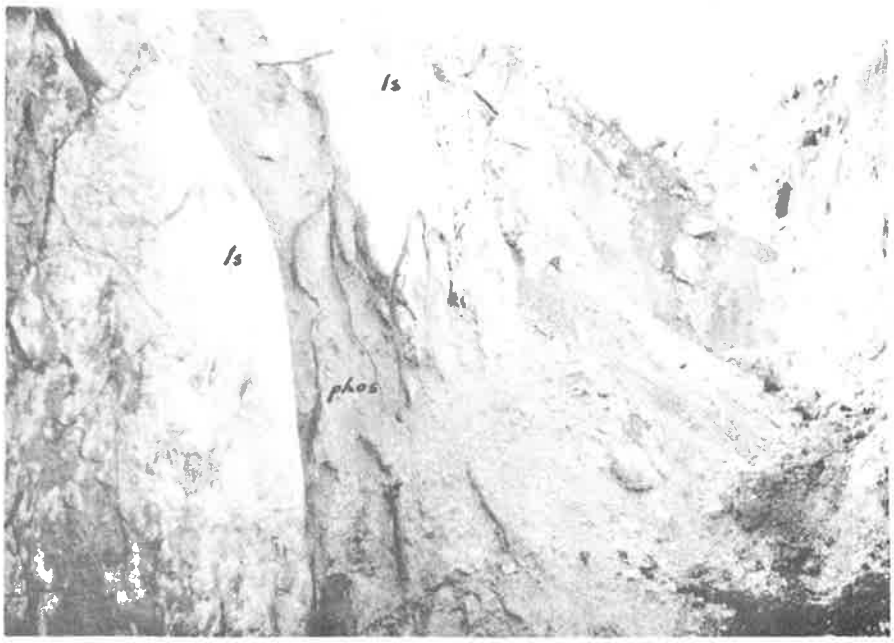

B. Phosphate Profile, Field 4, Phosphate Hill

PLATE 7

A - Phosphate Recovery beneath Pinnacles, West Quarry

B - Phosphatized "Limestone" Pinnacle, West Quarry

PLATE 8

A. Phosphate in fractures and replacing Dolomite, Old Limestone Quarry, South Point. ΔΔ SP2, SP3.

B. Phosphate Rock (massive apatite), Tom's Ridge. ΔΔ MH7.

PLATE 9

A. Basalt Glass (x100, ppl) ΔΔ FC12B.

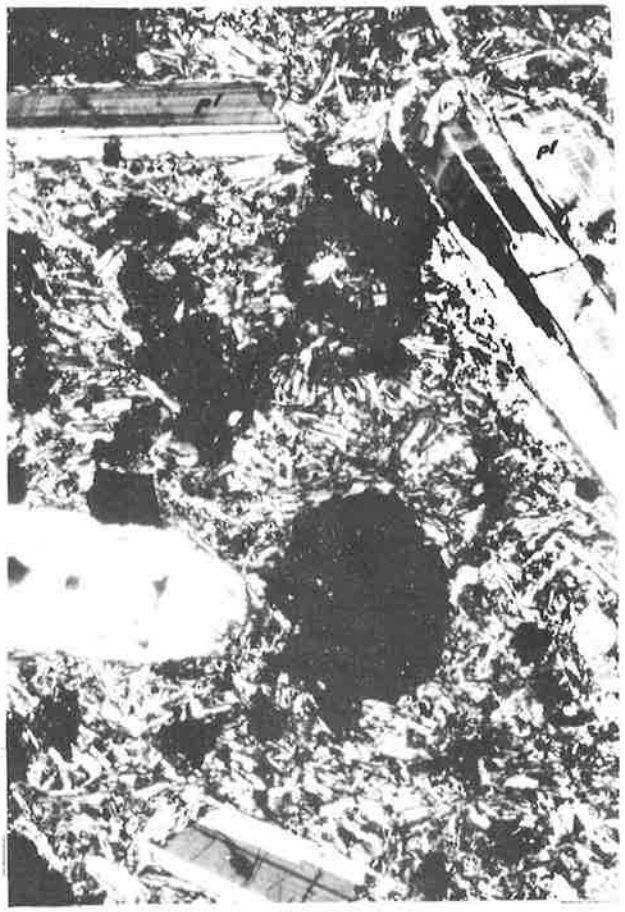

B. Andesite (x25, XN) ΔΔ RH6

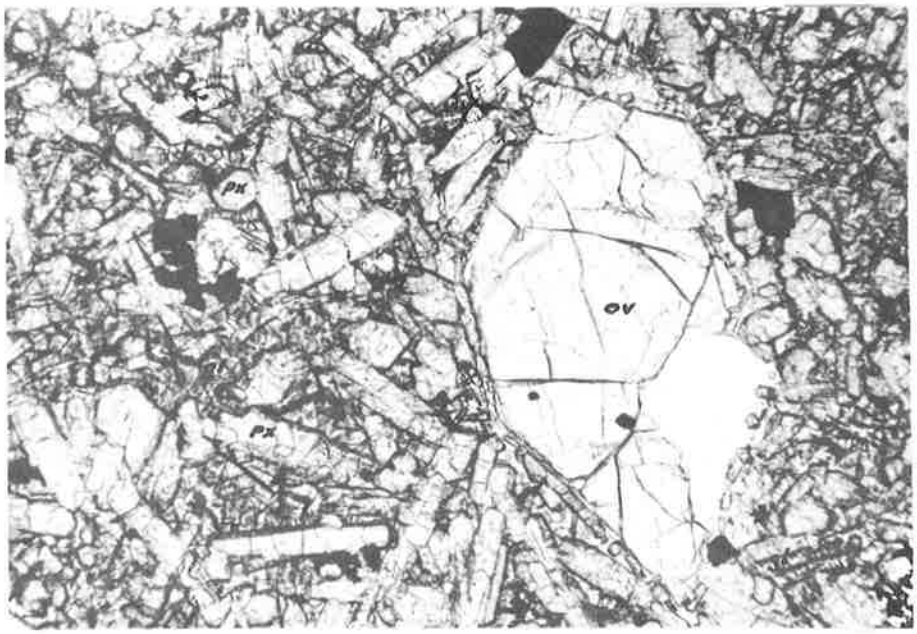

C. Limburgite (x100 ppl) ΔΔ RH3

PLATE 10

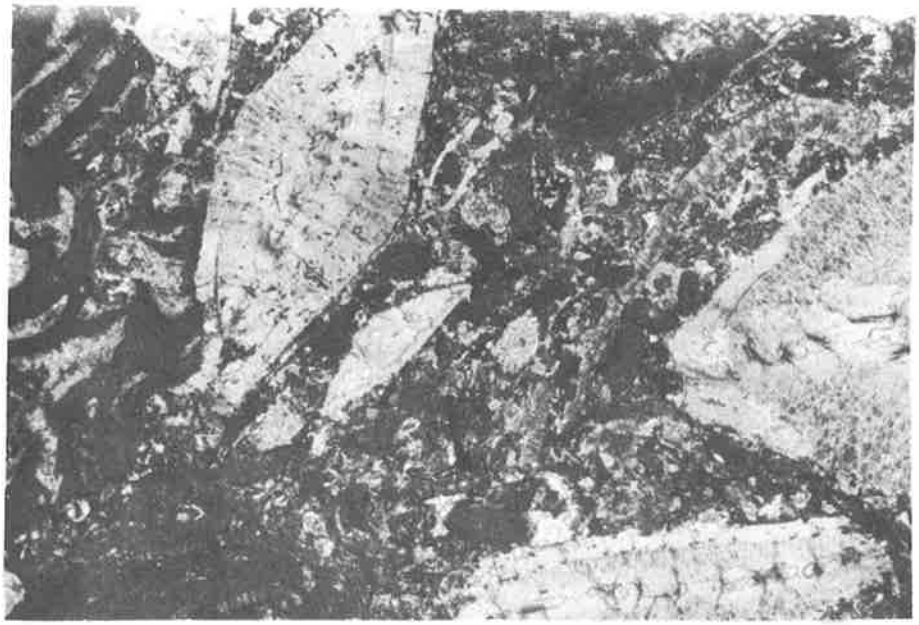

A. Eocene Foraminiferal Limestone (x25, ppl) ΔΔ FC8A

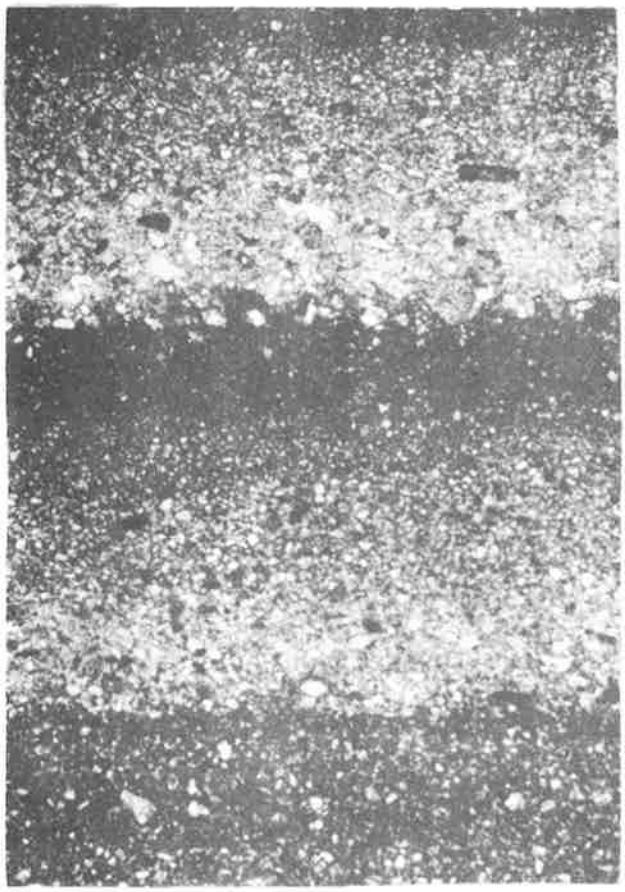

B. Graded bedding in Dolomite (x25, ppl) ΔΔ SP2A.

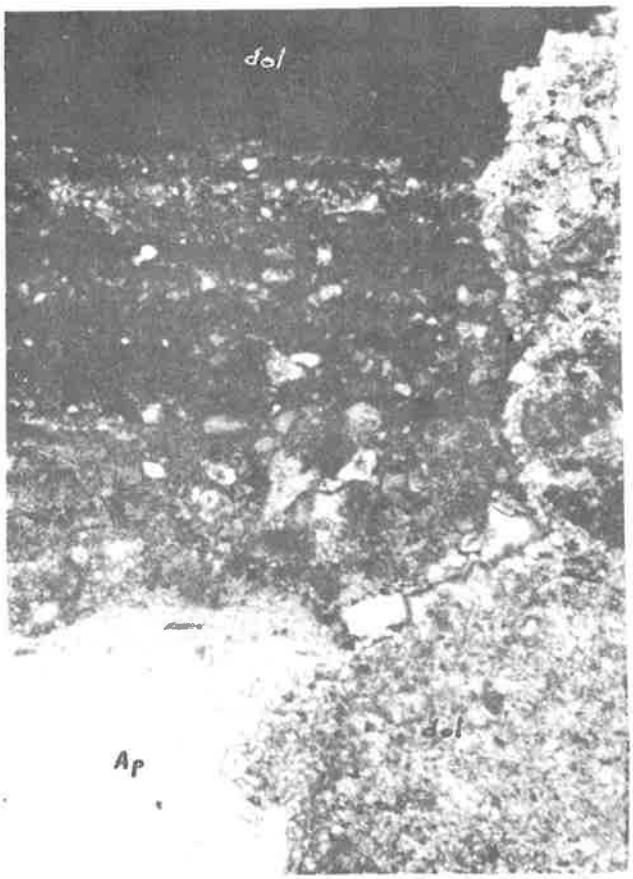

C. Phosphatized Dolomite (x25, ppl) ΔΔ SP3.

PLATE 11

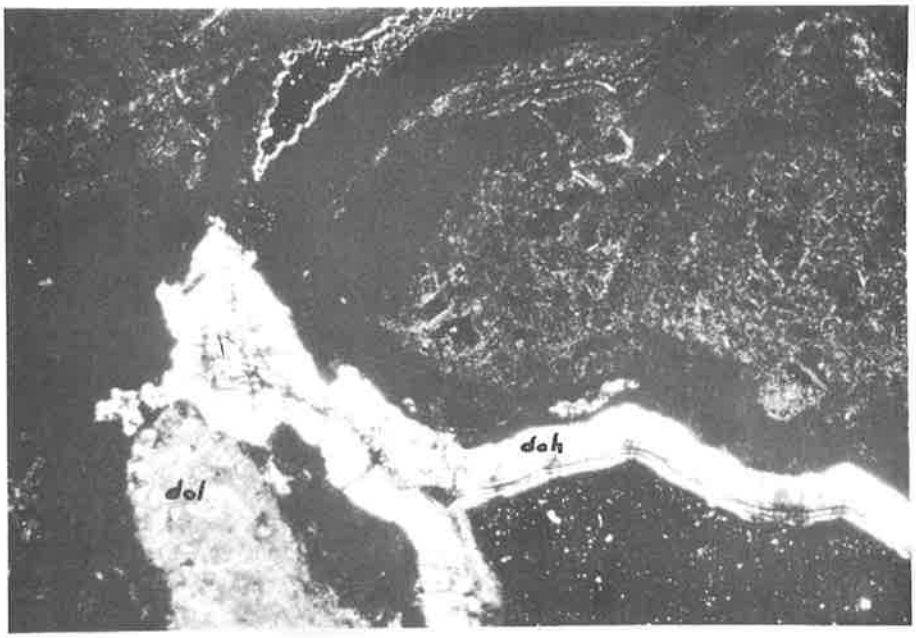

A. Collophane and Dolomite cemented by later Dahllite (x25, XN) ΔΔ 7A.

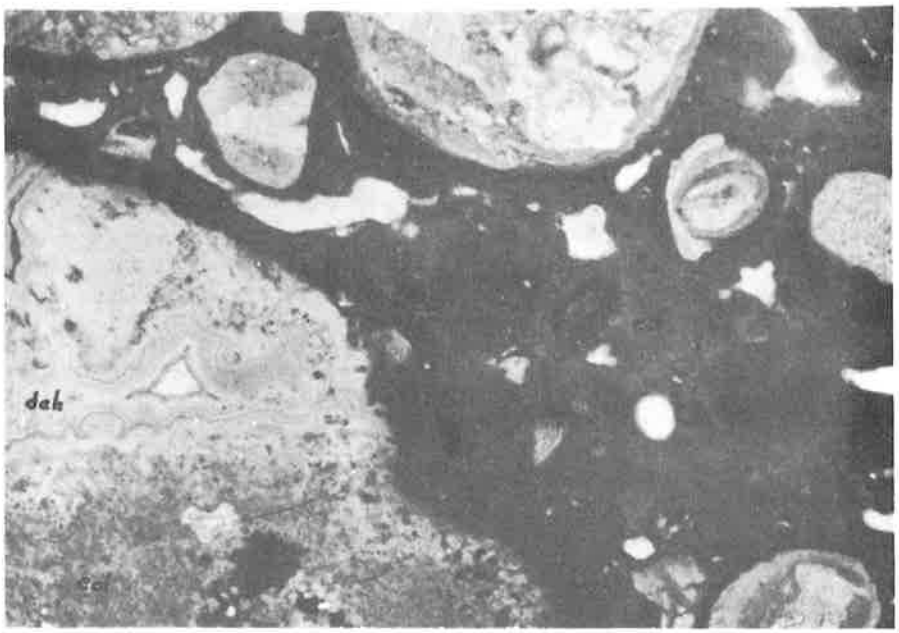

B. Collophane, Dahllite and later Crandallite (x25, ppl) ΔΔ 18A.

PLATE 12

Phosphatized Volcanic Rock (Barrandite) containing secondary vein of Barrandite, Crandallite and ?Apatite ΔΔ Cela.

A. x25, ppl

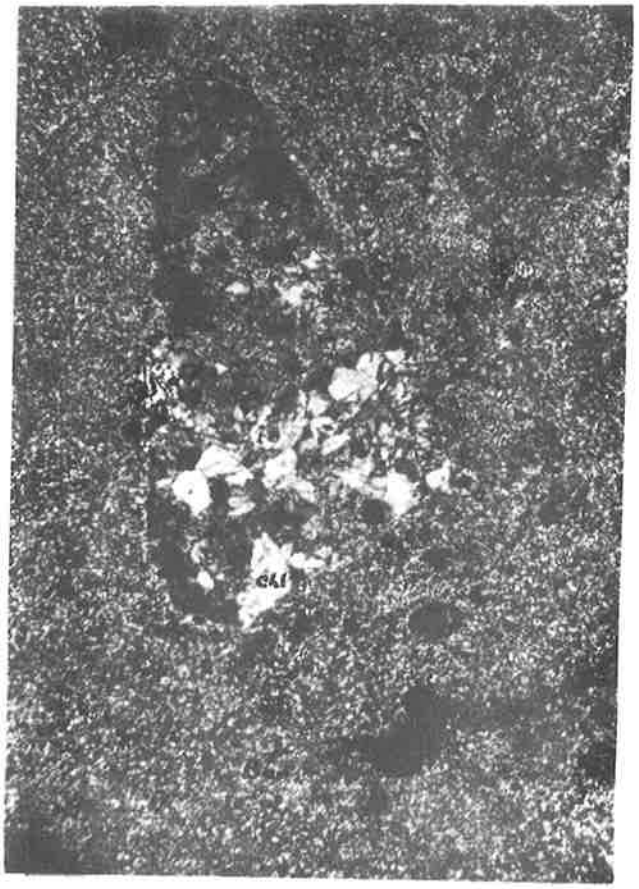

B. x40, XN

C. x40, ppl

PLATE 13

Electron Probe Microanalysis ΔΔ RH3

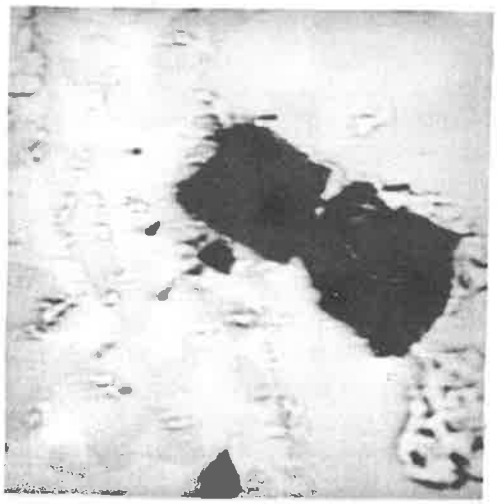

A. Absorbed Electron Image

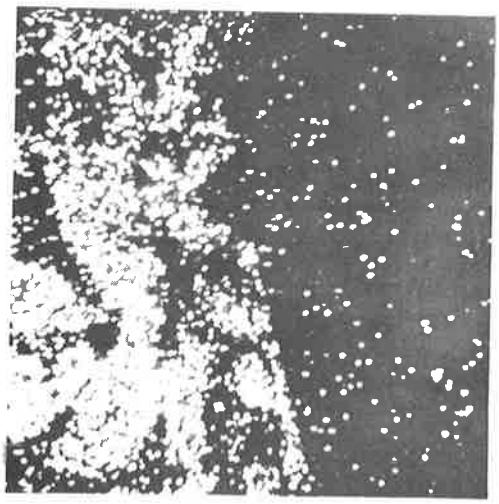

B. Calcium

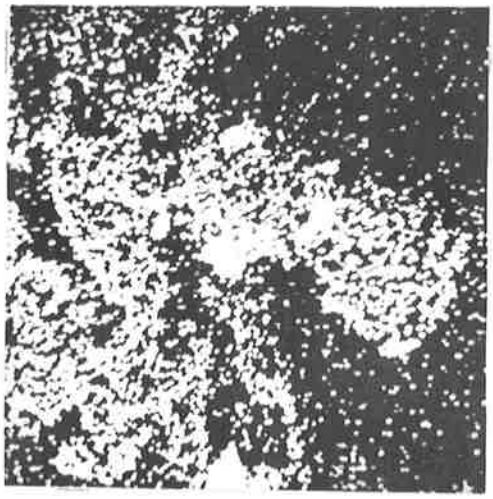

C. Titanium

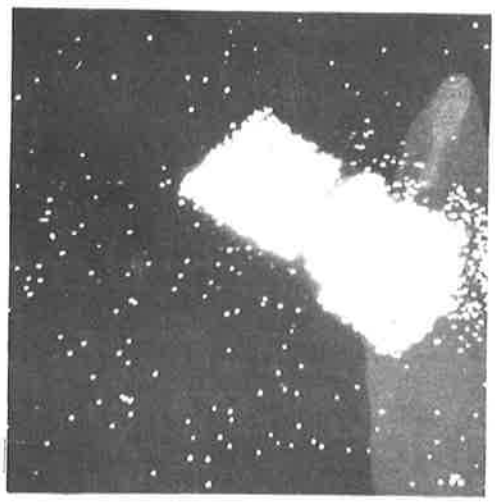

D. Chromium

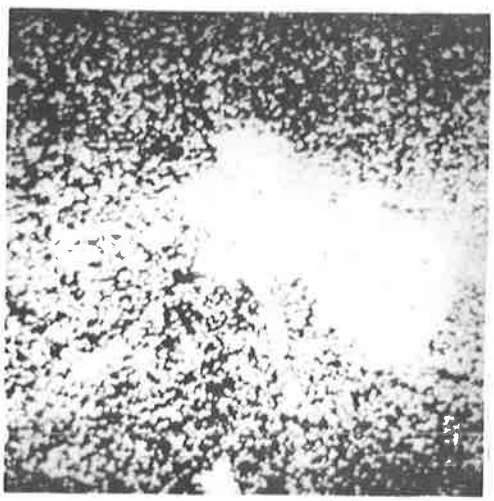

E. Iron

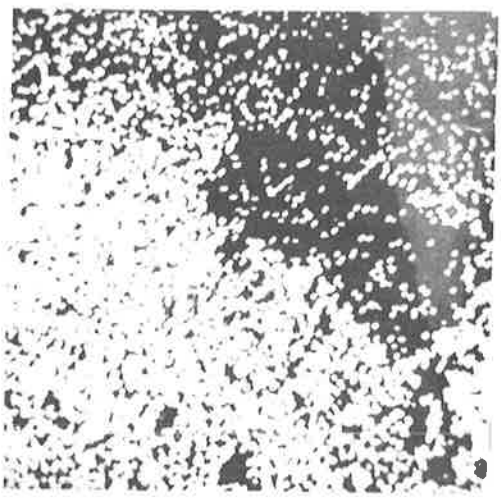

F. Silicon

PLATE 14

Electron Probe Microanalysis ΔΔ Cela, MH2

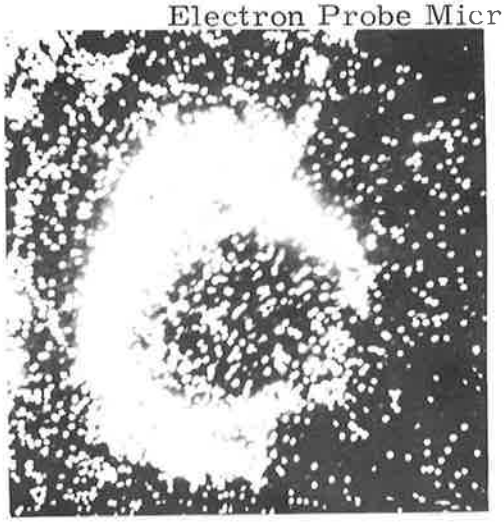

A. Cela, Titanium

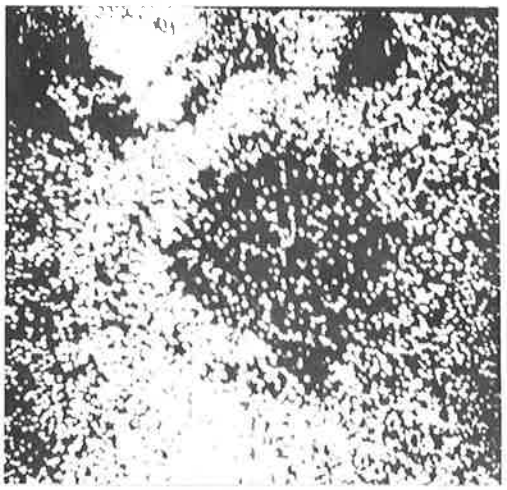

B. Cela, Phosphorus

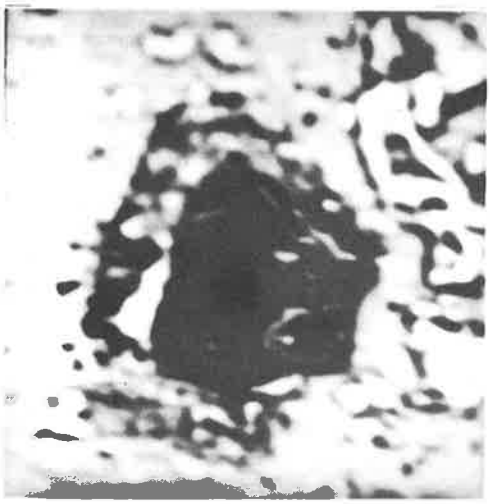

C. Cela, Absorbed Electron Image

D. Cela, Chromium

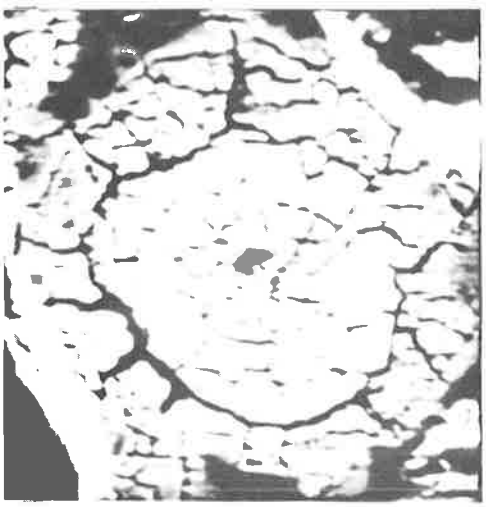

E. MH2, Absorbed Electron Image

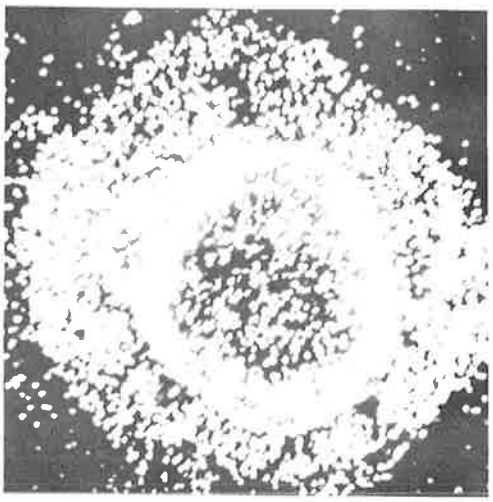

F. MH2, Titanium

TEXT FIGURES

KEY TO TEXT FIGURES

Figure 1. X-ray diffraction trace, sample consisting mainly of crandallite. Sample MH8.

Figure 2. X-ray diffraction trace, sample consisting mainly of millisite. Sample A17 (0-2 ft).

Figure 3. X-ray diffraction trace, sample consisting mainly of barrandite. Sample Ce1.

Figure 4. X-ray diffraction trace, Sample Ce1, heated to 300°C for 12 hours.

Figure 5. X-ray diffraction trace, Sample Ce1, heated to 1200°C for $^1/_2$ hour.

Figure 6. (F, OH, Cl) – Carbonate relationships of apatite samples, on a basis of 10 Ca etc. ions per two formula units.

Figure 7. (F, OH, Cl) – Carbonate relationships of apatite samples, on a basis of 26 (F, OH, Cl, O) ions per two formula units.

Figure 8. RO – R_2O relationships of the apatite samples, on a basis of 26 (F, OH, Cl, O) per two formula units.

Figure 9. Precipitation of normal and basic phosphates, after Britton (1956).

Figure 10. Semi-quantitative electron probe microanalysis, sample consisting of oolitic barrandite. Sample MH2.

Figure 11. Semi-quantitative electron probe microanalysis, sample consisting of limburgite. Sample RH3.

Figure 12. Semi-quantitative electron probe microanalysis, sample consisting of barrandite, phosphatized (?)limburgite. Sample Ce1a.

Figure 13. DTA trace, apatite samples. Samples W/2 (0-2 ft) and W/2 (8-10 ft).

Figure 14. DTA trace, sample consisting dominantly of crandallite. Sample MH8.

Figure 15. DTA trace, sample consisting mainly of millisite. Sample A17 (0-2 ft).

Figure 16. DTA trace, Sample A8 (6 in.).

Figure 17. DTA trace of samples consisting of barrandite. Sample Ce1, Ce2b.

Figure 18. TGA trace of sample consisting of apatite. Sample 16.

Figure 19. TGA trace of sample consisting of crandallite and millisite. Sample 24.

Figure 20. TGA trace of barrandite sample. Sample Ce1.

Figure 21. The origin of the principal phosphate minerals.

Legend to Figures 6, 7 and 8

A. Analyses of Christmas Island apatite samples marked thus: ●

B. Analyses of carbonate apatite samples from Deer, Howie and Zussman (1962, p 328) marked thus: ◬ 23.

Z1 = Blue apatite, pegmatite dyke in contact with limestone, Mansjo Mountain, Halsingland, Sweden.

Z2 = Colourless apatite, pegmatite dyke, Mansjo Mountain, Halsingland, Sweden.

Z3 = Francolite, oolitic ironstone, Robin Hood Quarry, Thorpe-on-the-Hill, Leeds, Yorkshire.

Z4 = Francolite, Wheal Franco, Buckland Monachorum, Tavistock, Devon.

Z5 = Francolite, altered lava, Annisfontein farm, Richtersveld, Namaqualand, South Africa.

C. Analyses of carbonate-apatite samples from Palache, Berman and Frondel (1951, p 883) marked thus: ⊙ D14.

D2 = Fluorapatite. Faraday Township, Ontario.

D6 = Carbonatian fluorapatite. Wheal Franco, Devonshire (Francolite).

D13 = Carbonate-apatite. St. Paul's Rocks, Atlantic Ocean.

D14 = Carbonatian fluorapatite. Richtersveld, South Africa.

D15 = Carbonatian fluorapatite. Milburn, New Zealand.

D. Analysis of dahllite from McConnell (1960) marked thus: × McC-1

McC-1 = post-Wisconsin (upper Pleistocene) fossilized dental enamel from a mastodon, Bluffton, Ohio.

E. Analyses of other apatites analysed at AMDEL marked thus: ⊡

"Sechura" – Sechura Desert, Peru. (Sample ex BPC).

"Peruvian" – Unspecified locality, Peru. (Sample ex BPC).

FIGURE-1 X-RAY DIFFRACTION TRACE - SAMPLE MH8
CRANDALLITE AND GOETHITE

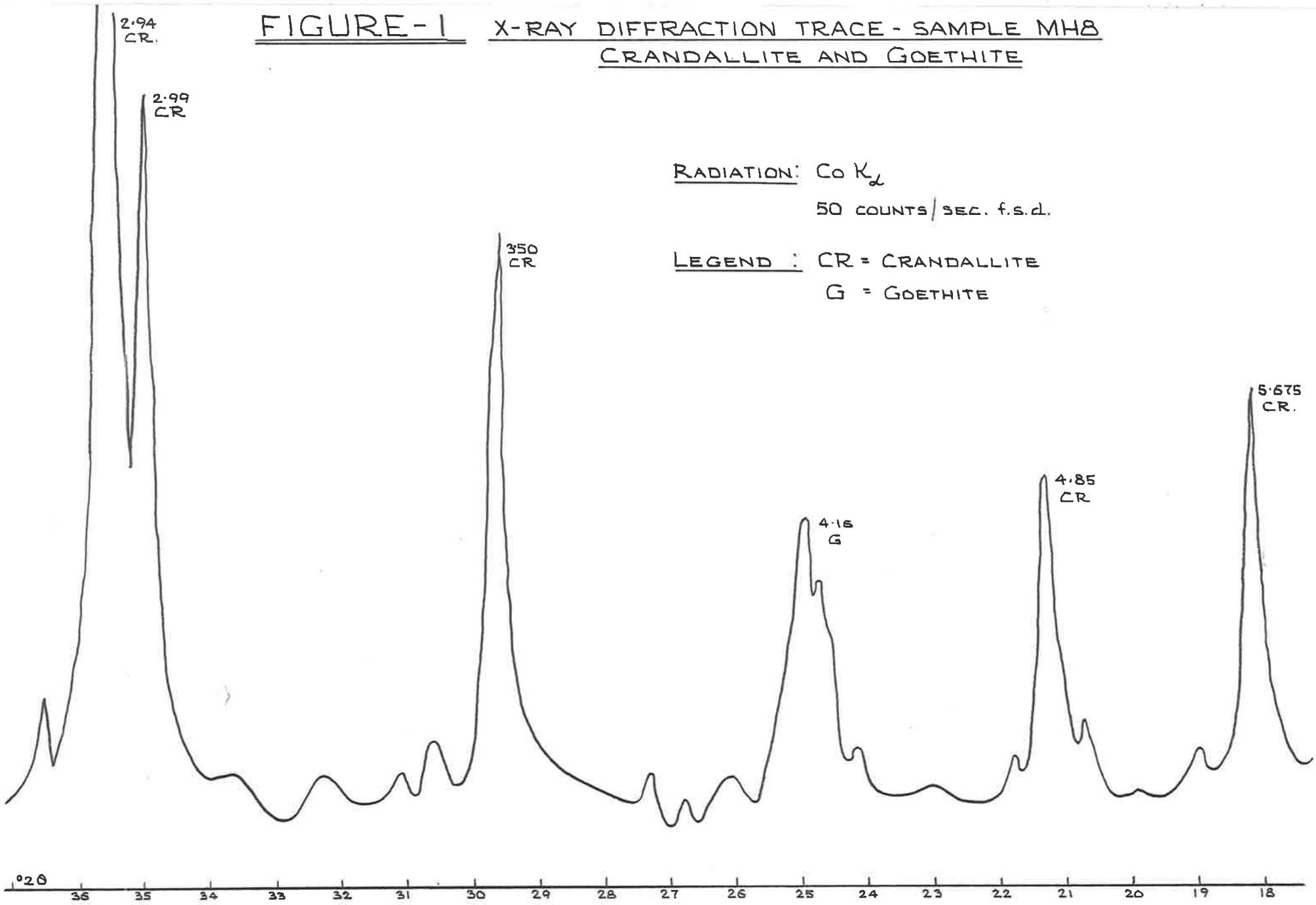

RADIATION: Co K_α

50 COUNTS / SEC. f.s.d.

LEGEND : CR = CRANDALLITE

G = GOETHITE

FIGURE-2 X-RAY DIFFRACTION TRACE - SAMPLE A17 (0-2ft.)

MILLISITE AND MINOR CRANDALLITE AND GOETHITE

RADIATION: CoK_α

50 COUNTS / SEC. f.s.d.

LEGEND: M = MILLISITE
CR = CRANDALLITE
G = GOETHITE

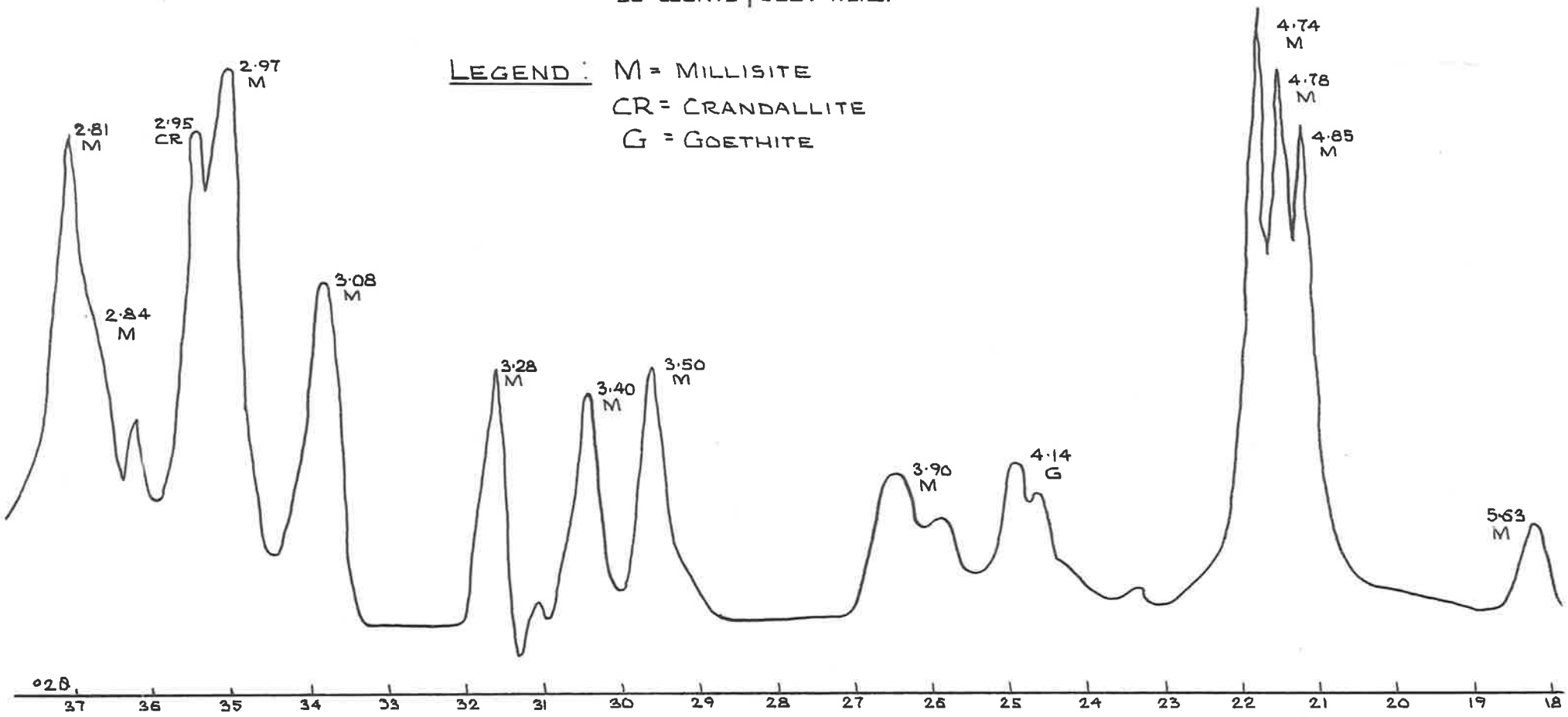

FIGURE-3 X-RAY DIFFRACTION TRACE - SAMPLE Ce 1

BARRANDITE AND MINOR GORCEIXITE

RADIATION: Co K_α

50 COUNTS / SEC. f.s.d.

LEGEND : B = BARRANDITE

GOR.= GORCEIXITE

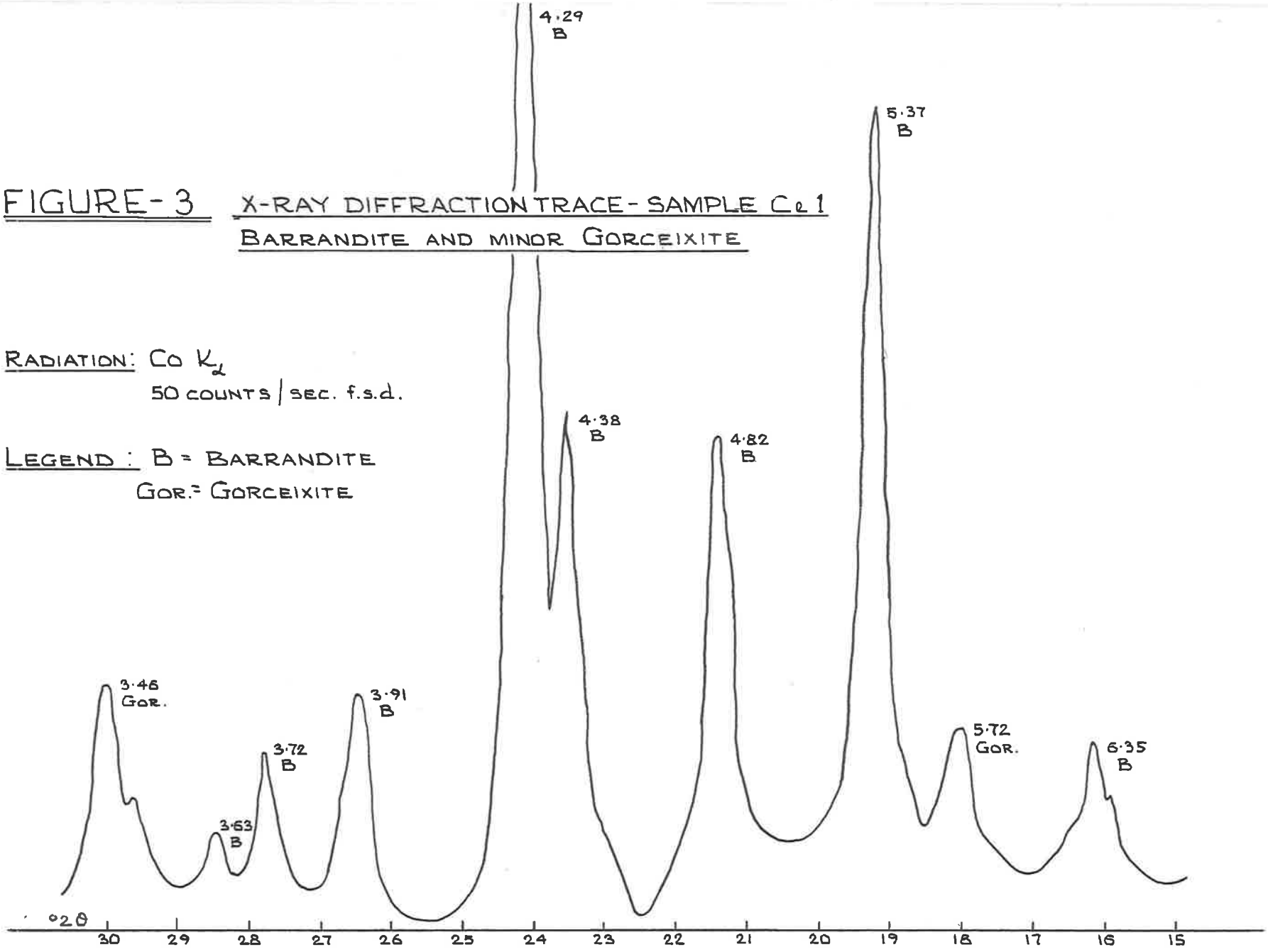

FIGURE. 4 SAMPLE Ce 1, HEATED 300°C/12 HRS. (Al, Fe) PO_4 LOW TEMPERATURE FORM AND BARRANDITE.

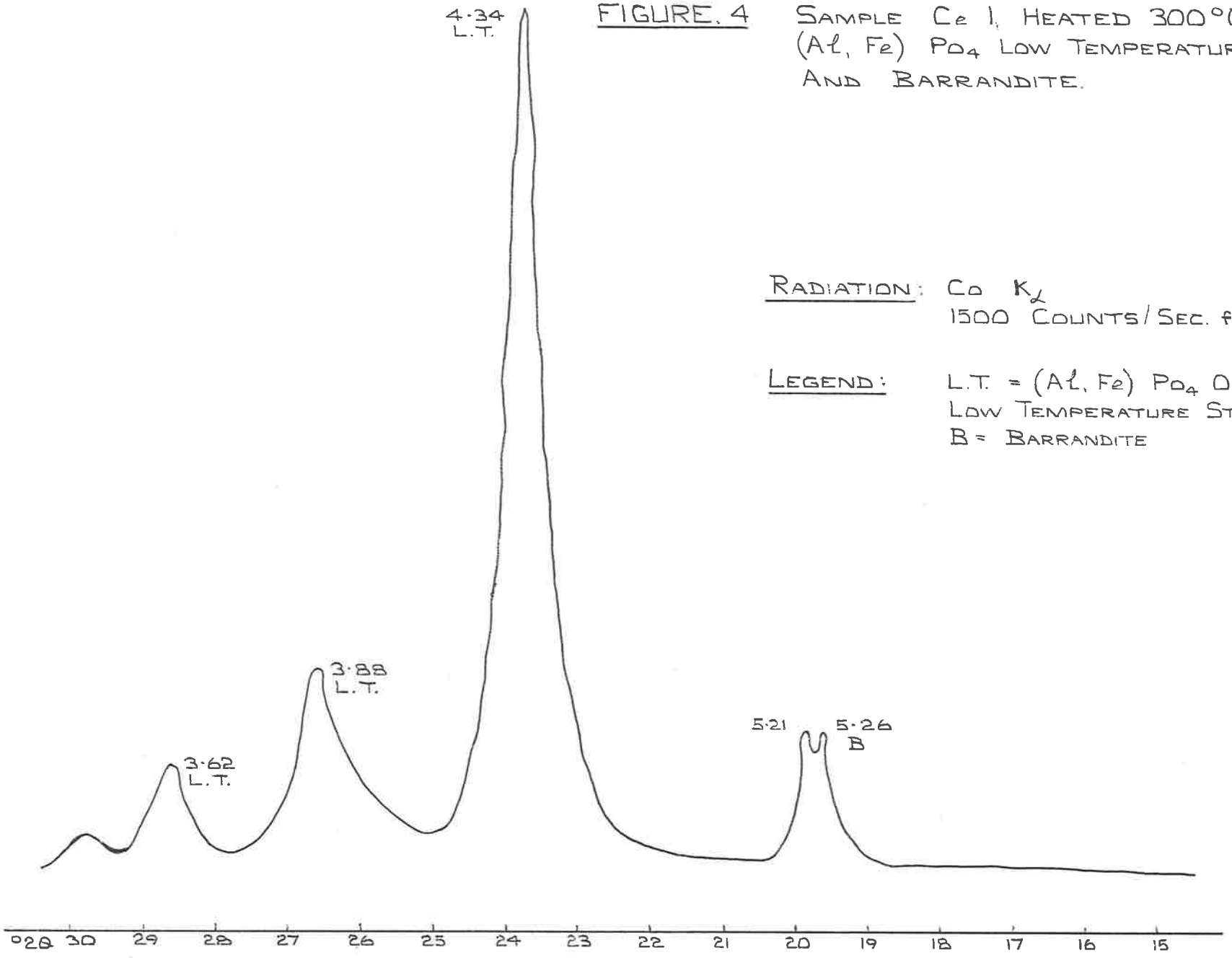

RADIATION: Co K_α
1500 COUNTS/SEC. f.s.d.

LEGEND: L.T. = (Al, Fe) PO_4 OF LOW TEMPERATURE STRUCTURE
B = BARRANDITE

FIGURE. 5 SAMPLE Ce 1. HEATED 1200°C/½ HR.
ORTHOPHOSPHATE & MINOR LOW TEMPERATURE
(Al, Fe) PO_4

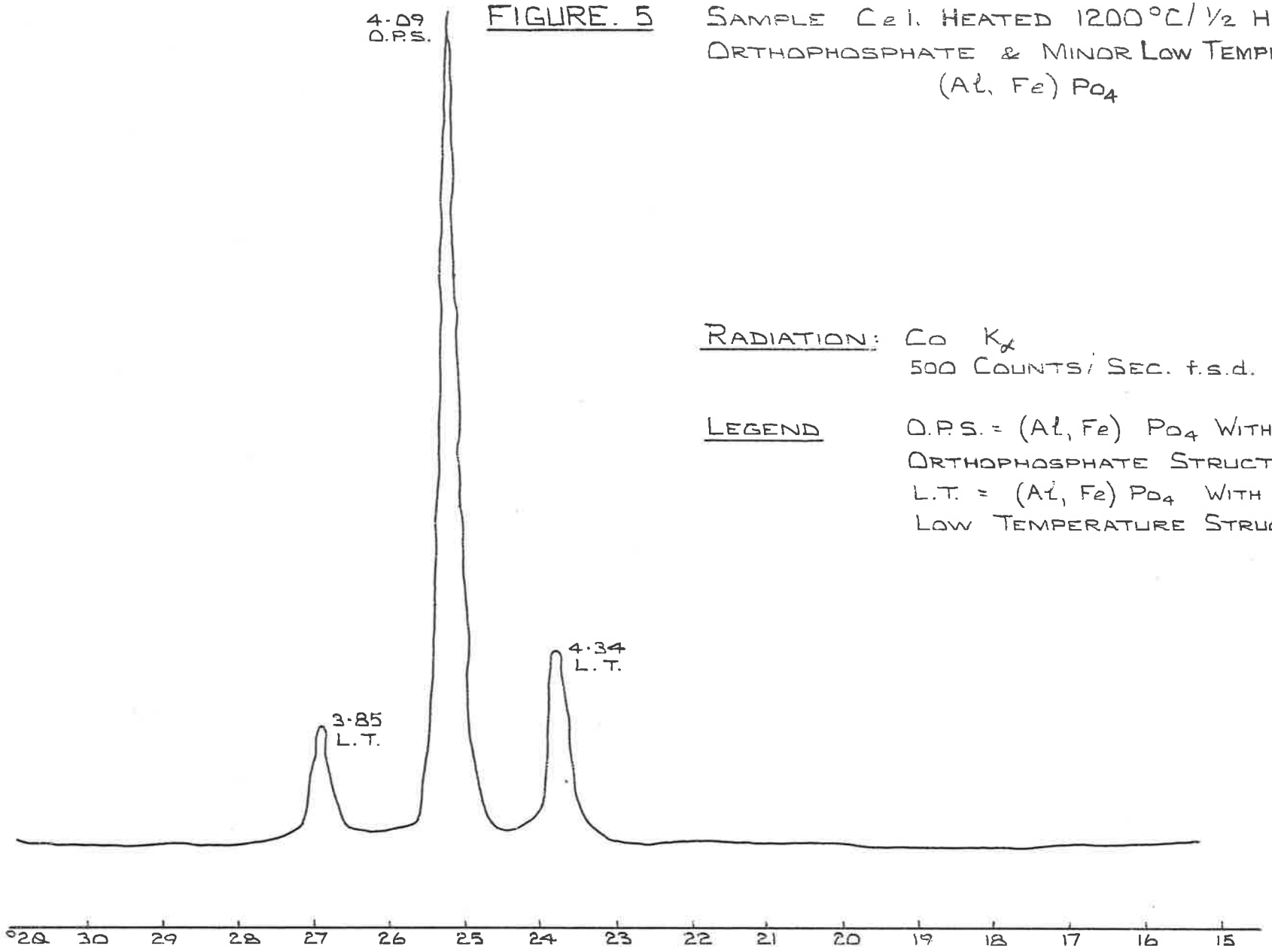

RADIATION: Co K_α
500 COUNTS/SEC. f.s.d.

LEGEND O.P.S. = (Al, Fe) PO_4 WITH
ORTHOPHOSPHATE STRUCTURE
L.T. = (Al, Fe) PO_4 WITH
LOW TEMPERATURE STRUCTURE

FIGURE-6 APATITE SAMPLES. CARBONATE/HALOGEN-HYDROXYL RELATIONSHIPS PLOTTED ON A BASIS OF 10 Ca ETC. IONS PER TWO FORMULAR UNITS

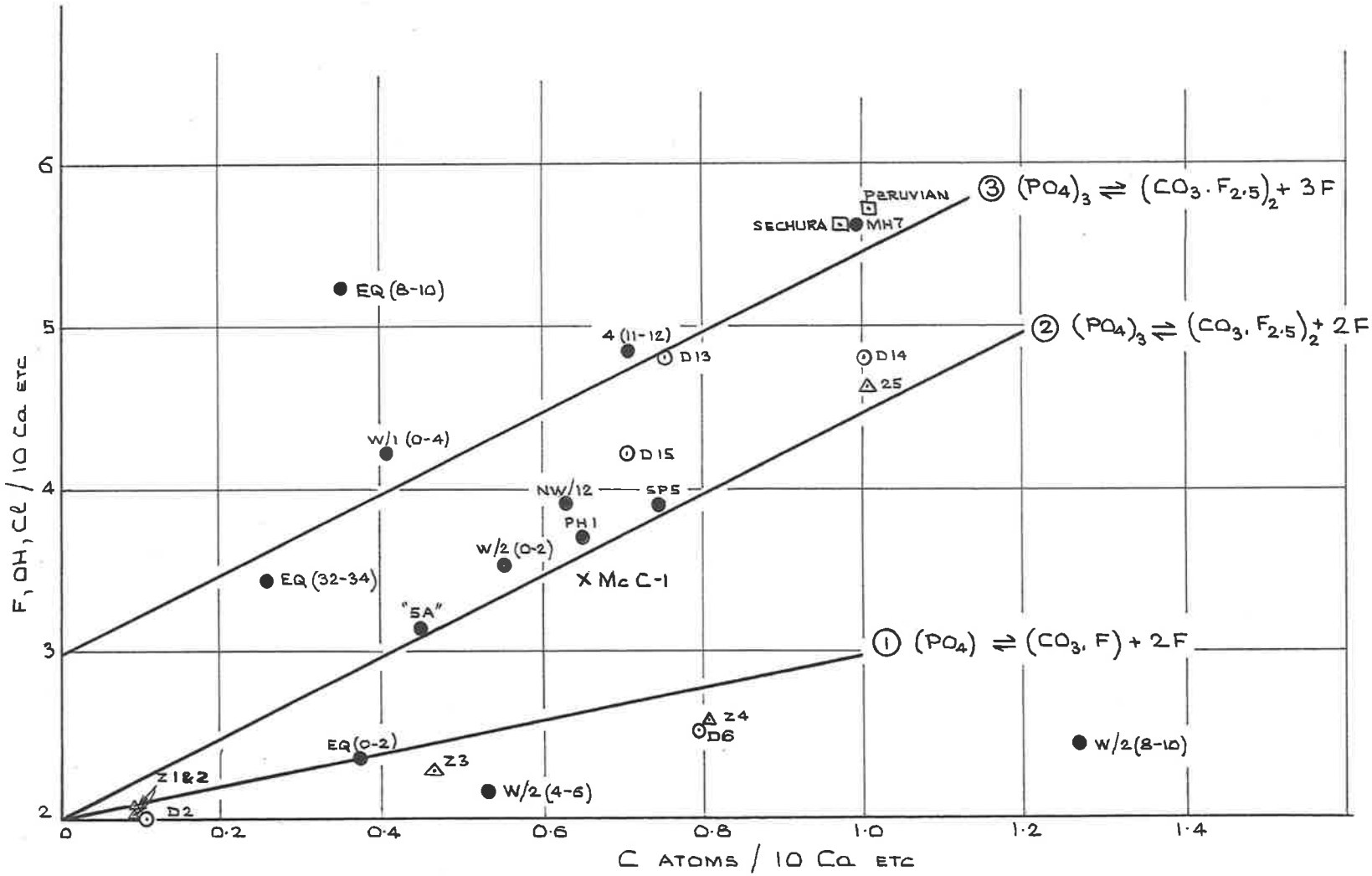

FIGURE-7 APATITE SAMPLES. CARBONATE/HALOGEN-HYDROXYL RELATIONSHIPS PLOTTED ON A BASIS OF 26 ANIONS PER TWO FORMULA UNITS.

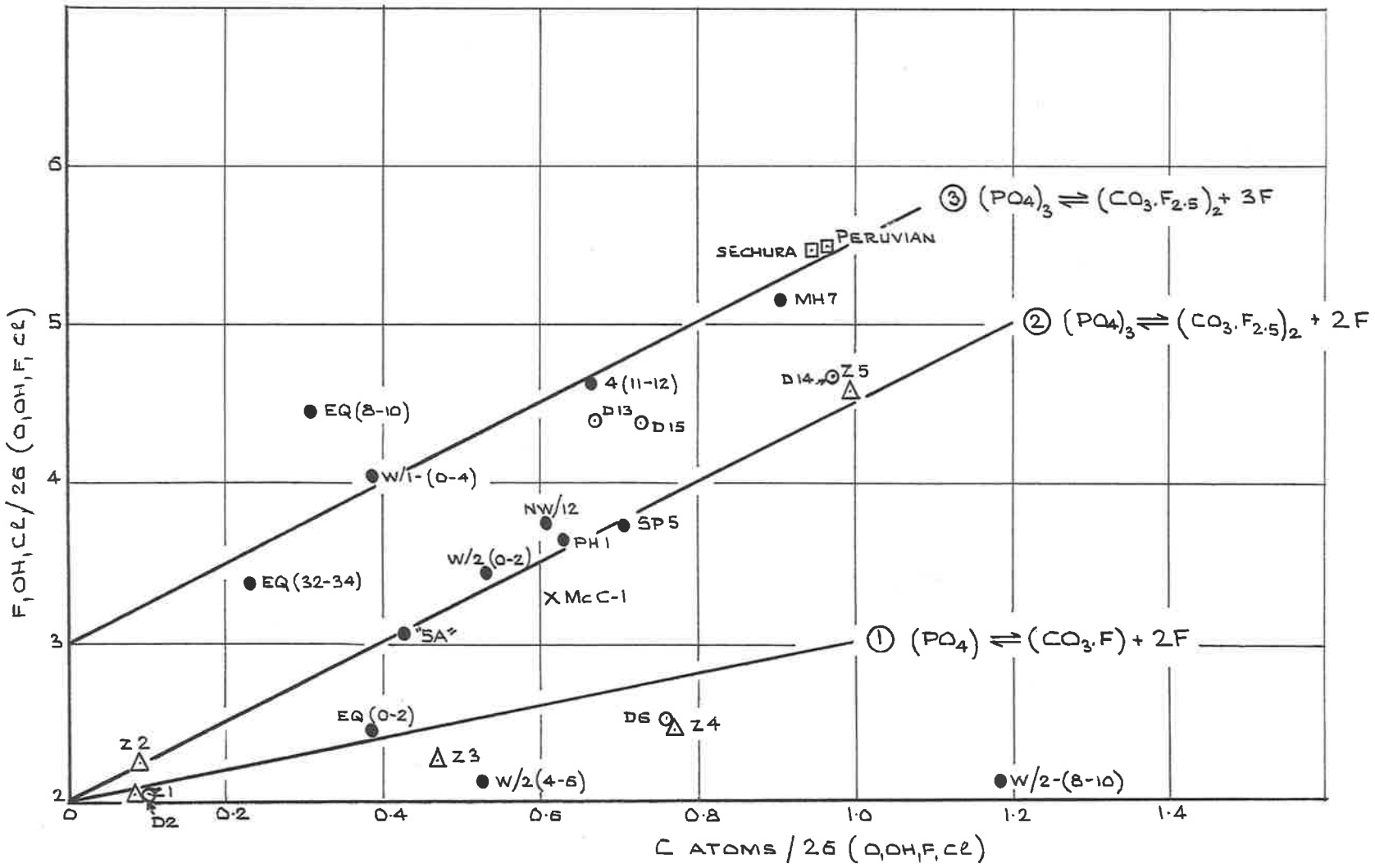

FIGURE-8

APATITE SAMPLES. RO/R_2O RELATIONSHIPS PLOTTED ON A BASIS OF 26 ANIONS PER TWO FORMULAR UNITS.

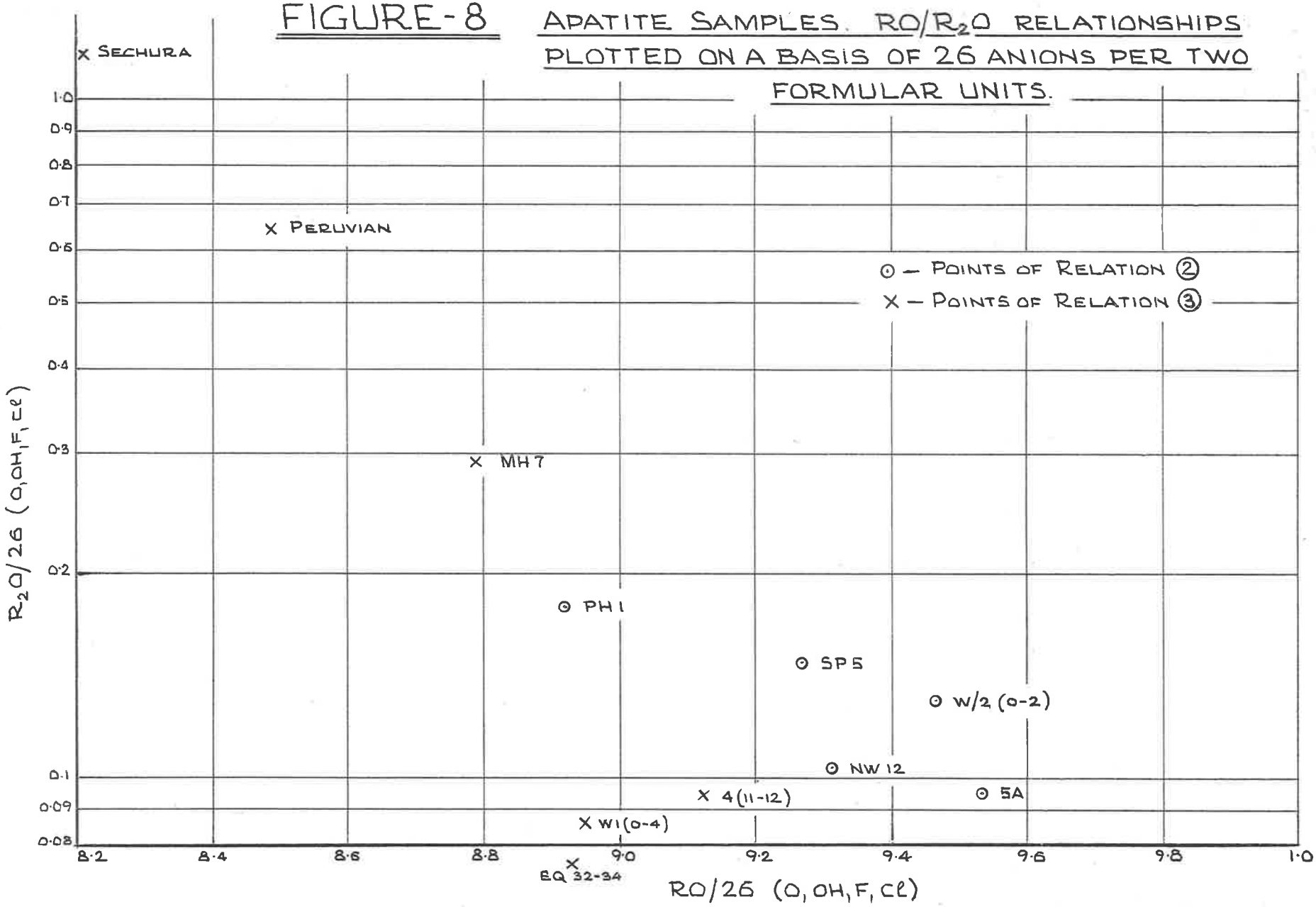

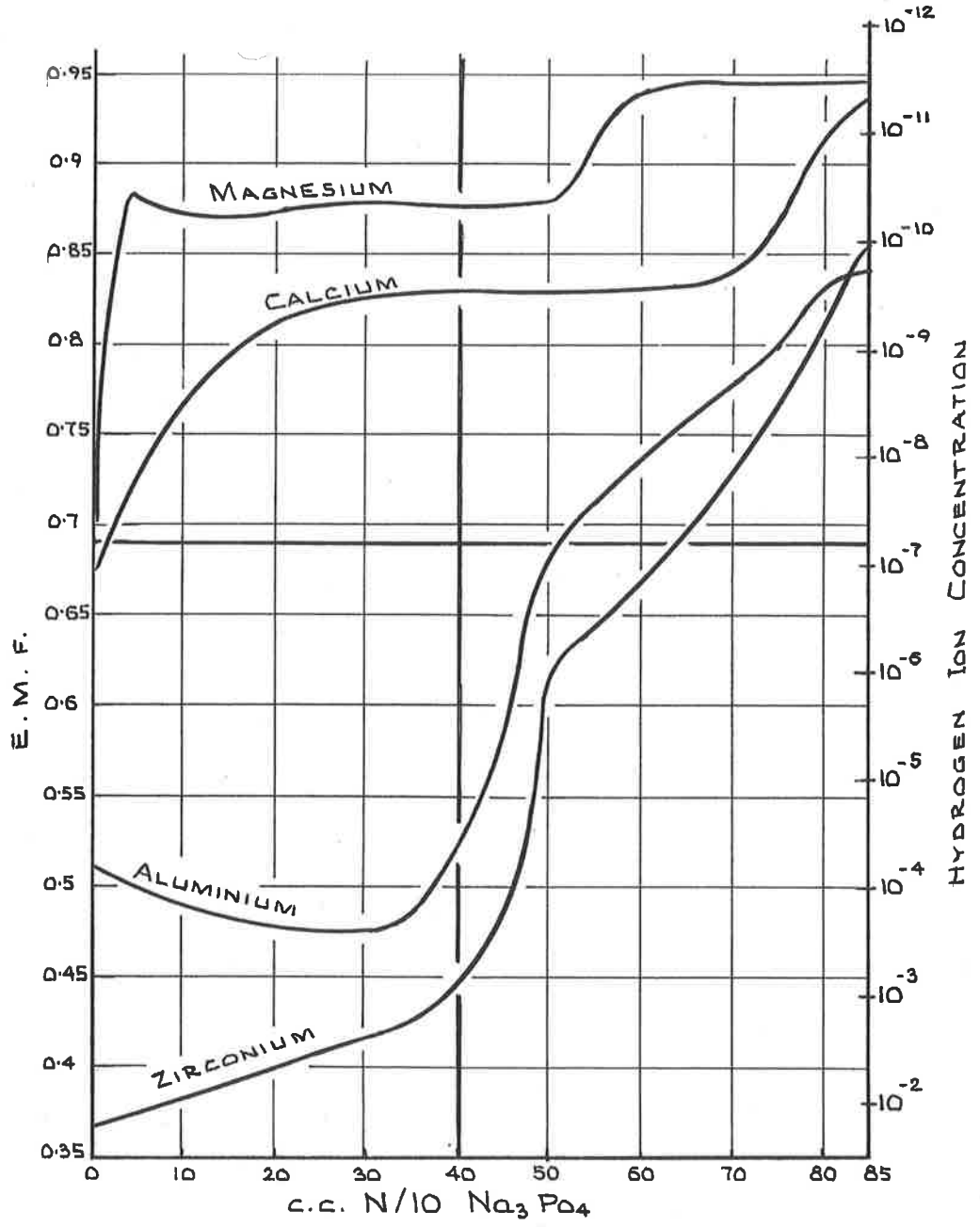

FIGURE-9 PRECIPITATION OF NORMAL AND BASIC PHOSPHATES AFTER BRITTON H.T.S. (1956)

FIGURE-13 DIFFERENTIAL THERMAL TRACES

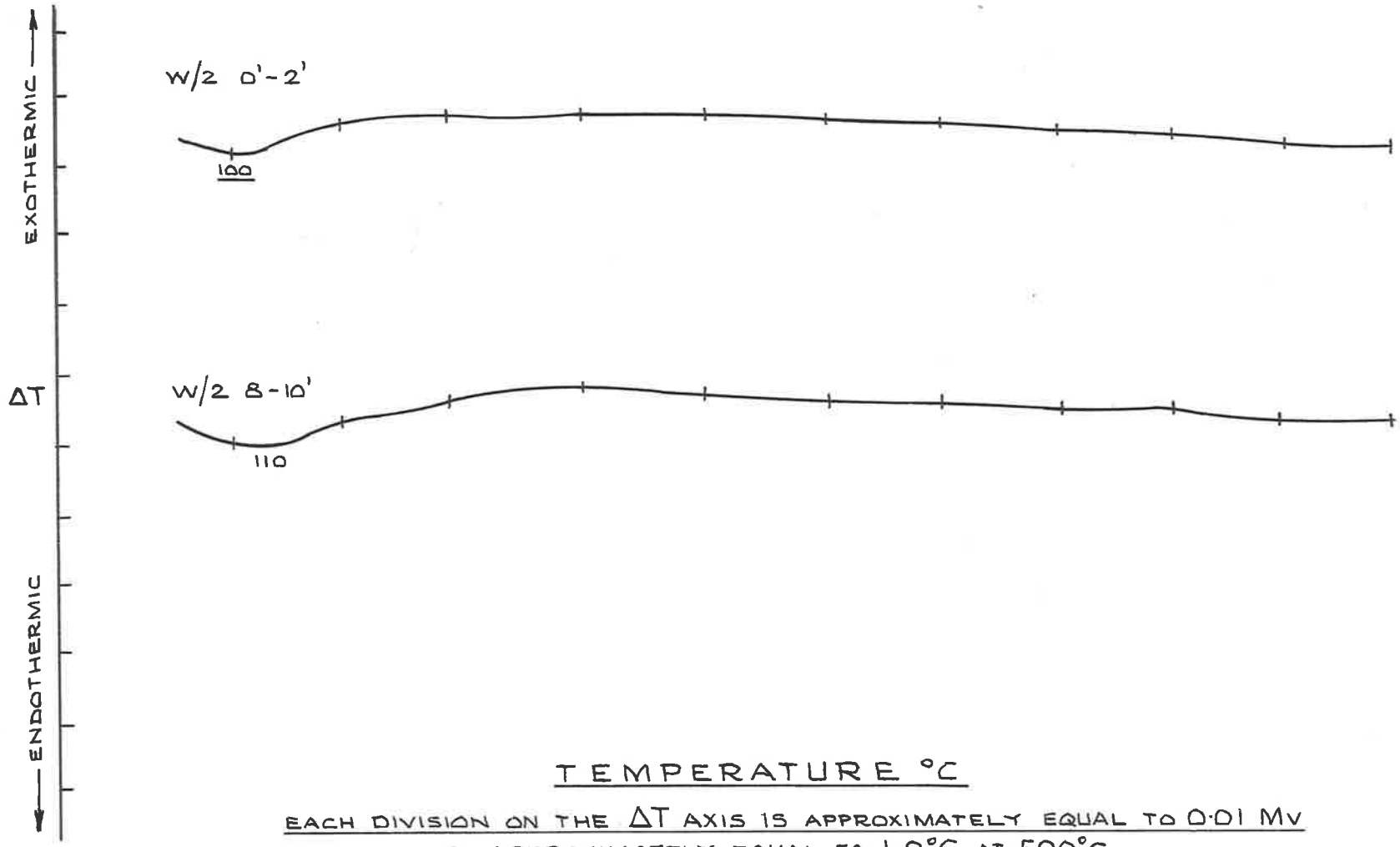

TEMPERATURE °C

EACH DIVISION ON THE ΔT AXIS IS APPROXIMATELY EQUAL TO 0·01 MV
I.E. APPROXIMATELY EQUAL TO 1·0°C AT 500°C

FIGURE-14 DIFFERENTIAL THERMAL TRACE - SAMPLE MH 8
SAMPLE CONSISTING MAINLY OF CRANDALLITE

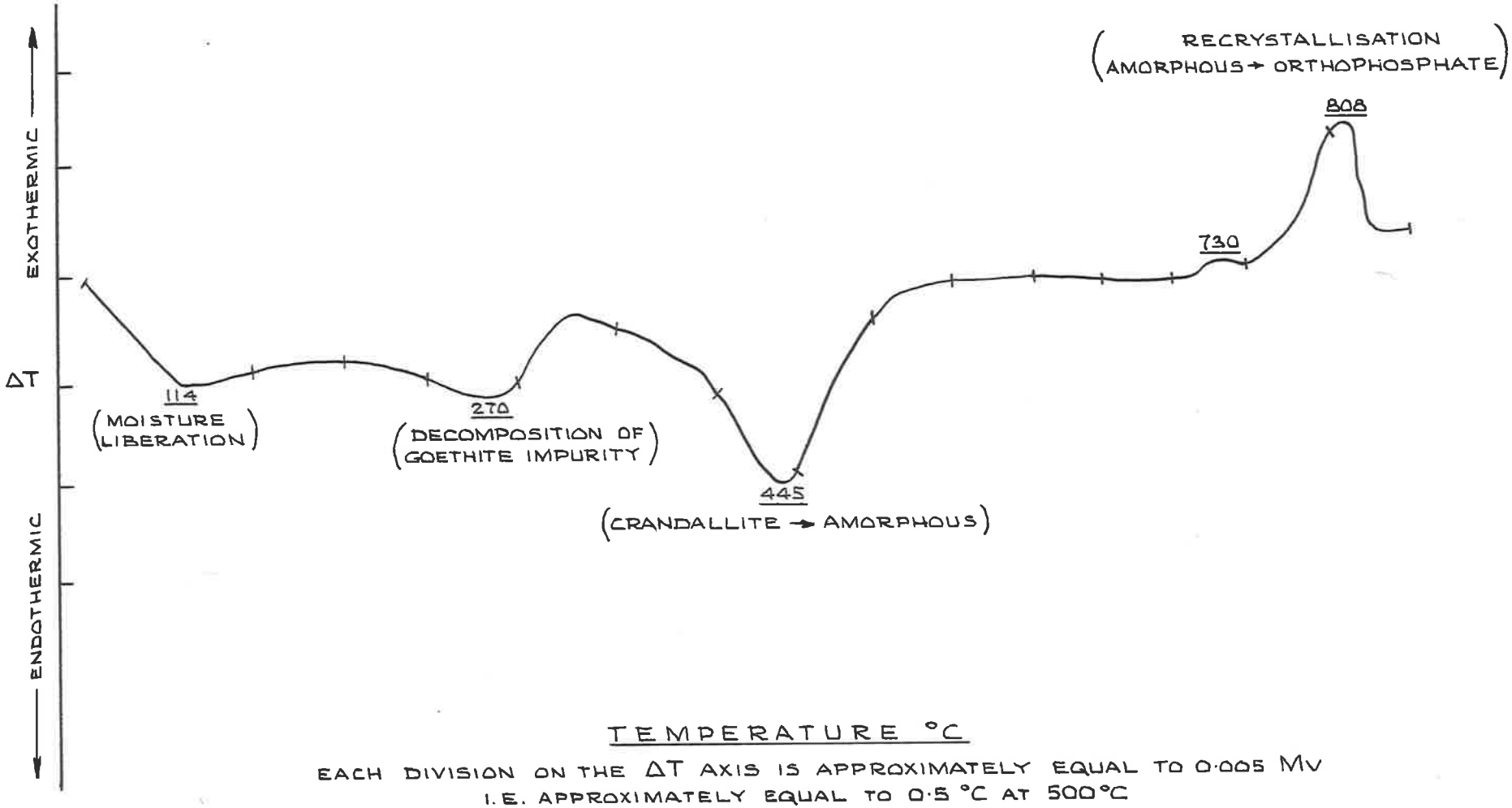

TEMPERATURE °C

EACH DIVISION ON THE ΔT AXIS IS APPROXIMATELY EQUAL TO 0·005 Mv
I.E. APPROXIMATELY EQUAL TO 0·5 °C AT 500°C

FIGURE-15 DIFFERENTIAL THERMAL TRACE - SAMPLE A17 (0-2ft)

SAMPLE CONSISTING MAINLY OF MILLISITE

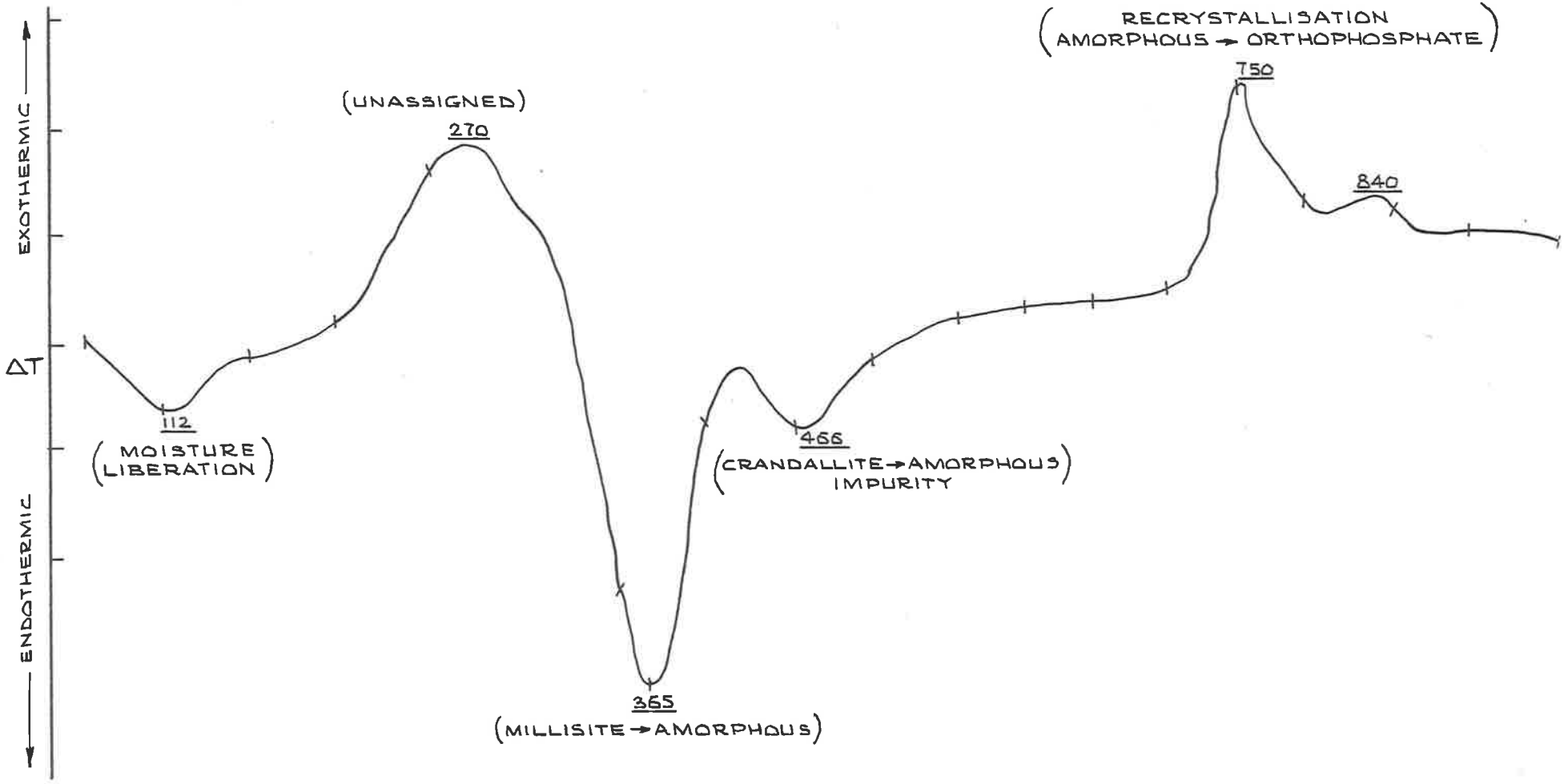

EACH DIVISION ON THE ΔT AXIS IS APPROXIMATELY EQUAL TO 0·005 Mv
I.E. APPROXIMATELY EQUAL TO 0·5 °C AT 500°/₀

FIGURE-16 DIFFERENTIAL THERMAL TRACE

SAMPLE A8-6 INS.

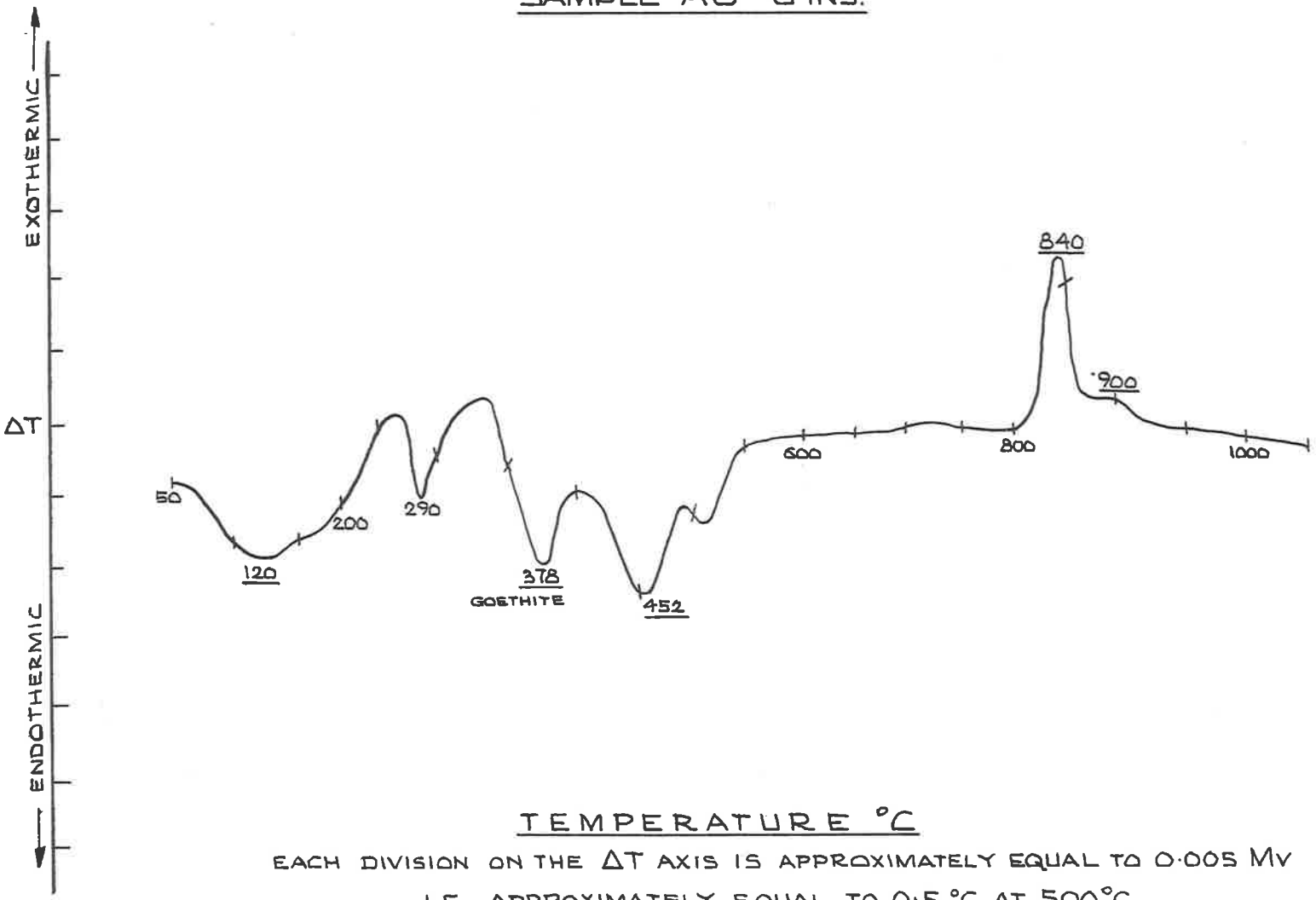

TEMPERATURE °C

EACH DIVISION ON THE ΔT AXIS IS APPROXIMATELY EQUAL TO 0·005 MV

I.E. APPROXIMATELY EQUAL TO 0·5 °C AT 500°C

FIGURE-17 DIFFERENTIAL THERMAL TRACES

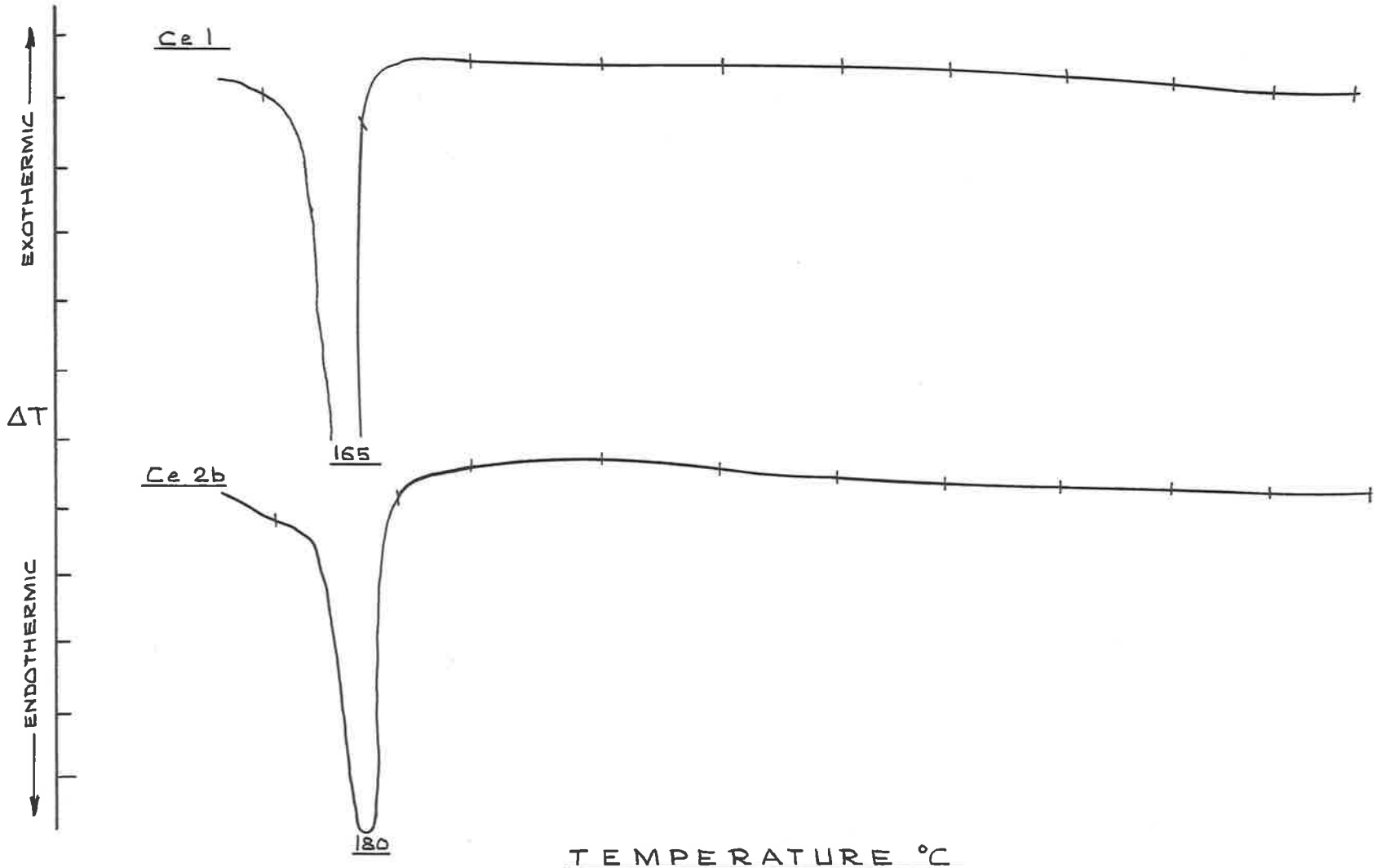

EACH DIVISION ON THE ΔT AXIS IS APPROXIMATELY EQUAL TO 0·01 Mv
I.E. APPROXIMATELY EQUAL TO 1·0°C AT 500°C

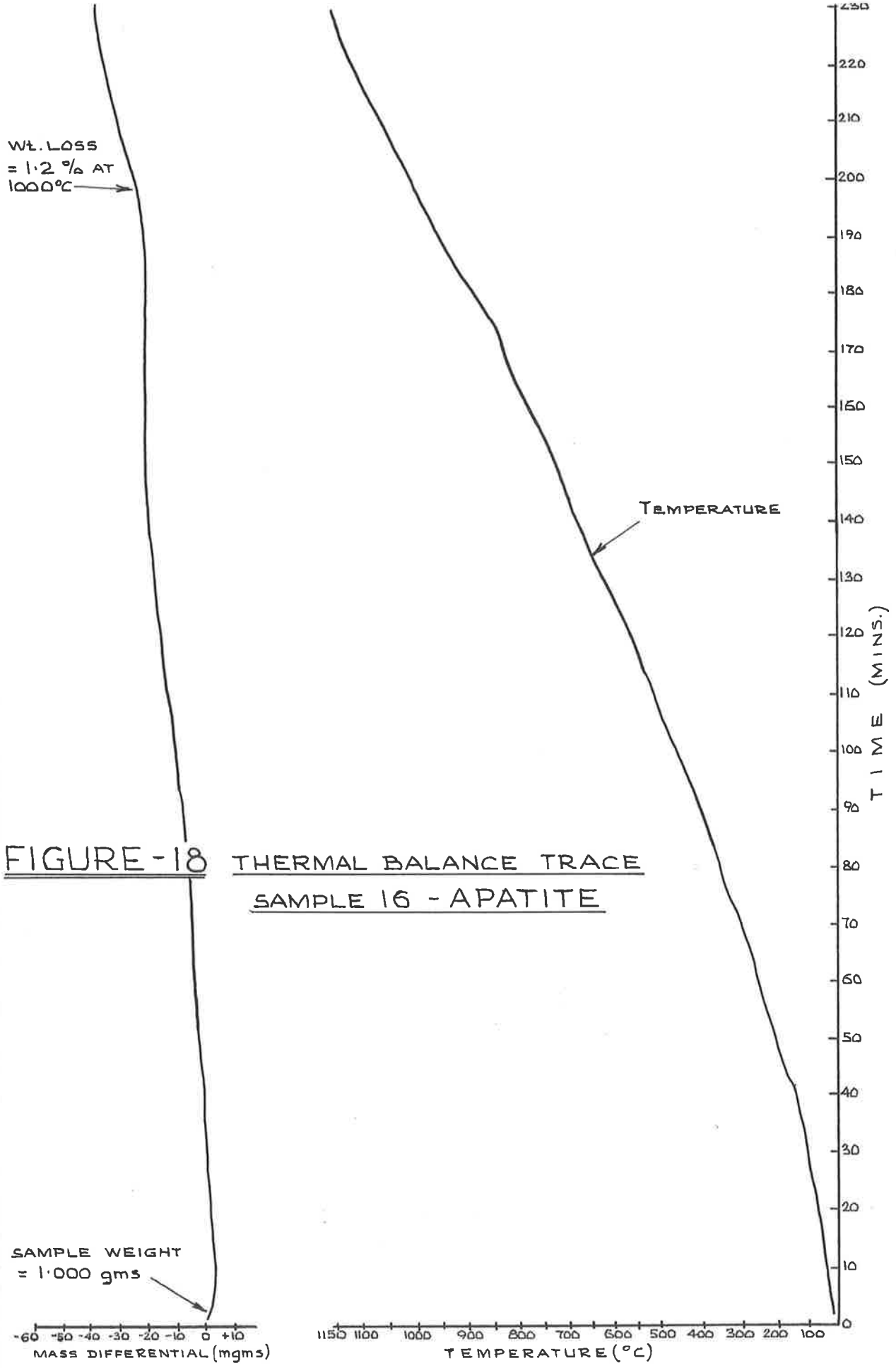

FIGURE-18 THERMAL BALANCE TRACE
SAMPLE 16 - APATITE

FIGURE-19 THERMAL BALANCE TRACE SAMPLE-24 CRANDALLITE & MILLISITE

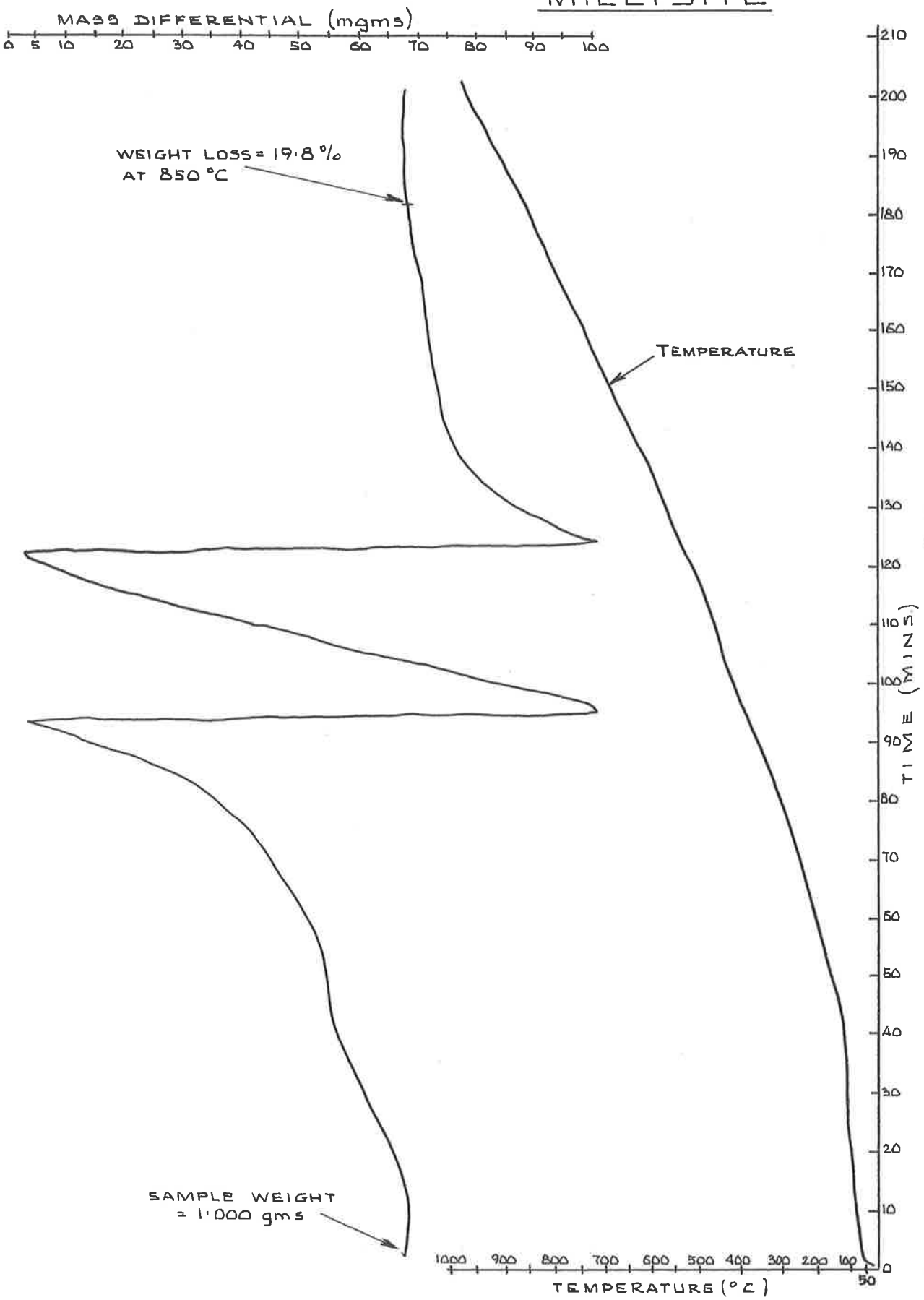

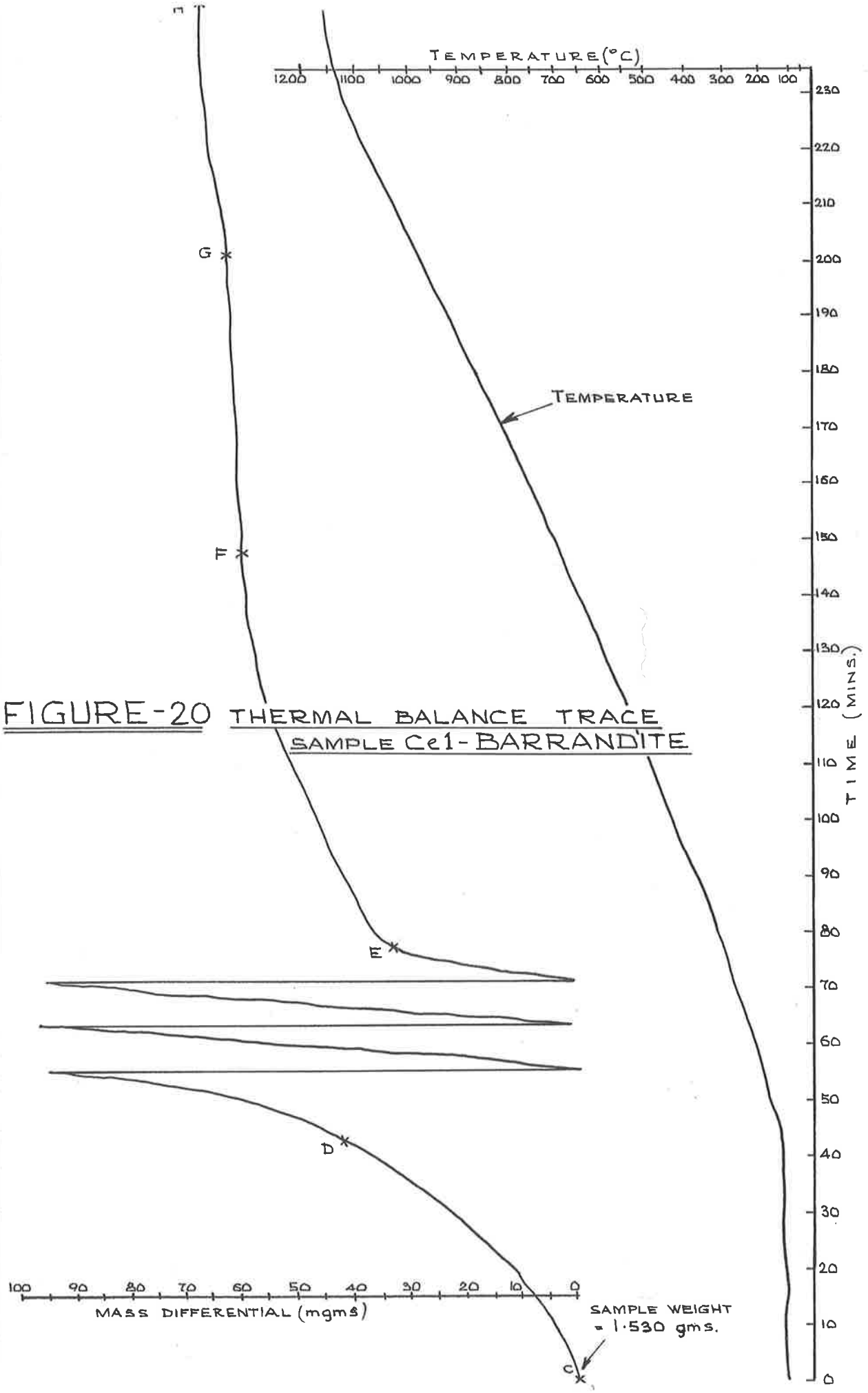

FIGURE-20 THERMAL BALANCE TRACE
SAMPLE Ce1-BARRANDITE

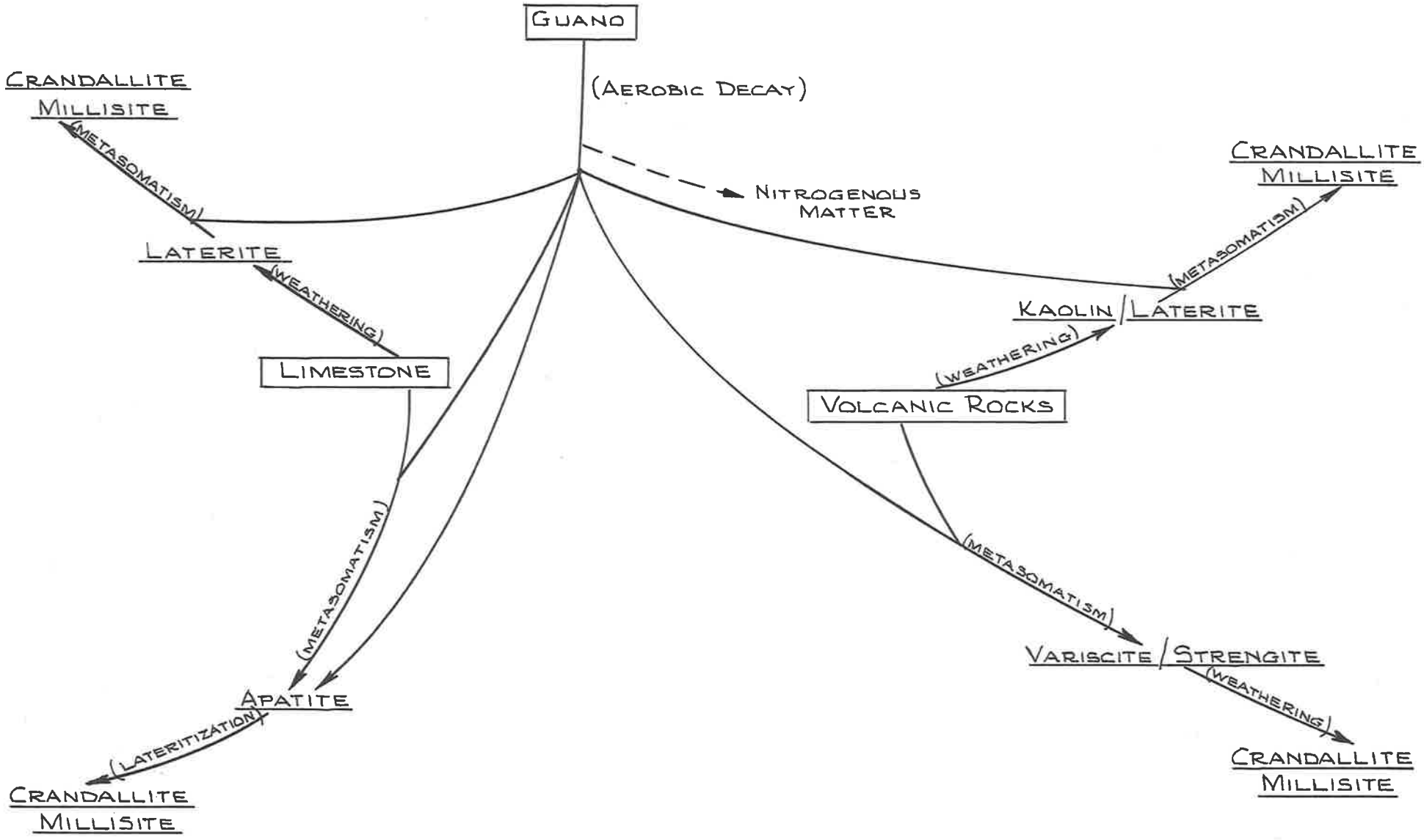

FIGURE-21 THE ORIGIN OF THE PRINCIPAL PHOSPHATE MINERALS CHRISTMAS ISLAND (INDIAN OCEAN)

APPENDIX

DEPARTMENT OF MINES SOUTH AUSTRALIA

TERTIARY LIMESTONES OF CHRISTMAS ISLAND (INDIAN OCEAN)

by

N. H. Ludbrook

ABSTRACT

The foraminiferal faunas of the Upper Eocene and Lower Miocene limestones of Christmas Island in the Indian Ocean are described. Except for the fringing reefs, no rocks younger than Burdigalian were identified.

1. INTRODUCTION

Christmas Island is a small island in the north east of the Indian Ocean about 190 miles south of Java and 550 miles north of east of Cocos Islands, latitude 10°25'13"S, longitude 105°42'40"E, based upon the flagstaff at Flying Fish Cove. It has been a territory of the Commonwealth of Australia since 1958 and is leased by the Christmas Island Phosphate Commission for the mining of important deposits of phosphate. The island has an area of 52 square miles, the greatest length north-south is $10^1/_2$ miles, greatest width east-west 11 miles.

The physiography, geology and natural history of the island were described by Andrews and others in 1900 in A Monograph of Christmas Island (Indian Ocean). British Museum (Natural History). From a suite of some 58 rock specimens Jones and Chapman described the larger foraminifera, the orbitoids being subsequently revised by Nuttall in 1926.

The present study is based on a collection of 54 rock specimens made by N. A. Trueman of the Australian Mineral Development Laboratories, Adelaide, in July-August, 1963, as part of an investigation of the phosphate deposits for the British Phosphate Commissioners.

2. GENERAL GEOLOGY

Van Bemmelen (1949, p. 59) briefly described the structural setting of Christmas Island as on an east-west trending submarine ridge forming part of the circum-Australian median ridge. Although no confirmatory deep drilling has been undertaken, the island is considered to be a Tertiary atoll formed upon a steep volcanic cone rising more than 13,000 feet from the ocean floor.

A general account of the geology was given by Andrews (1900, pp. 269-298). Most of his sampling was done in and around Flying Fish Cove where the main settlement is situated. The island is composed of Tertiary limestones interbedded with basalt and palagonite tuffs described by Campbell Smith (1926). Andrews distinguished three limestones – A, B, and C – in the Flying Fish Cove sections (1900, p. 272), the ages of which were determined by Jones and Chapman (pl. 20) as Upper Eocene or Oligocene, ? Oligocene, and Miocene respectively. Nuttall (1926) subsequently re-examined Jones and Chapman's material and determined the age of limestones A and B as Upper Eocene and of C as Lower Miocene probably Aquitanian. There are, in addition, younger limestones of the fringing reef (Andrews's D and E).

The material collected by Trueman includes resampling some of the localities of Andrews, but on the whole it is distributed over the island rather than concentrated on Flying Fish Cove. Particular attention was paid to the higher levels in the hope of determining an approximate age for the phosphate, which occurs above 500 feet above sea level. The sample localities are shown in Figure 1.

Except for sample P36 from the fringing reef at Flying Fish Cove, Trueman's material is of Upper Eocene (Tertiary 'b') and Lower Miocene (Tertiary 'e' to 'f_{1-2}' - Aquitanian to lower Burdigalian) age. No limestones younger than Burdigalian were recognized.

Allowing for the elevation of the atoll, the phosphates have the possibility of being as old as Middle Miocene. It is not feasible to date them more accurately than of Middle Miocene to Recent age.

3. FAUNAS OF THE LIMESTONES

Both the Upper Eocene and Lower Miocene are reef limestones with abundant corals and calcareous algae, and rich in foraminifera which appear to be localized in their distribution. Twelve of the samples collected consisted more or less entirely of reef corals. Fourteen samples mostly between 600 and 1020 feet contained molluscan moulds of relatively few species dominated by cerithiids.

Distribution of the foraminifera is tablulated in Figure 2. Assemblages contained in P 36, from the fringing reef, and P52, from talus, have been included, but their position in the vertical range is obviously anachronous. In addition to these species included in the systematic descriptions the following were recorded:

(1) From the Upper Eocene

Nummulites cf. pengaronesis, Gyroidina sp.,
Amphistegina sp.

(2) From the Lower Miocene

Miliolidae, Carpenteria sp., Bolivina cf. robusta, Rotalia cf. indica Le Roy

(3) From the fringing reef

Textularia sp., Borelis cf. melo (Fichtel and Moll) Homotrema rubrum (Lamarck), Eponides sp., Amphistegina sp., Globigerina bulloides d'Orbigny, Orbulina universa d'Orbigny, Globorotalia menardii (d'Orbigny), Globorotalia truncatulinoides (d'Orbigny).

The foraminiferal faunas of the Lower Miocene limestone are very similar to those of the Tagpochau Limestone of Saipan as described by Hanzawa (1957) and Cole (1957).

4. EVIDENCE FOR THE AGE OF THE LIMESTONES

The oldest limestone, limestone A of Andrews, is represented by sample P35. It is an algal limestone containing Discocyclina oceanica, abundant Heterostegina cf. saipanensis and an associated fauna with Gypsina globula and species of Pararotalia, Amphistegina, Gyroidina, with rare Nummulites which was seen only in a natural section on one of the surfaces of P35. This limestone occurs near sea level at the south end of Flying Fish Cove. Limestone B of Andrews is represented by Sample P 51 taken at about 300 feet $^1/_2$ mile south east of Smith Point at the south end of Flying Fish Cove. It is lithologically and faunally the same as P 35, with Discocyclina oceanica, Heterostegina saipanensis and, apart from Nummulites, the same associated foraminifera. As suggested by Nuttall (1926. p. 25) limestone B is considered to be the same limestone as A. The foraminiferal assemblage is indicative of Tertiary 'b' (Upper Eocene) age.

Limestone C, the "orbitoidal limestone" of Andrews and of Jones and Chapman is represented by sample P 13 collected about $^1/_2$ mile south of Flying Fish Cove at 600 feet and by P 52 collected at 200 feet in Flying Fish Cove. As P 52 was collected below the level of P 51, unless they are separated by a fault, P 52 was taken from talus. At the 600-foot level at Flying Fish Cove the limestones are rich in species of Lepidocyclina (Eulepidina). L. (E.) ephippioides, L. (E.) insulaenatalis, L. (E.) chapmani, L. (E.) murrayana, and L. (E.) inaequalis are all present in Trueman's material, associated with Borelis pygmaeus, Rotalia tectoria, Sorites martini, Cycloclypeus cf. eidae and Amphistegina sp.

Except for a fragment of a lepidocycline in sample P 40, neither Lepidocyclina (Eulepidina) ephippioides (= L.(E.) formosa), nor any of the other eulepidines were observed above this level.

At approximately the same level on the southwest side of the island sample P 48 contained Miogypsinoides dehaartii which continued to 880 feet (P 9).

The division at 600 feet between samples P 13, with the last appearance of Lepidocyclina (Eulepidina) ephippioides, and P 48 with the first appearance of Miogypsinoides dehaartii corresponds to the division between Tertiary e_{1-4} and e_5 as recognized in Borneo by Mohler (1950, p. 526).

The zone of Miogypsinoides dehaartii contains also Austrotrillina howchini, Sorites martini, Borelis pygmaeus, Borodinia septentrionalis, Gypsina marianensis, G. vesicularis, Acervulina inhaerens, Carpenteria capitata, and Amphistegina bikiniensis. Spiroclypeus globulus occurs in the lower part at 600-662 feet and Miogypsina neodispansa above the 800-foot level.

This assemblage is regarded as of upper Tertiary 'e' age.

Sample P 33, taken from approximately 800 feet, is a miliolid limestone containing Flosculinella bontangensis in association with Austrotrillina howchini, Sorites martini, Borelis pygmaeus, and Borodinia septentrionalis. The presence of Flosculinella bontangensis would indicate a Tertiary f_{1-2} age. As the relative levels of P 33 (? 800 feet) and P 9 (880 feet) may be approximate only or influenced by faulting, it may not be assumed with certainty that the zones of Miogypsinoides dehaartii and of Flosculinella bontangensis overlap on Christmas Island, although this has shown to be the case in Borneo (Mohler 1950, p. 526)

Tertiary 'e' on the assembled evidence most recently published by Glaessner (1959) and Eames and his colleagues (1961, pp. 12-15) is equivalent to the Aquitanian and Tertiary f_{1-2} to the Burdigalian. The Aquitanian age for the Miocene limestone of Christmas Island as suggested by Nuttall, (l.c. p. 24) is supported by the present investigation for all but the upper levels above approximately 800 feet which extend into the Burdigalian.

No evidence of age younger than Lower Miocene for any of the limestones other than the fringing reef was obtained. The fringing reef sample P 36 carried the planktonic foraminifera Orbulina universa, Globigerina bulloides, Globorotalia menardii and Globorotalia truncatulinoides, all of which are living species figured on Plate 7, figs. 1-5, 7-9.

5. SAMPLE DESCRIPTIONS

P4. 1 mile east of Flying Fish Cove at 1020 feet, dense miliolid limestone with Austrotrillina howchini, Sorites martini, Borelis pygmaeus, Acervulina inhaerens, algae, moulds of coral and gastropods.

P5. Phosphate Hill, 1 mile ESE of Flying Fish Cove, at 1000 feet. Granular unfossiliferous limestone.

P6. $1\frac{1}{2}$ miles south east of Flying Fish Cove at 890 feet. Chalky detrital miliolid limestone with Austrotrillina howchini, Borelis pygmaeus, algae, and mollusca Hipponix (Sabia) sp., Cypraea sp., Turbo sp.

P7. $1\frac{1}{2}$ miles south east of Flying Fish Cove at 800 feet. Unfossiliferous recrystallized limestone.

P8. $1\frac{1}{2}$ miles SSE of Flying Fish Cove at 925 feet. Recrystallized and leached limestone with internal cast of a lucinid mollusc.

P9. 2 miles south of Flying Fish Cove at about 800 feet. Leached chalky limestone with molluscan mould (carditid) and casts (cerithiids).

P11. $2\frac{1}{4}$ miles west of south of Flying Fish Cove at about 800 feet. Partially recrystallized coralline limestone.

P12. $\frac{1}{2}$ mile east of Smithson Bight and 3 miles north of South Point at about 650 feet. Dense recrystallized limestone with abundant Borodinia septentrionalis associated with Acervulina inhaerens, Borelis pygmaeus, Gypsina marianensis, Sorites martini, Carpenteria sp., miliolidae, algae

P13. $\frac{1}{2}$ mile south of Flying Fish Cove at 600 feet. The "Orbitoidal Limestone" of Jones and Chapman, containing Lepidocyclina (Eulepidina) ephippioides, L. (E.) insulaenatalis, L. (E.) murrayana, L. (E.) inaequalis, Borelis pygmaeus, Rotalia tectoria, Amphistegina sp.

P14. $2\frac{1}{2}$ miles south of Northwest Point at 600 feet or less. Partially leached and recrystallized coralline limestone.

P15. Sydney's Dale $3\frac{1}{4}$ miles south of Northwest Point at less than 600 feet. Coral.

P16. Near railway 2 miles north of South Point at 800 feet. Sugary leached limestone.

P17. 2 miles north of South Point at 800 feet. Sugary leached and recrystallized limestone.

P18. $1\frac{1}{2}$ miles north of Smithson's Bight at 600 to 700 feet. Sugary leached limestone with moulds of cerithiid mollusca.

P19. Centre of island on track 1/2 mile west of railway at about 730 feet. Limestone with molluscan moulds.

P20. Centre of island 1 mile west of railway at about 750 feet. Dense recrystallized limestone with abundant moulds and casts of mollusca - Cerithiopsis sp., Cerithium (Ptychocerithium) sp., lucinid, carditid.

P21. 1 mile north west of Middle Point at 300 feet. Coralline limestone with algae, Gypsina vesicularis, Carpenteria sp.

P22. 1/4 mile north cast of railway, 1/2 mile south west of Grant's Well at 700 feet. Dense coralline limestone.

P23. 1/2 mile east of Grant's Well at 750 feet. Coral.

P24. Jack's Hill 1 mile north east of Murray Hill at about 700 feet. Coralline limestone.

P25. Murray Hill at about 700 feet. Leached limestone.

P26. Murray Hill, west side, above 800 feet. Limestone with abundant Miogypsinoides dehaartii, Miogypsina neodispansa, Austrotrillina howchini and Rotalia tectoria.

P27. 1/4 mile south of Murray Hill at 700 to 800 feet. Coral.

P28. 1 mile north of Middle Point at about 700 feet. Limestone with Gypsina vesicularis, G. marianensis, Rotalia tectoria, Rotalia cf. indica, Bolivina cf. robusta, Operculinoides sp., algae

P29. 1/4 mile north west of Grant's Well at 750 feet. Recrystallized coralline limestone.

P30. 3/4 mile north of Smithson Bight at about 650-700 feet. Algal limestone with abundant Miogypsinoides dehaartii, and Gypsina marianensis, G. vesicularis, Carpenteria capitata.

P31. 3/4 mile north of Middle Point, at ?600 feet. Dense limestone with abundant Miogypsinoides dehaartii, Amphistegina bikiniensis, Gypsina vesicularis, G. marianensis, Acervulina inhaerens, algae

P32. Centre of island 1 mile west of railway at 600 feet. Leached limestone with abundant molluscan moulds, chiefly Cerithiopsis sp. with Callista sp. and lucinidae.

P33. 1 mile northwest of John D. Point at 800 feet. Recrystallized miliolid limestone containing Flosculinella bontangensis, Austrotrillina howchini, Borodinia septentrionalis, Sorites martini, Borelis pygmaeus, algae.

P34. Flying Fish Cove, 1/4 mile east of Smith Point. Coral.

P35. Flying Fish Cove, 1/4 mile south east of Smith Point at sea level. Yellow dense limestone with Discocyclina oceanica, Heterostegina saipanensis, Gypsina globula, Pararotalia sp., Amphistegina sp., Gyroidina sp., Nummulites cf. pengaronensis.

P36. On fringing reef, north end of Flying Fish Cove 1/4 mile south of Rocky Point at sea level. Limestone containing Sporadotrema cylindricum, Textularia sp., Borelis melo, Orbulina universa, Globigerina bulloides, Globorotalia menardii, Globorotalia truncatulinoides, Eponides sp., Homotrema rubrum, Amphistegina sp.

P37. On railway 1 mile south of Smith Point at 662 feet. Dense limestone containing abundant Spiroclypeus globulus with Miogypsinoides dehaartii, Acervulina inhaerens, algae.

P38. On railway 1 1/2 miles south of Smith Point at 678 feet. Corals.

P39. Centre of island, on railway at 700 feet. Leached and recrystallized miliolid limestone with Borodinia septentrionalis, corals, algae.

P40. On railway, 1 1/4 miles east of Smithson Bight at 653 feet. Detrital algal limestone containing Sorites martini, Borodinia septentrionalis, Gypsina vesicularis, Amphistegina bikiniensis, Lepidocyclina sp.

P41. 1 mile north of Smithson Bight at ?600 feet. Detrital limestone with fragmentary remains of miliolidae, algae, Austrotrillina howchini, Borelis pygmaeus.

P42. 1/2 mile north of Smithson Bight. Oolitic limestone with moulds of Cerithiopsis sp.

P43. Smithson Bight at less than 300 feet. Recrystallized limestone.

P45. West of railway, 1/2 mile east of Smithson Bight, at about 650 feet. Dense white detrital limestone with abundant Carpenteria capitata, Gypsina vesicularis, G. marianensis, Amphistegina bikiniensis, algae.

P46. 1 mile east of Smithson Bight at 650 feet. Recrystallized limestone crowded with moulds of small mollusca and Ptychocerithium.

P47. 1 1/2 miles north east of Egeria Point at ?600 feet. Calcite.

P48. 1 mile north east of Egeria Point at 600 feet. Partially recrystallized limestone, one specimen of which is crowded with molluscan moulds, including Cerithiopsis sp., the other with Miogypsinoides dehaartii, Borelis pygmaeus, Borodinia septentrionalis, Carpenteria capitata, miliolidae, algae.

P49. $1^1/_2$ miles north east of Egeria Point at ?600 feet. Coralline limestone with internal casts of cerithioid mollusca.

P50. $1^1/_4$ miles north of Smithson Bight at 600 - 800 feet. Leached detrital limestone crowded with moulds of molluscan fragments.

P51. Flying Fish Cove, $^1/_2$ mile southeast of Smith Point at about 300 feet. Bed B of Andrews, (p. 272) equivalent to No. 522 of Jones and Chapman (p. 231). Yellow limestone with Heterostegina saipanensis, Discocyclina oceanica, Gypsina globula, Gyroidina sp., Amphistegina sp., Pararotalia sp., algae.

P52. Flying Fish Cove, $^1/_2$ mile south east of Smith Point at 200 feet, presumed talus. Dense and partially recrystallized limestone rich in Lepidocyclinae - Lepidocyclina (Eulepidina) ephippioides, L. (E.) chapmani, L. (E.) insulaenatalis, L. (E.) andrewsiana, Rotalia tectoria, Cycloclypeus cf. eidae, Borelis pygmaeus, Amphistegina, Sorites martini, algae.

P53. $1^3/_4$ miles WSW of Low Point at 600 feet. Dense recrystallized limestone containing Spiroclypeus globulus, Amphistegina bikiniensis, Carpenteria capitata, algae.

P54 1 mile NNW of John D. Point at 600 feet. Recrystallized limestone with Miogypsinoides dehaartii, Carpenteria capitata Rotalia tectoria, Sorites martini, Gypsina vesicularis.

6. SYSTEMATIC RECORD OF THE FORAMINIFERA

The foraminifera are described from 86 random sections of 23 samples cut at Australian Mineral Development Laboratories and bearing the numbers 13262 - 13289, 13301 - 13303, 1333 - 13352, 13390 - 13414. All are deposited in the Palaeontological Collection of the Geological Survey of South Australia.

Family MILIOLIDAE

Genus Austrotrillina Parr, 1942

Austrotrillina howchini (Schlumberger)

pl. 1 figs. 13, 14.

1893 Trillina howchini Schlumberger, Bull. Soc. Geol. France, ser. 3, vol. 21, p 119, 120, text figs. 1, 2, pl. 3, fig. 6.

1908 Trillina howchini; Chapman Proc. Linn. Soc. N.S.W. vol. 32 pt. 4, No. 128, p. 753, pl. 39, figs. 7 - 9.

1913 Trillina howchini; Chapman, Proc. Roy. Soc. Vict vol. 26 (n.s.) p. 169 - 170, pl. 16, fig. 4.

1936 Trillina howchini; Crespin, Comm'lth Australia, Dept. Inst. Pal. Bull. No. 2 p. 6, pl. 1, figs. 1, 2.

1942 Austrotrillina howchini; Parr, Min. Geol. Journ. Victoria, Aust., vol. 2 No. 6, p. 361, figs. 1 - 3.

1953 Austrotrillina howchini; Crespin, Aust. Bur. Min. Res. Geol. Geophys. Bull. 21, pp. 62-3, pl. 9, fig. 4.

1953 Austrotrillina howchini; Cole and Bridge, U.S.G.S. Prof. Pap. No. 253, p. 20, pl. 14, fig. 12.

1954 Austrotrillina howchini; Todd and Post, U.S.G.S. Prof. Pap. 260-N, p. 555 (synonymy).

1954 Austrotrillina howchini; Cole, U.S.G.S. Prof. Pap. 260-0, p. 573, pl. 210, figs. 6 - 9.

1957 Austrotrillina howchini; Cole, U.S.G.S. Prof. Pap. 280-I, p. 329, pl. 101, figs. 4 - 6.

1957 Austrotrillina howchini; Hanzawa, Geol. Soc. Amer. Mem. 66, p. 38, pl. 22, figs. 12, 13, pl. 34, figs. 1, 2.

1960 Austrotrillina howchini; Todd and Low, U.S.G.S. Prof. Pap. 260-X, p. 825.

1961 Austrotrillina howchini; Ludbrook, Geol. Surv. S.Aust. Bull. 36, p. 48, table 10, pl. 4, fig. 5.

1962 Austrotrillina howchini; Eames et al., Fund. Mid.-Tert. Correl. p. 14 etc., pl. VI B, E.

1963 Austrotrillina howchini; Ludbrook, Trans. Roy. Soc. S.Aust. vol. 87 p. 12, fig. 2.

Distribution: Localities, P 4, P 6, P 33, P 41. 600 - 1020 feet above sea level. The species is especially abundant in P 4 at 1020 feet.

Occurrence elsewhere: In Aquitanian to Burdigalian rocks of North Africa and the southern Mediterranean, Middle East, East Africa, India and Pakistan, Indonesia, Papua, Marshall Islands, Mariana Islands, Western Australia, South Australia, and Victoria.

Family PENEROPLIDAE

Genus Sorites Ehrenberg, 1840

Sorites martini (Verbeek)

pl. 7 fig. 4

1896 Orbitolites martini Verbeek and Fennema, Desc. geol. Java et Madoura. Amsterdam. tome 2 p. 1159, pl., 9 figs. 134 - 135 (fide Ellis and Messina).

1957 Sorites martini: Hanzawa, Geol. Soc. Amer. Mem. 66, p. 55, pl. 6, figs. 3, 4, 8, 9; pl. 35, fig. 16. (synonymy).

1957 Sorites martini; Cole, U.S.G.S. Prof. Pap. 280 I, p. 335.

Distribution: Localities P 12, P 53, P 4, 650 to 1020 feet above sea level: P 52.

Occurrence Elsewhere: Java, Philippines; Tagpochau Limestone of Saipan, Tinian, and Rota.

Family ALVEOLINELLIDAE

Genus Borelis Montfort, 1808

Borelis pygmaeus Hanzawa

pl. 1 figs 8 - 12

1930 Borelis (Fasciolites) pygmaeus Kanzawa, Tohoku Imp. Univ. Sci. Rep., Sendai, Japan ser. 2 (Geol.) vol. 14, No. 1, p. 94-5, pl. 26, figs. 14 - 15.

1938 Neoalveolina pygmaea, Crespin, Comm'lth. Australia Dept. Interior Pal. Bull. No. 3, p. 10, pl. 3. figs 3, 5.

1947 Borelis pygmaeus; Hanzawa, Jap. Jour. Geol. Geol. vol. 20, Nos. 2-4, p. 9-11, pl. 5, figs. 1 - 4.

1953 Borelis pygmaeus; Cole, U.S.G.S. Prof. Pap. 253, p. 27, pl. 12, fig. 16; pl. 13, figs. 4 - 7 (synonymy).

1957 Borelis pygmaeus; Cole, U.S.G.S. Prof. Pap. 260-V, p. 767, pl. 240, figs. 11-13.

1957 Borelis pygmaeus; Hanzawa, Geol. Soc. Amer. Mem. 66, p. 55, pl. 34, figs. 8, 9.

1957 Borelis pygmaeus; Cole, U.S.G.S. Prof. Pap. 280-I, p. 336, pl. 102, fig. 1; pl. 110, figs. 5 - 7.

1961 Borelis pygmaea; Eames et al., Furd. Mid-Tert. Correl. p. 12 13, 14, 20, 67.

Distribution: Localities P 4, P 6, P 12, P 33, P 41, P 48, P 52, 600-1000 feet above sea level.

Occurrence elsewhere: Tertiary d-e, ?c, ?f, Oligocene to Miocene of Saipan, Eniwetok, Guam, Papua, Java, Tanganyika.

Genus FLOSCULINELLA Schubert, 1910

Flosculinella bontangensis (Rutten)

pl. 1 figs. 15, 16.

1913 Alveolinella bontangensis Rutten, Geol. Reichs.-Mus. Leiden Samml., ser. 1, vol. 9, p. 221-224, pl. 14.

1927 Alveolinella bontangensis; van der Vlerk and Umbgrove, Dienst. Mijnb. Ned. Indie. Wetensch. Meded. No. 6, p. 20, fig. 13.

1929 Alveolinella bontangensis: van der Vlerk, Dienst. Mijnb Ned. Indie Wetensch. Meded. No. 9, p. 14-15, figs. 1-5.

1937 Flosculinella bontangensis; Reichel, Soc. Paleont. Suisse Mem., vol. 59, p. 113-115, pl. 11, fig. 7; text figs. 23, 24.

1953 Flosculinella bontangensis; Crespin Comm'lth. Australia Bur. Min. Res. Geol. Geophys. Bull. 21, pt. 2, p. 66, pl. 9, fig. 5.

1962 Flosculinella bontangensis, Eames et al., Fund. Mid-Tert. Correl. p. 14, pl. 7E.

1963 Flosculinella bontangensis; Cole, U.S.G.S. Prof. Pap. 403-E p. E20, pl. 9, figs. 1 - 3.

Distribution: Locality P 33, at 800 feet.

Occurrence elsewhere: Tertiary f_{1-2}, Burdigalian, of Borneo, Java, New Guinea, Philippines, Soemba, North west Australia, Eucla Basin of South and Western Australia, East Africa.

Family PLANORBULINIDAE

Genus Borodinia Hanzawa, 1940

Borodinia septentrionalis Hanzawa

Pl. 2 figs, 5, 6.

1940 Borodinia septentrionalis Hanzawa, Jub. Publ. commem. Yabe's 60th Birthday, p. 790-791, pl. 42, figs 10-12.

1957 Borodinia septentrionalis Hanzawa, Geol. Soc. Amer. Mem. 66, p. 65, pl. 25, figs. 1-6.

Distribution: Localitites P 12, P 33, P 40, P 48, 600 to 800 feet above sea level.

Occurrence elsewhere: Tagpochau Limestone of Saipan and Tinian, Mariana Islands.

Genus Acervulina Schultze, 1854

Acervulina inhaerens, Schultze

1854 Acervulina inhaerens Schultze, Organismus Polythal. p. 68, pl. 6, fig. 12.

1954 Acervulina inhaerens; Cushman, Todd, and Post, U.S.G.S. Prof. Pap. 260-H, p. 372, pl. 91, figs. 37 38 (synonymy).

1960 Acervulina inhaerens; Todd and Low, U.S.G.S. Prof. Pap. 260-X p. 853.

Distribution: Localities P 4, P 12, P 31, P 37. 600-1000 feet above sea level.

Occurrence elsewhere: Widely distributed; Miocene to Recent of Eniwetok Atoll.

Family GYPSINIDAE

Genus Gypsina Carter, 1877

Gypsina globula (Reuss)

pl. 2, fig. 4; pl. 7, fig. 5.

1847 Ceriopora globulus Reuss, Naturwiss. Abh. Wien, Band 2, Abth. 1, p. 33, pl. 5, fig. 7 a-c.

1954 Gypsina globula; Cushman, Todd and Post, U.S.G.S. Prof. Pap. 260-H, p. 373, pl. 91, fig. 39.

1957 Gypsina globulus: Hanzawa, Geol. Soc. Amer. Mem. 66, p. 66, pl. 38, figs. 4, 8. 9 (synonymy).

1960 Gypsina globula; Todd and Low, U.S.G.S. Prof. Pap. 260-X, p. 853, pl. 258, fig. 9.

1963 Gypsina globula; Coleman, Micropal. vol. 9, (1), p. 10, pl. 1 fig. 2.

Distribution: P 35, P 36, P 51.

Occurrence elsewhere: Eocene to Recent of Europe, Middle East, Indo-Pacific region, Australia.

Gypsina marianensis Hanzawa

pl. 2 figs. 1 - 3

1957 Gypsina marianensis Hanzawa, Geol. Soc. Amer. Mem. 66, p. 66, pl. 21, fig. 8, pl. 27.

1957 Gypsina marianensis; Cole U.S.G.S. Prof. Pap. 280-I p. 337, pl. 103, figs. 1-4.

Ditribution: Localities P 9, P 12, P 28, P 30 P 31, P 45, 650 to 800 feet above sea level.

Occurrence elsewhere: Tagpochau Limestone of Saipan, Tinian, and Guam, Mariana Islands.

Gypsina vesicularis (Parker and Jones)

1860 Orbitolina concava Lamarck var. vesicularis Parker and Jones, Ann. Mag. Nat. Hist. ser. 3, vol. 6, p. 31, 38.

1954 Gypsina vesicularis; Cushman, Todd and Post, U.S.G.S. Prof. Pap. 260-H, p. 373, pl. 82, fig. 12. (synonymy).

1954 Gypsina vesicularis; Cole, U.S.G.S. Prof. Pap. 260-0 p. 585, pl. 210, figs. 14, 15 (synonymy).

1960 Gypsina vesicularis; Todd and Low, U.S.G.S. Prof. Pap. 260-X p. 853.

1963 Gypsina vesicularis; Coleman, Micropal. vol. 9, (1), p. 10, pl. 1, figs. 3 - 4.

Distribution: Localities P 9, P 21, P 28, P 31, 700-900 feet above sea level, ?300 feet.

Occurrence elsewhere: Mostly Pliocene to Recent Eniwetok, Bikini, Guam, Friendly Islands, Moluccas, Solomon Islands.

Family VICTORIELLIDAE

Genus Carpenteria Gray, 1858

Carpenteria capitata Jones and Chapman

pl. 7 fig. 10.

1900 Carpenteria capitata Jones and Chapman. Foram. Christmas I. Mon. Christmas I. B.M. (N.H.) p. 246, pl. 20, fig. 7.

Distribution: Samples P 9, P 45, P 48, 600-900 feet above sea level.

Family HOMOTREMIDAE

Genus Sporadotrema Hickson, 1911

Sporadotrema cylindricum (Carter)

pl. 7 figs. 1, 2.

1880 Polytrema cylindricum Carter, Ann. Mag. Nat. Hist. ser. 5, vol. 5, p. 441, pl. 18, fig. 1.

1963 Sporadotrema cylindricum; Coleman, Micropal. vol. 9, (1) p. 11, pl. 1, figs. 5-6 (synonymy).

Distribution: Locality P 36, on fringing reef.

Occurrence elsewhere: The species has been recorded from Eocene to Recent rocks in the Indo-Pacific region.

Family AMPHISTEGINIDAE

Genus Amphistegina d'Orbigny, 1826

Amphistegina cf. bikiniensis Todd and Post

pl. 3 figs. 8 - 10

1954 Amphistegina bikiniensis Todd and Post, U.S.G.S. Prof. Pap. 260-N, p. 563, pl. 201, fig. 4.

1960 Amphistegina bikiniensis; Todd and Low, U.S.G.S. Prof. Pap. 260-X p. 844.

Distribution: Localities P 31, P 33, P 40, 650-800 feet above sea level.

Occurrence elsewhere: Miocene of Bikini and Eniwetok Atolls.

Family ROTALIIDAE

"Rotalia" tectoria Todd and Post

pl. 1. figs. 1 - 4

1954 Rotalia tectoria Todd and Post, U.S.G.S. Prof. Pap. 260-N p. 561, pl. 202, figs. 2 - 4.

1957 Rotalia mecatepecensis; Hanzawa, Geol. Soc. Amer. Mem. 66, p. 59, pl. 2, figs. 1 - 11.

1960 Rotalia tectoria; Todd and Low, U.S.G.S. Prof. Pap. 260-X, p. 842.

Distribution: Localities P 13, P 28, P 52.

Occurrence elsewhere: Bikini, Tagpochau Limestone of Saipan, Tinian, and Rota, Mariana Islands; Eniwetok.

Remarks: Jones and Chapman's record of Rotalia schroeteriana from Christmas Island probably refers in part at least to this species. It is evidently close to Rotalia mexicana

mecatepecensis Nuttall with which it was synonymized by Hanzawa. Reiss (1958, pl. 2, figs. 18-24) has figured a species from Victoria, Australia, as Pararotalia mexicana mecatepecensis Nuttall, remarking (p. 15) that most specimens of Pararotalia from the Paris Basin are smooth. The Christmas Island specimens are heavily ornamented. No well preserved specimens are available and further study is required to determine whether the species should be placed in Pararotalia.

Genus PARAROTALIA Le Calvez, 1949

Pararotalia sp.

Pl. 1 figs 5-7

A species of Pararotalia is common in the Eocene samples P 35 and P 51.

Family MIOGYPSINIDAE

Genus Miogypsina Sacco, 1893

Miogypsina neodispansa (Jones and Chapman)

pl. 3 figs. 1 - 2.

1900 Orbitoides (Lepidocyclina) neodispansa, Jones and Chapman, Mon. Christmas I. p. 235-6, pl. 20, fig. 3

1926 Miogypsina neodispansa; Nuttall, Quart. J. Geol. Soc. Lond. vol. 82, p. 37-8, pl. 5, fig. 4 (synonymy).

Distribution: Sample P 26, 800 feet.

Occurrence elsewhere: Borneo, Philippines, New Guinea, New Hebrides.

Remarks: Miogypsina neodispansa was described from Andrews's sample 924, taken from the "orbitoidal limestones" immediately above their contact with the basalt south of Flying Fish Cove. No comparable sample was taken in the present collection, P 13 being nearest in location. The species occurs rarely and was seen only in P26 in association with Miogypsinoides dehaartii.

Genus MIOGYPSINOIDES Yabe and Hanzawa, 1928

Miogypsinoides dehaartii (van der Vlerk)

pl. 3 figs. 1 - 8

1924 Miogypsina dehaartii van der Vlerk, Eologae Geol. Helv. vol. 18, No. 3, p. 429-432, text figs. 1 - 3.

1957 Miogypsinoides dehaartii; Cole U.S.G.S. Prof. Pap. 280-I p. 339, pl. 111, figs. 6-16 (synonymy).

1962 Miogypsinoides dehaartii; Hanzawa, Micropal. vol. 8, No. 2, p. 157, text. fig. 11. (synonymy).

1962 Miogypsinoides dehaartii; Eames et al. Fund. Mid-Tert. Correl. p. 12, 15, 28, 30, 67.

1963 Miogypsinoides dehaartii; Coleman, Micropal. vol. 9, No. 1, p. 13, pl. 2, figs. 13-20.

Distribution: Localities P 9, P 26, P 30, P 31, P 37, P 48; 662-830 feet above sea level.

Occurrence elsewhere: Indonesia, Borneo, Guam, Taiwan, Saipan, Solomon Islands.

Remarks: M. dehaartii occurs abundantly at localities P 26, P 30 and P 31 on the south and south east of Murray Hill at elevations between 662 and 800 feet. It occurs rarely in P 9 at 800 feet. If the levels of P 9 (800 feet) and P 33 (800 feet) are correct, M. dehaartii persists for about 80 feet above the level at which Flosculinella bontangensis occurs in P 33, although it is not present with F. bontangensis in P 33. The continuance of M. dehaartii into the zone of F. bontangensis (Tertiary f, Burdigalian), as shown by Mohler (1950, p. 526) for the Tertiary of Borneo, would appear to be confirmed.

Family LEPIDOCYCLINIDAE

Genus Lepidocyclina Guembel, 1868

Subgenus Eulepidina Douvillé, 1911

Lepidocyclina (Eulepidina) andrewsiana (Jones and Chapman)

pl. 5 fig. 7

1900 Orbitoides (Lepidocyclina) andrewsiana Jones and Chapman, Mon. Christmas I., Brit. Mus. (Nat. Hist.) p. 255, pl. 21, fig. 14, fig. 15 (lower specimen only).

1926 Lepidocyolina (Eulepidina) andrewsiana; Nuttall, Quart. J. Geol. Soc. Lond. vol. 82, p. 27, pl. 4, figs. 1, 4, (synonymy).

1928 Lepidocyclina (Eulepidina) andrewsiana; van der Vlerk, Dienst Mijn. Ned. Indië. Wetensch. Meded. No. 8, p. 21, fig 1 a-b.

Distribution: Locality P 52; 200 feet above sea level.

Occurrence elsewhere: The recorded occurrences of this species in the opinion of Nuttall (l.c.p. 28) require confirmation.

Lepidocyclina (Eulepidina) ephippioides (Jones and Chapman) pl. 4, fig 6; pl. 5, fig. 4.

1950 Orbitoides (Lepidocyclina) ephippioides Jones and Chapman. Mon. Christmas Is. Brit. Mus. Nat. Hist. pp. 251-252, pl. 20, fig. 9, pl. 21, fig. 15.

1926 Lepidocyclina ephippoides; Nuttall, Quart. J. Geol. Soc. Lond. vol. 82, p. 34-36; pl. 5, figs. 1, 2, 3, 8 and 10.

1928 Lepidocyclina (Trybliolepidina) ephippoides; van der Vlerk, Dienst Mijn; Ned. Indië.Wetensch. Meded. No. 8, p. 26, fig. 10 a-c.

1957 Lepidocyclina (Eulepidina) ephippioides; Cole, U.S.G.S. Prof. Pap. 280-I p. 346, pl. 108, figs. 4-13; pl 109, figs. 11-15 (synonymy and discussion).

1963 Lepidocyclina (Eulepidina) ephippioides; Coleman, Micropal, vol. 9, No. 1, p. 15, pl. 4, figs 6-12; pl. 5, figs. 1-3 (synonymy).

Distribution: Locality P 13, at 600 feet; P 52, in talus at about 200 feet above sea level.

Occurrence elsewhere: Widely distributed in the Indo-Pacific region and possibly elsewhere.

Lepidocyclina (Eulepidina) inaequalis (Jones and Chapman) pl. 3 fig. 12

1900 Orbitoides (Lepidocyclina) insulae-natalis var inaequalis Jones and Chapman, Mon. Christmas I., Brit. Mus. Nat. Hist., p. 254, pl. 21, fig. 12.

1926 Lepidocyclina (Eulepidina) inaequalis; Nuttall, Quart. J. Geol. Soc. Lond. vol. 82, p. 33, pl. 4, fig. 3

1928 Lepidocyclina inaequalis; van der Vlerk, Dienst Mijn. Ned. Indië.Wetensch. Meded. No. 8, p. 31, fig. 46.

Distribution: Locality P 13, 600 feet above sea level.

Occurrence elsewhere: Santo, New Hebrides.

Lepidocyclina (Eulepidina) insulaenatalis (Jones and Chapman)
pl. 4 figs. 7 - 11; pl. 5, figs 1, 6.

1900 Orbitoides (Lepidocyclina) insulae-natalis Jones and Chapman, Mon. Christmas I., Brit. Mus. (Nat. Hist.), p. 242, pl. 20, fig. 5; pl. 21, fig. 16 (non pl. 21, fig. 13).

1911 Lepidocyclina (Eulepidina) insulae-natalis; Douvillé, Philippine J. Sci. ser. D, vol. 6, No. 2, p. 71, pl. A., fig. 7; pl. B, figs. 1,2, 3.

1926 Lepidocyclina (Eulepidina) insulae-natalis; Nuttall, Quart. J. Geol. Soc. Lond. vol. 82, p. 30, pl. 4, figs. 2, 5, 6. (synonymy).

1928 Lepidocyclina insulaenatalis; van der Vlerk, Dienst Mijnb. Ned. Indië. Wetensch. Meded. No. 8 p. 32, fig. 47 a-b (synonymy).

1938 Lepidocyclina (Eulepidina) insulae-natalis; Crespin, Commwlth. Aust. Dept. Interior Pal. Bull. No. 3, pl. 3, fig. 1.

Distribution: Locality P 13, 600 feet above sea level; P 52, talus about 200 feet above sea level.

Occurrence elsewhere: Borneo, New Guinea, New Hebrides, Philippines.

Remarks: Christmas Island specimens are inseparable from the matrix. Douvillé (1911, pl. B figs. 1, 2, 3.) figured external features of the species.

Lepidocyclina (Eulepidina) chapmani Nuttall
pl. 4 figs. 1 - 5

1900 Orbitoides (Lepidocyclina) insulae-natalis Jones and Chapman (pars) p. 256, pl. 21, fig. 13, specimen in upper part of figure,

1926 Lepidocyclina (Eulepidina) chapmani Nuttall, Quart. J. Geol. Soc. Lond. vol. 82, p. 31, pl. 4 figs. 7 - 9.

Distribution: Locality P 52 only, talus about 200 feet above sea level.

Lepidocyclina (Eulepidina) murrayana Jones and Chapman

1900 Orbitoides (Lepidocyclina) murrayana Jones and Chapman, Mon. Christmas I., Brit. Mus. Nat. Hist, p. 252-3, pl. 21, fig. 10.

1915 Lepidocyclina murrayana; Chapman, J. Proc. Roy. Soc. N.S.W. Vol. 48, pt. 3, p. 296, pl. 8. fig. 7.

1926 Lepidocyclina (Eulepidina) ?formosa, Nuttall, Quart. J. Geol. Soc. Lond. vol. 82, p. 29 (synonymy and discussion).

1938 Lepidocyclina (Eulepidina) murrayana, Crespin, Commw'lth Aust. Dept. Interior Pal. Bull. No. 3, p. 11, pl. 3, figs. 2, 3, 4, 9.

Distribution: Locality P 13, 600 feet above sea level.

Occurrence elsewhere: Borneo, New Guinea and Papua, Philippines.

Family DISCOCYCLINIDAE

Genus Discocyclina Guembel, 1870

Discocyclina oceanica Nuttall

pl. 5 figs. 2, 3

1900 Orbitoides (Discocyclina) dispansa Jones and Chapman, Mon. Christmas I., Brit. Mus. (Nat. Hist.) p. 229-230, pl. 20, fig. 1. (non Sowerby)

1926 Discocyclina oceanica Nuttall, Quart. J. Geol. Soc. Lond. vol. 82, pp. 38-40, pl. 5, fig. 9; text figs. 2, 3.

Distribution: Localities P 35, P 51; sea level to 300 feet above sea level.

Remarks: Several vertical sections are present in random sections of sample P 35, but the species is very rare in P 51, only one oblique section being observed. Nuttall (1926 p. 25) similarly records the rarity of Discocyclina in Andrews's sample 522, from the same limestone as P 51.

Family NUMMULITIDAE

Genus Spiroclypeus Douvillé, 1905

Spiroclypeus globulus Nuttall

pl. 6 figs. 8-10

1900 Orbitoides (Lepidocyclina) sumatrensis Jones and Chapman, Mon., Christmas I., Brit. Mus. (Nat. Hist.) p. 244, pl. 20, fig. 6 (non Brady)

1926 Spiroclypeus globulus Nuttall, Quart. J. Geol. Soc. Lond. vol. 82, p. 36, pl. 5, figs. 5-7, text fig. 1.

Distribution: Localities P 37, P 53, 600-662 feet above sea level; P 52, 200 feet above sea level.
The species is abundant in P 37

Remarks: S. globulus is closely related to Spiroclypeus orbitoideus Douville but is about half the size of orbitoideus. According to Nuttall the median lateral chambers differ in the two species.

Genus Heterostegina d'Orbigny, 1826
Heterostegina saipanensis Cole
pl. 6 figs. 1-7

1953 Heterostegina saipanensis Cole, U.S.G.S. Prof. Pap. 253, p. 23-24 pl. 2, figs. 4, 6.

1957 Heterostegina saipanensis Cole, U.S.G.S. Prof. Pap. 280-I, p. 331, pl. 102, figs. 17-19.

1957 Heterostegina saipanensis Cole, U.S.G.S. Prof. Pap. 260-V, p. 760, pl. 234, figs. 13-24; pl. 235, figs. 1-13.

Distribution: Abundant in samples P 35 and P 51.

Occurrence elsewhere: Saipan, Eniwetok, Guam.

Remarks: All the random sections cut yielded only transverse or oblique sections; two weathered specimens which were freed from the matrix yielded median sections which permit comparison with Heterostegina saipanensis. The dimensions of the initial and second chambers are approximately the same as those cited by Cole (1953, p. 24).

Genus Cycloclypeus Carpenter, 1856
Subgenus Cycloclypeus Carpenter, 1856
Cycloclypeus (Cycloclypeus) cf. eidae Tan.
pl. 5 fig. 5

1930 Cycloclypeus eidae Tan 1930, Mijningenieur vol. 12 p. 235 (fide Ellis and Messina).

1932 Cycloclypeus eidae Tan, Dienst Mijnb. Nederl. Indië.Wetensch. Meded. No. 19, p. 50-59; pl. 5, fig. 6; pl. 12, figs. 2, 3; pl. 13, figs. 1, 2, 4 - 6.

1953 Cycloclypeus (C.) eidae; Cole. U.S.G.S. Prof. Pap. 253, p. 27, pl. 5, figs. 13 - 19. (synonymy).

1953 Cycloclypeus eidae; Crespin, Aust. Bur. Min. Res. Geol. Gephys. Bull. 21, p. 66, pl. 9, fig. 1; pl. 10, fig. 3.

1963 Cycloclypeus (C.) eidae; Coleman, Micropal. vol. 9, No. 1, p. 34, pl. 9, fig. 12 (synonymy).

Distribution: Locality P 52, 200 feet above sea level.

Occurrence elsewhere: Tertiary "e" (Aquitanian) of Indonesia, Borneo, Saipan, Guam, Fiji, Solomon Islands, Northwest Australia.

Remarks: The species is very rare in the Christmas Island material; the section of the fragment figured is the only evidence of its presence.

REFERENCES

ANDREWS, C.A., 1900. A Monograph of Christmas Island (Indian Ocean). History and Physical Features, Geology, The Geographical Relations of the Flora and Fauna. British Museum (Natural History), 1-21, 269-298, 299-337.

CHAPMAN, F., 1905. Notes on the older Tertiary Foraminiferal Rocks on the West Coast of Santo, New Hebrides. Proc. Linn. Soc. N.S.W. 30, (2), (118), 261-274, pls. 5-8.

CHAPMAN, F., 1908. On the Tertiary Limestones and Foraminiferal Tuffs of Malekula, New Hebrides, Proc. Linn. Soc. N.S.W. 32, (4), (128), 745-760, pls. 37-41.

CHAPMAN, F., 1914-1915 Description of a Limestone of Lower Miocene Age from Bootless Inlet, Papua. J. Proc. Roy. Soc. N.S.W. 48, (2), 281-288; (3), 289-301, pls. 7-9.

COLE, W. STORRS, 1939. Large Foraminifera from Guam. J. Pal. 13, (2) 183-189, pls. 23-24, 1 text fig.

COLE, W. STORRS, 1953. Geology and Larger Foraminifera of Saipan Island. Correlation and Systematic Paleontology. U.S. Geol. Surv. Prof. Pap. 253, 17-45, pls. 2-15.

COLE, W. STORRS, 1954. Larger Foraminifera and Smaller Diagnostic Foraminifera from Bikini Drill Holes, U.S. Geol. Surv. Prof. Pap. 260-0, 569-608, pls. 204-222.

COLE, W. STORRS, 1957. Larger Foraminifera from Eniwetok Atoll Drill holes. U.S. Geol. Surv. Prof. Pap. 260-V, 743-784, pls. 231-249.

COLE, W. STORRS, 1957. Geology of Saipan, Mariana Islands, Part 3, Paleontology, Chapter 1. Larger Foraminifera. U.S. Geol. Surv. Prof. Pap. 280-I, 321-360, pls. 94-118.

COLE, W. STORRS, 1960. Upper Eocene and Oligocene Larger Foraminifera from Viti Levu, Fiji. U.S. Geol. Surv. Prof. Pap. 374-A, A 1 - A 3 pls. 1-3.

COLE, W. STORRS, 1963. Tertiary Larger Foraminifera from Guam. U.S. Geol. Surv. Prof. Pap. 403-E, E 1 - E 28, pls. 1 - 11.

COLEMAN, P.J., 1963. Tertiary larger foraminifera of the British Solomon Islands, southwest Pacific, Micropaleontology. 9, (1), 1-38, pls. 1-9.

CRESPIN, I., 1938. A Lower Miocene Limestone from the Ok Ti River, Papua, C'wealth Australia Dept. Interior, Pal. Bull. 3, 9-16, pl. 3.

CRESPIN, I., 1953. The Cape Range Structure, Western Australia. Part 2 Micropaleontology. C'wealth Australia. Bur. Min. Res. Geol. Geophys. Bull. 21, 43-75 pls. 7-10.

CUSHMAN, J.A., TODD, R., and POST, R.J., 1954. Recent Foraminifera of the Marshall Islands U.S. Geol. Surv. Prof. Pap. 260-H, 319-384, pls 82-93.

DOUVILLE, H., 1911. Les foraminiferes dans le Tertiare des Phillippines. Philippine Jour. Sci., ser. D, 6, (2), 53-80, pls A-D.

EAMES, F.E., BANNER, F.T., BLOW, W.H., AND CLARK, W.J., 1962. Fundamentals of Mid-Tertiary Stratigraphical Correlation. Camb. Univ. Press. 1-153, pls. 1-17, figs. 1-20.

GLAESSNER, M.F., 1959. Tertiary Stratigraphic Correlation in the Indo-Pacific Region and Australia. J. Geol. Soc. Ind. 1, pp. 53-67.

HANZAWA, S., 1957, Cenozoic Foraminifera of Micronesia. Geol. Soc. Amer. Memoir 66, 1-163, pls. 1-38, tables 1-5.

JONES, T.R., and CHAPMAN, F., 1900. Monograph of Christmas Island. Brit. Mus. (Nat. Hist.), 226-264 pls. 20-21.

LUDBROOK, N.H., 1961. Stratigraphy of the Murray Basin in South Australia. Geol. Surv. S.Aust. Bull. 36, 1-96, pls. 1-8. tabs. 1-11, text. figs. 1-36.

LUDBROOK, N.H., 1963. Correlation of the Tertiary Rocks of South Australia. Trans. Roy. Soc. S.Aust. 87, 5-15, figs. 1-4.

MOHLER, W.A., 1949. Uber das Vorkommen von Alveolina and Neoalveolina in Borneo. Eclog. Geol. Helvetiae 41, (2), (1948), 321-329, 1 tab. text figs. 1-2.

MOHLER, W. A., 1950. Flosculinella reicheli n. sp. aus dem Tertiar e_5 von Borneo. Eclog. Geol. Helvetiae 42, (2), 521-527, text figs. 1-3.

NUTTALL, W. L. F., 1926. A Revision of the Orbitoides of Christmas Island (Indian Ocean). Quart. J. Geol. Soc. Lond. 82, 22-43, pls. 4-5.

SMITH, W. CAMPBELL, 1926. The Volcanic Rocks of Christmas Island (Indian Ocean). Quart. J. Geol. Soc. Lond. 82, 44-66 pl. 6.

TAN SIN HOK, 1932. On the Genus Cycloclypeus Carpenter. Dienst Mijn Ned. - Indie, Wetensch. Meded, 19, 1-194, pls. 1-24, tables 1-7, text figs. 1-4.

TODD, R. and LOW, D., 1960. Smaller Foraminifera from Eniwetok Drill Holes. U. S. Geol. Surv. Prof. Pap. 260-X, 799-861, pls. 255-264.

VAN BEMMELEN, R. W., 1949. The Geology of Indonesia, 3 vols. Government Printing Office, The Hague.

8. EXPLANATION OF PLATES

PLATE 1.

1-4 "Rotalia" tectoria Todd and Post.

1. GSSA 13350, P 52, slightly oblique median section and vertical section X28; 2. GSSA 13351, P 52, median section showing surface ornament and umbilical plug X28; 3. GSSA 13284, P 52, slightly oblique vertical section X28; 4. GSSA 13303, P 52, 3 sections illustrating local abundance of the species X 28.

5-7 Pararotalia sp.

5. GSSA 13405, P 35, median section X28;
6. GSSA 13403, P 35, vertical section X28;
7. GSSA 13282, P 51, oblique section X 28.

8-12 Borelis pygmaeus Hanzawa

8. GSSA 13392, P 4, axial section X28; 9. GSSA 13391 P 4, transverse X80; 10. GSSA 13276, P 41, transverse section X28; 11. GSSA 13393, P 4, traverse section X80; 12; GSSA 13396, P 4, axial section X80.

13-14 Austrotrillina howchini (Schlumberger).

13; GSSA 13392, P 4, slightly oblique section X28;
14. GSSA 13396, P 4, oblique and axial section X28.

15-16 Flosculinella bontangensis (Rutten). 15, GSSA 13344, P 33, axial section X28; 16. GSSA 13344, P 33, slightly oblique axial section X28.

PLATE 2.

1. Association of Gypsina marianensis Hanzawa and Lithophyllum GSSA13267, P 30, X28.

2-3 Gypsina marianensis Hanzawa. 2. Three individuals on same slide as 1, GSSA 13267, P 30 X 28. 3. GSSA 13267, P 30, X28.

4 Gypsina globula (Reuss). GSSA 13404, P 35, transverse section X28.

5-6 Borodina septentrionalis Hanzawa. 5 GSSA 13412, P 48, X 28. 6. GSSA 13400, P 12, X 28.

PLATE 3.

1-2 Miogypsinoides dehaartii (van der Vlerk) and Miogypsina neodispansa (Jones and Chapman) 1. GSSA 13263, P 26, vertical sections of M. dehaartii (2 specimens at top). M. neodispansa (at bottom) X 28; 2. GSSA 13263, P 26, M. neodispansa on left, surrounded by 4 specimens of M. dehaartii X 28.

3-7 Miogypsinoides dehaartii (van der Vlerk). 3 GSSA 13263, P 26, equatorial section X 28; 4 GSSA 13263, P 26, equatorial section 28; 5 GSSA 13270 P 31, equatorial section X 28; 6 GSSA 13268, P 30 vertical section X 28; 7 GSSA 13270, P3, oblique section X 28.

8 Miogypsinoides dehaartii (van der Vlerk) and Amphistegina bikiniensis Todd and Post. GSSA 13270, P 31, oblique section X 28.

9-10 Amphistegina bikiniensis Todd and Post. 9 GSSA 13269 P 31, vertical section, X 28; 10 GSSA 13286, P 35, oblique vertical section X 80.

PLATE 4.

1-5 Lepidocyclina (Eulepidina) chapmani Nuttall.

1. GSSA 13301, P 52, vertical section X 7.5;
2. GSSA 13336, P 13, oblique section X 7.5;
3. GSSA 13283, P 52, oblique vertical section X 7.5;
4. GSSA 13285, P 62, vertical section of flange X 7.5;
5. GSSA 13342, P 13, oblique horizontal section X 7.5;

6 Lepidocyclina (Eulepidina) ephippioides (Jones and Chapman) GSSA 13340, P 13, vertical section X 7.5;

7-11 Lepidocyclina (Eulepidina) insulaenatalis (Jones and Chapman) 7. GSSA 13339, P 13, vertical section X 7.5; 8. GSSA 133301, P 52, oblique section, X 7.5; 9. GSSA, 13301, P 52, oblique vertical section X 7.5; 10. GSSA 13285, P 52, oblique section X 7.5; 11. GSSA, 13301 P 52, oblique section X 7.5.

12 Lepidocyclina (Eulepidina) inaequalis (Jones and Chapman) GSSA 13340, P 13, oblique section X 7.5.

PLATE 5.

1,6 Lepidocyclina (Eulepidina) insulaenatalis (Jones and Chapman) GSSA 13350, P 52, oblique section showing detail X 28; 6, GSSA 13352, P 52, vertical section showing detail, X 28.

2-3 Discocyclina oceanica Nuttall. 2. GSSA, 13403, P 35 vertical section X 80; 3. GSSA 13405, P 35, vertical section X 28;

4 Lepidocyclina (Eulepidina) ephippioides (Jones and Chapman) GSSA, 13350, P 52, vertical section X28.

5. Cycloclypeus cf. eidae Tan. GSSA, 13351, P 52, median section X80.

7 Lepidocyclina (Eulepidina) andrewsiana (Jones and Chapman). GSSA 13352, P 52, vertical section X 28.

PLATE 6.

1-7 Heterostegina saipanensis Cole, 1. GSSA, 13348, P 51, vertical section X 28; 2, GSSA, 13348, P 51, vertical section of flange X 28; 3. GSSA, Ff. 101 P 51, median section, slightly oblique X 28; 4. GSSA, 13406,

P 35, oblique vertical section X 28; 5. GSSA, 13348, P 51, vertical section X 28; 6. GSSA, 13281, P 51, vertical section X 28; 7. GSSA, 13408, P 35, vertical section X 28.

8–10 Spiroclypeus globulus Nuttall 8. GSSA, 13274, P 37, vertical section X 28; 9. GSSA, 13273, P 37, vertical section X 28; 10. GSSA, 13273, P 37, vertical section of flange X 28.

PLATE 7.

1-2 Sporadotrema cylindricum (Carter). GSSA, 13272, P 36, X 28.

3 Borelis cf. melo (Fichtel and Moll) GSSA, 13271, P 36, X 28

4 Sorites martini (Verbeek). GSSA, 13344, P 33, X 28.

5 Gypsina globula (Reuss). GSSA, 13271, P 36, X 28

6 Globigerina bulloides (d'Orbigny). GSSA, 13271, P 36, X 28.

7 Orbulina universa (d'Orbigny). GSSA, 13271, P 36, X 28.

8 Textularia sp. GSSA, 13271, P 36, X 28.

9 Globorotalia menardii (d'Orbigny). GSSA, 13271, P 36 X 28.

10 Carpenteria capitata (Jones and Chapman) GSSA, 13268 P 30, X 28.

11 Gyroidina sp. GSSA, 13349, P 51, X 80.

PLATE A1

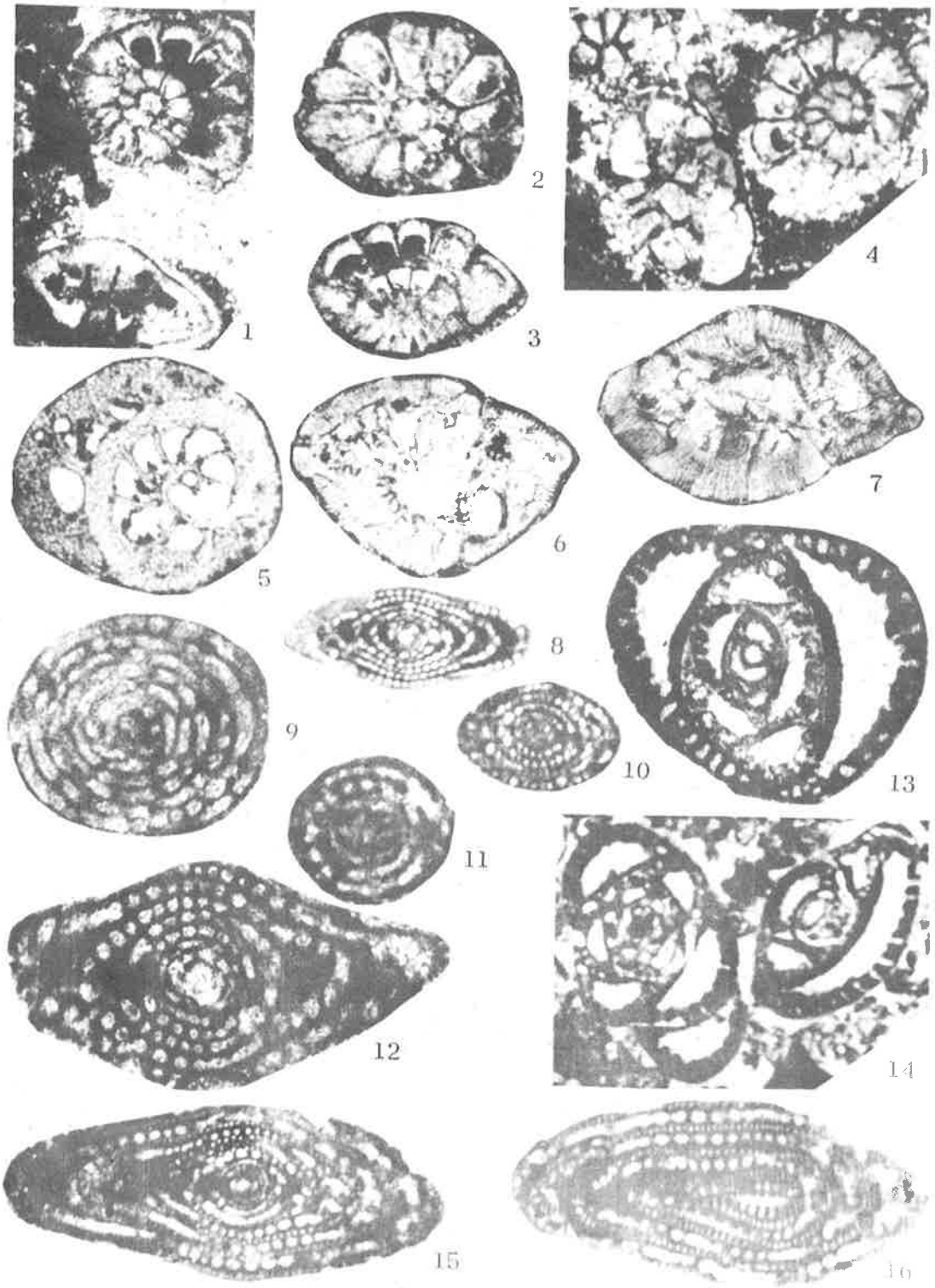

PLATE A2

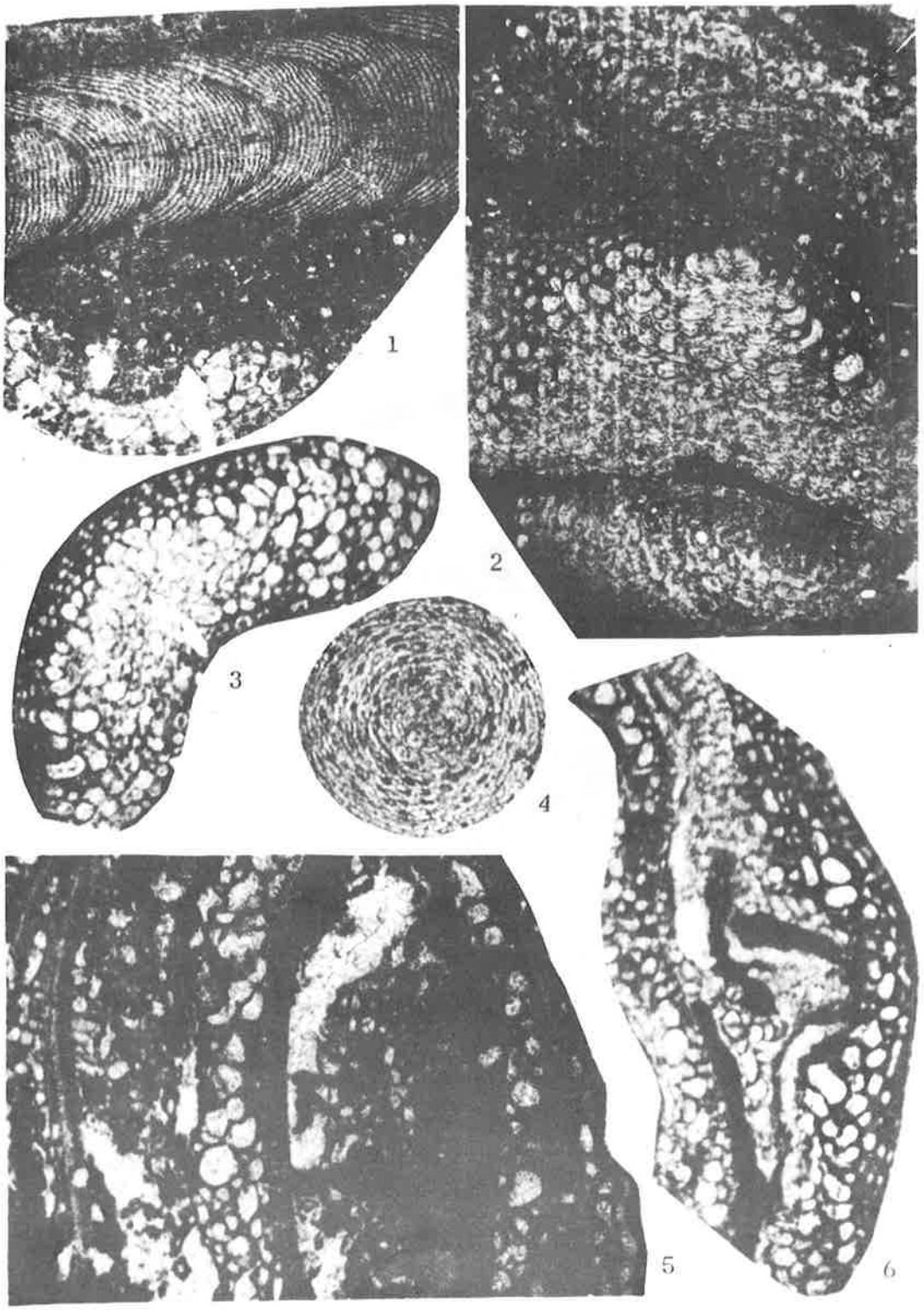

PLATE A3

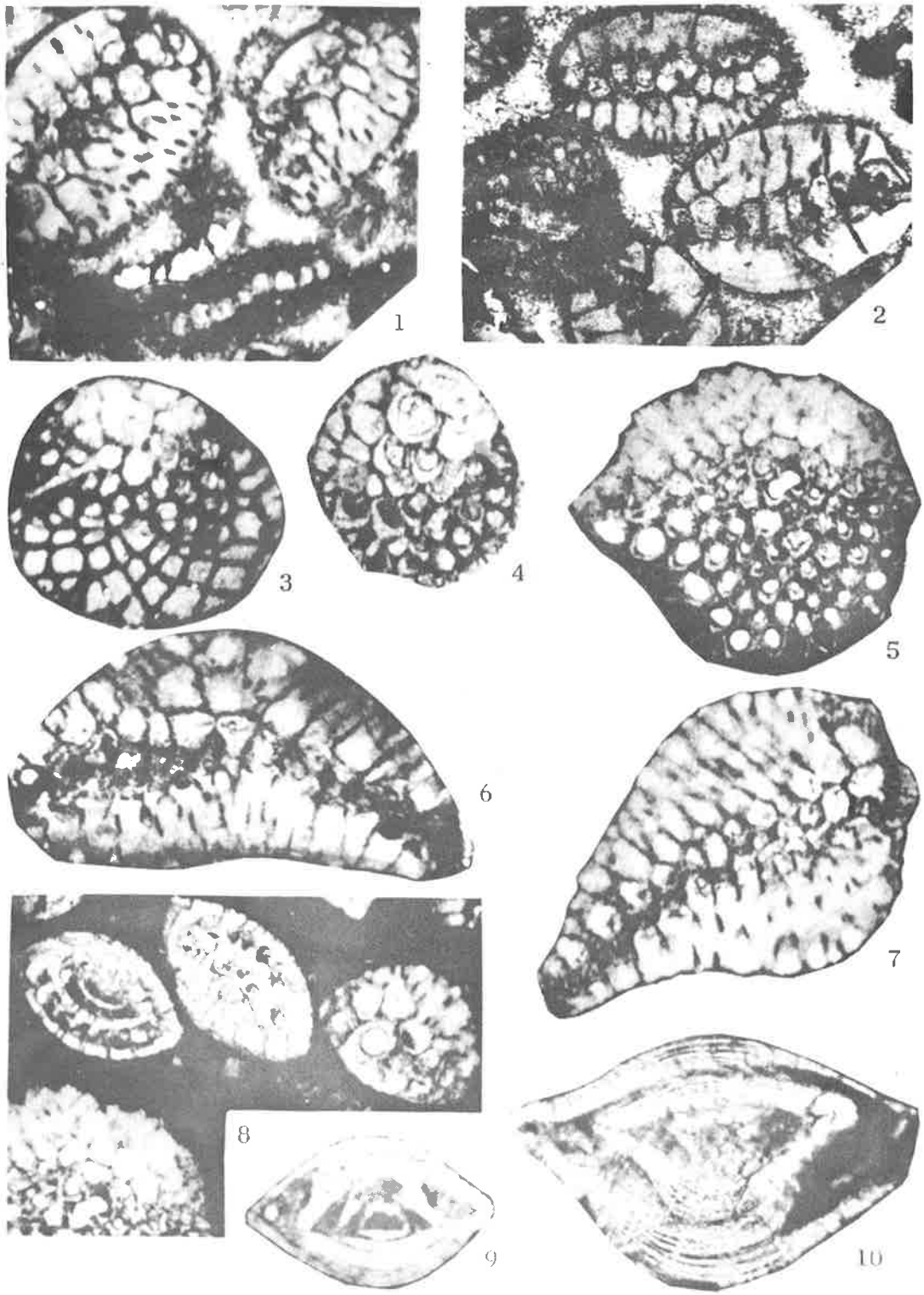

PLATE M

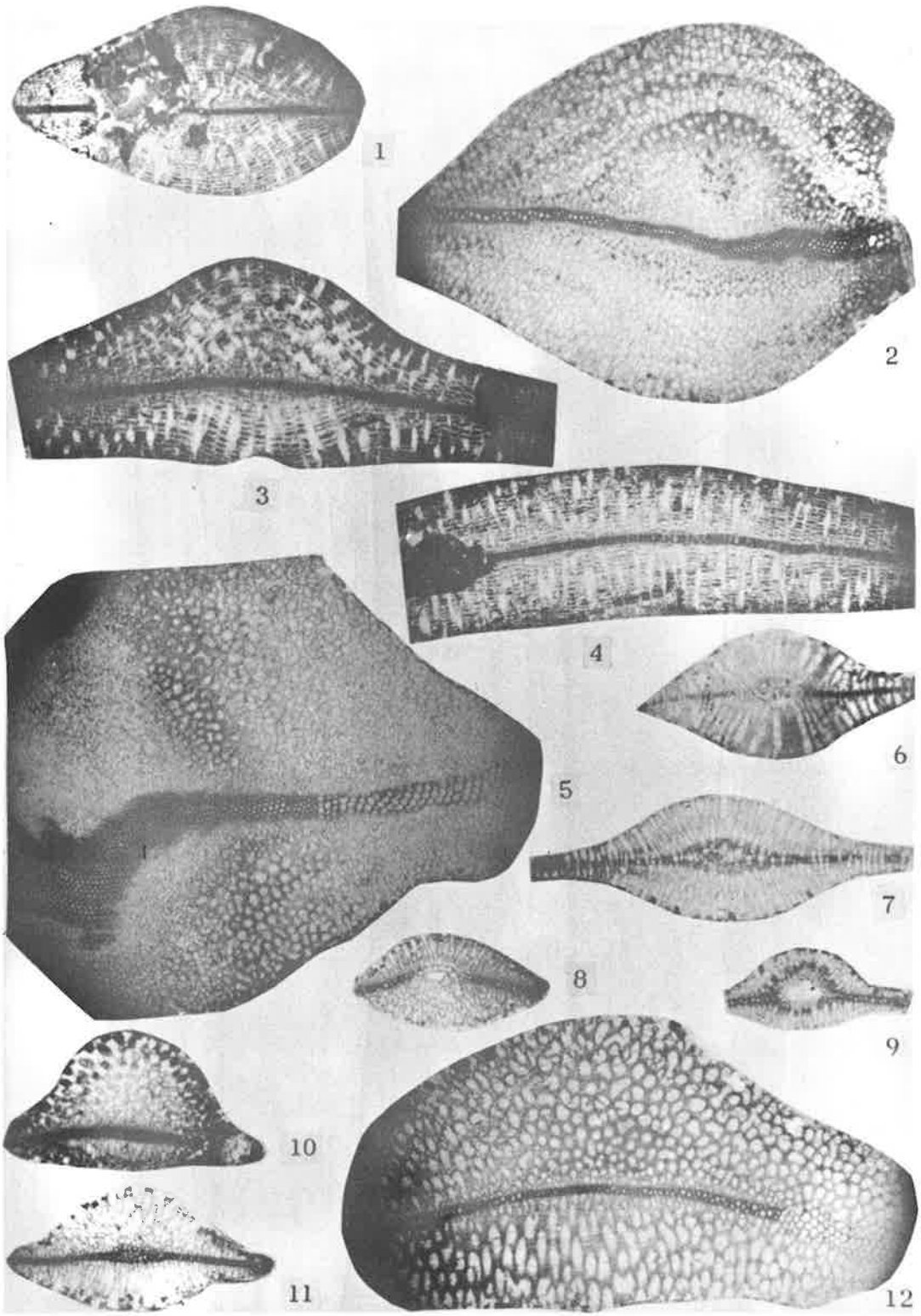

PLATE A5

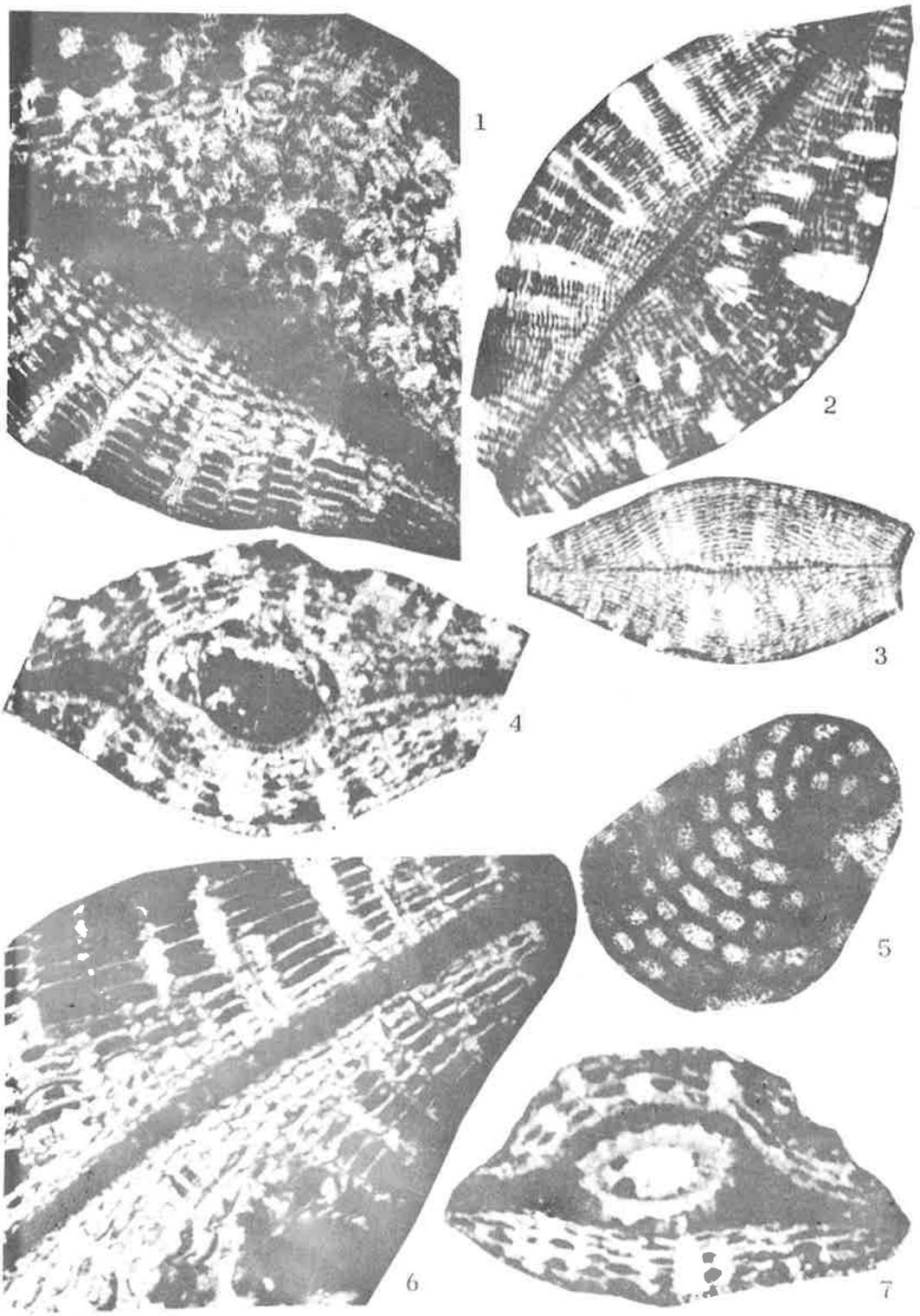

PLATE A6

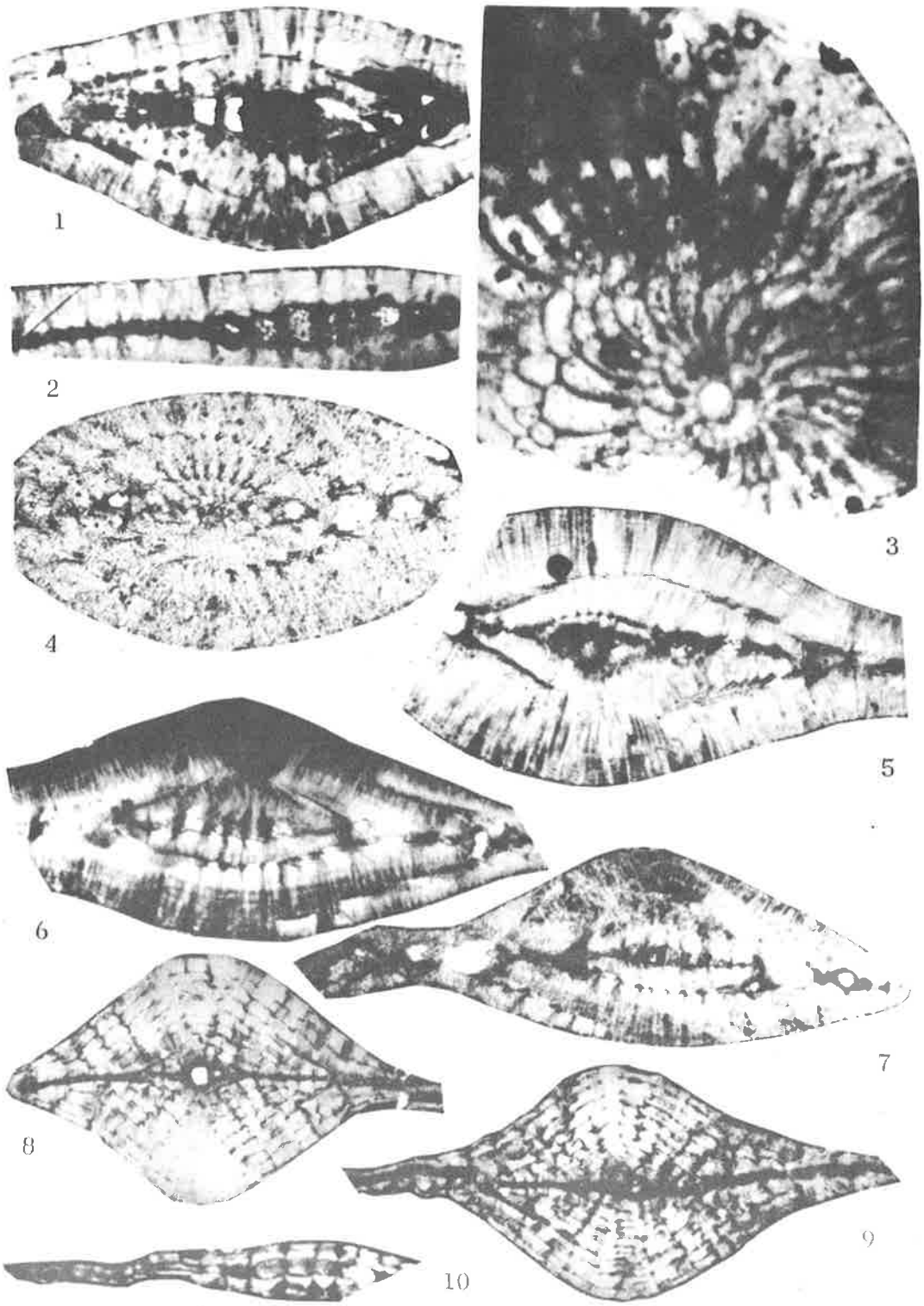

PLATE A7